

CHAPTER 1

INTRODUCTION

The acquired immunodeficiency syndrome (AIDS) caused by the virus, human immunodeficiency virus (HIV) is a debilitating and devastating disease, which has acquired pandemic proportion globally, in the past twenty-five years since its discovery in 1983 by Nobel laureate Professor Luc Montagnier [1]. In the initial years of the AIDS epidemic, the cause of AIDS eluded clinicians and researchers treating patients afflicted with this sinister disease. In 1984, Professor Robert C. Gallo established the linkage between HIV and acquired immunodeficiency syndrome (AIDS) by repeatedly isolating HIV from patients afflicted with AIDS [2]. HIV-1 and HIV-2, the causative agents of acquired immunodeficiency syndrome (AIDS), belong to the family of lentivirus and these are retroviruses that is they are capable of converting genomic RNA into proviral DNA. The closest relative of HIV-1 is the simian immunodeficiency virus (SIV) which have been isolated from chimpanzees (*Pan troglodytes*) [3]. AIDS is characterized by a marked depletion in CD4⁺ helper T-lymphocytes, thereby making the host vulnerable to many opportunistic infections viz. tuberculosis (TB), pneumonia, and other bacterial and fungal infections. The probable routes of HIV transmission are via intimate contact with infected body fluids, infected intravenous devices, maternal transmission and transfusion of contaminated blood.

Till date, sixty million people have been infected with HIV, of which 50% have perished, creating a profound socio-economic impact [4]. According to the 2008 report on the global AIDS epidemic released by UNAIDS, globally there were around 33 million people infected with HIV in 2007 [5]. In India, 2.47 million of the population is living with HIV as of 2007, which is approximately 0.36 percent of the adult population [6]. 25% of this infected populace requires anti-retroviral therapy (ART), out of which 147,400 receive ART [6].

1.1 Structure & anatomical considerations of HIV-1 virion

Mature, infectious HIV-1 virions contain a characteristic cone-shaped central, dense core which encloses viral RNA and replicative proteins. The virus is surrounded by a lipid membrane. A matrix protein lines the inner surface of the membrane. The outer surface is composed of an envelope protein structured as spikes, which is implanted in the lipid bilayer. HIV has a complement of nine genes of which three are common with other retroviruses, viz. *gag* (group antigen), *pol* (polymerase) and *env* (envelope) structural genes, which encode for proteins getting integrated into the virus particle [7]. The average size of HIV-1 virion is approximately 145 nm and with maturation the size does not change. Cryo-electron microscopic analysis revealed that these cores can be conical or tubular in shape with a stacked-disc arrangement possessing 7-, 8-, 9-10- fold axial symmetry. Intact, mature HIV-1 particles possess projecting spikes on their surface, which most likely interact with the viral glycoproteins. When released from cell surface as immature, non-infectious particles they possess a spherical layer of Gag polyproteins underneath the viral membrane. These Gag polyproteins are then processed by protease enzyme, which leads to maturation followed by budding. Proteolytic cleavage leads to protein matrix, capsid, nucleocapsid, p6 and two other small spacer peptides formation along with conferment of infectivity [8]. In the mature virion, the matrix is found underneath the viral membrane, the capsid corresponds to the core shell and the nucleocapsid forms the internal ribonucleotide complex. Localization of p6, which is involved in late stages of virus release, is not known till date. The proteins involved in viral replication are synthesized as part of a Gag-Pol fusion protein and are released proteolytically in the maturing virion. The Pol-derived proteins, protease, RT and integrase are located centrally in the immature virion, but following maturation RT and integrase form a part of the internal core and are retained in the genome during entry into the T-lymphocytes. The viral surface and transmembrane glycoproteins gp120 and gp41 are also synthesized as polyproteins and are transported and processed via the vesicular route and acquired by the budding virion at the plasma membrane [9].

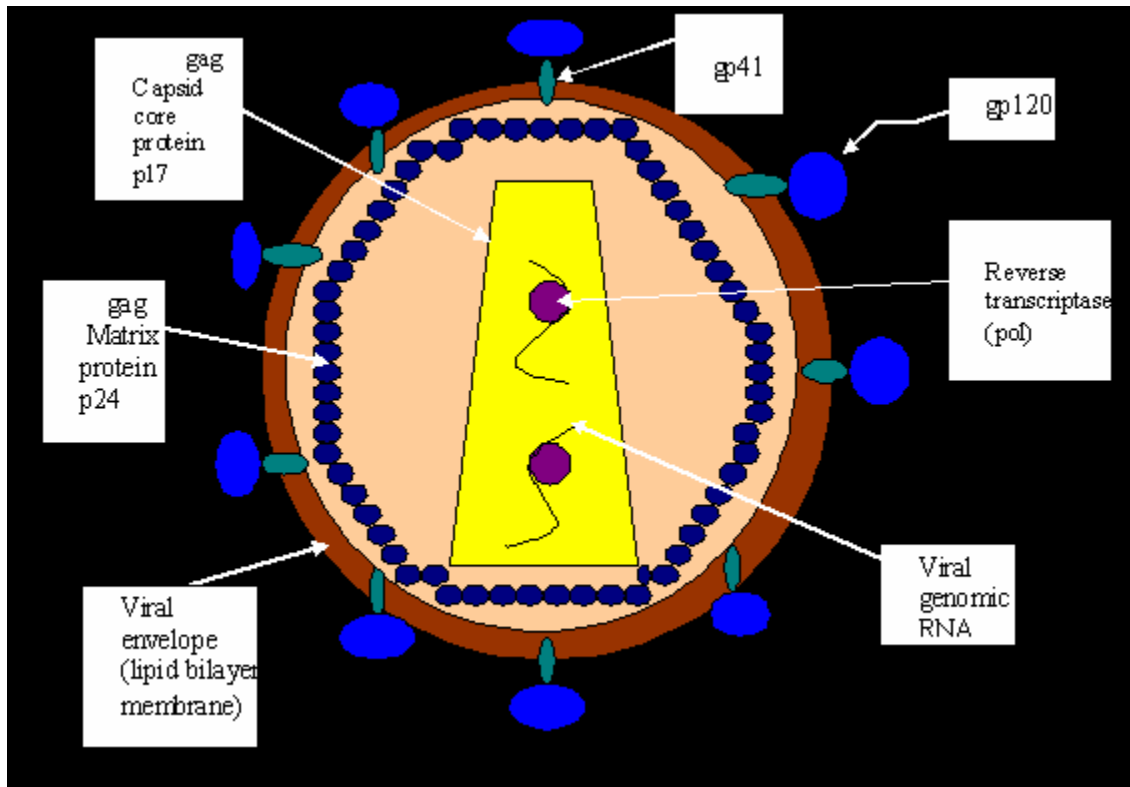


Fig. 1.1: Structure of the HIV-1 virion

Biochemical and electron microscopic studies afford an overview of the core geometry. Retroviral capsid and longer proteins containing the nucleocapsid domain assemble *in vitro* into helical tubes of diameter 300-800 Å and lengths of several microns. The capsid tubes are constituted of hexameric rings of capsid proteins. The hexamer exhibited an external diameter of ~100 Å surrounding a central hollow zone of ~25 Å. The ends of the conical cores were found to lie close near the viral membrane with a distinct gap between the two [8]. Other than Gag, Pol and Env proteins, HIV-1 also encode for three regulatory proteins viz. *rev* (regulator of virion protein), *tat* (trans-activator) and *nef* (negative regulatory factor). It also encodes for three proteins which assist in virus maturation and release namely, *vif* (virion infectivity factor), *vpu* (viral protein U) and *vpr* (viral protein R). But not much is known about the topology of these regulatory and accessory proteins [7,9].

1.2 HIV Life cycle

The life cycle of HIV, as illustrated in **Fig. 2** comprises of four distinct phase namely: infection, reverse transcription and integration; viral gene expression; virus assembly and maturation. The process involves initial binding of the HIV cell to the CD4 receptor on the host T-lymphocyte cell by virtue of its surface protein, gp 120. Following attachment of virus particles to CD4 receptor molecules, the virus enters the cell by a pH-dependent mechanism and/or endocytosis. The virus fuses with the host cell's cytoplasmic vacuole, leaving behind the outer lipid envelope thereby entering into the host cell, within a few minutes to a few hours of infection [7].

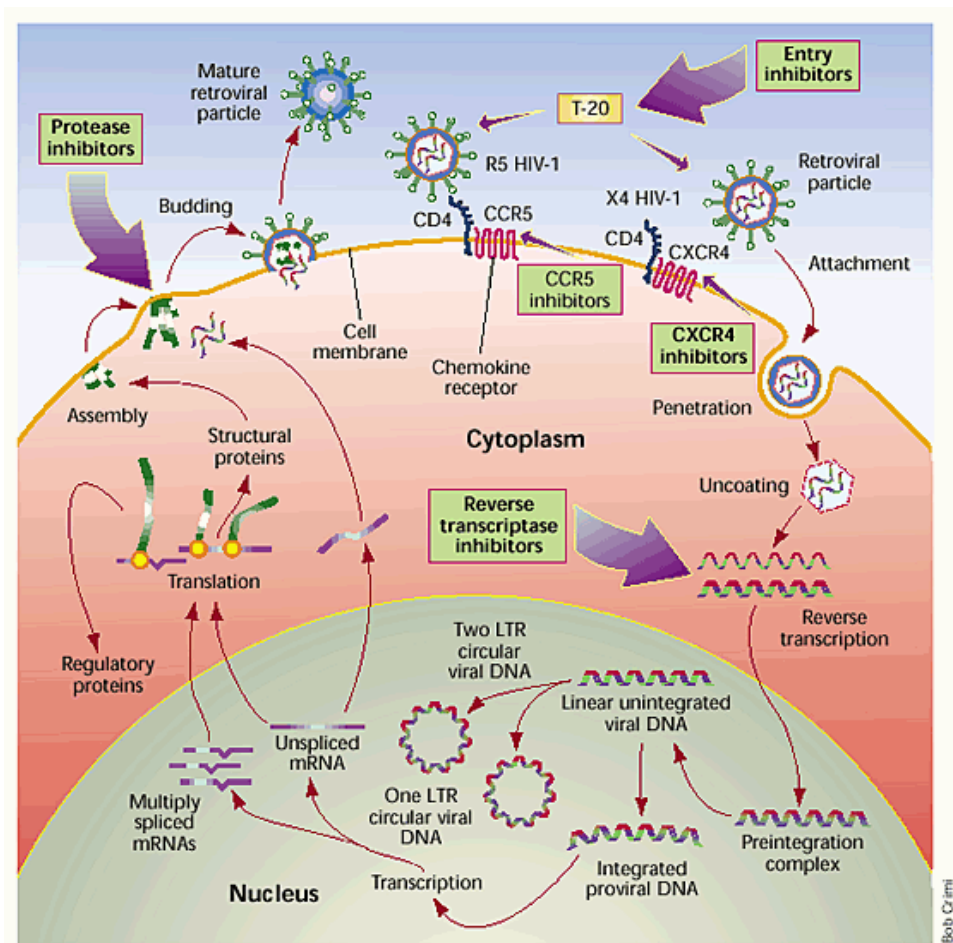


Fig 1.2: HIV Life cycle and the site of action of many anti-HIV agents [10]

Subsequent to the release of the proviral RNA, it gets converted into genomic DNA, the process being mediated by the conservative action of the viral reverse transcriptase

enzyme's two isoforms, polymerase and ribonuclease. This DNA then enters into the host nucleus and gets integrated into the host DNA, with the help of the catalytic enzyme, integrase, within a span of 2- 10 h of infection [7, 11]. Once part of the cellular DNA, the viral genetic information remains in the cell as long as the cell survives, by becoming a part of the host cellular DNA and this is the reason for life-long persistent infection of HIV [12]. Eight to twelve hours after infection, activation of the host cells results in the transcription of viral DNA into messenger RNA (mRNA), which is then translated into viral proteins [7]. Cellular enzymes process the initial RNA transcript, yielding a complex pattern of sub-fragments of the initial transcript which serves as messenger RNAs for some viral proteins [12]. The translational process occurs 12-24 h following infection [7]. The enzyme, HIV protease, processes these HIV proteins into their functional forms. The structural proteins are all derived from Gag polyprotein which gets myristoylated co-translationally [13]. These viral RNA and viral proteins then accumulate at the surface of the host cytoplasmic membrane. Amino-terminal myristoylation of the p55 *gag* and p160 *gag-pol* precursors guide these molecules to the cytoplasmic membrane. Dimerization of the proteinase region of the *gag-pol* precursor triggers the virally encoded enzyme. Cleavage of the *gag* precursor molecule produces mature, infectious particles with their distinctive bullet-shaped nucleoid core [7]. A new virion then buds forth and is released, continuing its saga of infecting new T-lymphocytes. Maturation and budding take place 36-48 h after infection [7]. The time spans mentioned for the different processes involved can vary depending on the metabolic status of the cell and the multiplicity of infection.

1.3 HAART

Considerable progress has been made in treating HIV-infected patients using highly active anti-retroviral therapy (HAART) involving multi-drug combinations. The indicator parameter which primarily determines the initiation of HAART in a patient is, when the subject's CD4 count plunges below 350 cells/mm³ or less. It combines two or three anti-HIV medications in a daily regimen. The antiretroviral drugs approved by the U.S Food and Drug Administration (USFDA) can be classified into five different classes as listed in **Table 1.1**.

Table 1.1: Antiretroviral drugs approved by the U.S FDA [14]

<i>Class</i>	<i>Generic Name</i>	<i>Brand name</i>	<i>Manufacturer</i>	<i>FDA Approval Date</i>
NNRTI	Delavirdine	Rescriptor	Pfizer	1997
	Efavirenz	Sustiva	Bristol-Myers Squibb	1998
	Etravirine	Intelence, Celsentri	Tibotec	2008
	Nevirapine	Viramune	Boehringer Ingelheim	1996
NRTI	Abacavir	Ziagen	Glaxo Smithkline	1998
	Didanosine	Videx, Videx EC	Bristol-Myers Squibb	1991, 2000 (EC)
	Emtricitabine	Emtriva	Gilead Sciences	2003
	Lamivudine	Epivir	Glaxo Smithkline	1995
	Stavudine	Zerit	Bristol-Myers Squibb	1994
	Tenofovir	Viread	Gilead Sciences	2001
	Zidovudine	Retrovir	Glaxo Smithkline	1987
PI (Protease Inhibitors)	Amprenavir	Agenerase	Glaxo Smithkline, vertex Pharmaceuticals	1999
	Atazanavir	Reyataz	Bristol-Myers Squibb	2003
	Darunavir	Prezista	Tibotec	2006
	Fosamprenavir	Lexiva	Glaxo Smithkline, vertex Pharmaceuticals	2003
	Indinavir	Crixivan	Merck	1996
	Lopinavir, Ritonavir	Kaletra	Abbott Laboratories	2000
	Nelfinavir	Viracept	Agouron Pharmaceuticals	1997
	Ritonavir	Norvir	Abbott Laboratories	1996
	Saquinavir	Invirase	Hoffman-La Roche	1995
	Tipranavir	Aptivus	Boehringer Ingelheim	2005
Fusion Inhibitors	Enfuvirtide	Fuzeon	Hoffman-La Roche, Trimeris	2003
	Maraviroc	Selzentry	Pfizer	2007
Integrase inhibitors	Raltegravir	Isentress	Merck	2007

The nucleoside reverse transcriptase inhibitors (NRTIs) are structural analogs of the nucleoside substrates and they competitively inhibit the RT by getting incorporated into the DNA and preventing further attachment of nucleosides [15]. The non-nucleoside reverse transcriptase inhibitors (NNRTIs) non-competitively inhibit the RT by binding to an allosteric site located almost 10 Å away from the catalytic site.

The protease inhibitors block the enzyme, protease, needed for splicing the core proteins into functional proteins which would form further new mature and infectious viruses [16]. The fusion inhibitors target both the viral surface glycoprotein (gp 120) as well as the host cell surface chemokine receptor (CXCR4 & CCR5), to which HIV gets attached [17-20]. The integrase inhibitors target the enzyme, integrase, required for integration of the viral reverse transcripts into the host chromosome [21].

1.4 Implications of RT in AIDS

In retroviruses, such as HIV-1, RT is the sole enzyme which catalyses the transformation of single-stranded viral RNA into the double-stranded linear DNA, which ultimately gets integrated into the host cell chromosome. It also possesses ribonuclease H (RNase H) activity that is it degrades the RNA strand of RNA-DNA complex into small pieces, once its use as the template for the first DNA strand is over [22]. HIV-1 RT is composed of 2 subunits of 66 kDa and 51 kDa (p66 & p51). The N-terminal 440 amino acids of p66 comprise the polymerase domain and the C-terminal 120 amino acids make up the RNase H domain. The p51 subunit of HIV-1 RT corresponds to the polymerase domain of the p66 subunit. The p51 subunit lacks the RNase H domain; but the corresponding domains in the p66 and p51 are similar in structure only differing in their relative organization. The polymerase domains of p66 and p51 each contain four sub-domains, which are denoted as fingers, palm, thumb and connection. The finger and thumb domains of p66 and p51 are structurally similar; but certain regions of palm and connection domains are strikingly different. Particularly the residues involved in formation of the carboxy terminus of p51 are in an entirely varying conformation from that of p66 [23].

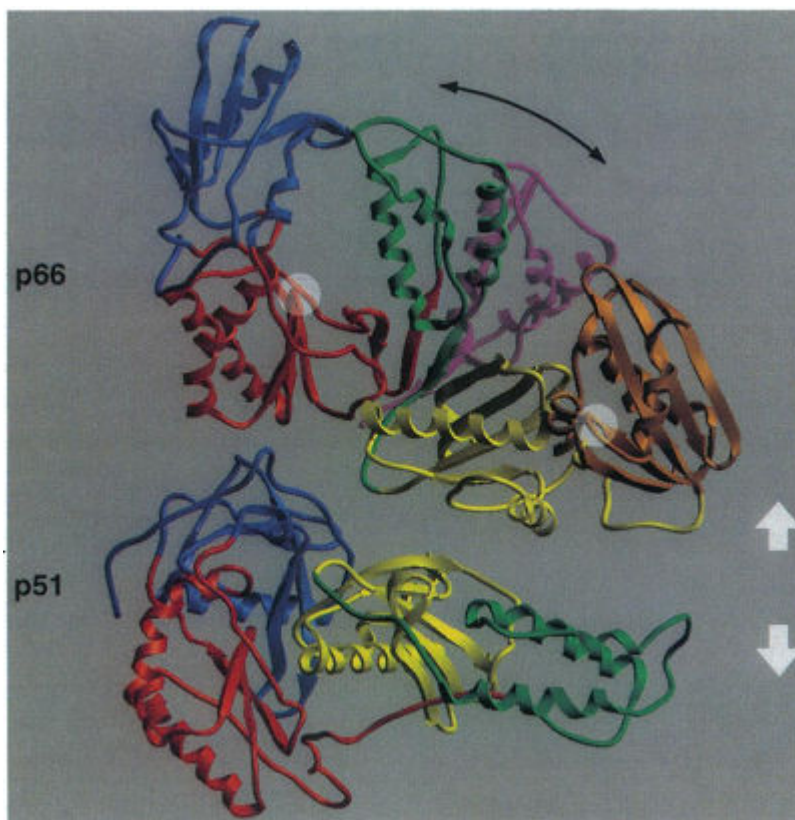


Fig 1.3: HIV-1 RT domain structure. Domains are color coded: blue, fingers; red, palm; green, thumb; yellow, connection; RNase H, brown. White disks indicate the polymerase (p66) and the RNase H active sites. [24]

In the p66 palm resides the polymerase active site that is defined by a triad of aspartates, viz. Asp 110, Asp 185 and Asp186. The 3'-OH of the primer terminus lies close to the catalytic aspartates and is positioned for nucleophilic attack on the α -phosphate of an incoming nucleoside triphosphate [25]. The p66 fingers and thumb form a gap which accommodates the template-primer. The four active site residues, namely, Tyr 183, Met 184, Asp 185 and Asp186 lie in a turn connecting β 7 and β 8; while the catalytic Asp 110 lies in the strand β 4, adjacent to the Asp 185 and Asp186 [23].

1.5 Non-nucleoside reverse transcriptase inhibitors

NNRTIs inhibit the chemical step of DNA polymerization by its presence. The crystal structure of RT complexed with NNRTIs reveals that the residues, Tyr 181 and Tyr 188 have significant implications in the interaction with NNRTIs. These tyrosine residues skirt the essential catalytic aspartates. Relatively minute changes in the positions of these residues dramatically affect the catalytic step, without affecting nucleotide binding [26]. In the absence of any inhibitor, the NNRTI binding pocket (NNIBP) does not exist. On its binding, a hydrophobic pocket is formed distorting the region near the polymerase active site, primarily by torsional swiveling of the side chains of Tyr 181 and Tyr 188 and repositioning of the second β -sheet containing Phe 227 and Trp 229. This NNIBP is almost devoid of any electrostatic charges. The NNIBP lies between 2 β -sheets, one containing the essential aspartates (β 9- β 10) and the other containing the primer grip (β 12- β 13- β 14). This leads to displacement of the β 12- β 13 hairpin, which directly interacts with a nucleic acid substrate. On comparison of an RT-dsDNA with an RT-NNRTI complex, it is found that NNRTI binding affects the structural elements of the enzyme, which are in contact with the DNA and the incoming dNTP [27].

Comparison of the apo and NNRTI-bound structures of RT demarcates the conformational changes involved in formation of the NNIBP. The NNRTIs achieve specificity by mimicking the protein-protein interaction that stabilizes the inactive p51 structure, thereby deforming the polymerase active site via movement of the functional aspartates. Hence this structurally diverse group of molecules attains specificity and possesses a common mechanism of inhibition of HIV-1 RT [28].

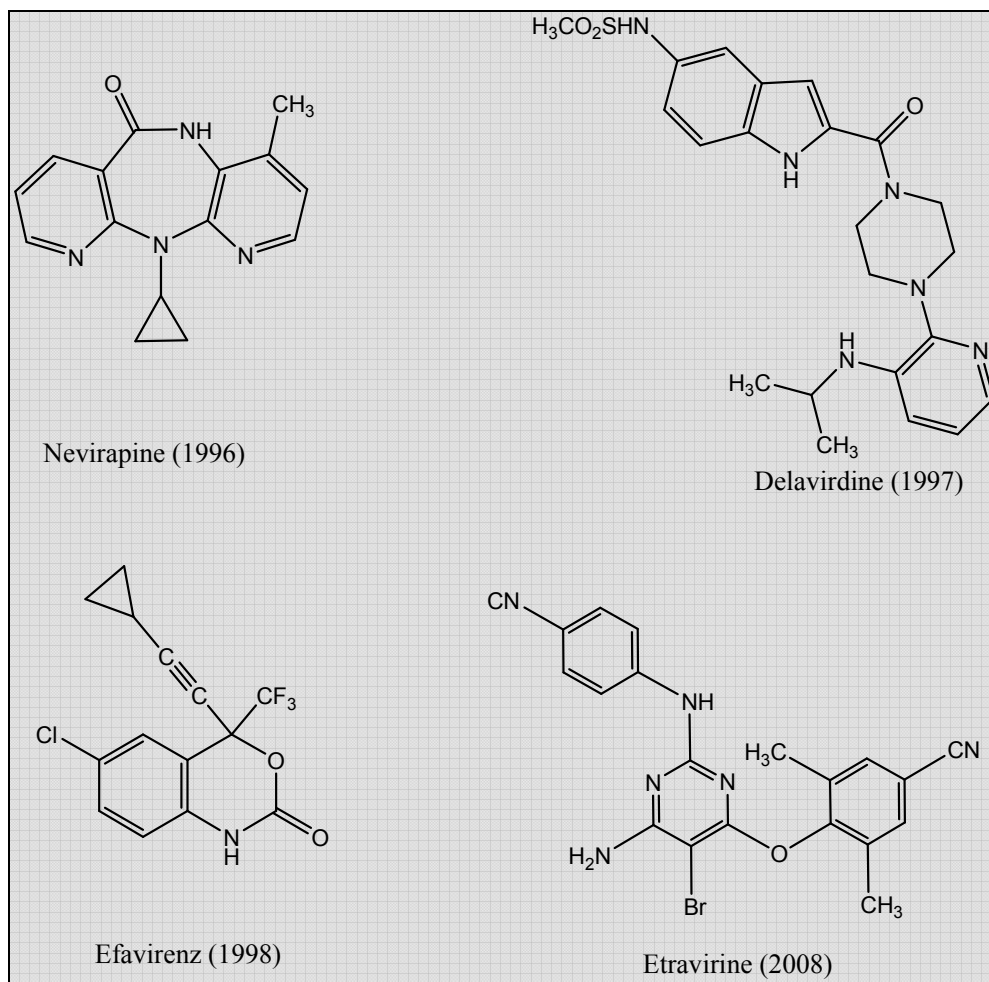


Fig 1.4: Chemical structures of USFDA approved NNRTIs; in parentheses year of approval

The NNRTIs came into vogue about a decade ago with the discovery of 1-[(2-hydroxyethoxy)methyl]-6-(phenylsulfanyl)thymine (HEPT)[29-31] and 4,5,6,7-tetrahydroimidazo[4,5,1-jk][1,4]benzodiazepin-2(1H) one and -thione (TIBO)[29] as specific HIV-1 inhibitor, targeted at HIV-1 RT. Following HEPT and TIBO, nevirapine, pyridinone, bis(heteroaryl)piperazine (BHAP) [32], 2', 5'-bis-O-(*tert*-butyldimethylsilyl)-3'-spiro-5''-amino-1'', 2''-oxathiole-2'', 2''-dioxide pyrimidine analogues (TSAO) [33], α -anilinophenyl acetamides [α -APA (R89439)] [34], PETT (LY 300046) [29,31], 3,4-

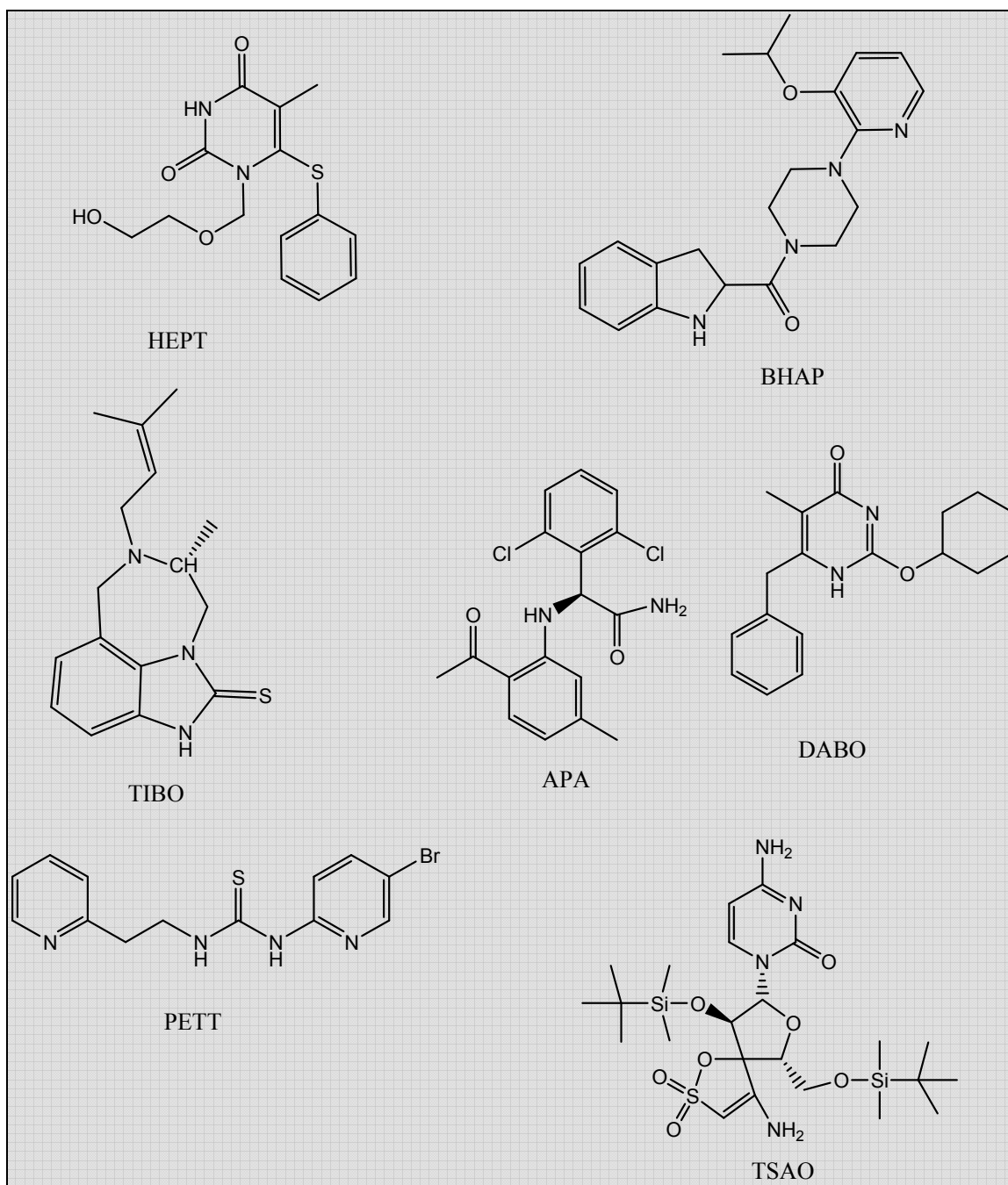


Fig 1.5: NNRTIs in research

dihydro-2- alkoxy-6-benzyl-4-oxopyrimidines (DABOs)[29,31] and various other compounds were identified as specific HIV-1 RT inhibitors.

1.6 Limitations of HAART

Though HAART is efficacious in lowering plasma viral load and also in protracting the life span of HIV-infected patients, it suffers from two major setbacks of toxicity and non-compliance. Since HAART involves a multi-drug regimen comprising of two NRTIs and one PI or NNRTI, it inevitably leads to shared toxicity due to metabolic and pharmacokinetic interferences. The high-pill burden and obligation to a lifetime therapy, associated with HAART has a profound psychological impact on the psyche of the patient, which leads to non-adherence and treatment discontinuation. Multiple side effects occur as a consequence of HAART, which is also one of the causes for HAART discontinuation. The most common but minor side-effects are fatigue, nausea and fever; but the severe ones are hepatotoxicity, hyperglycemia, hyperlipidemia, lactic acidosis, and osteoporosis [14]. Due to HAART, alterations in plasma cholesterol and triglyceride levels have been detected [35]. Some patients also tend to suffer from immune restoration inflammatory syndrome (IRIS) and neurological immune restoration inflammatory syndrome (NIRIS), following HAART [36].

1.7 Tuberculosis, an opportunistic infection associated with AIDS

Following HIV assault, the count of T-lymphocytes, which confer resistance against various viral, bacterial and fungal infections, dwindle and hence the body's immunological protective mechanism is compromised, thereby subjecting the patients to various opportunistic infections, the most rampant and grave of which is tuberculosis (TB). TB is one of the foremost causes of morbidity and death globally, particularly in Asia and Africa. There were an estimated 9.2 new million cases of TB in 2006, in comparison to 9.1 million cases of 2005. India ranks first in terms of absolute number of TB cases [37]. The pathogen, *Mycobacterium tuberculosis* (MTB), the causative agent of TB, is a facultative intracellular parasite that infects the alveolar macrophages, subsequent to aerosol transmission. This bacillus is non-motile and is incapable of surviving in an extracellular environment in the infected host. In order to disseminate infection, it first enters as air-borne particles into alveolar macrophages, which engulf these particles fervently with the aid of a plethora of phagocytic receptors. The cardinal criterion to the virulence of MTB is by virtue of its ability to prevent the fusion of its phagosome with host lysosome, inside which it replicates and can persist in a dormant state for many years [38]. The virulent MTB prevents the apoptosis of the host macrophages, inside which it proliferates to a

very high intracellular bacterial load, which then triggers necrotic macrophage cell death, leading to release of the new bacilli. These new bacilli then further infect new host macrophage cells [38].

1.8 HIV-TB dual pandemic

The 2008 WHO report on Tuberculosis (TB), states that 0.7 million cases of HIV-TB co-infection were reported in 2006 and an estimate of 0.2 million of the global populace died due to HIV-TB co-infection [37]. In developing countries, the foremost cause of mortality in HIV-positive patients is TB, which accounts for almost 13% of the death toll [39]. In India, a wide deviation was found in the cases of HIV seroprevalence in TB cases from 0.4 % in Delhi to 28.75 % in Pune [40].

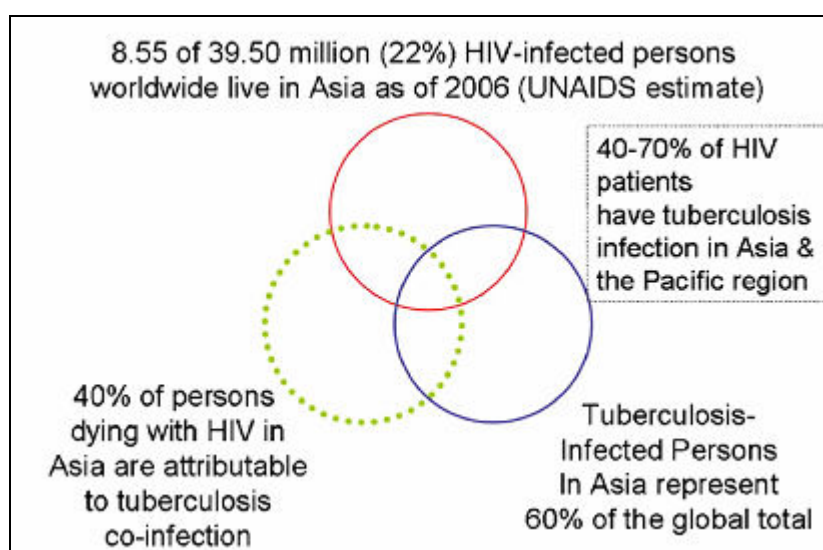


Fig 1.6: Prevalence of HIV-TB co-infection in Asia [39]

TB and HIV have a harmonized effect on the progression of each other and hence become a lethal threat to the patient. In HIV patients the low levels of T lymphocytes makes the patient more predisposed to mycobacterial diseases. *Mycobacterium tuberculosis* (MTB) in return up-regulates the replication of HIV by a probabilistic mechanism involving induction of macrophages to produce excess interleukins and tumor necrosis factors [41-43].

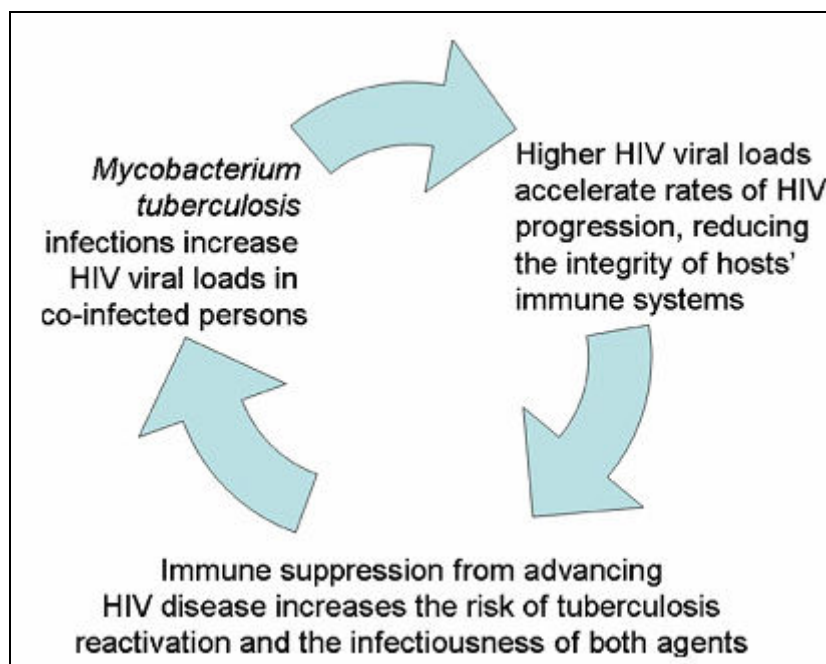


Fig 1.7: Mutual interaction between HIV & TB

MTB promotes HIV replication by increasing HIV long terminal repeat (LTR)-driven transcription in rapidly transfected CD4⁺-T cells. MTB also increases the secretion of pro-inflammatory cytokines which thereby up-regulate HIV replication [42, 44]. It was also observed that the surface expression of CXCR4 receptor is increased in HIV patients co-infected with MTB [45]. In TB, pleural fluids possess a very high content of cytokines, namely interleukin-2 (IL-2), tumor necrosis factor- α (TNF- α) and IL-6 in the milieu, stimulates HIV replication [41], thereby initiating life-threatening immunosuppression.

HIV complicates TB infection by escalating the risk of reactivating latent TB and also HIV patients who contract new TB infection have a more rapid disease progression rate [46]. Also following the initiation of ART in TB patients a contradictory aggravation of tuberculous lesions has frequently been observed [47].

Patients suffering from HIV-TB co-infection are currently being treated with a combination therapy involving non-nucleoside reverse transcriptase inhibitors viz. efavirenz, nevirapine, delaviridine and viral protease inhibitors viz. nelfinavir, ritonavir, saquinavir, to tackle the retrovirus and a combination regimen comprising of rifampicin (RIF), isoniazid (INH), ethambutol and pyrazinamide to combat the tubercle bacilli. Since this therapy involves a very high pill burden, it lessens patient compliance. The patients being treated with

combination anti-retroviral and anti-tubercular regimens are confronted with grave outcomes due to drug-drug and drug-disease interactions [48]. Administration of anti-retroviral and anti-tubercular drugs in parallel leads to various adverse effects viz. nausea, gastrointestinal tract disturbance, peripheral neuropathy, cutaneous reactions, renal and potentially fatal hepatotoxicity [49]. In TB-HIV co-therapy, many significant pharmacokinetic drug interactions arise, which leads to withdrawal from therapy. Many anti-TB drugs, specifically rifampicin, induce a multitude of metabolic enzymes namely; cytochrome P450s and p-glycoprotein; which therefore cause a reduction in the plasma levels of NNRTIs and PIs [50]. Majority of the PIs are contraindicated with rifampicin [51].

HIV-TB co-infected patients on HAART also tend to develop an immune reconstitution inflammatory syndrome (IRIS), which leads to worsening of tuberculous symptoms viz. aggravation of pulmonary infiltrates, pleural effusions, lymphadenitis and a highly critical neurological tuberculomata [47, 48]. The coupled effect of HIV-induced immunosuppression and HIV-TB drug side-effects also give rise to multiple pathologies of many vital organs, especially liver [48].

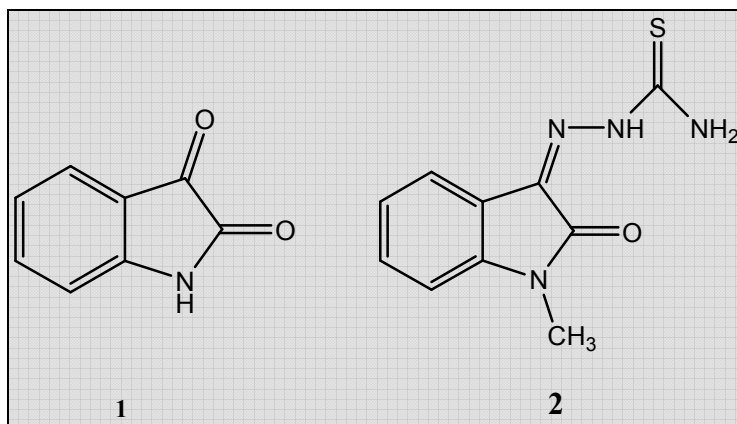
CHAPTER 2

LITERATURE REVIEW

Isatin (**1**) or indoline-2, 3-dione is a natural product found in various plants belonging to the genus *Isatis* [52]. It was also obtained as a metabolic derivative of adrenaline in humans [53]. Isatin and its various derivatives have been found to possess a multitude of biological activity against numerous viruses, bacteria, fungi and protozoa.

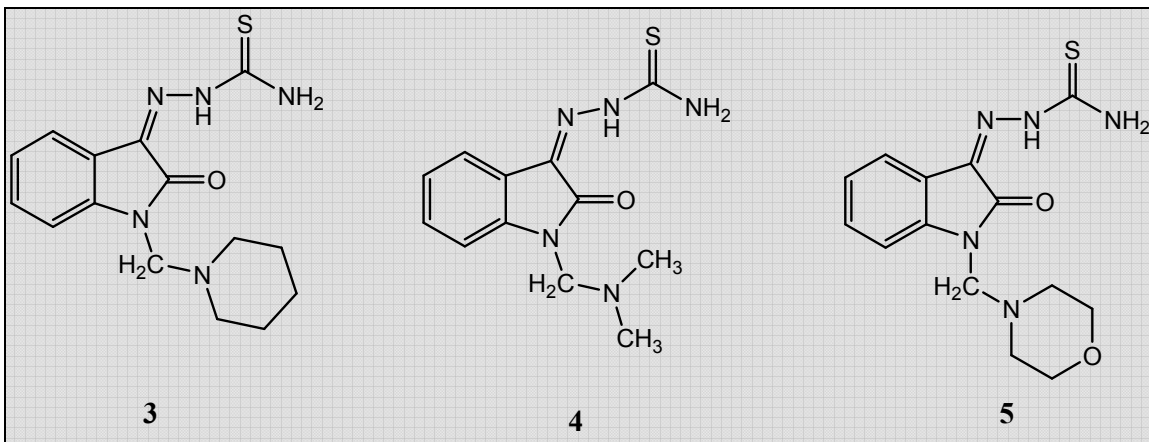
2.1 Isatin analogues as anti-viral agents

Isatin analogues have been in use as anti-viral agents since the past four decades. Methisazone ([[(1-methyl-2-oxoindol-3-ylidene)amino]thiourea) (**2**) an isatin analogue, is a drug that is in clinical use as a prophylactic as well as a therapeutic agent for viral diseases [54]. It exerts its antiviral action probably through inhibition of viral DNA polymerase, which is needed for replication; inhibition of viral penetration and by preventing viral assembly.

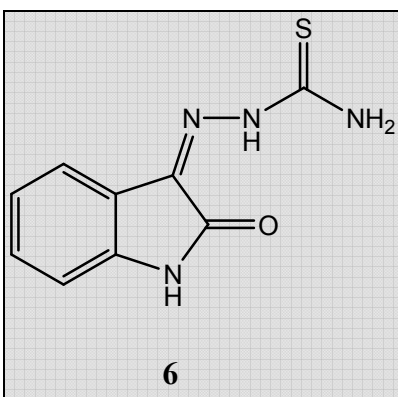


In 1967, the duo of Varma and Nobles, reported the activity of various N-dialkyldiaminomethyl derivatives (**3**, **4** and **5**) of isatin- β -thiosemicarbazone against replication of polio virus type II (RNA type) and parainfluenza3 (RNA type) virus. Compounds **3** and **5** were capable of inhibiting polio virus but were ineffective against

parainfluenza virus; whereas compound **3** was inactive against both polio and parainfluenza virus replication [55].



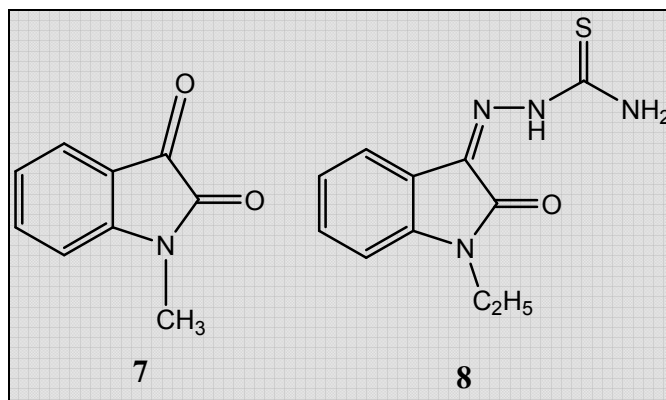
Isatin- β -thiosemicarbazone (IBT) (**6**) was found to inhibit the maturation of vaccinia virus. Woodson et al. investigated the prime core of action at which compound **6** inhibits the formation of mature vaccinia virion.



Their findings suggested that compound **6** do not interfere with viral DNA synthesis or mRNA synthesis; nor does it hinder the functioning of viral mRNA encoded from parental genome. But in the presence of compound **6**, the sedimentation coefficient of mRNA, synthesized after the first three hours of infection decreases; thereby diminishing the functional half-life of these viral mRNA from 30-40 minutes to less than 5 minutes. This in turn leads to a reduction in polyribosome formation and therefore cessation of translation of functional proteins [56].

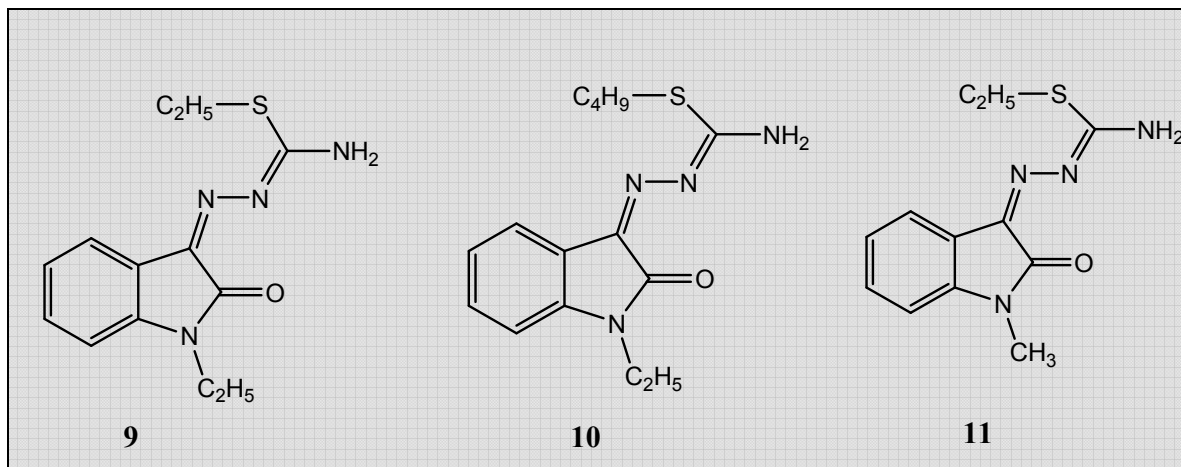
Compound **2** also displayed promising inhibitory activity against pox virus, smallpox virus, arbovirus, reovirus, myxo- and para-myxoviruses [57-61].

The RNA-dependent DNA polymerase of Rous sarcoma virus (RSV) as well as its transforming potential was also found to be inhibited by compound **2**. In the presence of cupric ions (Cu^{++}), compound **2** was more effective in inhibiting the action of DNA polymerase. Levinson et al. demonstrated that when compound **2** was used alone the activity of RNA-dependent DNA polymerase was 42% and RSV's transforming ability was 50%; whereas when used in combination with copper sulfate the activity of the polymerase as well as the transforming capability plummeted drastically to 1%. Levinson hypothesized that this synergism could be due to the chelating nature of thiosemicarbazones; whereby the active molecule is a copper complex of compound **2**. The activity of compound **2** can be attributed to the thiosemicarbazone moiety since N-methyl isatin (**7**) when used alone was ineffectual in hindering the DNA polymerase and also transformation of RSV [62].



In another study, N-methyl (**2**) and N-ethyl isatin-β-thiosemicarbazones (**8**) were found to inactivate various strains of arenaviruses viz. Parana and Pichinde viruses as well as three different strains of lymphocytic choriomeningitis virus. Concomitant addition of 20 μM of CuSO_4 along with 20 μM of compounds **2** or **8** lead to 94% and 96% loss of infectivity of arenavirus after being exposed for 30 min. After 2 h, the virus lost 99.75% of its infectivity when in contact with compound **2** and 99.85% after exposure to compound **8** [63].

Another study reported about the inhibition of [³H]uridine incorporation by three isatinisothiosemicarbazones into mengoviral RNA by restricting uridine transport. 1-Ethylisatin-S-ethyl-isothiosemicarbazone (**9**), 1-ethylisatin-S-*n*-butyl-isothiosemicarbazone (**10**) and 1-methyl-isatin-S-ethyl-isothiosemicarbazone (**11**) at the concentration levels of 70 μmol, 30 μmol and 200 μmol respectively displayed specific inhibition of mengoviral RNA synthesis of 98.5 %, 99.3% and 98.2% respectively [64].



Francis and Bradford reported the inhibitory property of compound **2** against two different strains of *Molluscum contagiosum* virus (MCV) in FL cell culture. At 2 μg/ml and 5 μg/ml concentration levels, compound **2** failed to show any decrease in the plaque forming units/ml (pfu/ml), probably since it was unable to inhibit the DNA synthesis [65].

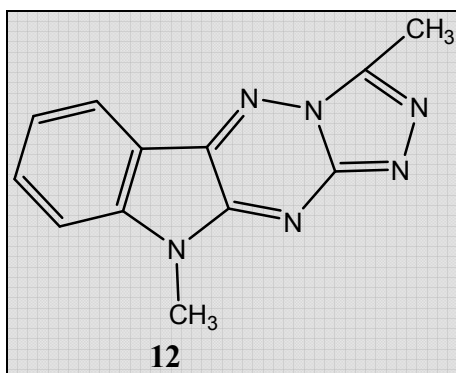
Enteroviruses belonging to the group *Picornaviridae*, are common cause of many infections in humans especially children. Protease 3C is a vital enzyme required for polyprotein processing and due to its unique folding character it differs widely from cellular proteases; thereby making it an attractive target for antiviral drugs. Isatin (**1**) also displays superlative binding ability for the pocket of protease 3C of enteroviruses [66].

Equine abortion virus (EAV), a DNA-containing virus, is a member of the herpes virus and it produces a lethal infection in hamsters. When compound **8** was tested at 60

mg/kg body weight of hamsters by subcutaneous route, it proved ineffective in protecting them from EAV [67].

The ability of compounds **2**, **7** and **8** to inhibit various strains of herpes simplex virus (HSV), causing infection in rabbit eye, was investigated by Levinson et al. Compound **2** showed considerably good capability in inactivating the infectivity of herpes simplex virus, by a probabilistic mechanism where the drug binds to herpes virus DNA within the virion, thereby impeding with the intracellular replicative steps. Compound **2** was found to inactivate strains of both type 1 and type 2 HSV, including a strain of HSV type 2 which is responsible for transforming hamster cells *in vitro*; but it was found to be ineffective in preventing the viral cytopathic effect when added to the cell after infection. At 40 μM concentration level, compounds **2** and **8** displayed 99% inhibition of plaque formation by herpes simplex virus; while compound **7** showed nil inhibition [68].

In another study a structural analogue of isatin- β -thiosemicarbazone, (3,10-dimethyl-10-H-s-triazolo[4',3':2,3]-as-triazino-[5,6-b]indole) (**12**) was investigated for its activity against two strains of herpes simplex virus.

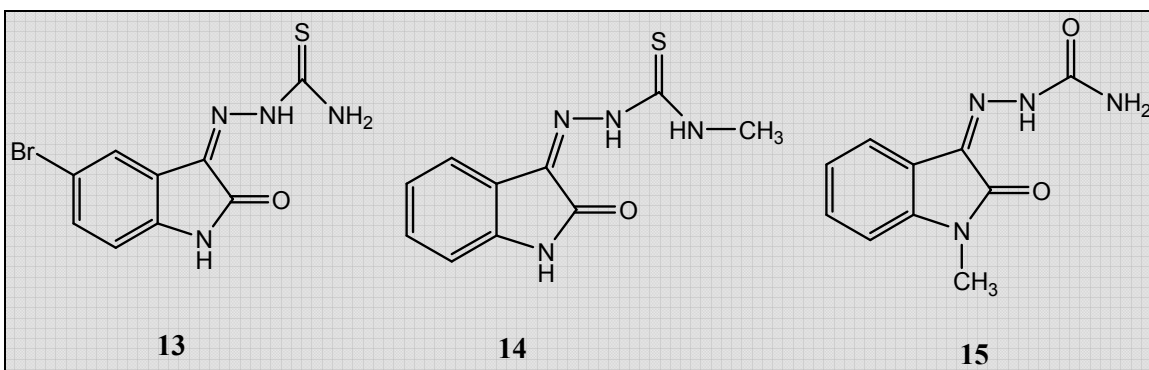


HSV-1 and HSV-2 were grown in BSC1 and BGM, two African green monkey cell lines in M199 medium and RPMI medium supplemented with fetal calf serum (FCS). When compound **12** was added at 60 $\mu\text{g/ml}$, the growth of HSV-1 was inhibited almost 70 fold. Compound **12**, when added in concentration lower than 10 $\mu\text{g/ml}$, was found to be ineffectual in inhibiting HSV. HSV-2 was found to be more susceptible than HSV-1 to

this compound. While analyzing the antiviral activity of compound **12** against HSV, it was observed that it successfully suppressed HSV DNA synthesis and also inhibited viral particle formation. However viral polypeptide synthesis was almost unaltered. These results hint that the mechanism of action of compound **12** is possibly different from that of compound **6** [69].

In a study by Katz et al. it was revealed that isatin- β -thiosemicarbazone (IBT) (**6**) is essential for the growth of IBT-dependent mutant vaccinia virus. Compound **6** is not needed for the synthesis of viral DNA but the formed DNA does not become resistant to deoxyribonuclease in its absence. The need for IBT by the IBT-dependent mutant vaccinia brought up the issue as to whether it is needed by the same stage of viral replication, which is inhibited in the wild type strain. In absence of compound **6**, in case of IBT-mutant strain it was observed that formation of vaccinia virus core polypeptide from its precursor was inhibited; whereas in case of the wild type strain this process was unaffected in presence of compound **6** [70].

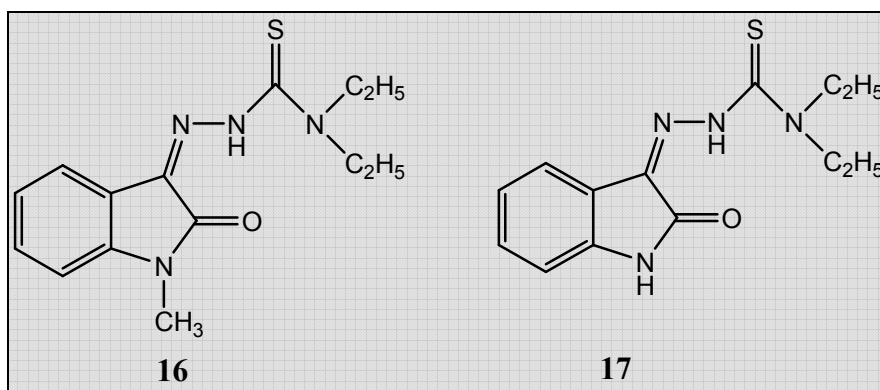
Another study by Katz et al. investigated the ability of four IBT-related compounds to inhibit wild-type and IBT-resistant mutants and their ability to support the growth of an IBT-dependent mutant.



The four analogues were IBT (**6**), 5-bromoisatin-3-semicarbazone (**13**), isatin-4'-methyl-3-thiosemicarbazone (**14**) and 1-methylisatin-3-semicarbazone (**15**). Amongst these compounds **6** and **13** were found to inhibit the growth of wild type vaccinia strain at a concentration of 14 μ M, and were ineffective against plaque formation of IBT-resistant

strain and supported the growth of IBT-dependent strain. Compounds **14** and **15** were unable to curb the growth of wild type strain; but also failed to support the growth of IBT-dependent vaccinia strain [71].

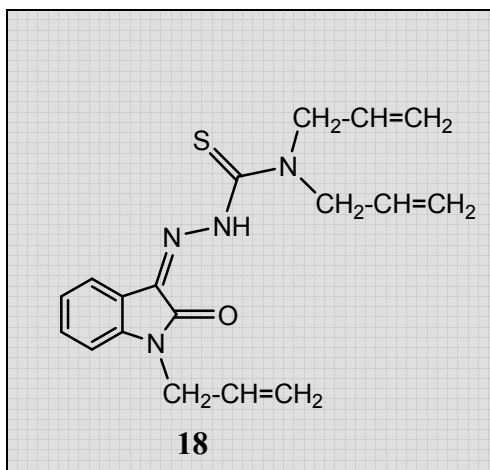
N-methylisatin- β -4', 4'-diethylthiosemicarbazone (**16**) demonstrated excellent inhibition of Moloney leukemia virus (MLV) production in contrast to N-methylisatin- β -thiosemicarbazone (**2**) and isatin- β -4',4'-diethylthiosemicarbazone (**17**). The effective drug concentrations ranged between 3.4 μ M and 34 μ M. But this drug failed to block viral reverse transcriptase activity even at very high concentrations. Compound **2** failed to inhibit MLV production but compounds **16** and **17** were able to inhibit virus production at 17 μ M. When compared to other antimetabolites viz. actinomycin D, cycloheximide and α -amanitin, in terms of the amount of MLV released into the culture medium within 6 hours of infection compound **16** was found to possess comparable activity. Compound **16** was found to exhibit reversible inhibition of cellular DNA synthesis [72].



The addition of dialkyl moieties to the terminal nitrogen of thiosemicarbazone endows these compounds with a broad spectrum of activity against both DNA and RNA containing viruses. Compound **16** targets the inhibition of synthesis of structural proteins of MLV. In the presence of compound **16** the precursor for the viral glycoprotein gp-70 was drastically reduced along with a drastic reduction in the formation of the *gag*-polypeptide precursor. Compound **16** was also found to interfere with protein translation of viral mRNA by cellular ribosomes [73].

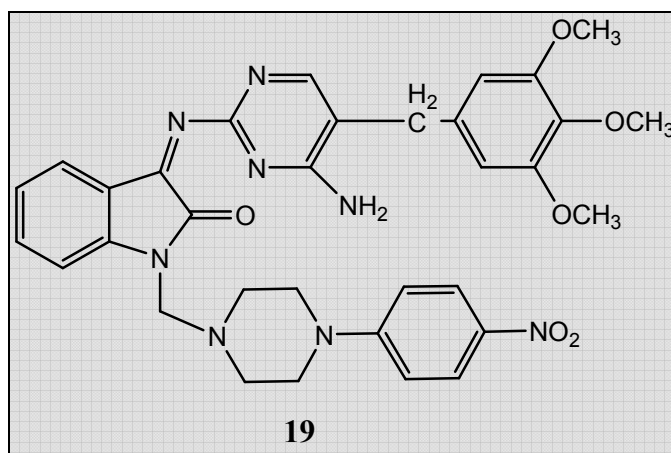
Ronen et al. probed the mode of inhibition of MLV production by compound **16**. An investigation of the effect of compound **16** on polysomes involved in translation of viral proteins showed a four-fold accumulation of polysomal virus-specific RNA in drug-treated cells. Thus this group proved that compound **16** exerts its antiviral activity on MLV by inhibiting translation of viral RNA rather than interfering with RNA transcription [74].

Teitz et al. explored the effect of compound **16** and N-allylisatin- β -4',4'-diallylthiosemicarbazone (**18**) on the production of viral transduced oncogene, *v-abl* protein of Abelson murine leukemia virus. *v-abl* is also associated with tyrosine kinase activity. Tyrosine kinase activity was appreciably decreased by compound **16** at concentrations ranging between 0.17 and 0.64 μ M and by compound **18** at concentrations ranging between 1.45 to 2.9 μ M. 0.64 μ M and 2.9 μ M of compounds **16** and **18** respectively completely impeded *V-abl* synthesis [75].



Methisazone (**2**) was tested for its ability to block the replication of foot-and-mouth-disease virus (FMDV). When administered singly it failed to inhibit FMDV replication; but when administered along with Cu^{2+} at 200 μ M and 250 μ M dose levels respectively in a contact inactivation study for 4 h at 37°C, they together reduced the infectivity of FMDV by about 0.5 log unit [76].

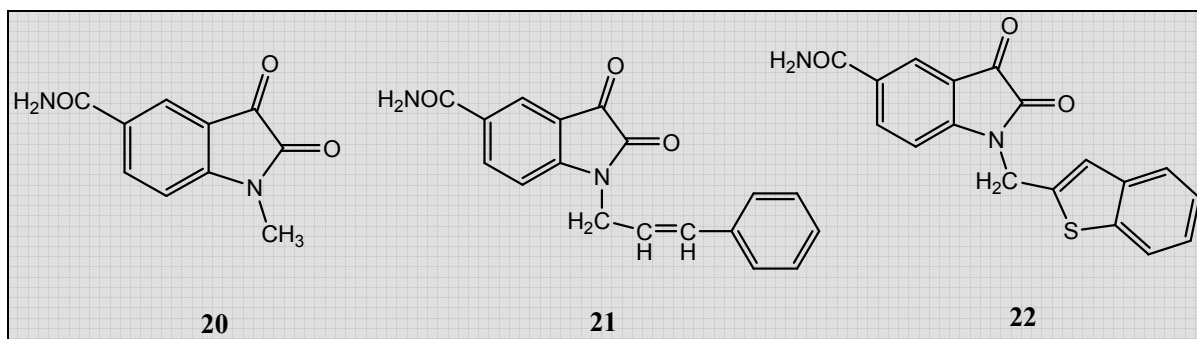
Several N-Mannich bases of N-methylisatin- β -thiosemicarbazone were tested for their activity against replication of Japanese encephalitis virus (JEV). Out of those (Z)-3-(4-amino-5-(3,4,5-trimethoxybenzyl)pyrimidin-2-ylimino)-1-((4-(4-nitrophenyl)piperazin-1-yl)methyl)indolin-2-one (**19**) displayed promising activity against flaviviral replication.



Compound **19** completely inhibited JEV as well as West Nile virus replication *in vitro*. Further compound **19** also totally inhibited JEV replication *in vivo* in a murine model challenged peripherally with 50 LD₅₀ of the virus in a dose-dependent manner. *In vitro* when compound **19** was added at a concentration of 76 $\mu\text{g/ml}$, in infected monolayers of PS cell lines at 2, 4, 6 and 8 h post-infection, it totally inhibited the replication of JEV, which was substantiated by the absence of viral antigens, viral RNA and inhibition of virus yield [77].

Human rhinoviruses (HRV) are the chief etiologic agents of common cold and they are small icosahedral RNA viruses belonging to the picornaviridae family [78]. In humans the primary locus of HRV infection and replication is nasal epithelium. Following binding to cell surface receptors the viral genome gets uncoated and is translated by the host cell machinery. The open reading frame codes for a precursor polyprotein, which is further processed by 3C protease, a cysteine protease, to yield many structural and functional proteins needed for viral replication. 3C protease is a cysteine protease with a trypsin-like polypeptide fold [79, 80]. In a quest to discover novel

nonpeptidic 3CP inhibitors of HRV, Webber et al. designed and synthesized a series of novel isatin analogues.



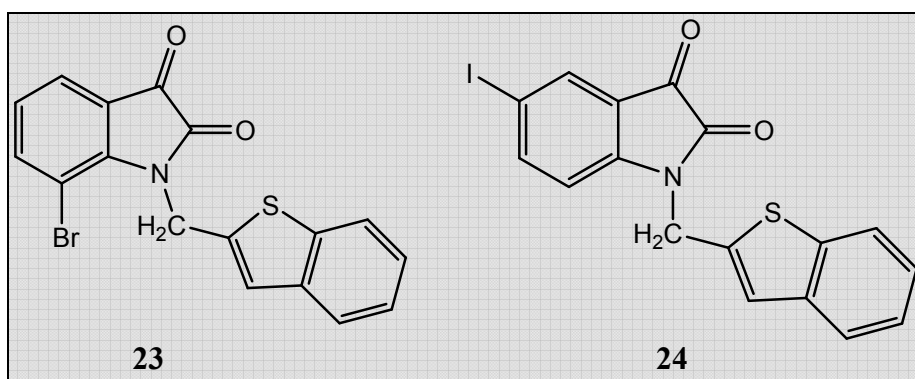
Amongst the entire battery of twenty-seven compounds that were synthesized and tested against HRV, 1-methyl-2,3-dioxindoline-5-carboxamide (**20**), 1-cinnamyl-2,3-dioxindoline-5-carboxamide (**21**) and 1-((benzo[b]thiophen-2-yl)methyl)-2,3-dioxindoline-5-carboxamide (**22**) displayed a 3CP enzyme inhibition value of 0.051, 0.011 and 0.002 μM respectively. All three of these compounds, viz. **20**, **21** and **22** were found to have exceptional selectivity for rhinoviral 3CP in comparison to other cellular proteases. Analogues **20** and **22** were found to be effective against 3CP of various serotypes of rhinovirus. In all these molecules the carboxamide moiety at C5, forms H-bonds to the imidazole of His-161 and the hydroxyl and the α -carbonyl of Thr-142. The C-2 carbonyl of isatin was envisaged to react in the active site of HRV 3CP with the cysteine responsible for catalytic proteolysis [80].

But in another effort undertaken by the same research group, compound **22**, which was earlier observed to have covalent attachment of Cys-147 to the electrophilic center of 3CP with the carboxamide and benzothiophene positioned in the S1 and S2 specificity pockets of 3CP; was found to possess greater toxicity profile due to their electrophilic feature [79].

Severe acute respiratory syndrome (SARS), a viral atypical pneumonia is caused by the human coronavirus, named as SARS coronavirus (SARS CoV) [81]. SARS CoV-3C like protease (SARS CoV 3CL) has significant implications in the viral life cycle and

hence has been targeted for developing novel inhibitors as a chemoprophylactic in SARS infection [82].

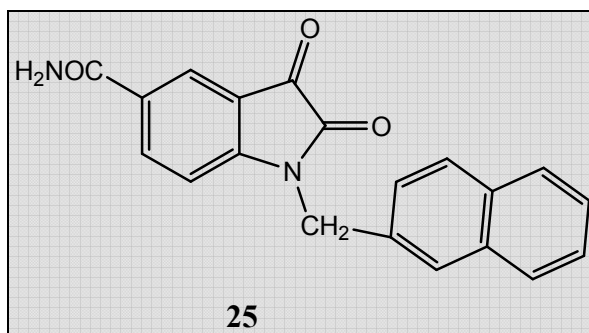
An array of twenty-six novel molecules with isatin scaffold was designed and synthesized with the motive to target them as SARS CoV 3CL inhibitors. All these derivatives inhibited SARS CoV 3CL with IC_{50} values lying in the range between 0.95 to 17.50 μM . Amongst these, two of them namely, 1-((benzo[b]thiophen-2-yl)methyl)-7-bromoindoline-2,3-dione (**23**) and 1-((benzo[b]thiophen-2-yl)methyl)-5-iodoindoline-2,3-dione (**24**), displayed promising SARS CoV 3CL inhibition with IC_{50} values of 0.98 μM and 0.95 μM respectively.



In terms of selectivity towards various proteases these two analogues were found to be highly selective for SARS CoV 3CL than other proteases like trypsin and papain. But comparison between the two revealed that compound **24** is more selective than compound **23** towards SARS CoV 3CL. Computational studies of this series revealed that the isatin moiety was docked in the S_1 site of the protease whereas the side chain at N-1 was docked into the S_2 site. The carbonyl group of isatin was hydrogen bonded to the NH group of Cys 145, Ser 144 and Gly 43 of the protease. Compounds with bulky groups at N-1 of isatin showed less inhibition of the enzyme. At C7 of isatin, non-polar and electron-withdrawing groups afforded the compounds with higher inhibitory potency than the ones with amino group [83].

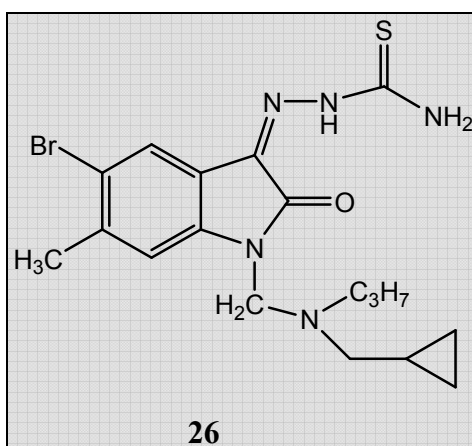
Another study performed by a research group in Peking University, China investigated the inhibitory potency of novel isatin analogues as SARS CoV 3CL inhibitors. Twenty-three compounds were synthesized and evaluated for their anti-SARS CoV 3CL protease activity, out of which eight of them had IC_{50} value below 100 μM . 1-

((naphthalen-2-yl)methyl)-2,3-dioxindoline-5-carboxamide (**25**) demonstrated the highest inactivation of the protease of SARS with an IC_{50} value of $0.37 \mu M$.



Compound **25** also exhibited high selectivity for SARS CoV 3CL protease in comparison to other proteases viz. papain (30 times), trypsin (92 times) and chymotrypsin (950 times). These analogues were found to bind non-covalently to SARS CoV 3CL protease. The isatin C-5 was found to favor carboxamide group and the N-1 position preferred large hydrophobic substituents in order to effectively inhibit the SARS protease [82].

A recent study by Pirrung et al. reported the solid-phase synthesis of libraries of isatin thiosemicarbazones, which were then screened for their anti-pox viral activity using a cell-based assay technique.

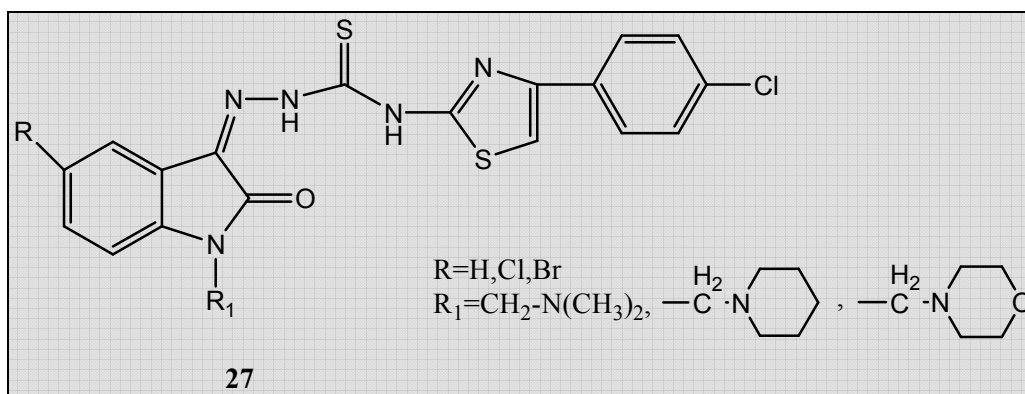


The compound with maximum anti-pox virus potential from amongst the pool of compounds generated was compound **26**. When investigated for its ability to inhibit plaque formation by vaccinia virus and cowpox virus in HFF cell lines, compound **26**

inhibited vaccinia virus plaque formation with an EC_{50} value of $0.6 \mu\text{M}$ and selectivity index of 302; and in case of cowpox virus it had an EC_{50} value of $6.0 \mu\text{M}$ and selectivity index of 30. This derivative was 30-fold more potent and more selective than cidofovir, a drug used in prophylaxis of pox infection [84].

Teitz et al. explored the prospect of *N*-methylisatin- β -4':4'-diethylthiosemicarbazone (**16**) and *N*-allylisatin- β -4',4'-diallylthiosemicarbazone (**18**) as effective anti-retroviral agents by evaluating them for their capability to inhibit HIV replication. Compound **16** was effective in the concentration range of $0.17 \mu\text{M}$ to $2.04 \mu\text{M}$ and compound **18** showed its inhibitory potency in the range of $1.45 \mu\text{M}$ to $17.4 \mu\text{M}$. On treatment of chronic infected HIV-1 cells with $0.34 \mu\text{M}$ of compound **16** and $2.9 \mu\text{M}$ of compound **18** for 48 h, 50% inhibition of virus yield was observed by the plaque forming unit assay method. Compounds **16** and **18** had therapeutic indices of 20 and 30 respectively. Both these molecules were also found to selectively inhibit the HIV structural proteins [85].

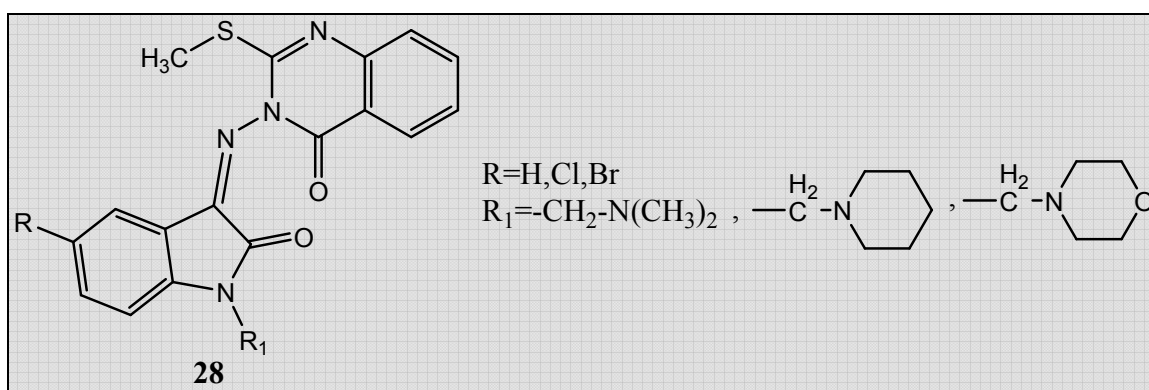
Isatin and its 5-substituted analogues were reacted with *N*-[4-(4-chlorophenyl)thiazol-2-yl]thiosemicarbazide to form the corresponding Schiff bases; which on further reaction with formaldehyde and three secondary amines yielded the respective *N*-Mannich bases, having the general structure as depicted in **27**.



These *N*-Mannich bases were subjected to anti-retroviral evaluation by an MTT assay based method; but were found to be ineffective due to their high toxicity which can

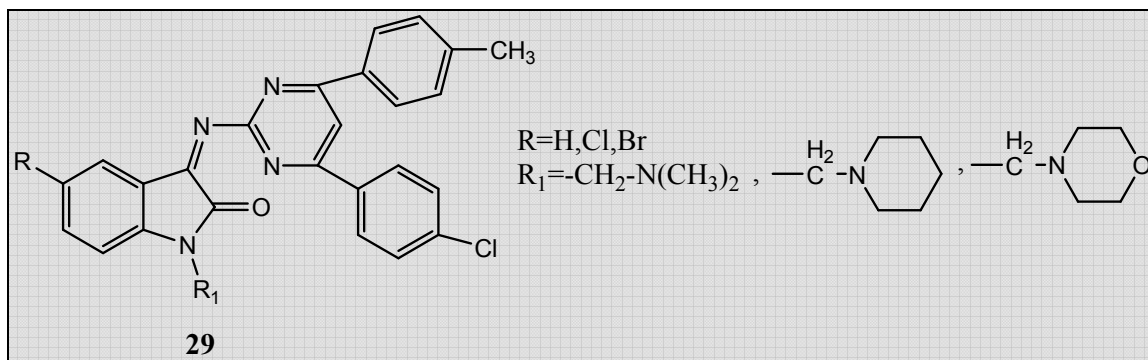
be attributed to the bulky *p*-chlorophenyl thiazolyl group at the thiosemicarbazide end [86].

Pandeya et al. investigated the effect of various isatin analogues on HIV-1 replication. These isatin derivatives were synthesized by reacting isatin and its 5-substituted analogues with 3-amino-2-methylmercaptoquinazolin-4(3H)-one to form the corresponding Schiff bases; which on further reaction with formaldehyde and three secondary amines yielded the respective *N*-Mannich bases, having the general structure as depicted in **28**.



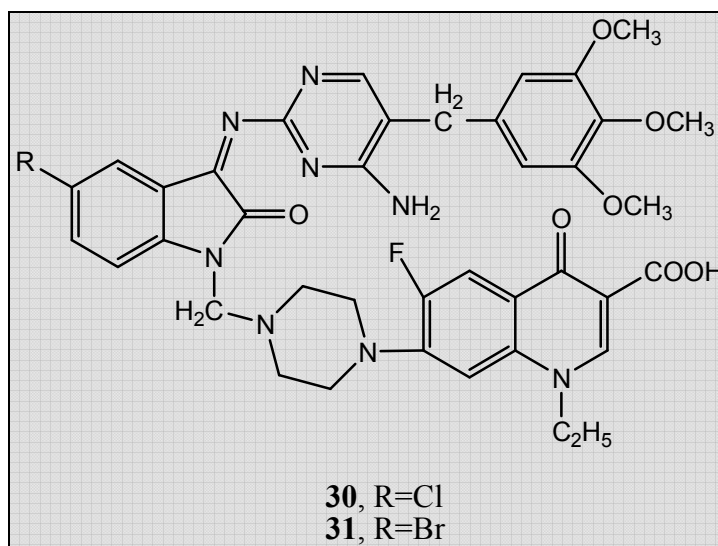
These compounds when evaluated for their inhibitory effect on HIV-1 replication in MT-4 cell lines did not display significant anti-retroviral activity owing to their high toxicity profile [87].

In another effort undertaken by Pandeya et al. Schiff bases of isatin and its 5-substituted derivatives were synthesized by reacting with 4-(4'-chlorophenyl)-6-(4'-methylphenyl)-2-aminopyrimidine which on reaction with formaldehyde and various secondary amines afforded the corresponding *N*-Mannich bases with the general structure as shown in **29**.



These analogues when evaluated for their potency to suppress HIV-1 replication were found to have very low selectivity indices; hence failed as effective anti-retroviral agents [88].

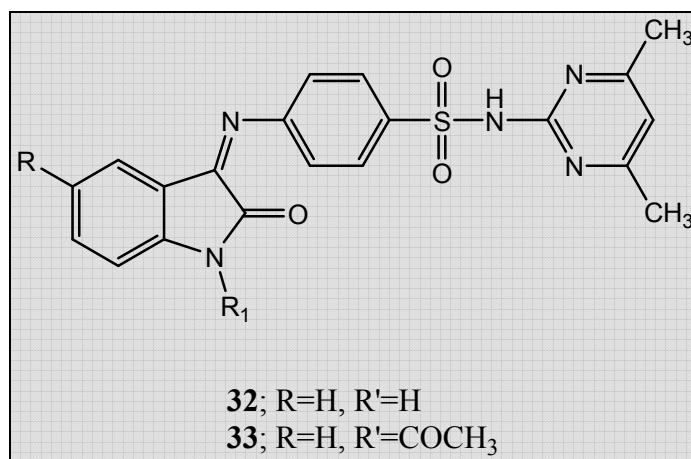
In another study, a series of norfloxacin Mannich bases of isatin were synthesized and evaluated for their HIV-1 replication inhibitory profile.



Amongst the entire series, only two analogues, 7-(4-(((Z)-3-(5-(3,4,5-trimethoxybenzyl)-4-aminopyrimidin-2-ylimino)-5-chloro-2-oxoindolin-1-yl)methyl)piperazin-1-yl)-1-ethyl-6-fluoro-1,4-dihydro-4-oxoquinoline-3-carboxylic acid (**30**) and 7-(4-(((Z)-3-(5-(3,4,5-trimethoxybenzyl)-4-aminopyrimidin-2-ylimino)-5-bromo-2-oxoindolin-1-yl)methyl)piperazin-1-yl)-1-ethyl-6-fluoro-1,4-dihydro-4-oxoquinoline-3-carboxylic acid (**31**) displayed prominent anti-retroviral activity when

tested in human MT-4 cell line with EC₅₀ of 11.3 and 13.9 µg/ml respectively and selectivity index above 5 [89].

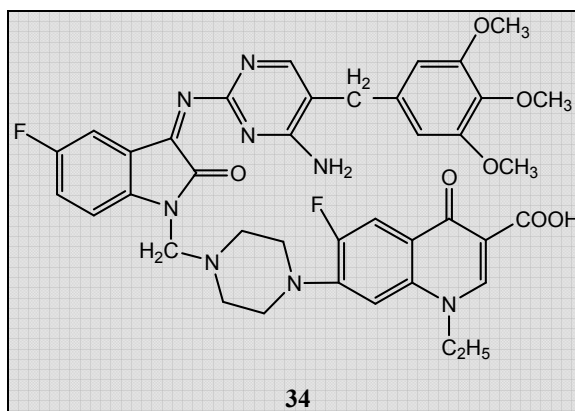
On reaction of isatin with sulfadimidine, a series of benzene sulfonamide analogues were obtained, which were put to test for their ability to prevent replication of HIV-1 (IIIB) and HIV-2 (ROD) strains in infected MT-4 cells.



Amongst the five compound subjected to anti-HIV evaluation, two of them namely, 4-[(1,2-Dihydro-2-oxo-3H-indol-3-ylidene)amino]-N-(4,6-dimethyl-2-pyrimidinyl)-benzenesulfonamide (**32**) and 4-[(1-Acetyl,1,2-dihydro-2-oxo-indol-3-ylidene) amino]-N-(4,6-dimethyl-2-pyrimidinyl) benzenesulfonamide (**33**) portrayed prominent inhibition of HIV replication. The EC₅₀ values of all the five compounds were found to lie in the range of 8.0 to 15.3 µg/ml for inhibition of HIV-1 replication; whereas for HIV-2 it was in the range of 41.5 to >125 µg/ml. In comparison the standard drug, azidothymidine had EC₅₀ values of 0.0012 µg/ml and 0.00062 µg/ml against HIV-1 and HIV-2 respectively. These analogues were far less cytotoxic in comparison to azidothymidine [90].

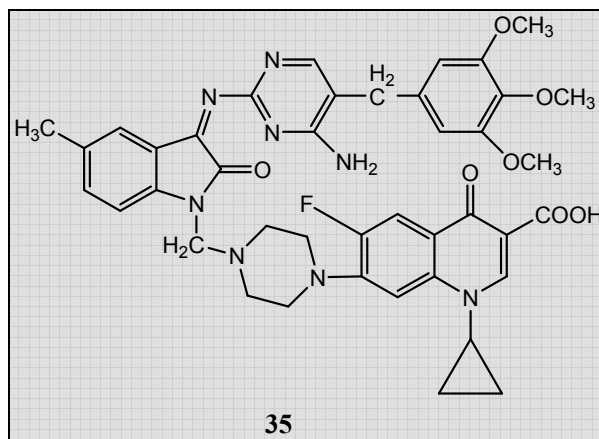
Sriram et al. investigated the inhibitory profile of various aminopyrimidinimino 5-fluoro isatin derivatives on HIV-1 replication in MT-4 and CEM cell lines. Amongst the fifteen compounds synthesized, 7-(4-(((Z)-3-(5-(3,4,5-trimethoxybenzyl)-4-aminopyrimidin-2-ylimino)-5-fluoro-2-oxoindolin-1-yl)methyl)piperazin-1-yl)-1-ethyl-6-fluoro-1,4-dihydro-4-oxoquinoline-3-carboxylic acid (**34**) showed maximum potential in

inhibiting HIV-1 replication with EC_{50} of 12.1 $\mu\text{g/ml}$ and selectivity index of 13 with maximum protection of 96.6%.



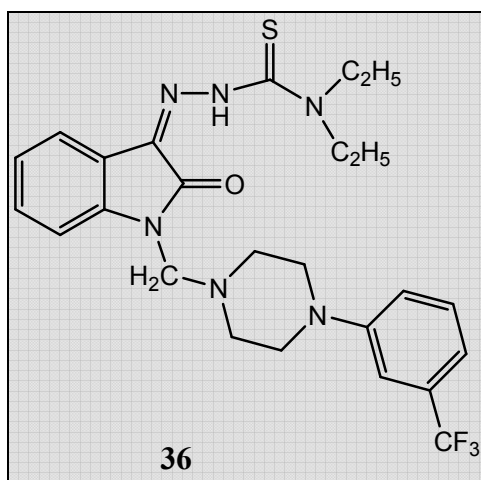
This compound was further evaluated for its capability to inhibit HIV-1 RT enzyme and it was found to possess an IC_{50} value of 32.6 μM [91].

In another effort to develop anti-retroviral isatin analogues, Sriram et al. synthesized a novel series of aminopyrimidinimino 5-methyl isatin analogues and evaluated these for their ability to inhibit HIV-1 replication in MT-4 and CEM cell lines. Four of the twelve synthesized compounds showed inhibition of HIV-1 replication in MT-4 cell line with their EC_{50} values lying in the range of 11.6 to 28.4 μM . 7-(4-(((Z)-3-(5-(3,4,5-trimethoxybenzyl)-4-aminopyrimidin-2-ylimino)-5-methyl-2-oxoindolin-1-yl)methyl)piperazin-1-yl)-1-cyclopropyl-6-fluoro-1,4-dihydro-4-oxoquinoline-3-carboxylic acid (**35**) exhibited the highest inhibition of HIV-1 replication in MT-4 and CEM cell lines with EC_{50} value of 11.6 μM and selectivity index greater than 7.



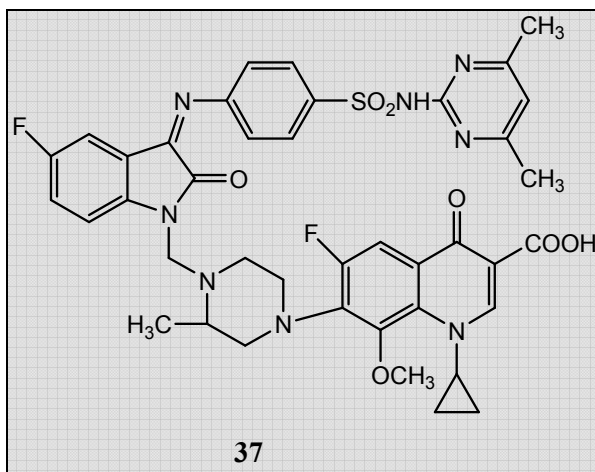
In CEM cell line compound **35** showed notable anti-HIV activity at a concentration much lower than its toxicity threshold. When further subjected to evaluation against HIV-1 RT, compound **35** was found to have an IC₅₀ value of 28.4 μM [92].

Novel isatin-thiosemicarbazone derivatives were synthesized and assessed for their ability to suppress HIV-1 replication in CEM cell line. Amongst the battery of nine compounds synthesized, three of them were able to suppress HIV-1 replication with EC₅₀ values in the range of 2.62 to 3.40 μM.



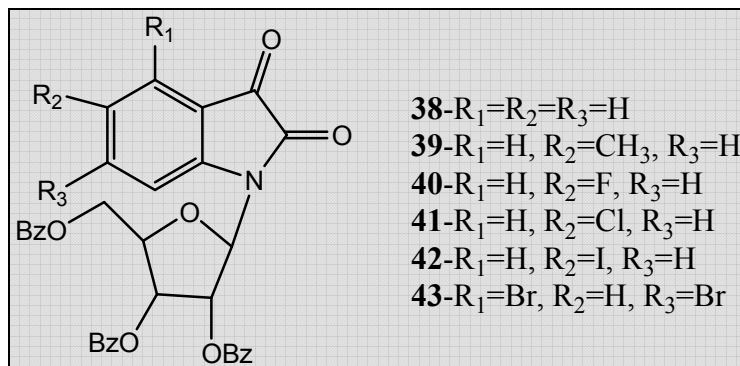
(Z)-4,4-diethyl-1-(1-((4-(3-(trifluoromethyl)phenyl)piperazin-1-yl)methyl)-2-oxoindolin-3-ylidene)thiosemicarbazide (**36**) was found to be the most active anti-retroviral agent in the entire series with an EC₅₀ value of 2.62 μM and selectivity index greater than 17 and CC₅₀ value of 44.90 μM [93].

A series of novel *N*-Mannich bases of 3-[[4,6-dimethylpyrimidin-2-yl)benzenesulfonamido-4'-yl]imino}-5-fluoro-1,3-dihydro-2H-indol-2-one were synthesized by reacting with formaldehyde and various aryl piperazines.



Amongst the twelve synthesized analogues, compound **37** was found to be the most potent in terms of inhibition of HIV-1 replication in MT-4 cell line with EC_{50} value of 12.1 $\mu\text{g/ml}$ and selectivity index greater than 13 [94].

In another endeavor undertaken by Oliviera et al. a series of novel isatin ribonucleosides (**38-43**) were synthesized employing a TMSOTf coupling reaction between the silylated isatins and 1-O-acetyl-2,3,5-tri-O-benzoyl- β -D-ribofuranose.

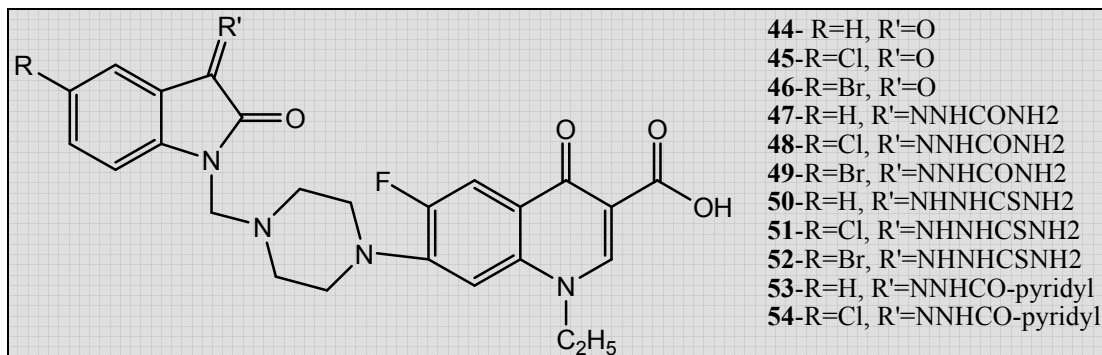


These analogues when tested for their ability to inhibit HSV replication proved effective by inhibiting 66% virus yield. 4,6-dibromo-2,3-dihydro-1-(2,3,5-tri-O-benzoyl- β -D-ribofuranosyl)indole-2,3-dione (**43**) proved most efficacious against HSV replication. But these agents failed to inhibit HIV-1 RT [95].

2.2 Isatin analogues as anti-tubercular agents

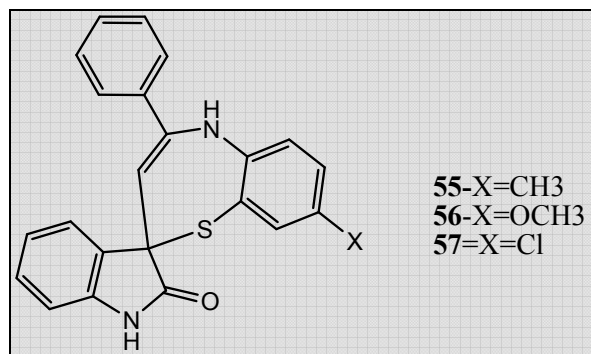
Isatin derivatives having established themselves as effective anti-microbial agents were also evaluated for their anti-tubercular potential.

A study by Pandeya et al. examined the anti-tubercular activity of various norfloxacin Mannich bases of isatin scaffolds, bearing isoniazid, semicarbazone or thiosemicarbazone moieties having the below mentioned general structure.



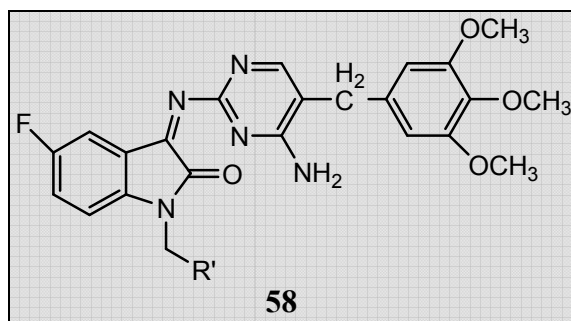
When subjected to evaluation against H37Rv strain of MTB these analogues showed activity with MIC values ranging from 6.25 $\mu\text{g/ml}$ to 12.5 $\mu\text{g/ml}$ and percentage inhibition ranging between 90 and 100%. Amongst the entire series, compound **53** displayed 100% inhibition of H37RV MTB with MIC less than 6.25 $\mu\text{g/ml}$ and compound **54** inhibited MTB up to 99% with MIC between 6.25 and 12.5 $\mu\text{g/ml}$; hence the isonicotinyl hydrazone derivatives of isatins were found to be most active anti-tubercular agents [96].

Various spiro [1,5]-benzothiazepin-2,3'[3'H]indol-2-[1'H]-ones were obtained by reacting various substituted aminobenzenethiols with 3-spiro-indolines and condensed indole derivatives having the general structure detailed below. These compounds when evaluated at a concentration of 12.5 $\mu\text{g/ml}$ for their ability to inhibit H37Rv MTB by BACTEC method showed inhibition ranging between 92 and 100%.



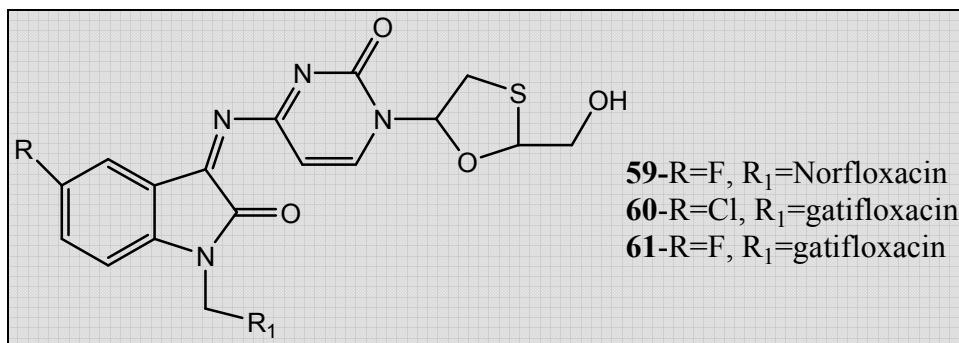
Compound **57** had the highest inhibitory potency with 100% inhibition followed by compounds **55** and **56** with 99% inhibition [97].

Sriram et al. investigated various aminopyrimidinimino isatin analogues with the following general structure (**58**) for their anti-tubercular activity against H37Rv strain of MTB in BACTEC 12B medium at a concentration of 6.25 µg/ml.



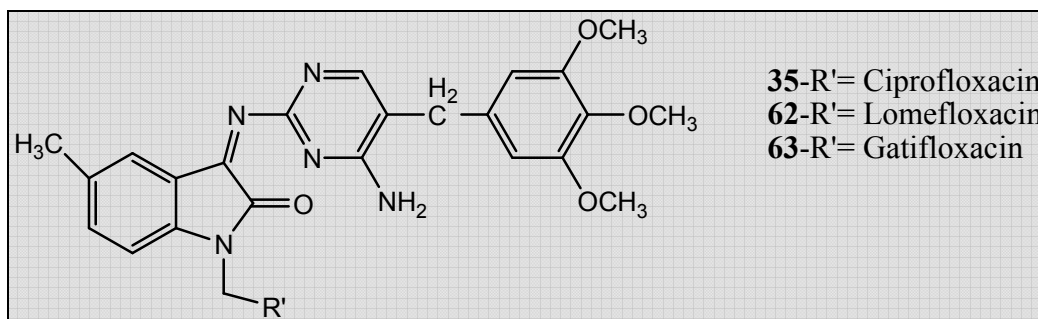
Amidst all the compounds in the series, four of them namely, 7-(4-(((Z)-3-(5-(3,4,5-trimethoxybenzyl)-4-aminopyrimidin-2-ylimino)-5-fluoro-2-oxoindolin-1-yl)methyl)piperazin-1-yl)-1-ethyl-6-fluoro-1,4-dihydro-4-oxoquinoline-3-carboxylic acid (**34**), 7-(4-(((Z)-3-(4-amino-5-(3,4,5-trimethoxyphenyl)pyrimidin-2-ylimino)-5-fluoro-2-oxoindolin-1-yl)methyl)piperazin-1-yl)-1-cyclopropyl-6-fluoro-1,4-dihydro-4-oxoquinoline-3-carboxylic acid, 7-(4-(((Z)-3-(4-amino-5-(3,4,5-trimethoxyphenyl)pyrimidin-2-ylimino)-5-fluoro-2-oxoindolin-1-yl)methyl)-3-methylpiperazin-1-yl)-1-ethyl-6,8-difluoro-1,4-dihydro-4-oxoquinoline-3-carboxylic acid and 7-(4-(((Z)-3-(4-amino-5-(3,4,5-trimethoxyphenyl)pyrimidin-2-ylimino)-5-fluoro-2-oxoindolin-1-yl)methyl)-3-methylpiperazin-1-yl)-1-cyclopropyl-6,8-difluoro-1,4-dihydro-4-oxoquinoline-3-carboxylic acid showed 100% mycobacterial inhibition [91].

Various prodrugs of lamivudine with substituted isatins were synthesized and were evaluated for their anti-tubercular potential at 6.25 $\mu\text{g/ml}$ using microplate alamar blue assay (MABA) against MTB H37Rv strain.



Three of them among the entire array proved beneficial in MABA screenings, which were *N*-Mannich bases of lamivudine prodrugs with various fluoroquinolones at R₁, viz. compounds **59**, **60** and **61**. These analogues were able to completely inhibit MTB growth [98].

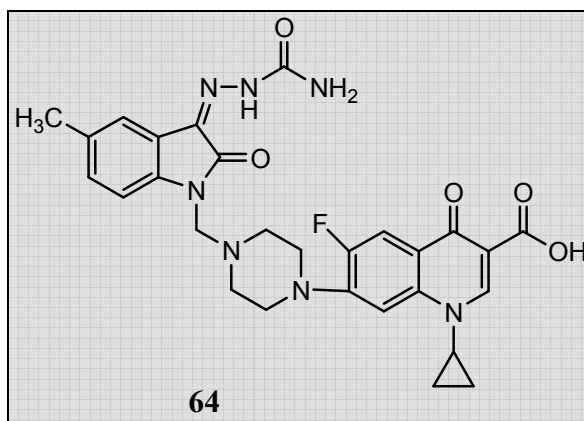
Schiff base of 5-methyl isatin with 5-(3',4',5'-trimethoxybenzyl)-2,4-diaminopyrimidine was initially synthesized which was then converted into *N*-Mannich bases using various secondary amines.



From all the twelve final compounds, three of them viz. 7-(4-(((*Z*)-3-(5-(3,4,5-trimethoxybenzyl)-4-aminopyrimidin-2-ylimino)-5-methyl-2-oxoindolin-1-yl)methyl)piperazin-1-yl)-1-cyclopropyl-6-fluoro-1,4-dihydro-4-oxoquinoline-3-carboxylic acid (**35**), 7-(4-(((*Z*)-3-(4-amino-5-(3,4,5-trimethoxyphenyl)pyrimidin-2-ylimino)-5-methyl-2-oxoindolin-1-yl)methyl)-3-methylpiperazin-1-yl)-1-ethyl-6,8-difluoro-1,4-dihydro-4-oxoquinoline-3-carboxylic acid (**62**) and 7-(4-(((*Z*)-3-(4-amino-5-

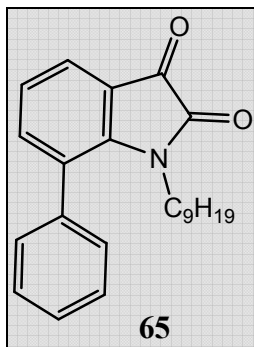
(3,4,5-trimethoxyphenyl)pyrimidin-2-ylimino)-5-methyl-2-oxoindolin-1-yl)methyl)-3-methylpiperazin-1-yl)-1-cyclopropyl-6-fluoro-1,4-dihydro-8-methoxy-4-oxoquinoline-3-carboxylic acid (**63**) demonstrated 100 % inhibition of H37Rv strain of MTB in BACTEC 12B medium at 6.25 µg/ml and were not cytotoxic to Vero cell line upto 62.5 µg/ml [92].

Various 7-substituted ciprofloxacin derivatives with isatin substitution were synthesized and assessed for their *in vitro* and *in vivo* antimycobacterial activity as well as their ability to inhibit the supercoiling property of DNA gyrase of *Mycobacterium smegmatis* [MC₂].

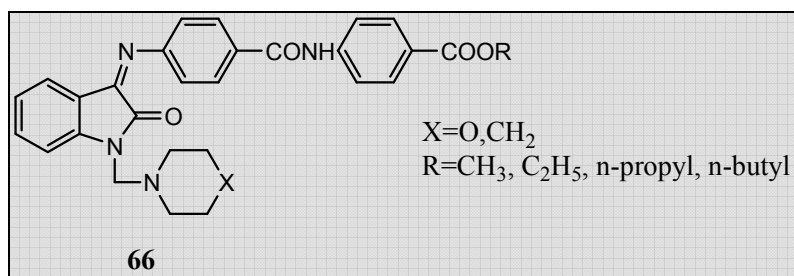


Compound 1-cyclopropyl-6-fluoro-1,4-dihydro-4-oxo-7-[[N4-[1'-(5-methylisatin-3-yl)methyl]N1-piperazinyl]-3-quinoline]carboxylic acid (**64**) decreased the bacterial load in spleen tissue with 0.76-log₁₀ protections and was considered to be moderately active in reducing bacterial count in spleen [99].

Ramachandran demonstrated that 1-nonyl-7-phenyl-1H-indol-2, 3-dione (**65**) was effective in inhibiting MTB growth with an MIC below 20 $\mu\text{g/ml}$ [100].

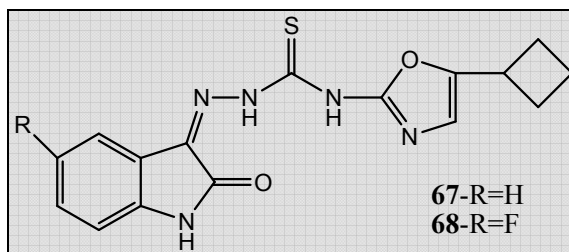


Varma and Pandeya synthesized various 3-[p-(p-(alkoxycarbonyl)-phenyl) carbamoyl]] phenyl) imino-1-aminomethyl-2-indolinones (**66**) and these were subjected to evaluation for their anti-mycobacterial property.



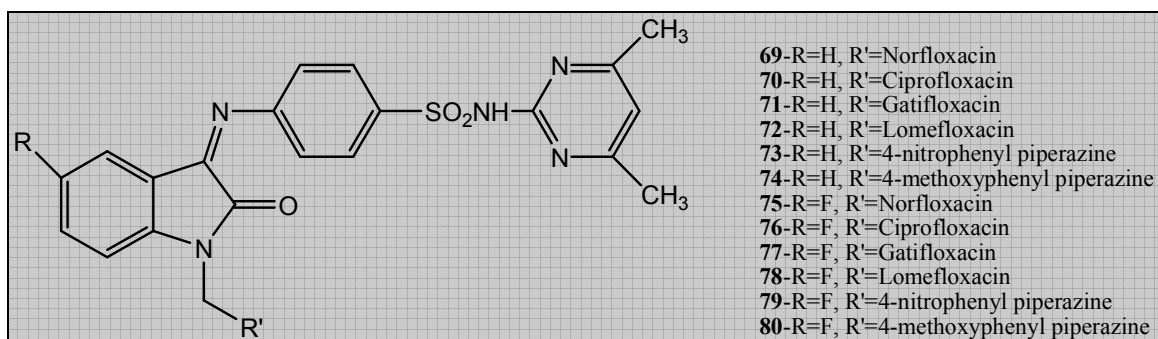
Nine analogues showed 100% inhibition of mycobacterial growth with MIC ranging from 10-20 $\mu\text{g/ml}$ [101].

(Z)-4-(5-cyclobutyloxazol-2-yl)-1-(2-oxoindolin-3-ylidene)thiosemicarbazide (**67**) and (Z)-4-(5-cyclobutyloxazol-2-yl)-1-(5-fluoro-2-oxoindolin-3-ylidene)thiosemicarbazide (**68**) were evaluated for *in vitro* and *in vivo* activity against H37Rv strain of MTB and multidrug-resistant TB (MDRTB).



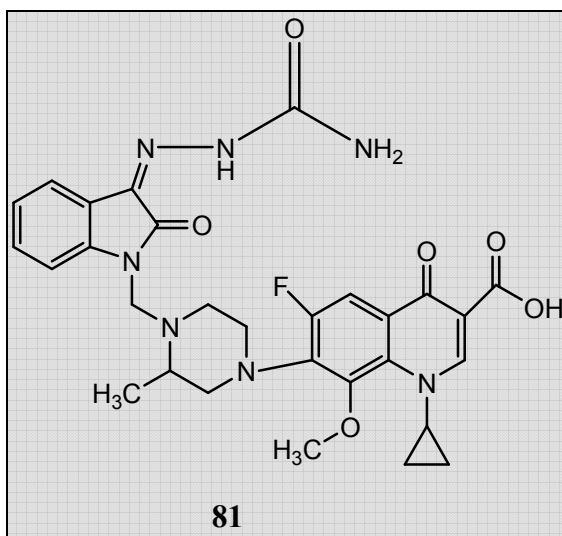
Compound **67** inhibited mycobacterial growth and also the growth of MDRTB at 25.0 µg/ml and compound **68** was able to inhibit H37Rv and also MDRTB at 12.5 µg/ml [102].

A number of isatin derivatives having the general structure as illustrated underneath were synthesized and appraised for their anti-mycobacterial potentials.



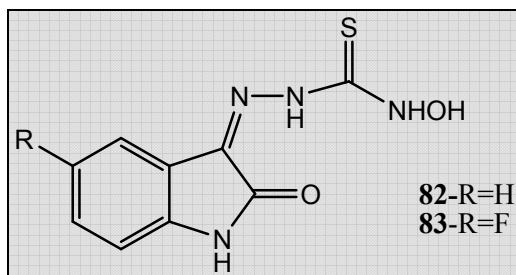
In preliminary screening, done in BACTEC 12B medium against H37Rv strain of MTB, compounds **69-72** and compounds **75-78** showed 100% inhibition of mycobacterial growth. In secondary level screening, **77** emerged as the most potent anti-mycobacterial agent with MIC of 1.22 µg/ml. All these compounds were not cytotoxic to Vero cells up to a concentration of 62.5 µg/ml [94].

In another effort by Sriram et al., sixteen *N*-Mannich bases of 5-substituted isatins were synthesized with gatifloxacin and these were then evaluated for their ability to inhibit MTB replication both *in vitro* and *in vivo* and were also tested against MDRTB.



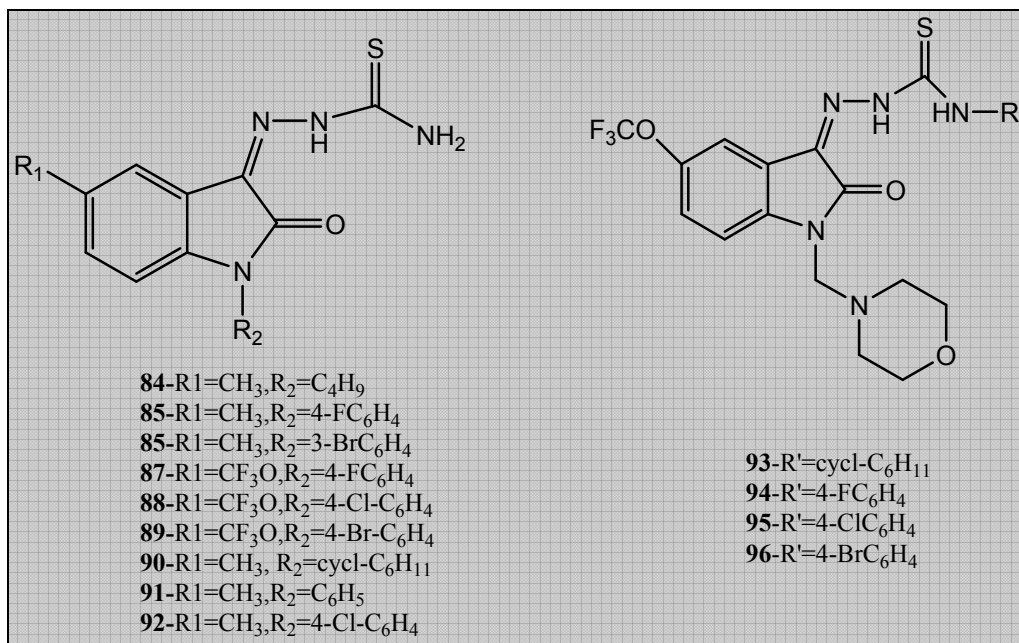
Amongst the complete array of synthesized analogues, 1-cyclopropyl-6-fluoro-8-methoxy-7-[[[N⁴-[1' -(5-isatinyl-β-semicarbazoyl)methyl]3-methyl]N¹ -piperazinyl]-4-oxo-1,4-dihydro-3-quinoline carboxylic acid (**81**) emerged as the most active compound *in vitro* with an MIC of 0.0125 µg/ml against H37Rv strain of MTB and was 16 times more potent than gatifloxacin, the parent drug. Against MDRTB, compound **81** displayed an MIC of 0.05 µg/ml and was 64 times more potent than gatifloxacin. When evaluated for their cytotoxicity compound **81** had a selectivity index greater than 1250. Compound **81** when tested *in vivo* in six-week old mice model at a dose level of 50mg/kg body weight decreased the bacterial load in lung and spleen tissues with 3.62- and 3.76- log₁₀protections respectively. It was also tested for its ability to hinder the supercoiling property of mycobacterial DNA gyrase enzyme. It inhibited DNA gyrase with an IC₅₀ value of 3 µg/ml [103].

(Z)-4-hydroxy-1-(2-oxoindolin-3-ylidene)thiosemicarbazide (**82**) and (Z)-1-(5-fluoro-2-oxoindolin-3-ylidene)-4-hydroxythiosemicarbazide (**83**) were synthesized by two different methods and were subjected to anti-mycobacterial screening against H37Rv strain of MTB.



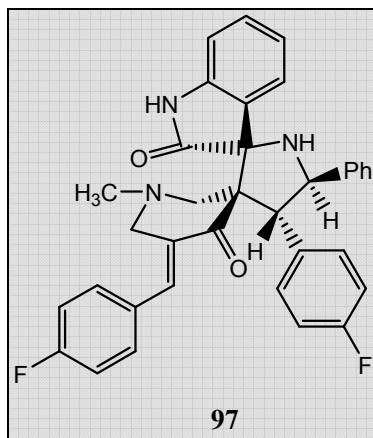
These two drugs could completely inhibit MTB replication at MIC values of 64.02 and 24.58 µg/ml respectively, and were far less potent than standard anti-tubercular agents viz. isoniazid, ethambutol and rifampicin [104].

New series of 5-methyl/trifluoromethoxy-1H-indole-2,3-dione 3-thiosemicarbazones; 1-methyl-5-methyl/trifluoromethoxy-1H-indole-2,3-dione 3-thiosemicarbazones; 5-methyl-1H-indole-2,3-dione 3-thiosemicarbazones and 5-trifluoromethoxy-1-morpholinomethyl-1H-indole-2,3-dione 3-thiosemicarbazones were synthesized and put to test against H37Rv strain of MTB.



In primary anti-tubercular screening the compounds **84-96** surfaced as potent anti-tubercular agents with EC₅₀ values ranging between 0.195 and 23.437 µg/ml. (Z)-1-(1-(4-fluorophenyl)-5-methyl-2-oxoindolin-3-ylidene)thiosemicarbazide (**85**) had an EC₅₀ value lesser than 0.195 µg/ml but proved to be cytotoxic to Vero cells with a selectivity index less than 0.1228 [105].

A series of 1-methyl-3, 5-bis [(E)-arylmethylidene] tetrahydro-4(1H)-pyridinones were synthesized via 1,3-dipolar cycloaddition reaction involving isatins and various α-amino acids.



These compounds were evaluated against H37Rv strain of MTB, MDRTB and *Mycobacterium smegmatis* (MC₂). Compound 4-(4-fluorophenyl)-5-phenylpyrrolo(spiro[2.3]oxindole)spiro[3.3]-1'-methyl-5'-(4-fluorophenylmethylidene)piperidin-4'-one (**97**) transpired as the most active compound against H37Rv MTB with an MIC of 0.07 µg/ml and was 5.1 times and 67.2 times more potent than isoniazid and ciprofloxacin respectively. When tested *in vivo*, compound **97** decreased the bacterial load in lungs and spleen tissues with 1.30 and 3.73 log₁₀protections respectively. It inhibited MDRTB with an MIC of 0.16 µg/ml and MC₂ with an MIC of 0.69 µg/ml [106].

2.3 Chemistry of Isatin

Isatin or 1H-indole-2, 3-dione is the lactam of *o*-amino benzoylformic acid [107]. It possesses both amide group and keto group and an active hydrogen atom attached to nitrogen (or oxygen, when it is in lactim form). In 1882, Bayer proved that isatin can exist both in its lactam as well as lactim form.

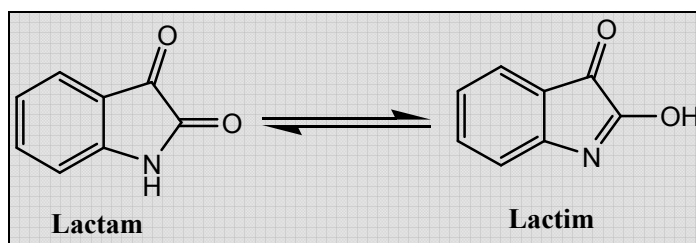


Fig. 2.1: Lactam-lactim tautomerism of isatin

Since isatin is a valuable intermediate in the synthesis of many pharmacologically active molecules, numerous endeavors have been undertaken in developing various synthetic protocols for it.

Synthetic protocols of Isatin:

I. Claisen and Shadwell method: This method involves the use of *o*-nitrobenzoyl chloride and potassium cyanide as the starting reagent for isatin synthesis; which thereby gives *o*-nitrobenzoyl cyanide, which on hydrolysis and reduction with ferrous hydroxide affords the salt of *o*-aminophenyl glyoxalic acid product [107].

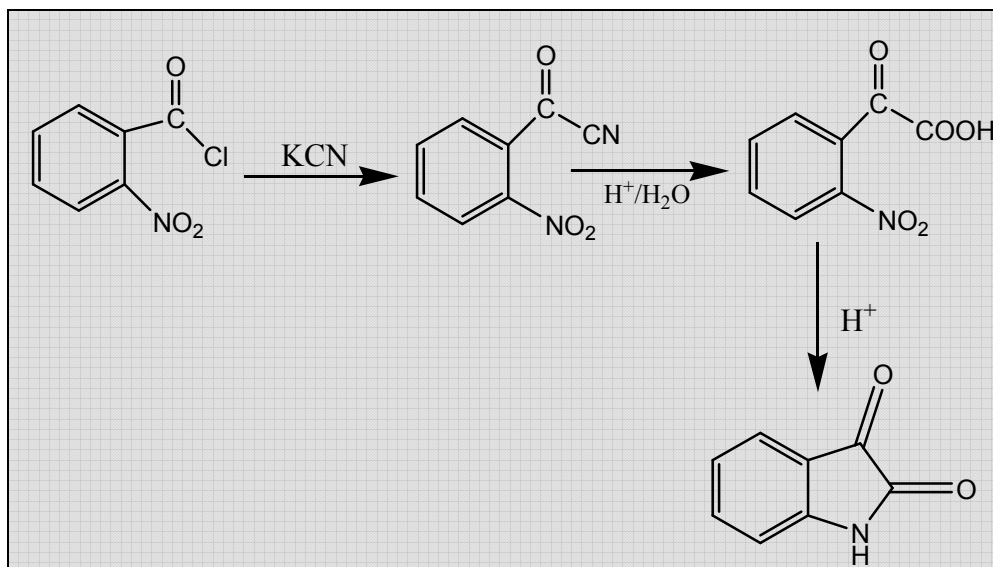


Fig. 2.2: Claisen Shadwell Isatin synthesis

This on further acidification yields isatin.

II. Baeyer's method:

- A. Baeyer and Forrer synthesized isatin by the action of alkali on *o*-nitrophenylpropionic acid [107].
- B. In another method, Baeyer first reduced *o*-nitrophenylacetic acid to aminooxindole, which was further converted into isatin [107].

III. Sandmeyer's method: Sandmeyer developed two methods for the synthesis of isatin and its derivatives.

- A. In one of the methods, thiocarbanilide was used as the starting reagent, which when reacted with hydrocyanic acid and lead carbonate yielded the cyano-*N,N*-diphenyl formamidine. This intermediate was converted into the isatin- α -anilide. The reaction scheme that was followed is outlined below:

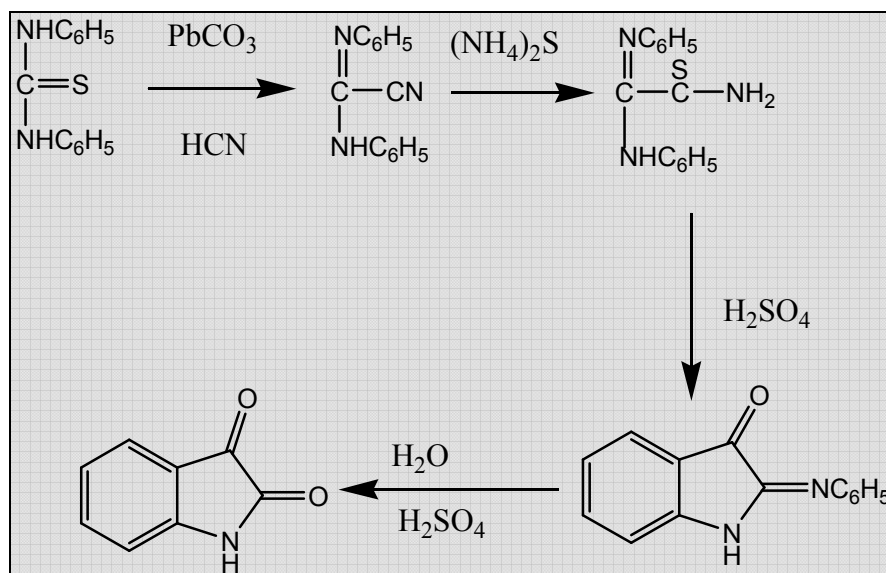


Fig. 2.3: Sandmeyer's thiocarbanilide isatin synthesis

The isatin- α -anilide can be readily hydrolyzed to isatin [108].

- B.** Sandmeyer's second method relies on the formation of isonitrosoacetanilide from aniline, chloral hydrate and hydroxylamine. Isatin is obtained on treating the isonitrosoacetanilide with concentrated sulfuric acid [107].

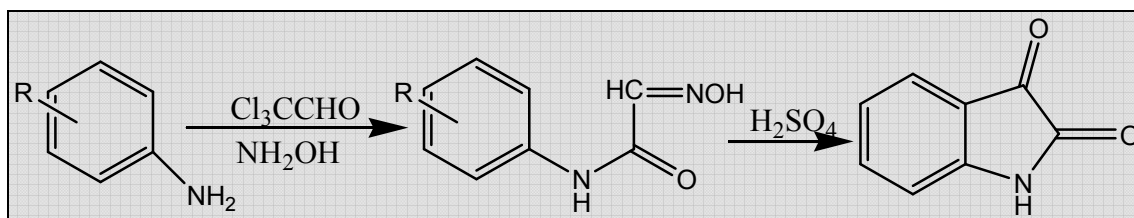


Fig 2.4: Sandmeyer's isonitrosoacetanilide isatin synthesis

IV. Bauer's method: Bauer synthesized isatin and nuclear substituted isatins by the action of sulfuric acid on substituted imide chlorides of oxalic acid [107].

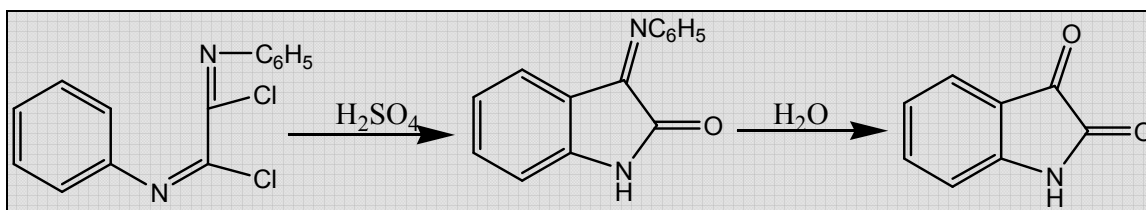


Fig. 2.5: Bauer's isatin synthesis

V. Ostromisslensky method: The method of Bauer was adopted and modified by Ostromisslensky and Meyer for the synthesis of substituted isatins from *o*-toluidine and *p*-toluidine and dichloroacetic acid. This procedure involves heating dichloroacetic acid

and arylamines thereby forming the intermediate oxindole; which further gets oxidized to the corresponding isatin anilide. The isatin anilide on hydrolysis yields the substituted isatin [107].

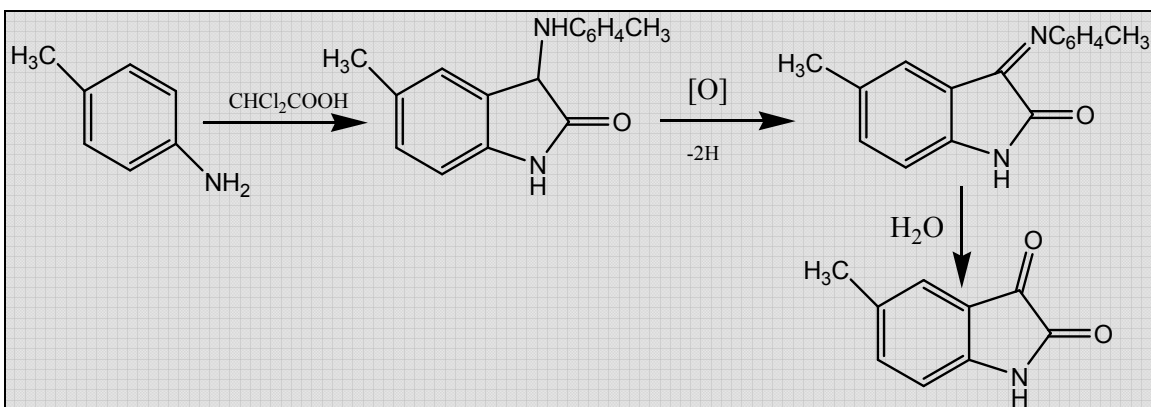


Fig. 2.6: Ostromisslensky isatin synthesis

VI. Stollé method: Stollé developed a facile method for the synthesis of many isatin derivatives, which involves the treatment of N-substituted aniline with oxalyl chloride. The resultant intermediate undergoes a Friedel-Crafts acylation type reaction on treatment with a strong Lewis acid viz. anhydrous aluminium chloride yields the corresponding isatin [107].

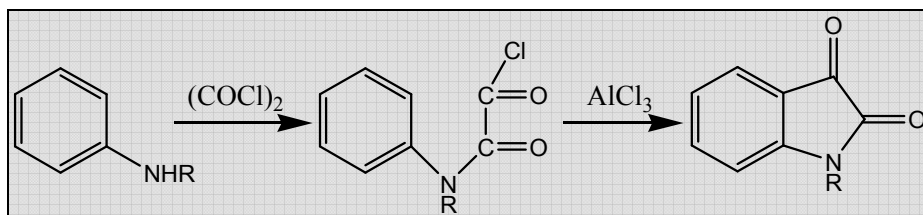


Fig. 2.7: Stollé's isatin synthesis

VII. Martinet's method: In this method, aniline or a substituted aromatic amine is condensed with the ethyl ester of oxomalonate. The intermediate obtained when treated with alkali in the absence of air yields dioxindole, but when subjected to alkali treatment in the presence of oxygen generates isatin [107].

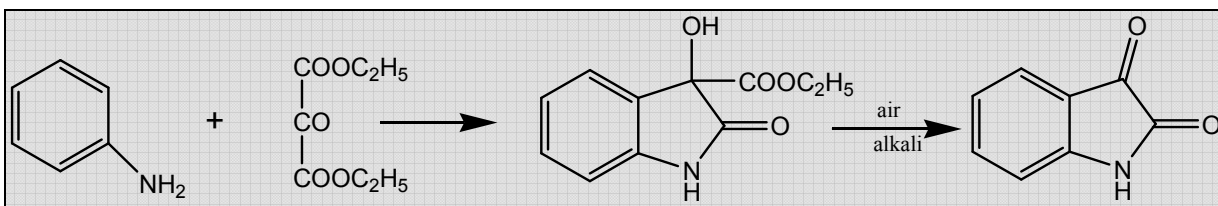


Fig. 2.8: Martinet's isatin synthesis

VIII. Heller's method: The method followed by Heller involves heating *o*-hydroxylaminomandelic acid with hydrochloric acid, which yields the intermediate *o*-aminobenzoyl cyanide. This intermediate on further hydrolysis and condensation yields isatin [107].

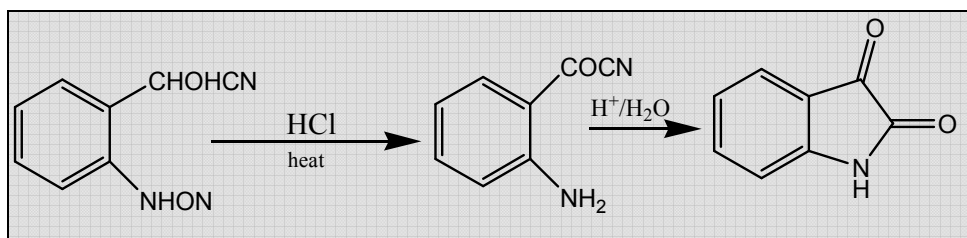


Fig. 2.9: Heller's isatin synthesis

IX. Reissert's method: This method entailed heating thiooxanilide with concentrated sulfuric acid thereby yielding isatin [107].

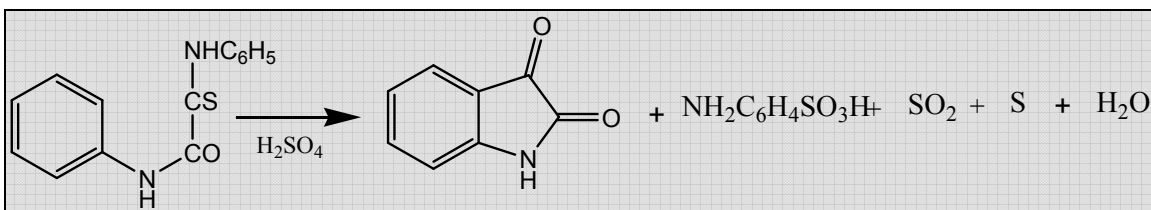


Fig. 2.10: Reissert's method of isatin synthesis

X. Gassman et al's method: This method involves the oxidation of anilines to 3-methoxythiooxindoles. This oxindole intermediate's methine carbon at 3rd position when oxidized with N-chlorosuccinimide gives a chlorinated intermediate. This chlorinated intermediate on hydrolysis with red mercuric oxide and boron trifluoride etherate in aqueous tetrahydrofuran gives the respective isatins [109].

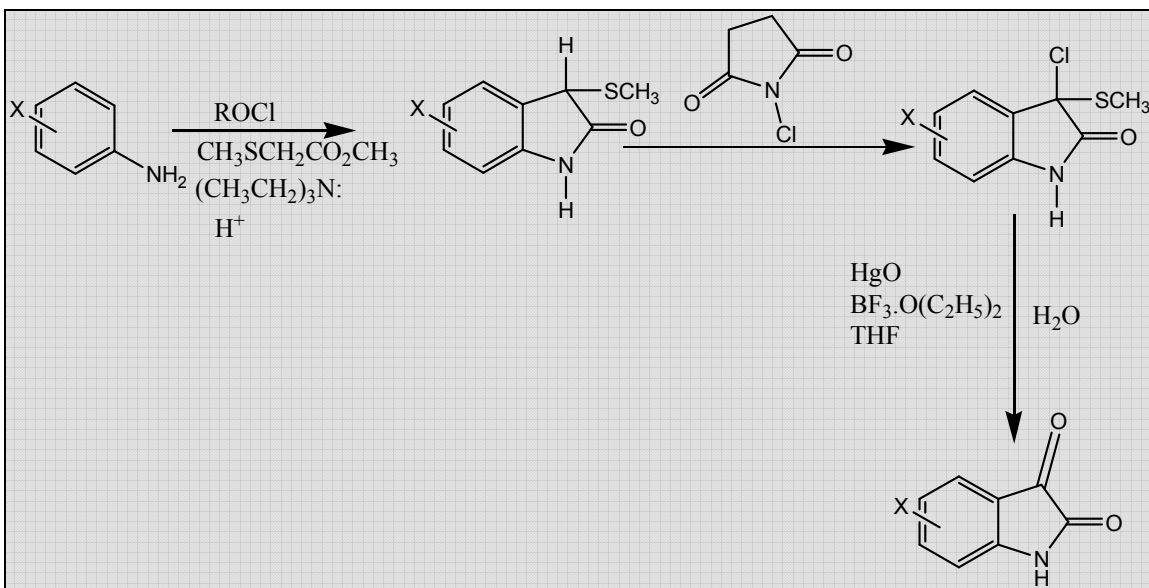


Fig. 2.11: Gassman's isatin synthesis

XI. Lamberton and Price's ring contraction method: A number of 2,4-dihydroxy quinolines, following the introduction of a 3-hydroxyamino, 3-nitroso, 3-hydroxy-3-amino, or 3,3-dihalo groups gives isatin on reaction with sulfuric acid or sodium hydroxide [110].

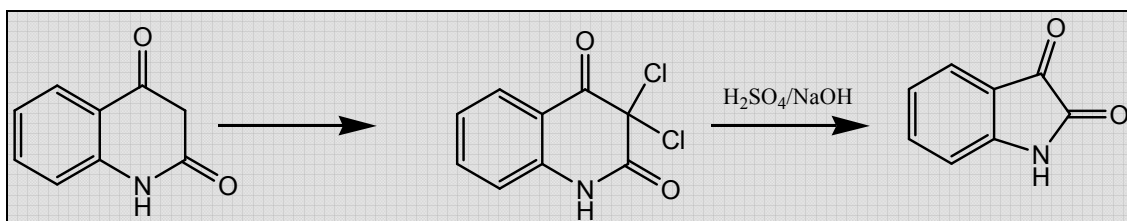


Fig. 2.12: Lamberton & Price's ring contraction method

XII. Giovanni and Portmann's method: This method employs indole as the starting reagent. Oxindoles on treatment with nitrous acid gives isatin-3-oximes. Reduction of oximes to 3-amino oxindoles followed by ferric chloride oxidation gives isatin [111].

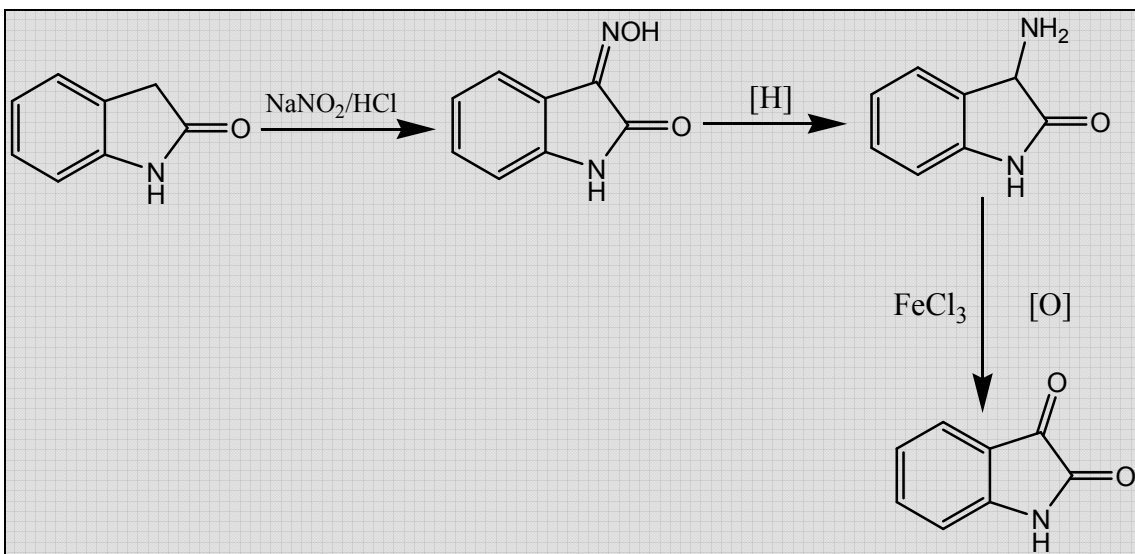


Fig. 2.13: Giovannini & Portmann's method of isatin synthesis

XIII. Erdmann and Laurent's method: This method involves the synthesis of isatin by oxidation of indigo using chromic acid or nitric acid or a mixture of the two [107].

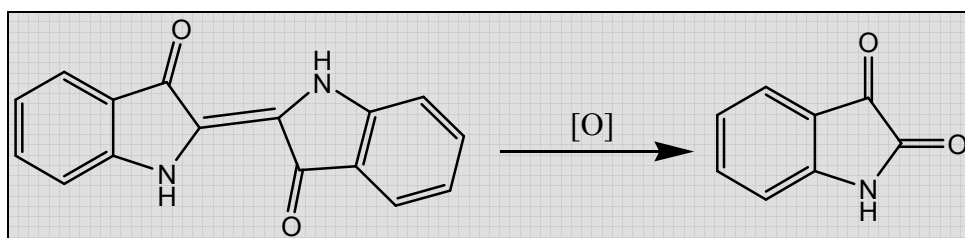


Fig. 2.14: Erdmann & Laurent's method

Reactions of isatin: By virtue of the reactive carbonyl moiety present at its 3rd position, isatin undergoes characteristic reactions with ketonic reagents namely hydroxylamine, phenylhydrazine and semicarbazide/thiosemicarbazide. In comparison to the carbonyl group at 3rd position, the one present at 2nd position possesses less nucleophilic character, due to the proximal amino group at N₁.

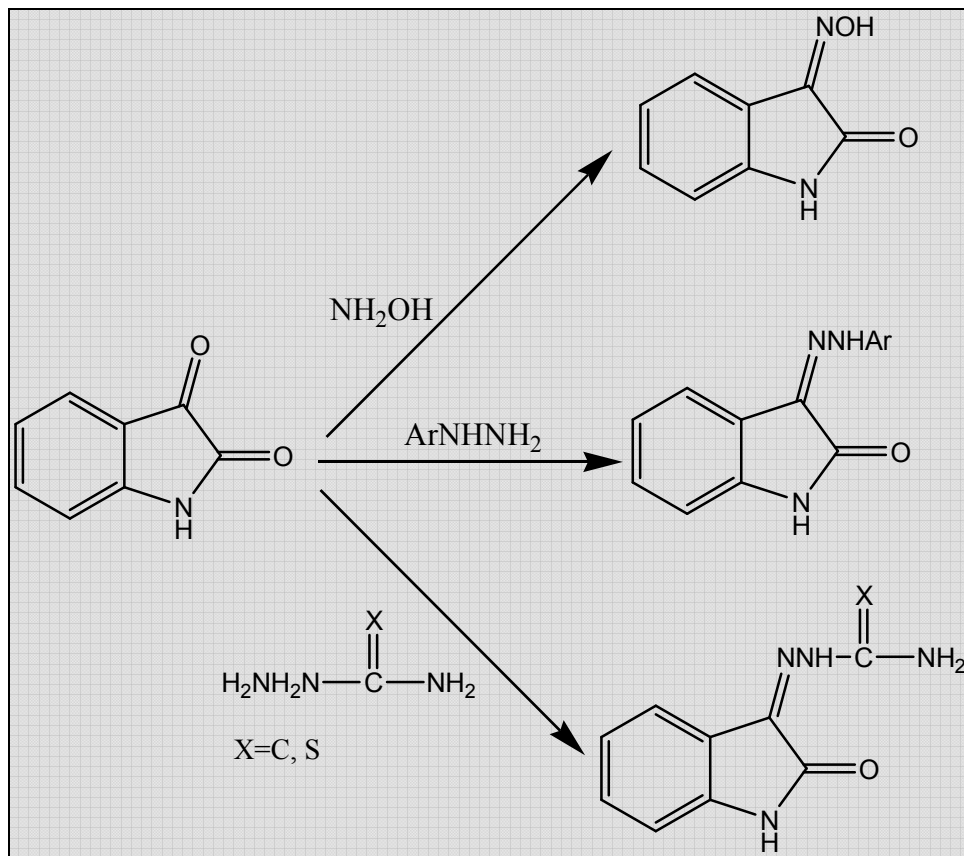


Fig. 2.15: Reactions of isatin

I. Schiff Reaction: Isatin reacts with a variety of aromatic amines and semicarbazides/thiosemicarbazides with the aid of the catalytic action of glacial acetic acid or sodium acetate to yield the corresponding Schiff bases namely the imines and semicarbazones/thiosemicarbazones.

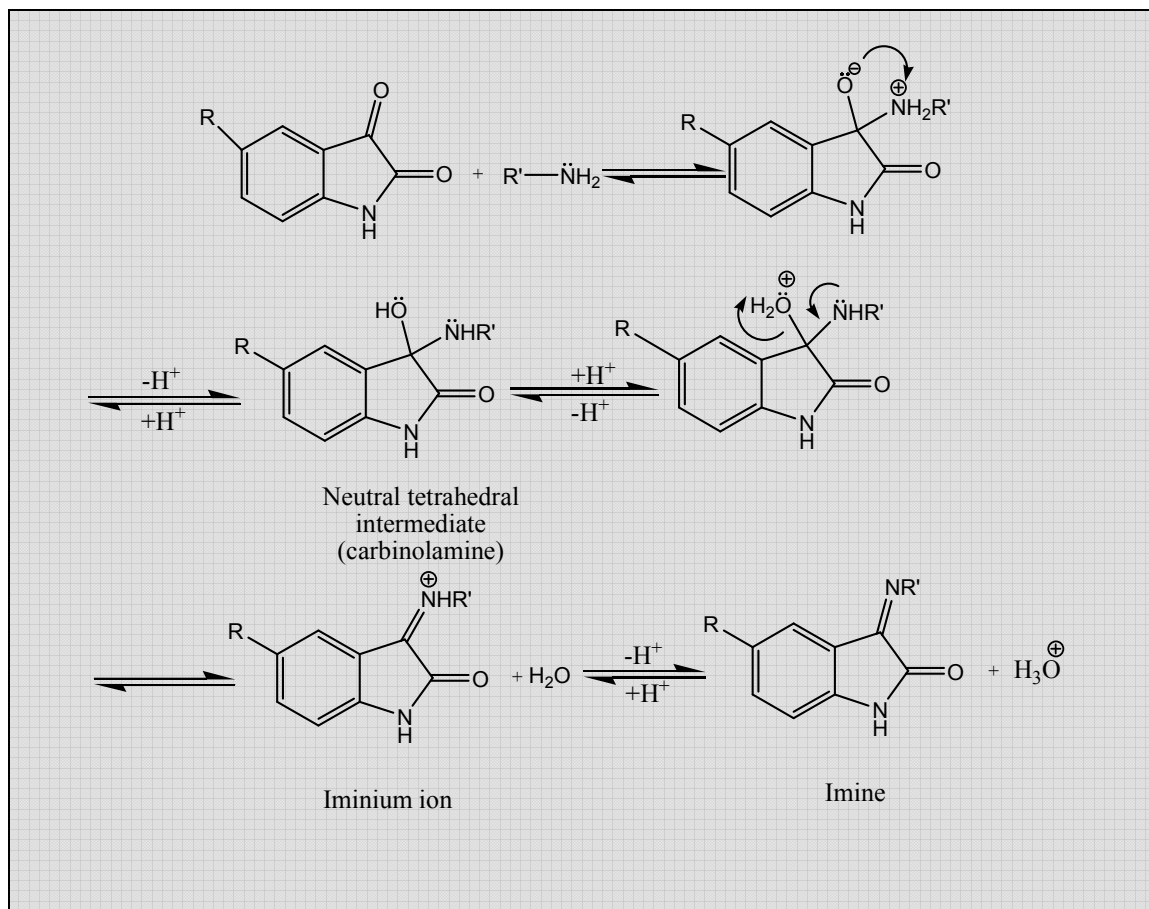
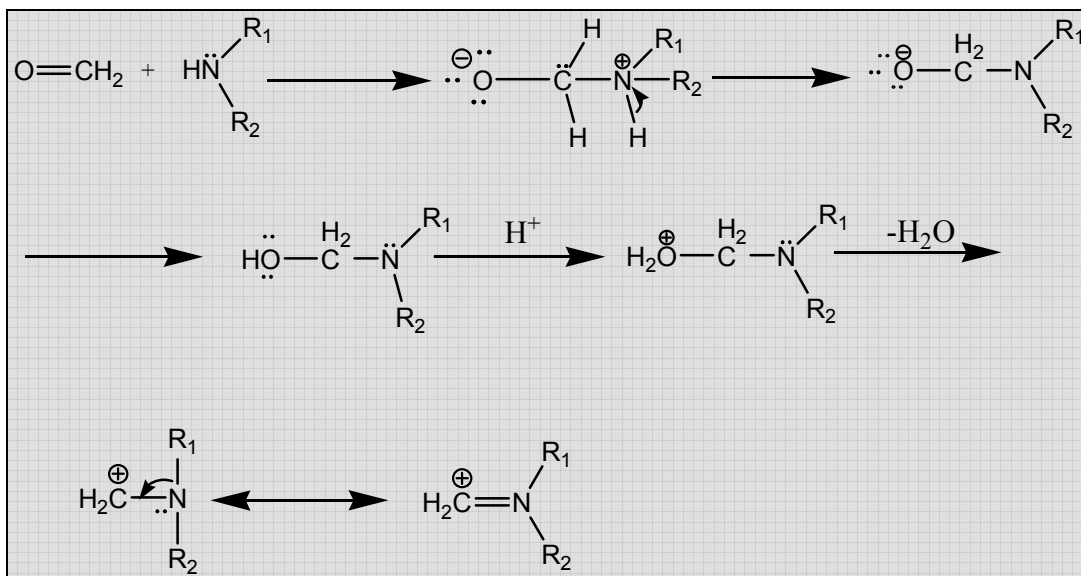


Fig. 2.16: Mechanism of Schiff reaction of isatin

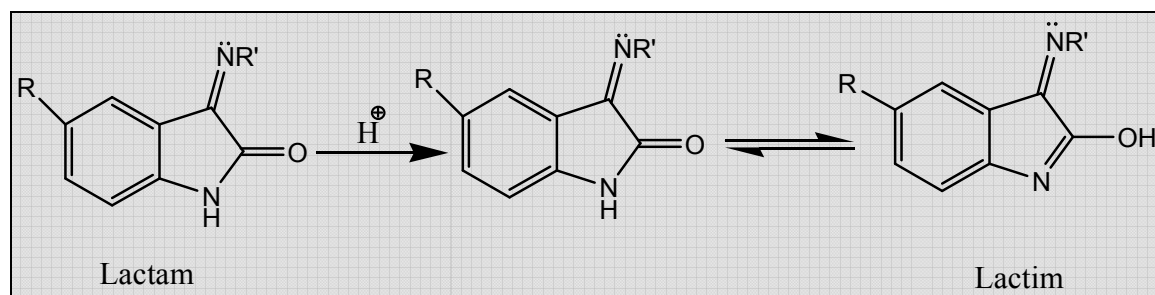
This is a nucleophilic addition-elimination reaction involving the nucleophilic addition of amine forming the unstable tetrahedral intermediate; which is followed by elimination of a water molecule. The first step involves the nucleophilic attack of amine onto the carbonyl carbon. Charge transfer from alkoxide to ammonium ion leads to generation of carbinolamine. pH is an important criteria for imine formation. There must be sufficient acid present to protonate the tetrahedral intermediate, so that the better leaving group i.e. water rather than the hydroxyl group is liberated. The amine lone pair pushes out water, giving rise to a protonated imine. Finally water accepts the proton from the iminium ion thereby regenerating the acid catalysts.

II. Mannich reaction: The active hydrogen atom at N-1 when condensed with formaldehyde and various secondary amines yields different N-Mannich bases.

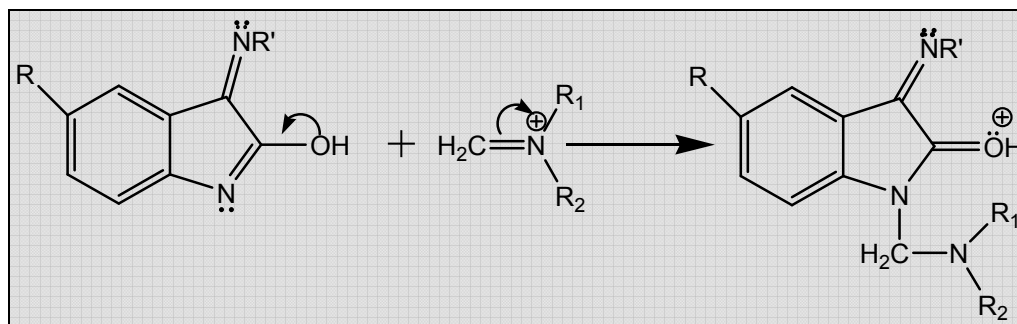
Step 1: Iminium ion formation



Step 2: Lactam-lactim tautomerism



Step 3: Carbon-nitrogen bond formation



Step 4: Proton transfer

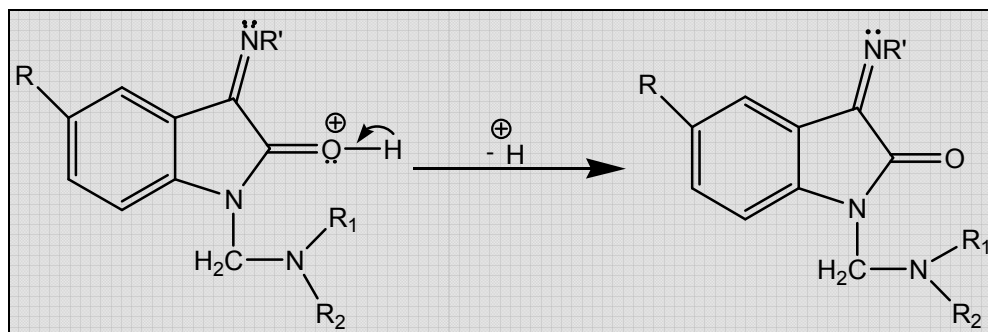


Fig. 2.17: Mechanism of Mannich base formation (Step 1-4)

In the first step, the electron lone pair present on the nitrogen of the secondary amine attacks the carbonyl carbon of formaldehyde; which leads to the intermediate protonated ion. Elimination of water from this intermediate gives the reactive species, iminium ion. The second step involves the tautomerism of the lactam to the lactim form, which serves as the nucleophile. The Schiff base's lactim form then attacks the electrophilic carbon of iminium ion thereby forming the carbon-nitrogen bond in the third step. Loss of proton from the oxonium ion thereby leading to the final product happens in the last step.

CHAPTER 3

OBJECTIVE AND PLAN OF WORK

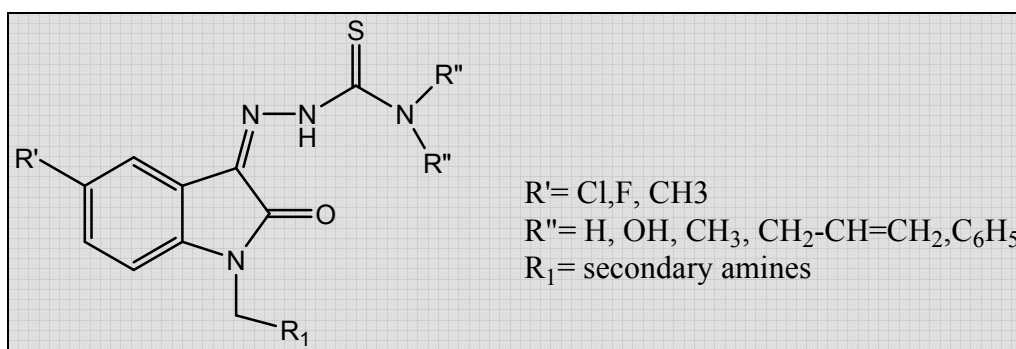
3.1 Objective

The objective of this present research work was to design, synthesize and evaluate various novel isatin- β -thiosemicarbazone analogues for their ability to treat HIV-TB co-infection.

3.2 Plan of work

The plan of work is briefly outlined below:

I Synthesis: The synthesis of various isatin- β -thiosemicarbazone analogues was accomplished in four steps. 5-substituted isatins were synthesized from 4-substituted anilines in two steps via Sandmeyer's method. Using hydroxylamine hydrochloride/ methoxylamine hydrochloride/ diphenylamine/diallylamine as starting reagents various thiosemicarbazides were attained, which on condensation with the 5-substituted isatins yielded the corresponding Schiff bases. These Schiff bases on reaction with formaldehyde and various secondary amines yielded the respective N-Mannich bases as the final products.



II. Biological activity: All the synthesized compounds were subjected to the following evaluations:

a) Anti-HIV activity against the replication of HIV-1 (HTLV-III_B) in MT-4 cell lines and cytopathogenicity in MT-4 cell line was determined using 3-(4,5-dimethylthiazol-2-yl)-2,5-diphenyltetrazolium bromide (MTT) assay based method.

b) Selected compounds were evaluated for their ability to inhibit HIV-1 RT enzyme using homopolymer template primers.

c) Anti-tubercular activity of all the synthesized compounds was evaluated against the replication of H37Rv strain of MTB in logarithmic phase employing an agar dilution method.

d) Few of these compounds were also evaluated for their ability to inhibit dormant MTB.

e) Selected compounds were also tested for their ability to repress the enzyme isocitrate lyase (ICL) of MTB, which has significant implication in persistent TB.

f) Selected compounds were also assessed for their ability to inhibit *Mycobacterium smegmatis*' DNA gyrase supercoiling.

g) Few analogues were tested for their antiviral and cytotoxicity activity against hepatitis C virus (HCV) in Huh7 ET cell line.

h) Antiviral and cytotoxicity assays were also performed for few of the compounds against influenza type A and B viruses and severe acute respiratory syndrome (SARS) virus.

III. Computational studies: **a)** 3D QSAR studies, namely comparative molecular field analysis (CoMFA) and comparative molecular similarity index analysis (CoMSIA) analyses were performed on the two series of compounds based on their anti-HIV activity.

b) Molecular docking simulations were performed on the two series of compounds to assess their binding mode to HIV-1 RT enzyme using the softwares, Genetic optimization of ligand docking (GOLD) and Autodock 4.0.

c) Molecular docking simulations were performed on the two series of compounds to evaluate their mode of binding to MTB ICL enzyme with the aid of the softwares, GOLD and Autodock 4.0.

CHAPTER 4

MATERIALS AND METHODS

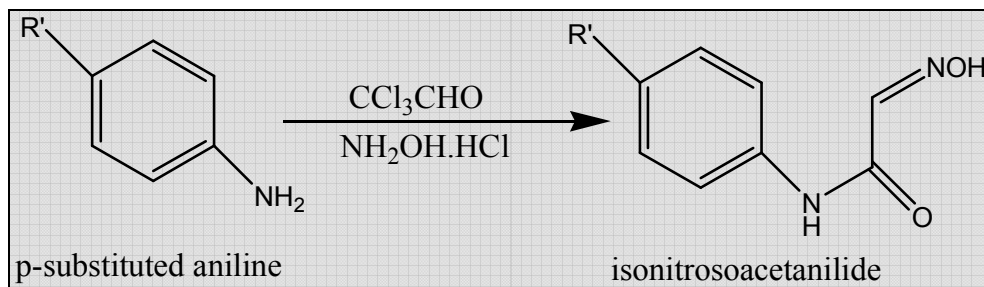
Chemistry

A scientific microwave reactor (Catalyst, India) was employed for the final step of the synthetic protocol. Melting points were determined on an electro thermal melting point apparatus (Büchi BM530) in one end open capillary tubes and are uncorrected. The homogeneity of the compounds was monitored by ascending thin layer chromatography (TLC) on silica gel-G (Merck) coated aluminium plates and visualized under UV irradiation or by using iodine vapor. The solvent system used was chloroform – methanol (9:1). IR spectra for the compounds were recorded using Jasco IR Report 100 (KBr pellet) Spectrophotometer. ¹H-NMR spectra were recorded on a JEOL Fx 400MHz NMR spectrometer using DMSO-d₆ as solvent. Chemical shifts are expressed in δ (ppm) relative to tetramethylsilane as an internal standard. Mass spectra were recorded with Shimadzu GC-MS-QP5000 spectrophotometer. Elemental analyses (C, H, and N) were performed on Perkin Elmer model 240C analyzer. The logP values were determined using ChemOffice 2004 software.

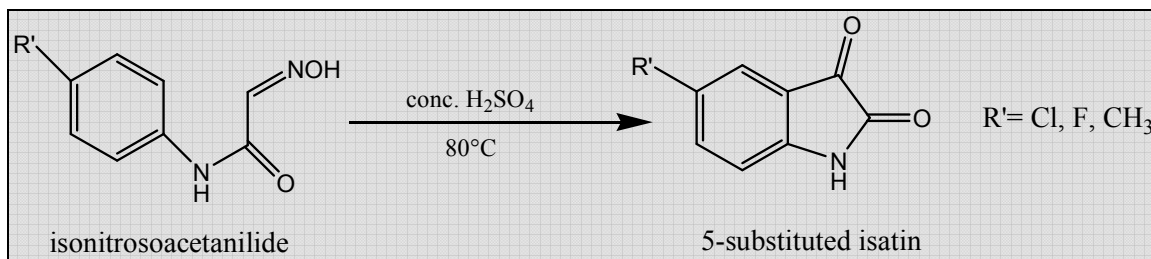
I. Synthesis:

The synthesis of the various isatin- β -thiosemicarbazone analogues were accomplished via the following steps:

Step 1: The first step consisted of synthesis of various isonitrosoacetanilide from various 4- substituted anilines employing Sandmeyer's method [108].

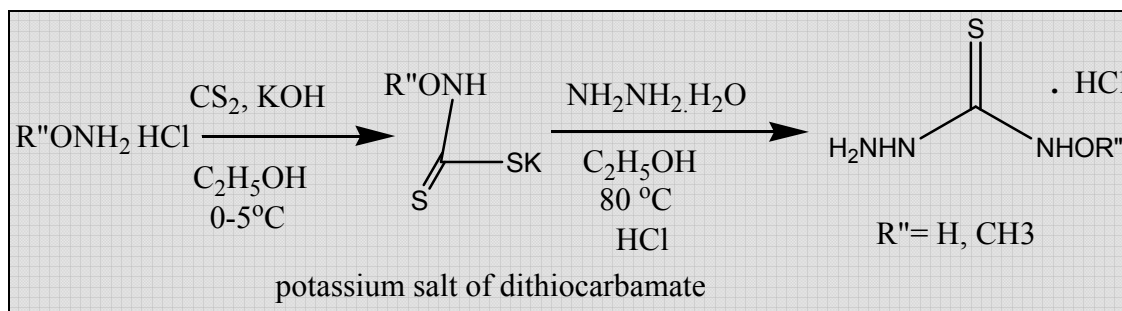


Step 2: The second step consisted of synthesis of 5-substituted isatins from the isonitrosoacetanilide obtained in Step 1 via a condensation step using concentrated sulfuric acid [108].

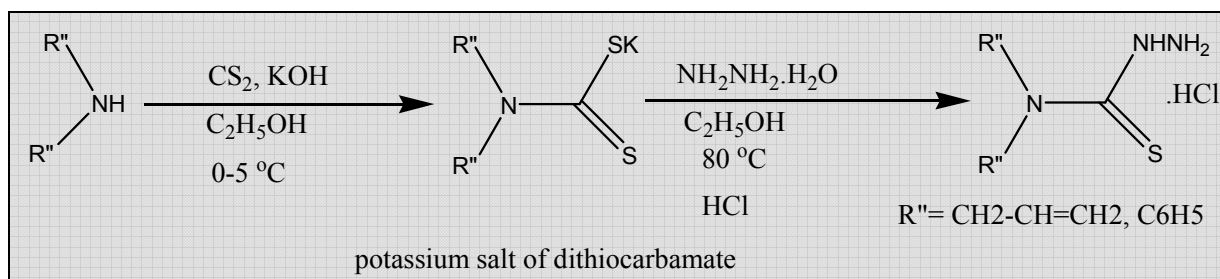


Step 3: The third step comprised of synthesis of various thiosemicarbazides using the following synthetic protocols: [102]

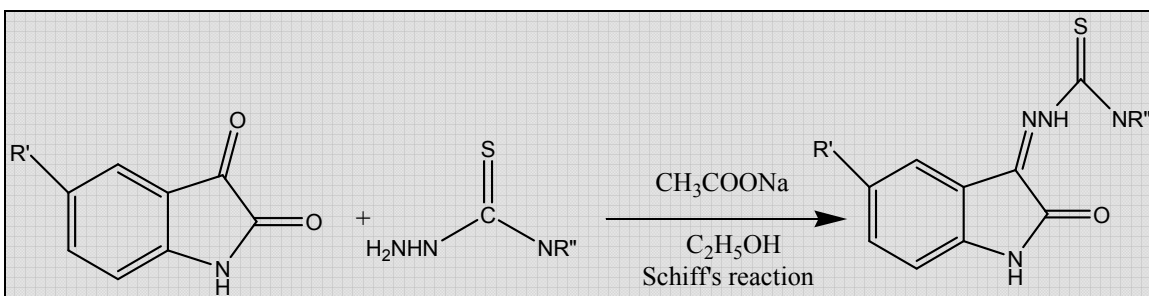
a) Preparation of hydroxyl/methoxy thiosemicarbazides:



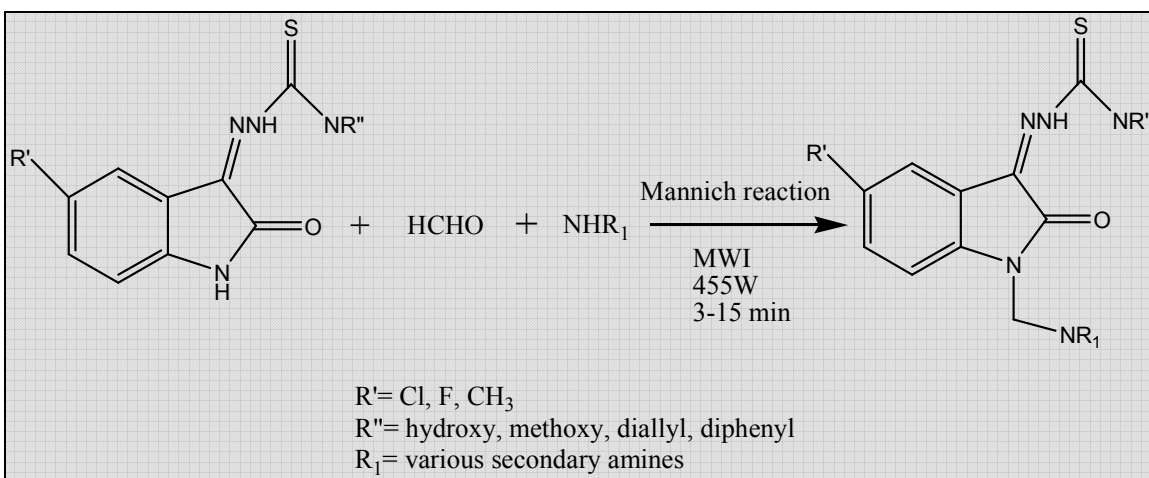
b) Preparation of diallyl/diphenyl thiosemicarbazides:



Step 4: The fourth step consisted of the synthesis of the isatin- β -thiosemicarbazones using the thiosemicarbazides obtained from Step 3 and the 5- substituted isatins of Step 2 as the starting reagents employing the reaction conditions of Schiff reaction, in the presence of sodium acetate and ethanol [102].



Step 5: The fifth and last step consisted of the synthesis of N-Mannich bases of the isatin- β -thiosemicarbazones obtained in the fourth step by reacting with various secondary amines and formaldehyde in the presence of microwave irradiation.



II. Biological intervention:

A. Anti-HIV activity

Cell Cultures

The compounds were tested for anti-HIV activity against replication of HIV-1 (IIIB) in MT-4 cells. The MT-4 cells were grown in RPMI-1640 DM (Dutch modification) medium (Flowlab, Irvine Schotland), supplemented with 10% (v/v) heat-inactivated fetal calf serum (FCS) and 20 µg/ml gentamicin (E. Merck, Darmstadt, Germany) [112, 113]. The cells were incubated at 37°C in a humidified atmosphere of 5% CO₂ in air. Every 3-4 days, cells were spun down and seeded at 3 x 10⁵ cells/ml in new cell culture flasks. At regular time intervals, the MT-4 cells were analyzed for the presence of mycoplasma and consistently found to be mycoplasma- free.

Virus

HIV-1 (strain HTLV – IIIB) [114] were obtained from the culture supernatant of HIV-1 infected MT-4 cell lines [115]. This virus titer of the supernatant was determined in MT – 4 cells. The virus stocks were stored at - 70°C until used.

Anti –HIV assay

Flat bottom, 96-well plastic microtiter trays (Falcon, Becton Dickinson, Mountain View, CA) were filled with 100 µL of complete medium using a Titertek Multidrop dispenser (Flow Laboratories). This eight-channel dispenser could fill a microtiter tray in less than 10s. Subsequently, stock solutions (10 x final test concentration) of compounds were added in 25 µl volumes to two series of triplicate wells so as to allow simultaneous evaluation of their effect on HIV and mock-infected cells. Serial five-fold dilutions were made directly in the microtiter trays using a Biomek 1000 robot (Beckman). Untreated control HIV– and mock-infected cell samples were included for each compound.

50 µl of HIV at 100 CCID₅₀ or medium was added to either infected or mock-infected part of microtiter. Exponentially growing MT-4 cells were centrifuged for 5 min at 140 x g and the supernatants were discarded. The MT-4 cells were resuspended at 6 x 10⁵ cells/ml in a flask, which was connected with an autoclavable dispensing cassette of a Titertek Multidrop dispenser. Under slight magnetic stirring 50 µl volumes were

then transferred to the microtiter tray wells. The outer row wells were filled with 200 μ l of medium. The cell cultures were incubated at 37 °C in a humidified atmosphere of 5 % CO₂ in air. The cells remained in contact with the test compounds during the whole incubation period. Five days after infection the viability of mock- and HIV-infected cells was examined spectrophotometrically by the 3-(4,5-dimethylthiazol-2-yl)-2, 5-diphenyltetrazolium bromide (MTT) method.

MTT assay

The MTT assay is based on the reduction of the yellow coloured 3-(4,5-dimethylthiazol-2-yl)-2, 5-diphenyltetrazolium bromide (MTT) (Sigma Chemical Co., St.Louis, MO) by mitochondrial dehydrogenase of metabolically active cells to a blue formazan which can be measured spectrophotometrically. Therefore, to each well of the microtiter trays, 20 μ l of a solution of MTT (7.5 mg/ml) in a phosphate-buffered saline was added using a Titertek Multidrop. The trays were further incubated at 37C in a CO₂ incubator for 1 h. A fixed volume of medium (150 μ l) was then removed from each cup using a M96 Washer (ICN flow) without disturbing the MT – 4 cell clusters containing the formazan crystals.

Solubilization of the formazan crystals was achieved by adding 100 μ l 10 % (v/v) Triton X-100 in acidified isopropanol (2 ml concentrated HCl per 500 ml solvent) using the M96 Washer (ICN flow). Complete dissolution of the formazan crystals could be obtained after the trays had been placed on a plate shaker for 10 min (ICN flow). Finally, the absorbances were read in an eight-channel computer-controlled photometer (Multiskan MCC, ICN flow) at two wavelengths (540 and 690 nm). The absorbance measured at 690 nm was automatically subtracted from the absorbance at 540 nm, so as to eliminate the effects of non-specific absorption. Blanking was carried out directly on the microtiter trays with the first column wells which contained all reagents except for the MT – cells. All data represent the average values for a minimum of three wells. The 50% cytotoxic dose (CD₅₀) was defined as the concentration of compound that reduced the absorbance (OD₅₄₀) of the mock-infected control sample by 50%. The percent protection achieved by the compounds in HIV-infected cells was calculated by the following formula:

$$\text{Expressed in \%} \quad \frac{(\text{OD}_T)_{\text{HIV}} - (\text{OD}_C)_{\text{HIV}}}{(\text{OD}_C)_{\text{mock}} - (\text{OD}_C)_{\text{HIV}}}$$

Whereby $(\text{OD}_T)_{\text{HIV}}$ is the optical density measured with a given concentration of the test compound in HIV-infected cells; $(\text{OD}_C)_{\text{HIV}}$ is the optical density measured for the control untreated HIV-infected cells; $(\text{OD}_C)_{\text{MOCK}}$ is the optical density measured for the control untreated mock-infected cells; all OD values determined at 540 nm. The dose achieving 50% protection according to the above formula was defined as the 50% effective dose (ED_{50}).

B. HIV-1 RT enzyme inhibition assay

The assay protocol involved a reaction mixture (50 μL) comprising of 50mM tris-HCl (pH 7.8), 5mM dithiothreitol, 30 mM glutathione, 50 μM EDTA, 150 mM KCl, 5mM MgCl_2 , 1.25 μg bovine serum albumin, an appropriate concentration of radiolabelled substrate [^3H] dGTP, 0.1 mM poly (vC)•oligo (dG) as the template/primer, 0.06 % Triton X-100, 10 μL of inhibitor solution (containing various concentrations of compounds), and 1 μL of RT preparation. The reaction mixtures were incubated for 15 min at 37°C, after which 100 μL of calf thymus DNA (150 $\mu\text{g}/\text{mL}$), 2mL of $\text{Na}_4\text{P}_2\text{O}_7$ (0.1 M in 1M HCl), and 2 ml of trichloroacetic acid (10 %v/v) were added. The solutions were kept on ice for 30 min, after which the acid-insoluble material was washed and analyzed for radioactivity. For the experiments in which 50 % inhibitory concentration (IC_{50}) of the test compounds was determined, fixed concentration of 2.5 μ [^3H] dGTP was used [116].

C. *In vitro* anti-tubercular activity in log phase cultures

All compounds were screened for their *in vitro* antimycobacterial activity against log-phase cultures of MTB in Middlebrook 7H11 agar medium supplemented with OADC by agar dilution method similar to that recommended by the National Committee for Clinical Laboratory Standards for the determination of MIC in

triplicate. The MIC is defined as the minimum concentration of compound required to produce complete inhibition of bacterial growth [117].

Test protocol:

(i) Micro-organism: *Mycobacterium tuberculosis* H37Rv ATCC 27294 obtained from Tuberculosis research center, Chennai, India.

(ii) Culture media: Middlebrook 7H11 agar with OADC growth supplement

Composition:

Middlebrook 7H9 broth base-	0.47g
Distilled water-	90 ml
Glycerol-	0.4 ml
Tween 80-	0.2 ml
OADC growth supplement:	
Bovine albumin fraction V-	0.5 g
Oleic acid-	0.02 ml
Dextrose-	0.2 g
Sodium chloride-	0.085 g
Distilled water-	10 ml

Method:

10 fold serial dilutions of each test compound was dissolved in DMSO and then incorporated into Middlebrook 7H11 agar medium supplemented with OADC. Inoculum of MTB H37RV were prepared from fresh Middlebrook 7H11 agar slants with OADC growth supplement adjusted to 1 mg/ml (wet weight) in Tween 80 (0.05%) saline diluted to 10^{-2} to give a concentration of approximately 10^7 cfu/ml. 5 μ l of bacterial suspension were then added into 7H11 agar tubes incorporated with the drug dilutions. Final readings were recorded after incubation at 37 °C for 28 days.

D. *In vitro* anti-tubercular activity in 6 week starved cultures

For starvation experiments, MTB cells were grown in Middlebrook 7H9 medium supplemented with 0.2% (v/v) glycerol, 10% (v/v) Middlebrook oleic acid-albumin-dextrose-catalase (OADC) enrichment, and 0.025% (v/v) Tween 80 at 37°C with constant rolling at 2 rpm until they reached an optical density at 600 nm of ~0.6. The

cells were then washed twice and re-suspended in phosphate-buffered saline (PBS) at the same cell density. Cells (50 ml of culture) were incubated at 37°C for an additional 6 weeks in 1-liter roller bottles. Compounds, dissolved in DMSO, were added to either 1 ml PBS containing $\sim 1 \times 10^7$ starved MTB cells at various concentrations. Cultures were incubated in 15-ml conical tubes at 37°C with constant shaking for 7 days and then washed twice in PBS before dilutions were plated on Middlebrook 7H11 plates supplemented with 0.2% (v/v) glycerol, 10% (v/v) Middlebrook OADC enrichment, and 0.025% (v/v) Tween 80, containing no antibiotics. Bacterial growth was determined after incubation for 4 weeks at 37°C. The MIC is defined as the minimum concentration of compound which brings about complete inhibition of bacterial growth. All values were determined in triplicate [118].

E. MTB ICL enzyme assay

Isocitrate lyase activity was determined at 37°C by measuring the formation of glyoxylate-phenylhydrazone at 324 nm. The reaction mixture contains 100 μ L of 0.5mM potassium phosphate buffer, 1.2 μ L of 1mM magnesium chloride, 24 μ L of 100 mM 2-mercaptoethanol, 7 μ L of 4mM phenylhydrazine hydrochloride, 6 μ L of 50 mM trisodiumisocitricacid and ICL enzyme (usually 3 to 6 μ L). This mixture is made up to 200 μ L with MilliQ water. At the end of the 10th minute this reaction mixture is made up to 1mL and UV absorbance is measured at 324nm which serves as a control. For the test compounds 3 μ L of 100mM 3-NPA was used and in case of the candidate molecules 10 μ L of 10mM concentration were added with the above mentioned reaction mixture. At the end of the 10th minute this reaction mixture is made up to 1mL and UV absorbance is measured at 324nm which serves as a test. The % inhibition is calculated by the formulae control absorbance minus test absorbance divided by control absorbance multiplied by 100 [119].

F. MTB DNA gyrase enzyme assay

In order to carry out gyrase inhibition assays, DNA gyrase purified from MC₂ was used. The enzyme was prepared and stored by standardized procedures [120]. The

compounds tested were dissolved in 5 % DMSO and pre-incubated with gyrase. Supercoiling assays were carried out as described previously [120], by incubating 400 ng of relaxed pUC18 at 37°C in supercoiling buffer [35 mM Tris-HCl pH 7.5, 5mM MgCl₂, 25 mM potassium glutamate, 2 mM spermidine, 2 mM ATP, 50 µ/ml bovine serum albumin, and 90 µ/ml yeast t-RNA in 5 % v/v glycerol] for 1 hour. Ciprofloxacin at 10µg/mL and moxifloxacin at 5µg/mL final concentrations were used as positive controls and a control reaction having 5 % DMSO in absence of compounds was also performed. The reaction samples were heat inactivated and applied on to 1% agarose gel electrophoresis in Tris-acetate-EDTA buffer for 12 hours. The gels were stained with ethidium bromide and recorded by gel documentation.

G. Antiviral and Cytotoxicity assay for HCV

Cell culture

The cell line Huh7 ET (luc-ubi-neo/ET), which contains a new HCV RNA replicon with a stable luciferase (LUC) reporter, was maintained in Dulbecco's modified Eagle's medium (DMEM) (Life Technologies) supplemented with 10% fetal bovine serum, 1% L-glutamine, 1% L-pyruvate, 1% penicillin and 1% streptomycin supplemented with 500 µg/mL G418 (Geneticin, Invitrogen) [121]. Cells were passaged every four days.

Primary HCV RNA replicon assay

The effect of drugs added in triplicate, was examined at a single high-test concentration of 20 µM on HCV RNA-derived LUC activity and cytotoxicity. Human interferon α -2b was included in each run as a positive control compound. Subconfluent cultures of the ET line were plated out into 96-well plates that were dedicated for the analysis of cell numbers (cytotoxicity) or antiviral activity and the next day drugs were added to the appropriate wells. Cells were processed 72 hr later when the cells were still subconfluent. Compounds that reduced the LUC signal by 50% or more relative to the untreated cell controls moved forward in the

program. Compound cytotoxicity was assessed as the percent viable cells relative to the untreated cell controls. [122].

H. Antiviral and Cytotoxicity assay against Influenza Type A and B viruses and SARS virus

Cell culture used

- (i) For Influenza Type A and B viruses: Madin Darby canine kidney (MDCK) cells.
- (ii) For SARS virus: Vero 76 cells.

This procedure involved testing of the drugs at 2 concentrations (200, 20 µg/ml). These were diluted 1:2 when virus was added, thus making the final concentrations 100 and 10 µg/ml. The standard CPE test used an 18 h monolayer (80-100% confluent) of the appropriate cells, the medium was drained and each of the concentrations of test compound or placebo were added, which was followed within 15 min by virus or virus diluent. Two wells were used for each concentration of compound for both antiviral and cytotoxicity testing. The plate was sealed and incubated for the standard time period required to induce near-maximal viral CPE. The plate was then stained with neutral red by the method described below and the percentage of uptake indicating viable cells read on a microplate autoreader at dual wavelengths of 405 and 540 nm, with the difference taken to eliminate background. An approximated virus-inhibitory concentration, 50% endpoint (EC₅₀) and cell-inhibitory concentration, 50% endpoint (IC₅₀) were determined from which a general selectivity index was calculated: $SI = (IC_{50}) / (EC_{50})$. An SI of 3 or greater indicated that confirmatory testing was needed.

Standard Assay: Inhibition of Viral Cytopathic Effect (CPE)

This test, run in 96 well flat-bottomed microplates, was used for the initial antiviral evaluation of all new test compounds. In this CPE inhibition test, four log₁₀ dilutions of each test compound (e.g. 1000, 100, 10, 1 µg/ml) were added to 3 cups containing the cell monolayer; and within 5 min, the virus was then added and the plate sealed, incubated at 37°C and CPE read microscopically when untreated infected controls developed a 3 to 4+ CPE (approximately 72 to 120 h).

A known positive control drug was evaluated in parallel with test drugs in each test. This drug was ribavirin for influenza A and B and alferon (interferon α -n3) for SARS virus.

The data were expressed as 50% effective concentrations (EC_{50}).

Standard Assay: Increase in Neutral Red (NR) Dye Uptake

This test was run to validate the CPE inhibition seen in the initial test, and utilized the same 96-well micro plates after the CPE was read. Neutral red was added to the medium; cells not damaged by virus took up a greater amount of dye, which was read on a computerized micro plate autoreader. An EC_{50} is determined from this dye uptake.

Cytotoxicity assay

In the CPE inhibition tests, two wells of uninfected cells treated with each concentration of test compound were run in parallel with the infected, treated wells. At the time CPE was determined microscopically, the toxicity control cells were also examined microscopically for any changes in cell appearance compared to normal control cells run in the same plate. These changes were enlargement, granularity, cells with ragged edges, a filmy appearance, rounding, detachment from the surface of the well, or other changes. These changes were given a designation of T (100% toxic), PVH (partially toxic–very heavy–80%), PH (partially toxic–heavy–60%), P (partially toxic–40%), Ps (partially toxic–slight–20%), or 0 (no toxicity–0%), conforming to the degree of cytotoxicity seen.

A 50% cell inhibitory (cytotoxic) concentration (IC_{50}) was determined by regression analysis of these data [123, 124].

III. Computational methodology:

A. 3D-QSAR Analysis

The molecular modeling studies namely, CoMFA, Advanced CoMFA and CoMSIA were performed using SYBYL6.9 molecular modeling software running on a Silicon Graphics Octane R12000³⁸ workstation. The structures were built in 2D using MDL ISIS Draw 2.5 software, and were imported to Discovery Studio 2.0 (Catalyst) software. CHARMM force field was applied to the molecules and later energy minimized. These 3D structures were then exported to the SYBYL6.9 workstation where partial charges were calculated using Gasteiger-Hückel method geometry optimized using Tripos force field with a distance-dependent dielectric function until a root mean square deviation (RMSD) of 0.01kcal/mol Å was achieved. Two different alignment techniques viz. (a) common substructure fitting method and (b) manual alignment method were compared to obtain the most efficient alignment for this set of structurally diverse molecules. The common substructure fitting method involves superimposition of all the molecules to a common substructure of the template molecule. In the manual method, the molecules were aligned manually over a template molecule. Amongst the two, manual alignment method gave better results.

Data Sets. The compounds were divided into training set and test set taking into account either the structural aspects or the anti-HIV inhibitory profile of compounds. The training set was chosen according to these criteria: (i) the most- and least-active compounds were both included.; (ii) compounds were chosen in such a way that the entire activity range was uniformly sampled; and (iii) structural superfluity was avoided by selecting compounds with different substituents or substitution patterns.

CoMFA Studies. The CoMFA calculations were done using Tripos Standard and Advanced CoMFA modules in SYBYL. For each alignment, an sp³ carbon atom having a charge of +1 and a radius of 1.52 Å was used as a probe to calculate various steric and electrostatic fields, the grid spacing was set to 2Å and the region was calculated automatically. To investigate the influence of different parameter settings on CoMFA, various steric and electrostatic cutoffs and grid spacing were set to 30kcal/mol [125].

Advanced CoMFA. H-bonding, indicator and parabolic fields were used in the Advanced CoMFA routine. Lattice points with steric energies below the steric cutoff

energy were assigned nominal energies equal to the steric cutoff energies if they were close to H-bond accepting or donating atoms. Indicator fields replaced all lattice energies with magnitudes below a designated threshold with zero values. All energies at or above that threshold were replaced with a nominal energy equal in magnitude to the relevant field cutoff value. When both fields were included in a single CoMFA column, the greater of the steric and electrostatic cutoffs was used. The sign of the original lattice energy is retained. Parabolic fields are those in which the magnitude of a standard steric and/or electrostatic field at each lattice point has been squared; the original sign of the energy is retained.

CoMFA Region Focusing. CoMFA region focusing is a method of application of weights to the lattice points in a CoMFA region to enhance or attenuate the contribution of these points to subsequent analysis. In this study, discriminant power values as weights and different factors were applied in addition to grid spacing for getting better models.

CoMSIA Studies. Five similarity fields namely, steric, electrostatic, and hydrophobic, hydrogen bond donor and acceptor were calculated. The lattice dimensions were selected with a sufficiently large margin extended up to 4 Å surrounding all aligned molecules. In CoMSIA, the steric indices are related to the third power of the atomic radii, the electrostatic descriptors are derived from atomic partial charges, the hydrophobic fields are derived from atom-based parameters, and the hydrogen bond donor and acceptor indices are obtained by a rule-based method derived from experimental values. In the present work, similarity indices were computed using a probe atom with radius 1.0 Å, charge +1, hydrophobicity +1, hydrogen bond donor and acceptor properties of +1 and attenuation factor of 0.3 for the Gaussian type distance function [126].

Validation of Models. PLS analysis was used to correlate the activities with CoMFA and CoMSIA values containing the steric and electrostatic potentials. The models were cross-validated using the Leave One Out (LOO) method by SAMPLS method. The LOO method involves excluding one compound from the data set and then deriving a model using the rest. Then with the help of this derived model, the activity of the excluded molecule is determined. CoMFA standard scaling was applied to all the CoMFA analyses. The full PLS analysis was run with a column filtering of 2.0kcal/mol to reduce

the noise and to speed up the calculations. In case of CoMSIA as well, SAMPLS method was used. This was followed by a full PLS analysis, which was run using column filtering of 2.0kcal/mol. Autoscaling was applied to all CoMSIA analyses.

B. Docking calculations onto HIV-1 RT

A crystallographic structure of HIV-1 RT in complex with nevirapine (PDB code 1VRT) [127] was used as protein starting structure for the docking simulation. Each inhibitor was built using Schrodinger Maestro and energy minimized in the same program and then docked onto RT using GOLD [128] and Autodock 4.0 [129] with the active site being defined using active atoms generated while redocking nevirapine onto HIV-1 RT. All the water molecules and the metal ions were removed from the protein structure prior to docking. Fifty genetic algorithms were performed for each ligand, with 100000 energy evaluations.

C. Docking calculations onto MTB ICL

Three dimensional coordinates of the MTB ICL/BP complex (RCSB PDB entry 1F8M) [130] were used as the input structure for docking simulations performed on Autodock 4.0 due to the highly rigid structure of the molecule. The cocrystallized ligand was deleted from the protein structure. The protein was prepared using Schrodinger's protein preparation wizard only for hydrogen minimization. Schrodinger Maestro was used for ligand building and energy minimized and saved in *.mol format and then imported to Autodock 4.0. Grids of molecular interactions were considered in a cubic box of 50×50×50 with grid spacing of 0.375 Å. The active site was centered on the coordinate 19.4465, 41.903, and 53.181. Few of the residues were assigned flexibility. Docking was performed 50 times using the Lamarckian genetic algorithm and a maximum of 250 000 energy evaluations. The final docked conformations were ranked according to their binding free energy.

CHAPTER 5

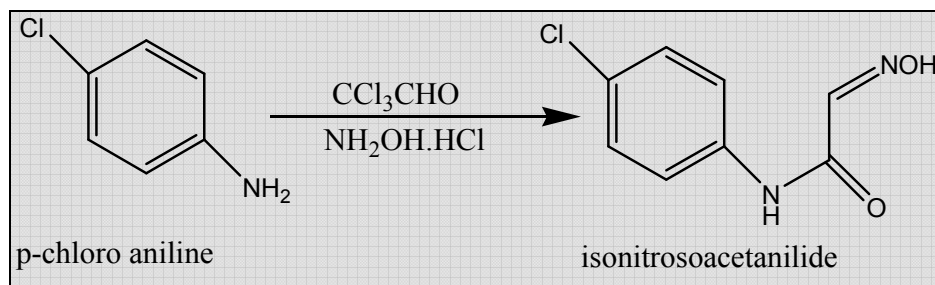
SYNTHESIS, BIOLOGICAL INTERVENTION AND COMPUTATIONAL STUDY OF N-MANNICH BASES OF 5-SUBSTITUTED-1H-INDOLE-2, 3-DIONE 3-(N-HYDROXY/METHOXYTHIOSEMICARBAZONES)

This chapter describes the synthesis, biological intervention and computational study of N-Mannich bases of 5-substituted-1H-indole-2, 3-dione 3-(N-hydroxy/methoxythiosemicarbazones, since it was observed from earlier works that N-Mannich bases of 1H-indole-2,3-dione-3-(N,N-diethylthiosemicarbazone) have considerable potential against the replication of HIV-1 cells along with broad-spectrum chemotherapeutic properties [93]. Considering this molecule as a lead, the titled compounds were designed and synthesized with the aim to treat HIV-TB co-infection.

5.1 Synthesis

Step I: Synthesis of Isatin

a) Synthesis of 4-chloroisitonrosoacetanilide from 4-chloro aniline



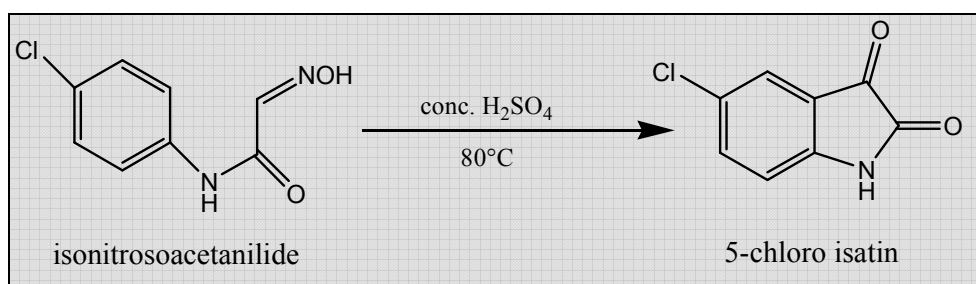
18 g (0.108 moles) of chloral hydrate dissolved in 240 ml of water was placed in a round-bottomed flask, to which was added, in sequence, 26 g of sodium sulfate, a solution of 12.7 g (0.1 mole) of *p*-chloro aniline in 60 ml water containing 10.24 g (8.6 ml, 0.104 mole) of concentrated hydrochloric acid to dissolve the aniline, followed by a solution of 22g (0.316 moles) of hydroxylamine hydrochloride solubilised in 100 ml of water. The flask was then slowly heated so that vigorous boiling began in approximately forty to forty-five minutes. The reaction attained completion following one to two minute of vigorous boiling. The flask was then subjected to cooling under running tap-water;

whereby the crystals of 4-chloro isonitrosoacetanilide separated out. It was then filtered with suction and then air-dried. The yield was 9.77 g (49.5% of theoretical yield) and melting point was reported to be between 158-160°C.

% yield of 4-methyl isonitrosoacetanilide- 52.6 % and M.P- 192-194°C

% yield of 4-fluoro isonitrosoacetanilide- 64% and M.P- 196°C.

b) Synthesis of 5-chloro isatin from 4-chloroisonitrosoacetanilide



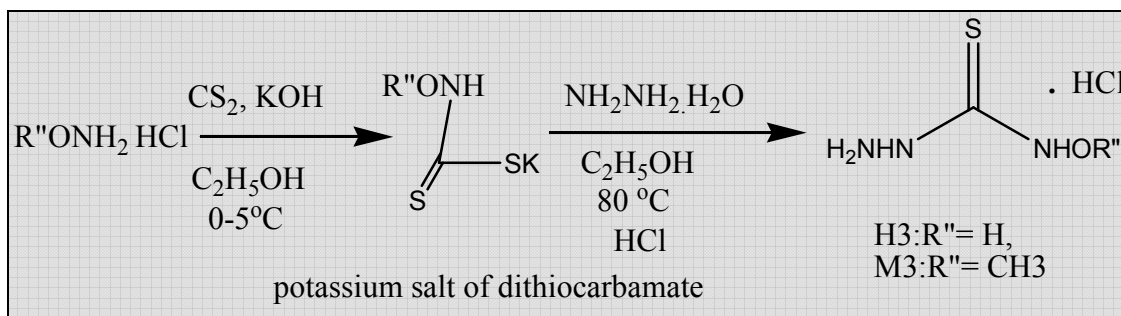
78.1 g (42.3 ml) of concentrated sulfuric acid was warmed to 50°C and to this warm sulfuric acid was added slowly the dry 4-chloroisonitrosoacetanilide in such a manner that the temperature was maintained between 60°C and 70°C. During addition the reaction vessel was also subjected to external cooling for speeding up the reaction rate. After the completion of isonitrosoacetanilide addition, the reaction mixture was heated to 80°C and this temperature was maintained for about 10 minutes till the reaction attained completion. After which it was cooled to room temperature and was poured upon ten to twelve times its volume of crushed ice. This was allowed to stand for about 90 minutes and was then filtered with suction, washed several times with cold water to remove any residual sulfuric acid, and then dried in air. The yield of crude isatin was reported to be 5.74 g (64.27 % of theoretical yield) and melting point was reported to be between 236-238°C. IR (KBr pellet) ν_{max} 3200, 1720, 1610 cm^{-1} ; $^1\text{H-NMR}$ (DMSO $-\text{d}_6$) δ 7.53-7.80 (d, 3H, Ar-H), 8.7 (s, 1H, N-H D_2O exchangeable).

5-fluoro and 5-methyl isatins were also prepared in similar manner using appropriate moles of 4-fluoroaniline and p-toluidine respectively employing the above mentioned synthetic protocol.

% yield of 5-methyl isatin-87.22% and M.P- 186-188°C

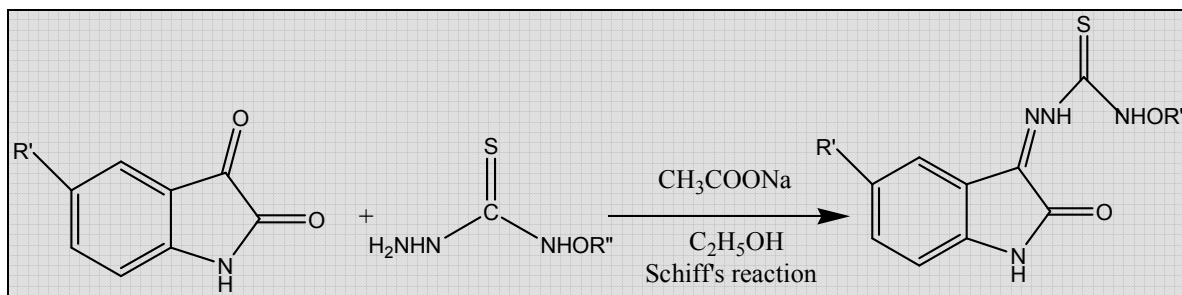
% Yield of 5-fluoro isatin- 74.13 % and M.P- 225°C.

Step II: Synthesis of hydroxy/methoxy thiosemicarbazides (H3, M3)



To a solution of *N*-hydroxylamine(**H1**)/*N*-methoxylamine(**M1**) (0.01 mol) in absolute ethanol (20 ml) was added potassium hydroxide (0.01 mol) and carbon disulphide (0.75 ml), and the mixture was stirred at 0-5°C for 1 h to form the corresponding potassium salt of dithiocarbamates (**H2**,**M2**). To the stirred mixture of dithiocarbamate salts was added hydrazine hydrate (0.01 mol) and the stirring was continued at 80°C for 1 h and on adding upon crushed ice the corresponding thiosemicarbazide was obtained which is converted to hydrochloride salts (**H3**,**M3**). **H3**: Yield: 6.96%; M.P: 258-260°C; **M3**: Yield: 50.96%; M.P: 100-102°C.

Step III: Synthesis of isatin-β-thiosemicarbazones (H4-6, M4-6)



To a hot dispersion of **H3**/**M3** (0.001M) in ethanol was added an equimolar aqueous solution of sodium acetate. To this solution further an equimolar ethanolic solution of various 5-substituted isatin was added and the mixture was stirred while being heated on

a hot plate for 4-15 minutes, with immediate precipitation of a bulky solid. The resultant precipitate was filtered off and dried. The product was recrystallized from 95% ethanol.

Table 5.1: Physical data of synthesized Schiff base

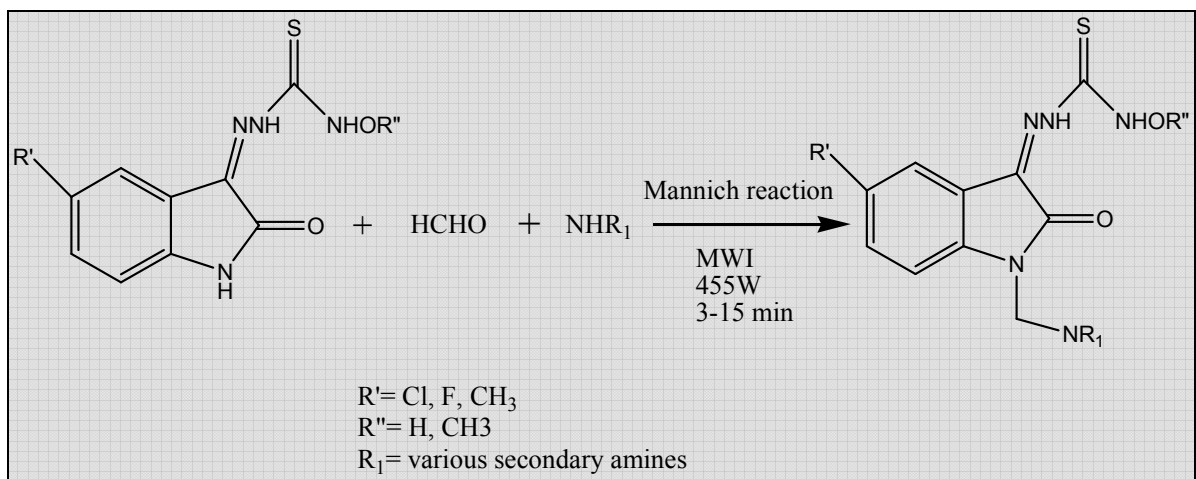
Compound code	R'	R''	% Yield	M.P (°C)	Molecular formula	Mol. Wt.
H4	Cl	H	62.96	210 ^a	C ₉ H ₇ ClN ₄ O ₂ S	270.7
H5	F	H	56.57	223-225	C ₉ H ₇ FN ₄ O ₂ S	254.24
H6	CH ₃	H	63.63	197-200	C ₁₀ H ₁₀ N ₄ O ₂ S	250.28
M4	Cl	CH ₃	35.63	223-225	C ₁₀ H ₉ ClN ₄ O ₂ S	284.72
M5	F	CH ₃	27.54	214-216	C ₁₀ H ₉ FN ₄ O ₂ S	268.27
M6	CH ₃	CH ₃	34.72	186-188	C ₁₁ H ₁₂ N ₄ O ₂ S	264.3

^a Melting point of the compounds at their decomposition.

Table 5.2: Spectral data of the synthesized Schiff bases

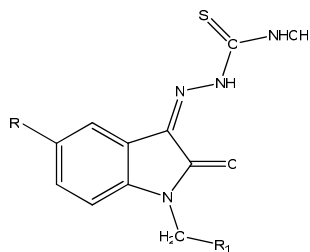
Compound code	IR spectroscopy (cm ⁻¹ ; KBr pellet)	¹ H-NMR (δ ppm, DMSO-d ₆)
H5	1740 (amide stretch), 1625 (C=N stretch), 3010 (Aromatic C-H stretch), 3300 (amide NH stretch)	7.02 (d, 1H at C ₆ of indolyl), 7.37 (d, 1H at C ₇ of indolyl), 7.61 (s, 1H at N ₁ of indolyl), 7.79 (s, 1H at C ₄ of indolyl), 8.37 (m, 3H, hydroxythiosemicarbazone protons).
M6	1740 (amide stretch), 1625 (C=N stretch), 3010 (Aromatic C-H stretch), 3300 (amide NH stretch)	2.57 (s, 3H, methoxy), 3.53 (s, 3H, CH ₃ of methoxy), 6.92 (d, 1H at C ₆ of indolyl), 7.16 (d, 1H at C ₇ of indolyl), 7.63 (s, 1H at N ₁ of indolyl), 7.89 (s, 1H at C ₄ of indolyl), 8.87 (s, 1H at N of hydrazine), 9.17 (s, 1H at N of N-methoxy).

Step IV: Synthesis of *N*-Mannich bases of isatin- β -thiosemicarbazones (H7-36, M7-36)

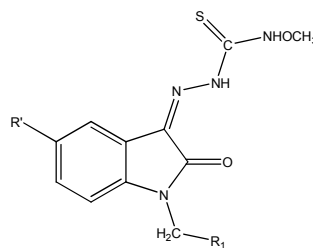


To an ethanolic solution of *N*-hydroxy/methoxy thiosemicarbazones (0.00045M) was added an equimolar amount of various secondary amines, dissolved in ethanol or dimethyl sulfoxide. To this mixture, an equimolar amount of 30% formaldehyde solution was then added and this mixture was then irradiated with microwave of 455W in a scientific microwave reactor accompanied by continuous stirring, which was attained by means of a magnetic plate, placed underneath the floor of the magnetic cavity and a Teflon-coated magnetic bead in the reaction vessel, for approximately three to fifteen minutes. At the end of the reaction period, the product precipitated out, which was filtered off and dried. The resultant precipitate was recrystallized from ethanol. The physical data of the Mannich bases are given in Tables 5.3-5.5. The spectral and elemental data of representative compounds are presented in Table 5.6-5.11.

Table 5.3: Physical data of *N*-Mannich bases of isatin- β -thiosemicarbazones (H7-H16)



H7-H36



M7-M36

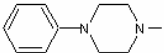
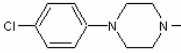
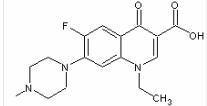
Compound code	Substituents		M.P (°C)	% Yield	Molecular Formula	Mol. Wt.	R _f ^b	logP ^c
	R'	R ₁						
H7	Cl	---N(CH ₃) ₂	102-104	97.05	C ₁₂ H ₁₄ ClN ₅ O ₂ S	327.79	0.52	1.72
M7	Cl	-do-	60-62	98.28	C ₁₃ H ₁₆ ClN ₅ O ₂ S	341.82	0.56	1.98
H8	F	-do-	40-42	87.10	C ₁₂ H ₁₄ FN ₅ O ₂ S	311.34	0.51	1.31
M8	F	-do-	56-58	82.45	C ₁₃ H ₁₆ FN ₅ O ₂ S	325.36	0.53	1.58
H9	CH ₃	-do-	110	95.85	C ₁₃ H ₁₇ N ₅ O ₂ S	307.37	0.56	1.64
M9	CH ₃	-do-	82-84	93.45	C ₁₄ H ₁₉ N ₅ O ₂ S	321.4	0.59	1.91
H10	Cl	---N(C ₂ H ₅) ₂	125-127	98.61	C ₁₄ H ₁₈ ClN ₅ O ₂ S	355.84	0.58	2.39
M10	Cl	-do-	52-54	69.28	C ₁₅ H ₂₀ ClN ₅ O ₂ S	369.87	0.61	2.65
H11	F	-do-	80-82	79.90	C ₁₄ H ₁₈ FN ₅ O ₂ S	339.39	0.55	1.99
M11	F	-do-	98-100	83.50	C ₁₅ H ₂₀ FN ₅ O ₂ S	353.42	0.58	2.25
H12	CH ₃	-do-	114-116	71.47	C ₁₅ H ₂₁ N ₅ O ₂ S	335.42	0.62	2.32
M12	CH ₃	-do-	88-90	68.81	C ₁₆ H ₂₃ N ₅ O ₂ S	349.16	0.64	2.58
H13	Cl		46-48	56.43	C ₁₄ H ₁₆ ClN ₅ O ₃ S	369.83	0.46	1.32
M13	Cl	-do-	72-74	98.90	C ₁₅ H ₁₈ ClN ₅ O ₃ S	383.85	0.47	1.58
H14	F	-do-	36-38	64.75	C ₁₄ H ₁₆ FN ₅ O ₃ S	353.37	0.41	0.92
M14	F	-do-	80-84	89.53	C ₁₅ H ₁₈ FN ₅ O ₃ S	367.4	0.43	1.18
H15	CH ₃	-do-	58-62	64.47	C ₁₅ H ₁₉ N ₅ O ₃ S	349.41	0.46	1.24
M15	CH ₃	-do-	86-90	75.70	C ₁₆ H ₂₁ N ₅ O ₃ S	363.43	0.48	1.51
H16	Cl		148-150	87.21	C ₂₀ H ₂₁ ClN ₆ O ₂ S	444.94	0.51	3.55

^a Melting point of the compound at their decomposition.

^b Mobile phase CHCl₃ : CH₃OH (9 : 1).

^c LogP was calculated using ChemOffice 2004

Table 5.4: Physical data of *N*-Mannich bases of isatin- β -thiosemicarbazones (M16-M27)

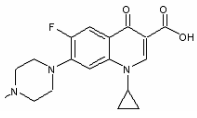
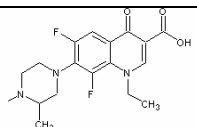
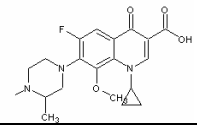
Compound code	Substituents		M.P (°C)	% Yield	Molecular Formula	Mol. Wt.	R _f ^b	logP ^c
	R'	R ₁						
M16	Cl		80-82	93.33	C ₂₁ H ₂₃ ClN ₆ O ₂ S	458.96	0.52	3.81
H17	F	-do-	78-80	86.09	C ₂₀ H ₂₁ FN ₆ O ₂ S	428.48	0.43	3.15
M17	F	-do-	108-110	79.94	C ₂₁ H ₂₃ FN ₆ O ₂ S	442.51	0.45	3.41
H18	CH ₃	-do-	68-70	79.93	C ₂₁ H ₂₄ N ₆ O ₂ S	424.52	0.47	3.47
M18	CH ₃	-do-	87-89	83.57	C ₂₂ H ₂₆ N ₆ O ₂ S	438.55	0.49	3.74
H19	Cl		110-112	92.40	C ₂₀ H ₂₀ Cl ₂ N ₆ O ₂ S	479.38	0.44	4.1
M19	Cl	-do-	208-210	74.26	C ₂₁ H ₂₂ Cl ₂ N ₆ O ₂ S	493.41	0.45	4.37
H20	F	-do-	72-74	73.50	C ₂₀ H ₂₀ ClFN ₆ O ₂ S	462.93	0.39	3.7
M20	F	-do-	202	76.87	C ₂₁ H ₂₂ ClFN ₆ O ₂ S	476.95	0.41	3.97
H21	CH ₃	-do-	178-182	76.34	C ₂₁ H ₂₃ ClN ₆ O ₂ S	458.96	0.42	4.03
M21	CH ₃	-do-	140	85.46	C ₂₂ H ₂₅ ClN ₆ O ₂ S	472.99	0.43	4.3
H22	Cl		140	58.32	C ₂₁ H ₂₃ ClN ₆ O ₃ S	474.96	0.45	3.42
M22	Cl	-do-	108-110	73.92	C ₂₂ H ₂₅ ClN ₆ O ₃ S	488.99	0.47	3.68
H23	F	-do-	54-56	60.38	C ₂₁ H ₂₃ FN ₆ O ₃ S	458.51	0.42	3.02
M23	F	-do-	116-118	69.35	C ₂₂ H ₂₅ FN ₆ O ₃ S	472.54	0.43	3.28
H24	CH ₃	-do-	216-218	88.66	C ₂₂ H ₂₆ N ₆ O ₃ S	454.55	0.49	3.35
M24	CH ₃	-do-	98-102	61.11	C ₂₃ H ₂₈ N ₆ O ₃ S	468.57	0.51	3.61
H25	Cl		166-168	71.55	C ₂₆ H ₂₅ ClFN ₇ O ₅ S	602.04	0.37	3.21
M25	Cl	-do-	170-174	98.59	C ₂₇ H ₂₇ ClFN ₇ O ₅ S	616.06	0.39	3.48
H26	F	-do-	88-90	72.88	C ₂₆ H ₂₅ F ₂ N ₇ O ₅ S	585.58	0.35	2.81
M26	F	-do-	66-68	93.50	C ₂₇ H ₂₇ F ₂ N ₇ O ₅ S	599.61	0.37	3.08
H27	CH ₃	-do-	180-182 ^a	47.33	C ₂₇ H ₂₈ FN ₇ O ₅ S	581.62	0.41	3.14
M27	CH ₃	-do-	158-162 ^a	67.23	C ₂₈ H ₃₀ FN ₇ O ₅ S	595.65	0.42	3.41

^a Melting point of the compound at their decomposition.

^b Mobile phase CHCl₃ : CH₃OH (9 : 1).

^c LogP was calculated using ChemOffice 2004

Table 5.5: Physical data of *N*-Mannich bases of isatin- β -thiosemicarbazones (H28-M36)

Compound code	Substituents		M.P (°C)	% Yield	Molecular Formula	Mol. Wt.	R _f ^b	logP ^c
	R'	R ₁						
H28	Cl		210 ^a	92.05	C ₂₇ H ₂₅ ClFN ₇ O ₅ S	614.05	0.51	3.17
M28	Cl	-do-	128-130 ^a	72.53	C ₂₈ H ₂₇ ClFN ₇ O ₅ S	628.07	0.53	3.43
H29	F	-do-	230 ^a	90.62	C ₂₇ H ₂₅ F ₂ N ₇ O ₅ S	597.59	0.49	2.77
M29	F	-do-	184 ^a	65.08	C ₂₈ H ₂₇ F ₂ N ₇ O ₅ S	611.62	0.51	3.03
H30	CH ₃	-do-	40	71.67	C ₂₈ H ₂₈ FN ₇ O ₅ S	593.63	0.52	3.1
M30	CH ₃	-do-	150-154 ^a	85.67	C ₂₉ H ₃₀ FN ₇ O ₅ S	607.66	0.54	3.36
H31	Cl		226-228	88.59	C ₂₇ H ₂₆ ClF ₂ N ₇ O ₅ S	634.05	0.47	3.69
M31	Cl	-do-	>230	48.33	C ₂₈ H ₂₈ ClF ₂ N ₇ O ₅ S	648.08	0.48	3.95
H32	F	-do-	130 ^a	61.75	C ₂₇ H ₂₆ F ₃ N ₇ O ₅ S	617.6	0.46	3.29
M32	F	-do-	180 ^a	72.90	C ₂₈ H ₂₈ F ₃ N ₇ O ₅ S	631.63	0.47	3.55
H33	CH ₃	-do-	140-144	72.36	C ₂₈ H ₂₉ F ₂ N ₇ O ₅ S	613.64	0.49	3.62
M33	CH ₃	-do-	206-210 ^a	81.22	C ₂₉ H ₃₁ F ₂ N ₇ O ₅ S	627.66	0.52	3.88
H34	Cl		136-138	90.92	C ₂₉ H ₂₉ ClFN ₇ O ₆ S	658.1	0.53	3.36
M34	Cl	-do-	154-156	28.47	C ₃₀ H ₃₁ ClFN ₇ O ₆ S	672.13	0.55	3.63
H35	F	-do-	70-74	66.79	C ₂₉ H ₂₉ F ₂ N ₇ O ₆ S	641.65	0.49	2.96
M35	F	-do-	88-90	70.23	C ₃₀ H ₃₁ F ₂ N ₇ O ₆ S	655.67	0.51	3.23
H36	CH ₃	-do-	70	77.75	C ₃₀ H ₃₂ FN ₇ O ₆ S	637.68	0.54	3.29
M36	CH ₃	-do-	70-72	46.09	C ₃₁ H ₃₄ FN ₇ O ₆ S	651.71	0.56	3.56

^a Melting point of the compound at their decomposition.

^b Mobile phase CHCl₃ : CH₃OH (9 : 1).

^c LogP was calculated using ChemOffice 2004

Table 5.6: Spectral and elemental data of *N*-Mannich bases of isatin- β -thiosemicarbazones

Compound	IR Spectroscopy (cm ⁻¹ ; KBr)	¹ H-NMR (δ ppm, DMSO-d ₆)	Elemental Analyses (Calculated/Found) ^a			Mass Spectrometry (m/z)
			C (%)	H (%)	N (%)	
H7	3030, 2850, 1730, 1620, 1210, 850.	2.07 (s, 6H, dimethylamine), 5.92 (s, 2H, -NCH ₂ N-), 6.61 (d, 1H, indolyl C ₇), 6.92 (d, 1H, indolyl C ₆), 7.35 (s, 1H, indolyl C ₄) 8.51 (s, 1H, hydrazino), 9.48 (d, 1H, NH of hydroxylamine), 10.52 (d, 1H, OH proton)	43.97 43.79	4.30 4.26	21.37 21.35	327.06
H11	3040, 2855, 1735, 1621, 1215, 843.	1.03 (t, 6H, (CH ₂ CH ₃) ₂), 2.59 (q, 4H, (CH ₂ CH ₃) ₂), 5.94 (s, 2H, -NCH ₂ N-), 6.65 (d, 1H, C ₇ of indolyl), 7.22 (d, 1H, C ₆ of indolyl), 7.83 (s, 1H, C ₄ of indolyl), 8.52 (s, 1H, hydrazino), 9.49 (d, 1H, NH of hydroxylamine), 10.45 (d, 1H, OH proton)	49.54 49.37	5.35 5.33	20.64 20.69	339.12
H13	3020, 2847, 1725, 1615, 1220, 852.	2.64 (t, 4H, C ₃ ,C ₅ of morpholiny), 3.55 (t, 4H, C ₂ , C ₆ of morpholiny), 5.67 (s, 2H, -NCH ₂ N-), 6.91 (d, 1H, C ₇ of indolyl), 7.41 (d, 1H, C ₆ of indolyl), 8.04 (s, 1H, C ₄ of indolyl), 8.49 (s, 1H, hydrazino), 9.46 (d, 1H, NH of hydroxylamine), 10.51 (d, 1H, OH proton)	45.47 45.44	4.36 4.35	18.94 18.89	369.07
H18	3030, 2850, 1731, 1622, 1210, 845.	2.26 (s, 3H, CH ₃), 3.15 (t, 4H, C ₂ , C ₆ of piperaziny), 3.17 (t, 4H, C ₃ ,C ₅ of piperaziny), 5.13 (s, 2H, -NCH ₂ N-), 6.41 (d, 2H, C ₂ , C ₆ of phenyl), 6.71 (d, 1H, C ₇ of indolyl), 6.77 (m, 1H, C ₄ of phenyl), 7.11 (d, 1H, C ₆ of indolyl), 7.35 (d, 2H, C ₃ , C ₅ of phenyl), 7.76 (s, 1H, C ₄ of indolyl), 8.52 (s, 1H, hydrazino), 9.47 (d, 1H, NH of hydroxylamine), 10.53 (d, 1H, OH proton)	59.41 59.39	5.70 5.71	19.80 19.78	424.17

^a Elemental analyses for C, H, N were within ± 0.4 % of the theoretical values.

Table 5.7: Spectral and elemental data of *N*-Mannich bases of isatin- β -thiosemicarbazones

Compound	IR Spectroscopy (cm ⁻¹ ; KBr)	¹ H-NMR (δ ppm, DMSO-d ₆)	Elemental Analyses (Calculated/Found) ^a			Mass Spectrometry (m/z)
			C (%)	H (%)	N (%)	
H21	3015, 2853, 1727, 1625, 1220, 853.	2.56 (s, 3H, CH ₃), 3.14 (t, 4H, C ₂ , C ₆ of piperazinyl), 3.18 (t, 4H, C ₃ , C ₅ of piperazinyl), 5.73 (s, 2H, -NCH ₂ N-), 6.34 (d, 2H, C ₂ , C ₆ of phenyl), 6.63 (d, 1H, C ₇ of indolyl), 6.81 (d, 2H, C ₃ , C ₅ of phenyl), 7.54 (s, 1H, C ₄ of indolyl), 8.53 (s, 1H, hydrazino), 9.47 (d, 1H, NH of hydroxylamine), 10.53 (d, 1H, OH proton)	54.96 55.16	5.05 5.03	18.31 18.27	458.13
H22	3025, 2845, 1720, 1622, 1230, 848.	3.15 (t, 4H, C ₂ , C ₆ of piperazinyl), 3.21 (t, 4H, C ₃ , C ₅ of piperazinyl), 3.77 (s, 3H, 4-methoxyphenyl) 5.16 (s, 2H, -NCH ₂ N-), 6.16(d, 2H, C ₂ , C ₆ of phenyl), 7.43 (d, 1H, C ₇ of indolyl), 6.62 (d, 2H, C ₃ , C ₅ of phenyl), 6.89 (d, 1H, C ₆ of indolyl), 8.14 (s, 1H, C ₄ of indolyl), 8.53 (s, 1H, hydrazino), 9.46 (d, 1H, NH of hydroxylamine), 10.51 (d, 1H, OH proton)	53.10 52.91	4.88 4.89	17.69 17.63	474.12
H27	3455, 3040, 2835, 1728, 1615, 1225, 846.	1.21 (t, 3H, CH ₃ of C ₂ H ₅), 2.37 (s, 3H, methyl at C ₅ of indole), 3.11 (t, 4H, C ₂ , C ₆ of piperazinyl), 3.15 (t, 4H, C ₃ , C ₅ of piperazinyl), 4.26 (q, 2H, CH ₂ of C ₂ H ₅), 5.16 (s, 2H, methylene CH ₂), 6.21 (s, 1H at C ₈ of quinoliny), 6.73 (d, 1H at C ₇ of indolyl), 7.14 (d, 1H at C ₆ of indolyl), 7.25 (s, 1H at C ₅ of quinoliny), 7.29 (s, 1H at C ₄ of indolyl), 7.35 (s, 1H at C ₂ of quinoliny), 8.52 (s, 1H, hydrazino), 9.47 (d, 1H, NH of hydroxylamine), 10.51 (d, 1H, OH proton)	55.76 55.57	4.85 4.86	16.86 16.89	581.19

^a Elemental analyses for C, H, N were within ± 0.4 % of the theoretical values.

Table 5.8: Spectral and elemental data of *N*-Mannich bases of isatin- β -thiosemicarbazones

Compound	IR Spectroscopy (cm ⁻¹ ; KBr)	¹ H-NMR (δ ppm, DMSO-d ₆)	Elemental Analyses (Calculated/Found) ^a			Mass Spectrometry (m/z)
			C (%)	H (%)	N (%)	
H29	3500, 3020, 2841, 1725, 1621, 1217, 845.	0.39 (m, 4H, CH ₂ of cyclopropyl), 2.51 (t, 1H, CH of cyclopropyl), 3.11 (t, 4H, C ₂ , C ₆ of piperaziny), 3.17 (t, 4H, C ₃ , C ₅ of piperaziny), 5.09 (s, 2H, methylene), 6.41 (s, 1H at C ₈ of quinoliny), 6.61 (d, 1H at C ₇ of indoly), 6.97 (s, 1H at C ₅ of quinoliny), 7.18 (d, 1H at C ₆ of indoly), 7.51 (s, 1H at C ₂ of quinoliny), 7.73 (s, 1H at C ₄ of indoly), 8.53 (s, 1H, hydrazino), 9.46 (d, 1H, NH of hydroxylamine), 10.51 (d, 1H, OH proton)	54.27 54.08	4.22 4.23	16.41 16.35	597.16
H36	3458, 3035, 2851, 1732, 1618, 1210, 852.	0.39 (m, 4H, CH ₂ of cyclopropyl), 0.94 (s, 3H, CH ₃ at C ₃ of piperaziny), 2.41 (s, 3H, methyl at C ₅ of indoly), 2.44 (t, 1H, CH of cyclopropyl), 2.89 (d, 2H at C ₂ of piperaziny), 3.14 (t, 2H at C ₆ of piperaziny), 3.18 (m, 1H at C ₃ of piperaziny), 3.56 (t, 2H at C ₅ of piperaziny), 3.61 (s, 3H, methoxy at C ₈ of quinoliny), 5.15 (s, 2H of methylene), 6.71 (d, 1H at C ₇ of indoly), 7.08 (d, 1H at C ₆ of indoly), 7.30 (s, 1H at C ₄ of indoly), 7.34 (s, 1H, C ₅ of quinoliny), 7.41 (s, 1H, C ₂ of quinoliny), 8.51 (s, 1H, hydrazino), 9.46 (d, 1H, NH of hydroxylamine), 10.52 (d, 1H, OH proton)	56.50 56.68	5.06 5.08	15.38 15.34	637.21

^a Elemental analyses for C, H, N were within ± 0.4 % of the theoretical values.

Table 5.9: Spectral and elemental data of *N*-Mannich bases of isatin- β -thiosemicarbazones

Compound	IR Spectroscopy (cm ⁻¹ ; KBr)	¹ H-NMR (δ ppm, DMSO-d ₆)	Elemental Analyses (Calculated/Found) ^a			Mass Spectrometry (m/z)
			C (%)	H (%)	N (%)	
M8	3020, 2847, 1726, 1615, 1205, 854.	2.45 (s, 6H, dimethylamino), 3.67 (s, 3H, methoxyl), 5.14 (s, 2H, -NCH ₂ N-), 6.63 (d, 1H, C ₇ of indolyl), 7.31 (d, 1H, C ₆ of indolyl), 7.82 (s, 1H, C ₄ of indolyl), 8.51 (s, 1H, hydrazino proton), 9.48 (s, 1H, NH proton)	47.99 47.85	4.96 4.98	21.52 21.55	325.1
M15	3030, 2853, 1731, 1623, 1190, 845.	2.43 (s, 3H, CH ₃), 2.65 (t, 4H, C ₃ , C ₅ of morpholinyl), 3.56 (t, 4H, C ₂ , C ₆ of morpholinyl), 3.66 (s, 3H, methoxyl), 5.17 (s, 2H, -NCH ₂ N-), 6.73 (d, 1H, C ₇ of indolyl), 7.13 (d, 1H, C ₆ of indolyl), 7.32 (s, 1H, C ₄ of indolyl), 8.52 (s, 1H, hydrazino proton), 9.47 (s, 1H, NH proton)	52.88 53.09	5.82 5.83	19.27 19.21	363.14
M16	3027, 2850, 1725, 1615, 1210, 848.	3.15 (t, 4H, C ₂ , C ₆ of piperazinyl), 3.18 (t, 4H, C ₃ , C ₅ of piperazinyl), 3.43 (s, 3H, methoxyl), 5.15 (s, 2H, -NCH ₂ N-), 6.73 (d, 2H, C ₂ , C ₆ of phenyl), 6.83 (d, 1H, C ₄ of phenyl), 6.81 (d, 1H, C ₇ of indolyl), 7.21 (m, 2H, C ₃ , C ₅ of phenyl), 7.25 (d, 1H, C ₆ of indolyl), 8.13 (s, 1H, C ₄ of indolyl), 8.51 (s, 1H, hydrazino proton), 9.46 (s, 1H, NH proton)	54.96 55.14	5.05 5.03	18.31 18.36	458.13

^a Elemental analyses for C, H, N were within ± 0.4 % of the theoretical values.

Table 5.10: Spectral and elemental data of *N*-Mannich bases of isatin- β -thiosemicarbazones

Compound	IR Spectroscopy (cm ⁻¹ ; KBr)	¹ H-NMR (δ ppm, DMSO-d ₆)	Elemental Analyses (Calculated/Found) ^a			Mass Spectrometry (m/z)
			C (%)	H (%)	N (%)	
M19	3024, 2855, 1727, 1618, 1195, 846.	3.17 (t, 4H, C ₂ , C ₆ of piperazinyl), 3.20 (t, 4H, C ₃ , C ₅ of piperazinyl), 3.51 (s, 3H, methoxyl), 5.13 (s, 2H, -NCH ₂ N-), 6.65 (d, 2H, C ₂ , C ₆ of phenyl), 6.79 (d, 1H, C ₇ of indolyl), 6.82 (m, 2H, C ₃ , C ₅ of phenyl), 7.34 (d, 1H, C ₆ of indolyl), 8.07 (s, 1H, C ₄ of indolyl), 8.53 (s, 1H, hydrazino proton), 9.48 (s, 1H, NH proton)	51.12 50.96	4.49 4.47	17.03 17.06	492.09
M23	3035, 2851, 1730, 1620, 1210, 852.	3.14 (t, 4H, C ₂ , C ₆ of piperazinyl), 3.19 (t, 4H, C ₃ , C ₅ of piperazinyl), 3.59 (s, 3H, methoxyl), 3.71 (s, 3H, 4-methoxyl), 5.11 (s, 2H, -NCH ₂ N-), 6.15 (d, 2H, C ₂ , C ₆ of phenyl), 6.47 (d, 1H, C ₇ of indolyl), 6.57 (m, 2H, C ₃ , C ₅ of phenyl), 7.23 (d, 1H, C ₆ of indolyl), 7.73 (s, 1H, C ₄ of indolyl), 8.51 (s, 1H, hydrazino proton), 9.47 (s, 1H, NH proton)	55.92 55.78	5.33 5.31	17.78 17.82	472.17
M26	3455, 3028, 2845, 1724, 1616, 1208, 850.	1.21 (t, 3H, CH ₃ of C ₂ H ₅), 3.13 (t, 4H, C ₂ , C ₆ of piperazinyl), 3.16 (t, 4H, C ₃ , C ₅ of piperazinyl), 3.62 (s, 2H, methylene), 3.68 (s, 3H, methoxy), 4.31 (q, 2H, CH ₂ of C ₂ H ₅), 6.23 (s, 1H, C ₈ of quinoliny), 7.21 (s, 1H, C ₅ of quinoliny), 7.29 (d, 1H, C ₆ of indolyl), 7.31 (s, 1H, C ₂ of quinoliny), 7.73 (s, 1H, C ₄ of indolyl), 8.52 (s, 1H, hydrazino proton), 9.49 (s, 1H, NH proton), 10.53 (s, 1H, carboxylate)	54.08 54.23	4.54 4.56	16.35 16.38	599.18

^a Elemental analyses for C, H, N were within ± 0.4 % of the theoretical values.

Table 5.11: Spectral and elemental data of *N*-Mannich bases of isatin- β -thiosemicarbazones

Compound	IR Spectroscopy (cm ⁻¹ ; KBr)	¹ H-NMR (δ ppm, DMSO-d ₆)	Elemental Analyses (Calculated/Found) ^a			Mass Spectrometry (m/z)
			C (%)	H (%)	N (%)	
M28	3465, 3031, 2847, 1730, 1615, 1202, 845.	0.39 (m, 4H, CH ₂ of cyclopropyl), 2.51 (t, 1H, CH of cyclopropyl), 2.95 (t, 4H, C ₃ , C ₅ of piperazinyl), 3.13 (t, 4H, C ₂ , C ₆ of piperazinyl), 3.61 (s, 3H, methoxy), 5.09 (s, 2H, methylene), 6.43 (s, 1H at C ₈ of quinoliny), 6.67 (d, 1H at C ₇ of indolyl), 6.95 (s, 1H at C ₅ of quinoliny), 7.16 (d, 1H at C ₆ of indolyl), 7.54 (s, 1H at C ₂ of quinoliny), 7.72 (s, 1H at C ₄ of indolyl), 8.51 (s, 1H, hydrazino proton), 9.46 (s, 1H, NH proton), 11.03 (s, 1H, carboxylate)	53.54 53.71	4.33 4.35	15.61 15.64	627.15
M30	3452, 3030, 2854, 1727, 1620, 1195, 852.	0.43 (m, 4H, CH ₂ of cyclopropyl), 2.48 (s, 3H, methyl at C ₅ of indolyl), 2.53 (t, 1H, CH of cyclopropyl), 3.11 (t, 4H, C ₂ , C ₆ of piperazinyl), 3.18 (t, 4H, C ₃ , C ₅ of piperazinyl), 3.61 (s, 3H, methoxy), 5.13 (s, 2H, methylene), 6.43 (s, 1H at C ₈ of quinoliny), 6.67 (d, 1H at C ₇ of indolyl), 6.95 (s, 1H at C ₅ of quinoliny), 7.16 (d, 1H at C ₆ of indolyl), 7.54 (s, 1H at C ₂ of quinoliny), 7.72 (s, 1H at C ₄ of indolyl), 8.53 (s, 1H, hydrazino proton), 9.47 (s, 1H, NH proton), 11.34 (s, 1H, carboxylate)	57.32 57.23	4.98 4.99	16.14 16.11	607.20

^a Elemental analyses for C, H, N were within ± 0.4 % of the theoretical values.

Results and Discussion

Synthesis & Characterization:

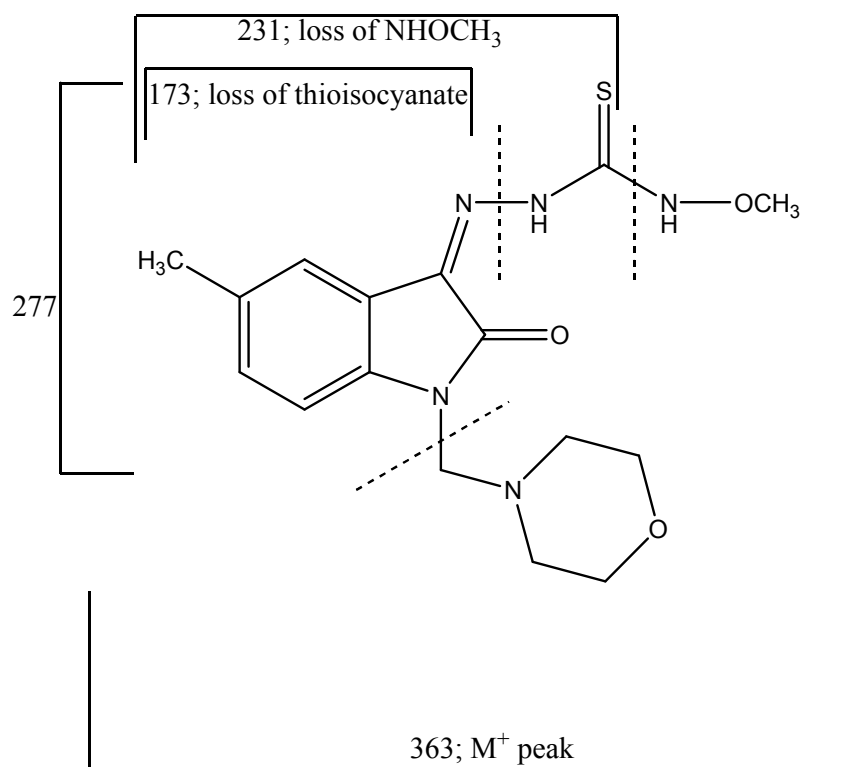
The *N*-Mannich bases of the isatin- β -thiosemicarbazones (**H7-M36**) were synthesized by condensing the acidic imino group of isatin with formaldehyde and various secondary amines.

The % yield of these final products ranged from 28.47 to 98.61 % following recrystallization from ethanol. The purity of the compounds was assessed by ascending TLC using chloroform and methanol in the ratio of 9:1 as eluant. The elemental analysis of the compounds for C, H and N were within ± 0.04 % of the theoretical values.

The logP values ranged between 0.92 and 4.37 with **H14** having the lowest logP value and **M19** being the most lipophilic with a logP of 4.37. Hence it can be seen that all the compounds were within the limits of lipophilicity as defined in Lipiniski's rule of five [131].

The assignments of structures were based on elemental and spectroscopic methods and the chemical shifts obtained from $^1\text{H-NMR}$ spectra supported the proposed structures. The IR spectra displayed new absorption band in the region of 2850 cm^{-1} due to the methylene group ($-\text{CH}_2-$). Absence of peak at 3200 cm^{-1} , due to amide group (N-H group), indicated the replacement of active hydrogen atom of isatin with aminomethyl group. The aromatic CH stretching was observed at 3030 cm^{-1} , the C=O stretch of $-\text{amide}$ at 1620 cm^{-1} , the C=N peak at 1730 cm^{-1} , the C=S peak at 1210 cm^{-1} , and the aromatic CH bending vibrations at 850 cm^{-1} . In the case of molecules like **M26**, **M30** which has a fluoroquinolone moiety a broad OH stretch of the carboxylic acid at C_3 was observed around 3500cm^{-1} .

In the NMR spectra for the isatin- β -thiosemicarbazones (Schiff bases), sharp singlet was observed at $\delta 10.6$ ppm due to $-\text{NH}$ group of isatin; whereas in the case of the *N*-Mannich bases this singlet disappeared and a new singlet appeared at $\delta 5.92$ ppm due to the $-\text{NCH}_2\text{N}-$ protons of the methylene Mannich group. A singlet was also observed for the NH of thiosemicarbazono group at $\delta 9.02$ ppm.



The mass spectrum of **M15** showed an M^+ peak at 363, base peak at 277. The remaining major fragmentation peaks were at m/z 231 and 173.

5.2 Biological activity

Results:

The titled compounds were screened for their anti-HIV activity and cytotoxicity against HIV-1 (HTLV-III_B) in MT-4 cell line.

Table 5.12: Anti-HIV activity and cytotoxicity of compounds (H7-M17) against HIV-1 (HTLV-III_B) in MT-4 cell line

Compound code	EC ₅₀ ^a (μM)	CC ₅₀ ^b (μM)	S.I ^c
H7	129.96	610.15	4.69
M7	57.93	551.75	9.52
H8	47.22	599.15	12.68
M8	37.80	559.69	14.80
H9	113.22	650.68	5.75
M9	64.09	622.28	9.71
H10	120.84	562.05	4.65
M10	58.40	454.21	7.78
H11	36.24	520.93	14.37
M11	29.71	490.07	16.49
H12	57.61	534.25	9.27
M12	53.27	572.80	10.75
H13	35.13	347.72	9.89
M13	28.40	322.26	11.35
H14	61.41	465.01	7.57
M14	28.85	274.09	9.50
H15	93.59	572.39	6.12
M15	45.13	365.41	8.09
H16	28.32	273.07	9.64
M16	17.65	267.13	15.13
H17	19.60	250.89	12.80
M17	18.08	226.89	12.55

^a Effective concentration of the drug that reduces HIV-1 induced cytopathic effect by 50% in MT-4 cells.

^b Cytotoxic concentration of the drug that decreases MT-4 cell's viability by 50%.

^c Selectivity index or ratio of CC₅₀ to EC₅₀.

Table 5.13: Anti-HIV activity and cytotoxicity of compounds (H18-H29) against HIV-1 (HTLV-III_B) in MT-4 cell line

Compound code	EC₅₀^a (μM)	CC₅₀^b (μM)	S.I^c
H18	19.32	420.00	21.74
M18	17.3	276	15.95
H19	11.06	268.14	24.24
M19	2.43	228.61	94.07
H20	6.85	193.55	28.25
M20	3.77	346.79	91.98
H21	6.10	335.11	54.94
M21	1.69	300.22	177.64
H22	21.26	278.76	13.11
M22	13.09	220.86	16.87
H23	14.66	259.54	17.70
M23	12.7	276	21.73
H24	14.96	320.98	21.46
M24	9.82	324.39	33.03
H25	27.24	185.54	6.81
M25	19.15	192.51	10.05
H26	18.44	207.66	11.26
M26	10.51	143.76	13.68
H27	16.88	326.67	19.35
M27	11.42	237.72	20.82
H28	33.38	229.30	6.87
M28	10.99	142.66	12.98
H29	16.50	222.23	13.47

^a Effective concentration of the drug that reduces HIV-1 induced cytopathic effect by 50% in MT-4 cells.

^b Cytotoxic concentration of the drug that decreases MT-4 cell's viability by 50%.

^c Selectivity index or ratio of CC₅₀ to EC₅₀.

Table 5.14: Anti-HIV activity and cytotoxicity of compounds (M29-M36) against HIV-1 (HTLV-III_B) in MT-4 cell line

Compound code	EC₅₀^a (μM)	CC₅₀^b (μM)	S.I^c
M29	11.43	254.78	22.29
H30	20.89	303.72	14.54
M30	9.22	231.71	25.13
H31	23.18	209.45	9.04
M31	9.26	180.38	19.48
H32	9.93	186.85	18.82
M32	4.43	178.27	40.24
H33	11.73	243.95	20.80
M33	5.74	155.50	27.09
H34	15.35	233.73	15.23
M34	7.14	164.25	23.00
H35	4.18	205.88	49.25
M35	1.88	170.51	90.70
H36	11.13	276.00	24.80
M36	1.86	154.06	82.83
Nevirapine	0.13	156	1200.00
Trovirdine	0.016	87	5437.50

^a Effective concentration of the drug that reduces HIV-1 induced cytopathic effect by 50% in MT-4 cells.

^b Cytotoxic concentration of the drug that decreases MT-4 cell's viability by 50%.

^c Selectivity index or ratio of CC₅₀ to EC₅₀.

Selected compounds were analyzed for their ability to repress HIV-1 RT enzyme.

Table 5.15: HIV-1RT enzyme inhibition data for selected N-Mannich bases of isatin- β -thiosemicarbazones^a

Compound code	IC₅₀ (μM) against HIV-1 RT^b
H21	23.4 \pm 1.2
M19	18.3 \pm 2.1
M20	16.7 \pm 2.3
M21	11.5 \pm 1.5
Nevirapine	0.25
Trovirdine	0.017 \pm 0.007

^a Enzyme assays done with WT RT.

^b IC₅₀ is the quantity of drug that reduced WT RT enzyme activity by 50%.

All the analogues were screened for their ability to inhibit the growth of H37 Rv strain of MTB in logarithmic phase. MIC was the concentration at which the H37Rv MTB strain showed complete inhibition.

Table 5.16: Anti-tubercular activity of compounds (H7-M22) against H37Rv strain of MTB in logarithmic phase

Compound code	MIC in μM	Compound code	MIC in μM
H7	76.27	H15	8.96
M7	18.28	M15	4.29
H8	10.05	H16	28.09
M8	9.62	M16	13.62
H9	81.34	H17	7.30
M9	19.45	M17	7.07
H10	70.26	H18	14.72
M10	16.90	M18	12.36
H11	9.22	H19	13.04
M11	4.41	M19	6.34
H12	11.83	H20	3.37
M12	8.96	M20	3.27
H13	6.11	H21	6.82
M13	4.06	M21	3.30
H14	4.41	H22	13.16
M14	4.25	M22	12.78

Table 5.17: Anti-tubercular activity of compounds (H23-M36) against H37Rv strain of MTB in logarithmic phase

Compound code	MIC in μM^a	Compound code	MIC in μM^a
H23	6.83	H30	0.67
M23	6.14	M30	0.66
H24	13.75	H31	1.23
M24	6.68	M31	1.20
H25	1.30	H32	0.65
M25	0.65	M32	0.63
H26	1.33	H33	0.65
M26	0.67	M33	1.24
H27	1.34	H34	1.19
M27	1.31	M34	0.30
H28	2.54	H35	0.16
M28	0.64	M35	0.15
H29	0.33	H36	0.63
M29	0.31	M36	0.31
Isoniazid	0.36	Rifampicin	0.12

^aMIC was the concentration at which the H37Rv MTB strain showed complete inhibition.

Few of the analogues were screened for their ability to suppress dormant MTB.

Table 5.18: Anti-tubercular activity of selected compounds against dormant MTB

Compound code	Dormant MTB MIC (μM)^a
H20	13.48
H21	27.28
H29	20.92
H30	42.11
H32	10.12
H33	20.37
H35	9.74
H36	19.60
M14	17.01
M19	25.36
M20	13.08
M21	12.11
M24	38.01
M25	36.86
M26	19.24
M28	34.62
M30	18.44
M32	9.45
M35	9.17
M36	17.81
Isoniazid	182.31
Rifampicin	15.19

^aMIC was the concentration at which the dormant H37Rv MTB strain showed complete inhibition.

Few of the analogues were analyzed for their ability to inhibit MTB ICL enzyme.

Table 5.19: MTB ICL suppression by selected compounds

Compound code	MTB ICL % Inhibition (conc. of stock solution used)
H20	18.54 (10mM)
H21	11.03 (10mM)
M12	18.9 (10mM)
M14	15.93 (10mM)
M19	6.38 (10mM)
M20	28.37 (10mM)
M21	9.49 (10mM)
M24	23.3 (10mM)
M30	63.44 (10mM)
3-NPA	65.99 (100mM)

Few of the analogues were tested for their ability to inhibit supercoiling of DNA gyrase of *Mycobacterium smegmatis* (MC₂).

Table 5.20: *Mycobacterium smegmatis* (MC₂) DNA gyrase supercoiling inhibition by selected compounds

Compound code	IC₅₀ (μM)	Compound code	IC₅₀ (μM)
H25	66.44	M25	81.16
H26	85.39	M26	83.39
H27	34.39-51.58	M27	83.94
H28	4.89-8.14	M28	63.69-79.61
H29	66.94-83.67	M30	82.28
H30	67.38-84.23	M31	77.15
H31	63.09	M32	>79.16
H32	>80.96	M33	79.66
H33	16.30	M34	74.39
H34	45.59-60.78	M35	76.26
H35	15.58	M36	76.72
H36	15.68-31.36	Ciprofloxacin	15.09
		Moxifloxacin	12.46

Selected compounds were screened for their antiviral activity against HCV in Huh 7 ET cell line.

Table 5.21: Antiviral and Cytotoxicity activity of selected compounds against HCV

Compound code	High Test Conc	Drug Units	Activity (% inhibition virus control)	Cytotoxicity (% cell control)	SI
H8	20	μM	41.4	61.6	<1
H9	20	μM	0.0	77.0	<1
H16	20	μM	12.3	102.4	<1
H19	20	μM	0.0	52.3	<1
H20	20	μM	86.9	32.7	<1
H21	20	μM	0.0	75.2	<1
H22	20	μM	37.8	0.0	<1
H23	20	μM	17.5	76.7	<1
H24	20	μM	38.1	0.1	<1
H31	20	μM	30.9	28.5	<1
rIFNα-2b	2	IU/mL	94.8	102.1	>1
rIFNα-2b	2	IU/mL	94.7	96.3	>1

Selected analogues were analysed for their activity against influenza type A and B virus in MDCK cell line.

Table 5.22: Activity of selected compounds against Influenza Type A virus

Compound code	EC₅₀ (µM)	IC₅₀ (µM)	SI
H27	55.02	>55.02	>1
H28	52.11	53.74	1
H31	>53.62	53.62	0
H32	32.38	>161.92	>5
H35	49.87	>155.85	>3

Table 5.23: Activity of selected compounds against Influenza Type B virus

Compound code	EC₅₀ (μM)	IC₅₀ (μM)	SI
H7	94.57	97.62	1
H8	28.91	89.93	3
H9	>104.11	120.38	1
H10	87.12	281.03	3
H11	17.68	94.29	5
H14	73.58	282.99	4
H15	>91.58	286.20	3
H16	71.92	224.75	3
H17	74.68	233.38	3
H19	22.95	70.92	3
H20	23.76	64.80	3
H21	84.97	>217.88	>3
H22	63.16	69.48	1
H23	65.43	152.67	2
H24	61.60	>61.60	0
H25	11.63	94.68	8
H26	6.83	56.35	8
H27	46.42	46.42	0
H28	45.60	52.11	1
H29	51.88	>167.34	>3
H30	52.22	168.46	3
H31	48.89	55.20	1
H32	142.49	>161.92	>1
H33	>143.41	>162.96	1
H34	>48.62	50.14	1
H35	56.11	>155.85	>3
H36	48.61	>156.82	>3

Selected compounds were tested for their antiviral activity against SARS virus in Vero 76 cell line.

Table 5.24: Activity of selected compounds against SARS virus

Compound code	EC₅₀ (μM)	IC₅₀ (μM)	SI
H7	97.62	>97.62	>1
H8	28.91	102.78	4
H9	117.12	>117.12	0
H10	84.31	>126.46	>2
H11	91.34	>94.29	>1
H14	87.73	166.96	2
H19	16.27	66.75	4.1
H21	143.80	217.88	2
H26	56.35	>63.19	>1
H30	38.74	>69.07	>2
H33	162.96	>162.96	>1
H34	>72.94	72.94	0
H36	>86.25	156.82	2

Discussion:

A. In-vitro anti-HIV assays:

The titled compounds were tested for their ability to inhibit the replication of HIV-1 (III_B) cells in MT-4 cells. All the sixty analogues had EC₅₀ lying in the range of 1.69 μM to 129.96 μM (Table 5.12-5.14). Fifteen derivatives had EC₅₀ less than 10 μM. Amongst the thirty hydroxythiosemicarbazone derivatives **H35** was found to be the most promising with EC₅₀ of 4.18 μM. Amongst the various substituted piperazinyl analogues the most potent ones were found to be the 4-chlorophenyl piperazinyl derivatives (**H19-H21**) followed by 4-methoxyphenyl piperazine (**H22-H24**) and then phenyl piperazine (**H16-H18**) derivatives. The presence of dialkylamine at R₁ ruled anti-HIV activity by the following order: N,N-diethylamine > N,N-dimethylamine. When R₁ was substituted by various fluoroquinolones (FQ), gatifloxacin analogues (**H34-H36**) showed the greatest inhibition of HIV replication followed by lomefloxacin derivatives (**H31-H33**) and then by ciprofloxacin (**H28-H30**) and norfloxacin analogues (**H25-H27**) which were almost equipotent to each other. The methoxythiosemicarbazone analogues when compared to those of hydroxy thiosemicarbazone derivatives displayed better inhibitory profile. The higher activity of the methoxythiosemicarbazones in comparison to the hydroxythiosemicarbazones can be attributed to the methoxy moiety, being involved in steric interaction with the aromatic residues of HIV-1 RT; which was confirmed with the docking results obtained. In the series of methoxy thiosemicarbazone analogues, 2-(1-{{4-(4-chlorophenyl)tetrahydropyrazin-1(2H)-yl}methyl}-5-methyl-2-oxo-1,2-dihydro-3H-indol-3-yliden)-N-(methoxy)hydrazine-1-carbothioamide (**M21**) was found to be the most potent in suppressing the replication of HIV-1 cells with an EC₅₀ of 1.69 μM. The anti-HIV potency of **M21** may be ascribed to the electronegative chlorine present at the 4th position of phenyl piperazinyl methyl which probably forms an ionic bond with positive residues present in the active site pocket and also owing to the methyl group at the 5th position of the indolyl moiety which helps it in establishing steric interactions with aromatic residues of the enzyme. Between morpholinyl and piperazinyl substitution at R₁ of the methoxy thiosemicarbazones, piperazinyl analogues (**M16-M24**) showed improved anti-HIV potency. Comparison between the various substituted piperazinyl showed that 4-chlorophenyl piperazine derivatives (**M19-M21**) were most active followed by 4-

methoxyphenyl piperazine (**M22-M24**) and lastly phenyl piperazinyl analogues (**M16-M18**). 4-Chlorophenyl piperazinyl methyl substituted molecules showed higher inhibitory activity against replication of HIV-1 cells in comparison to other phenyl piperazines namely phenyl piperazine and 4-methoxy phenyl piperazine due to the halogen group present at the 4th position of the phenyl ring forming a bond with some positively charged residues of the RT enzyme. Presence of various FQs at R₁ guides activity in the following sequence: gatifloxacin > lomefloxacin > ciprofloxacin ≈ norfloxacin. The presence of FQs at N-1 makes the molecule **M36** the second most potent molecule amongst the total 60 reported compounds against HIV replication. When considering the substituent at 5th position of the indole-2,3-dione it was observed that activity was governed by the order of F ≈ CH₃ > Cl. Compounds with N, N-diethylaminomethyl substitution at N-1 of indole-2, 3-dione (**H10-M12**) showed better inhibitory activity than those with N,N-dimethylamine methyl substitution (**H7-M9**) possibly due to the longer aliphatic chain length contributing to improved interaction with the bulky groups present at the active site. The nature of substituents at R₁ also governed the activity possessed by the compounds. Presence of piperazinylmethyl and substituted piperazinylmethyl group at N-1 enhanced the anti-HIV activity when compared to morpholinylmethyl group. This can be attributed to the repulsion experienced by the oxygen of morpholine ring.

The cytotoxic effect of these molecules was measured in MT-4 cells in parallel with the antiviral activity. Amongst the entire series **H9** was found to be least cytopathic to MT-4 cells with a CC₅₀ value of 650.68 μM. The CC₅₀ values of the entire series of sixty compounds were found to lie in the range of 143.76-650.68 μM (**Table 5.12-5.14**). When compared to standard non-nucleoside reverse transcriptase inhibitors (NNRTI) like nevirapine and delaviridine, which have CC₅₀ of around 25 μM, these new molecules are far less cytotoxic. Cytotoxicity was found to be regulated by the occurrence of greater bulky groups at N-1 of indolyl moiety. While comparing between the terminal substituent present at the hydrazino carbothioamide it was seen that molecules belonging to series of methoxythiosemicarbazone analogues were mostly less toxic than that of the series of hydroxythiosemicarbazones except for a few isolated cases, which can be ascribed to the

probable hydrogen bond formation by the hydroxyl group with residues of the MT-4 cells.

B. HIV-1 RT enzyme inhibition assay:

HIV-1 reverse transcriptase (RT) is a predominant target for many anti-HIV drugs that are being used clinically and are there in the developmental stages. RT is a multifunctional heterodimeric enzyme needed in HIV replicative cycle, which catalyzes the conversion of genomic HIV RNA into proviral DNA [23, 132]. Drugs targeting RT are classified into two broad categories: nucleoside reverse transcriptase inhibitors (NRTI) and non-nucleoside reverse transcriptase inhibitors (NNRTI). NNRTIs inhibit RT in a non-competitive manner by binding at an allosteric site that is situated 10 Å away from the catalytic HIV-RT site [133]. NNRTIs are specific to HIV-1 RT and hence are comparatively less toxic to the host. Though NNRTIs are structurally diverse, they act on RT by inducing conformational changes that form the NNRTI binding pocket (NNIBP). They achieve this by distorting the polymerase active site by means of movement of the catalytic aspartates [28].

Four compounds were assessed for their activity against wild type HIV-1 RT. Compound **M21** showed the highest inhibitory activity with IC_{50} of $11.5 \pm 1.5 \mu\text{M}$ (**Table 5.15**) on HIV-1 RT amongst all four, which can be ascribed to the methyl moiety present at thiosemicarbazone moiety, which may be involved in steric interaction with some residues present in the RT active site. Activity can moreover be guided by the phenyl ring attached to the piperazinyl moiety at R_1 , which can contribute to significant interaction with aromatic residues of the RT enzyme as is evident from the docking simulations performed.

C. *In vitro* anti-tubercular evaluation:

The titled compounds when evaluated for their inhibitory activity against the replication of MTB in the logarithmic growth phase displayed activity ranging from 0.15 to 81.34 μM (**Table 5.16-5.17**). Forty-four compounds had minimum inhibitory concentrations (MIC) below 10 μM out of which fifteen molecules' MIC were found to lie below 1 μM . 1-Cyclopropyl-6-fluoro-7-[4-{{[5-fluoro-3-((Z)-2-{{[(methoxy)amino]carbothioyl}hydrazono)-2-oxo-1H-indol-1(2H)-yl]methyl}}-3-methyltetrahydropyrazin-1(2H)-yl]-8-(methoxy)-4-oxo-1,4-dihydroquinoline-3-carboxylic acid (**M35**) was found to be the most active against the logarithmic growth of MTB with MIC of 0.15 μM , even more potent than INH (MIC: 0.36 μM). In contrast to the hydroxythiosemicarbazone analogues, the methoxythiosemicarbazones exhibited superior activity against MTB growth. Amongst the hydroxythiosemicarbazone analogues the most active compound was found to be **H35** with an MIC of 0.16 μM (**Table 5.16-5.17**). Keeping the functional group present at C₅ (R') constant in the hydroxysemicarbazone series when the substituent attached to N₁ (R₁), was varied the order of activity was as follows: *N,N*-dimethylamino < *N,N*-diethylamino < phenylpiperazinyl < 4-methoxyphenyl piperazinyl < 4-chlorophenyl piperazinyl < morpholinyl < norfloxacin < ciprofloxacin < lomefloxacin < gatifloxacin. Substituents at R' influenced the anti-tubercular activity in the following order: fluorine > chlorine \approx methyl, with moderate to lowest activity swaying between chlorine and methyl, which might be due in part to the combined effect of the substituent present at R₁. Compound **M35** was found to be the most promising in the methoxythiosemicarbazone series. Varying substituents at R₁ led to the same order of activity as that of hydroxy thiosemicarbazones. The greater activity profile of the fluoroquinolone substituted analogues (**H25-M36**) can be accredited to their increased lipophilicity permitting them to penetrate into the mycolic acid cell wall of the bacilli. In case of the morpholinyl derivatives (**H13-M15**) the enhanced activity in contrast to the piperazinyl derivatives may be due in part to the electronegative oxygen which might be involved in some ionic interaction or some hydrogen bonding interaction with residues at the active site. Amongst the substituted piperazinyl analogues, the 4-chlorophenyl piperazinyl analogues demonstrated highest activity, which can be attributed to the chlorine atom being

involved in some probable ion-dipole interaction with the residues of the active site pocket. In the presence of dialkylamino group at R₁, increased alkyl chain length contributed to greater inhibition of MTB replication possibly due to increased steric factor. These results were further established by the docking simulations that were performed.

D. Anti-tubercular activity of compounds against dormant MTB:

An MTB-infected individual transmits the bacilli as a droplet nucleus to the next human host who inhales it. Almost 30 % of exposed individual becomes infected; whereas 60 -90 % of this population launches an immune response against it thereby containing the pathogen. When more T cells and macrophages slowly surround this pathogen it slows its replicative cycle and is unable to transmit infection. Due to this feature of MTB, approximately one-third of the global population is estimated to be infected with this bacillus. The tuberculosis pathogen can endure within an infected individual for extended period of time without triggering any clinical symptoms of the disease. Though the replicative cycle of this mycobacterium during this stage is not clearly delineated, current breakthroughs in this area indicates that this pathogen needs the regulated expression of a set of genes and metabolic pathways to maintain chronicity in an immunocompetent host. Since the currently available anti-tubercular drugs are incapable of treating dormant TB, novel chemotherapeutic agents are needed which would target the phagocytosed bacilli present in the alveolar macrophages [134, 135].

These compounds showed exemplary inhibitory profile against starved MTB culture. Twenty compounds from amongst the sixty derivatives were tested for their activity against the replication of dormant MTB culture (**Table 5.18**). Compound **M35** proved superior in curbing the growth of dormant MTB (MIC: 9.17 μ M) in comparison to first-line anti-tubercular drugs, INH (MIC: 182.31 μ M) and RIF (MIC: 15.19 μ M). All the twenty analogues were found to be more active (MIC ranging from 9.17-42.11 μ M) in suppressing the proliferation of dormant MTB when compared to INH. Seven of them were found to be more beneficial (MIC ranging from 9.17-13.48 μ M) than RIF in inhibiting dormant MTB.

E. MTB ICL enzyme inhibition assay:

TB is marked by the ability of the bacilli, MTB, to endure in macrophages of the infected patients thereby maintaining chronicity. In chronic tuberculosis, the bacillus exists in diverse metabolic phases, spanning from active cell growth to stationary phase [93]. All the currently available anti-tubercular drugs that are being clinically used do not target various stages that MTB uses for its persistence in the macrophages and hence prolonging the treatment regimen. A lot of research activity is currently aimed at understanding the biology of persistence of the tubercle bacillus and developing new drugs that target the persister bacteria [136]. Gene products involved in mycobacterial persistence, such as isocitrate lyase (ICL) [137], PcaA (methyl transferase involved in the modification of mycolic acid) [138], RelA (ppGpp synthase) [139], and DosR (controlling a 48-gene regulation involved in mycobacterial survival under hypoxic conditions) [140], have been identified and could be good targets for the development of drugs that target persistent bacilli. As the compounds reported in this article, demonstrated excellent activity against dormant mycobacterium, we decided to explore the possible mechanism by screening some compounds against ICL enzyme of MTB. Mycobacterium survives during chronic infection by undergoing a shift in the metabolic cycle in the bacillus' carbon source to C₂ substrates. Due to this, the glyoxalate shunt is up regulated and it assimilates carbon by converting isocitrate to succinate and glyoxalate with the aid of isocitrate lyase enzyme. The glyoxylate cycle being absent in higher animals, and due to its role for survival for the persistent phase of the tubercular infection, ICL is considered an ideal drug target for combating persistent MTB [141]. Several small-molecule inhibitors have been described [140] as MTB ICL inhibitors; however, none has been developed as a drug for MTB. In this work, isocitrate lyase activity was determined at 37°C by measuring the formation of glyoxylate-phenylhydrazone in the presence of phenylhydrazine and isocitrate lyase at 324nm based on the method described [119]. The compounds were screened with a single concentration of 10 mM and percentage inhibitions of the screened compounds along with the standard MTB ICL inhibitor 3-nitropropionic acid (3-NP) (at 100 mM) for comparison are reported (**Table 5.19**).

Among nine compounds which were assessed for their ability to inhibit ICL of MTB, **M30** demonstrated excellent inhibitory action of the ICL enzyme of about 63.44% and was more potent than standard ICL inhibitors like 3-NP. Compounds **M20** and **M24** showed mild ICL inhibition with range of 20-30%. Amongst the hydroxythiosemicarbazone analogues evaluated, **H20** showed an inhibition of 18.54%. The inhibitory activities of **M24** and **M30** can be assigned to the methyl group present at R' and also to the bulky groups present at R₁, which might be contributing to significant steric interaction with bulky residues present in the enzyme active pocket. This was also confirmed by the docking study performed.

F. MTB DNA Gyrase enzyme assay:

Selected analogues were tried for their ability to inhibit the supercoiling of *Mycobacterium smegmatis* DNA gyrase (Table 5.20). The IC₅₀ of these twenty-three analogues ranged between 3 and 50 µg/mL. **H28** displayed the most promising DNA gyrase inhibition with an IC₅₀ of 3-5 µg/mL, followed by **H33** and **H35** with IC₅₀ of 10 µg/mL.

G. Antiviral and Cytotoxicity assay for HCV:

Selected compounds belonging to this series were evaluated for their ability to inhibit HCV and also for their cytotoxicity on Huh 7 ET cell line at a concentration of 20 µM. None of the compounds were found to be active against HCV replication. Four compounds namely, **H20**, **H22**, **H24** and **H31** were found to be cytotoxic to Huh 7 ET cell line (Table 5.21).

H. Antiviral and Cytotoxicity activity against Influenza Type A virus:

Selected compounds were also analyzed for their ability to inhibit the replication of Influenza type A virus, strain Vietnam/1203/2004H in MDCK cell line (Table 5.22). Only **H32** was found to be slightly active with an EC₅₀ of 20 µg/mL and selectivity index greater than 5.

I. Antiviral and Cytotoxicity activity against Influenza Type B virus:

Selected compounds were also analyzed for their ability to inhibit the replication of Influenza type B virus, strain Malaysia/2506/2004 in MDCK cell line (Table 5.23). Five analogues, namely **H8**, **H11**, **H14**, **H25** and **H26** were found to be slightly active in inhibiting the replication of Influenza type B virus. Their EC₅₀ ranged between 6 and 26 µg/mL. **H25** and **H26** had the greatest selectivity index of 8.

J. Antiviral and Cytotoxicity activity against SARS virus

Few of the analogues were also tested for their ability to inhibit the replication of SARS virus, Urbani strain in Vero 76 cell line (Table 5.24). Two of the analogues, viz. **H8** and **H19** showed slight activity against the replication of SARS virus replication with selectivity indices of 4.0 and 4.1 respectively.

5.3 Computational studies

A. CoMFA and CoMSIA Analyses based on HIV-1 screening

Results:

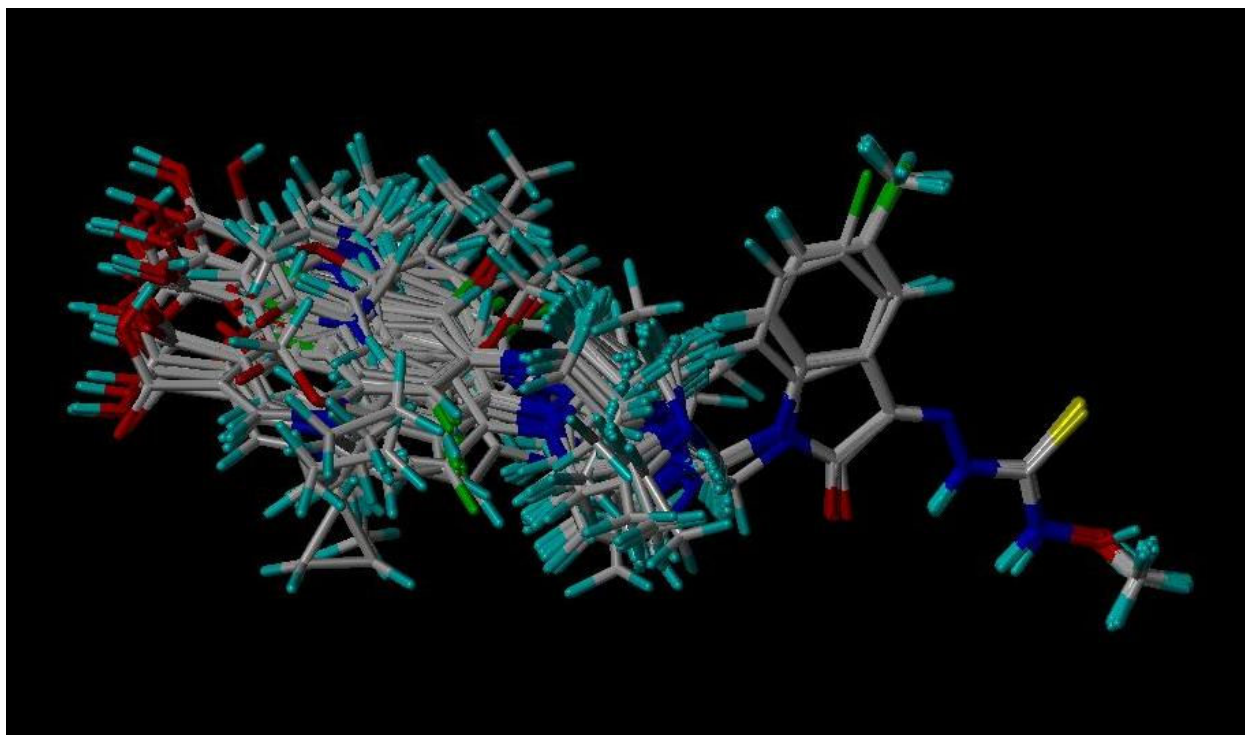


Fig. 5.1: Manual alignment of the analogues belonging to Series I

Table 5.25: Experimental and predicted pEC₅₀ values of training set compounds

Compound	Experimental pEC ₅₀	CoMFA model		CoMSIA model	
		Predicted pEC ₅₀	Residual	Predicted pEC ₅₀	Residual
H7	0.89	0.76	0.13	1.03	-0.14
H8	1.33	1.29	0.04	1.37	-0.04
H11	1.44	1.46	-0.02	1.53	-0.09
H14	1.21	1.27	-0.06	1.13	0.08
H16	1.55	1.43	0.12	1.73	-0.18
H17	1.71	1.85	-0.14	1.68	0.03
H18	1.72	1.7	0.02	1.69	0.03
H19	1.96	2.03	-0.07	1.84	0.12
H20	2.15	2.31	-0.16	2.21	-0.06
H23	1.82	1.65	0.17	1.94	-0.12
H26	1.74	1.83	-0.09	1.81	-0.07
H29	1.78	1.69	0.09	1.77	0.01
H30	1.68	1.51	0.17	1.74	-0.06
H31	1.64	1.32	0.32	1.55	0.09
H32	2.05	2.24	-0.19	2.13	-0.08
H33	1.92	2.37	-0.45	2.05	-0.13
M8	1.43	1.59	-0.16	1.56	-0.13
M10	1.24	1.16	0.08	1.09	0.15
M12	1.23	1.14	0.09	1.38	-0.15
M13	1.55	1.34	0.21	1.48	0.07
M15	1.35	1.44	-0.09	1.39	-0.04
M16	1.75	1.86	-0.11	1.86	-0.11
M17	1.74	1.63	0.11	1.65	0.09
M19	2.62	2.82	-0.20	2.53	0.09
M20	2.43	2.56	-0.13	2.51	-0.08
M22	1.88	1.79	0.09	1.73	0.15
M24	2.01	1.96	0.05	2.11	-0.10
M26	1.98	2.04	-0.06	2.03	-0.05
M27	1.94	1.99	-0.05	1.86	0.08
M28	1.96	1.73	0.23	2.08	-0.12
M31	2.05	1.92	0.13	1.98	0.07
M32	2.36	2.57	-0.21	2.42	-0.06
M33	2.24	2.18	0.06	2.35	-0.11
M35	2.74	2.91	-0.17	2.85	-0.11

Table 5.26: Experimental and predicted pEC₅₀ values of test set compounds

Compound	Experimental pEC ₅₀	CoMFA model		CoMSIA model	
		Predicted pEC ₅₀	Residual	Predicted pEC ₅₀	Residual
H9	0.95	0.958	-0.008	1.022	-0.072
H10	0.92	0.997	-0.077	1.164	-0.244
H15	1.03	1.053	-0.023	1.088	-0.058
H21	2.22	1.951	0.269	2.08	0.14
H22	1.68	1.596	0.084	1.687	-0.007
H24	1.82	1.122	0.698	1.187	0.633
H25	1.57	2.267	-0.697	1.744	-0.174
H27	1.77	1.897	-0.127	1.55	0.22
H28	1.48	1.644	-0.164	1.581	-0.101
H34	1.82	1.551	0.269	1.789	0.031
H35	2.38	1.925	0.455	2.057	0.323
H36	1.96	1.525	0.435	1.754	0.206
M7	1.24	1.277	-0.037	1.344	-0.104
M9	1.19	1.272	-0.082	1.369	-0.179
M11	1.54	1.538	0.002	1.518	0.022
M14	1.55	1.608	-0.058	1.605	-0.055
M21	2.8	2.103	0.697	2.203	0.597
M25	1.72	2.094	-0.374	1.939	-0.219
M30	2.05	2.251	-0.201	2.093	-0.043
M34	2.15	2.349	-0.199	2.009	0.141
M36	2.74	2.357	0.383	2.588	0.152

Table 5.27: Summary of CoMFA, Advanced CoMFA and CoMSIA results

	CoMFA			CoMSIA
Parameters	SCT(RF)	PBL	PBL(RF)	SEADH
q^2	0.71	0.642	0.666	0.823
S_{press}	0.262	0.290	0.280	0.209
r^2	0.970	0.971	0.955	0.970
SE	0.089	0.086	0.108	0.088
F	148.08	156.397	99.186	151.306
N	6	6	6	9
<i>fractions</i>				
S	0.653	0.669	0.954	0.123
E	0.347	0.331	0.046	0.241
H	-	-	-	0.329
A	-	-	-	0.242
D	-	-	-	0.064
r^2_{bs}	0.984	0.986	0.978	0.981
SD_{bs}	0.007	0.003	0.007	0.005
r^2_{cv}	0.694	0.661	0.632	0.792

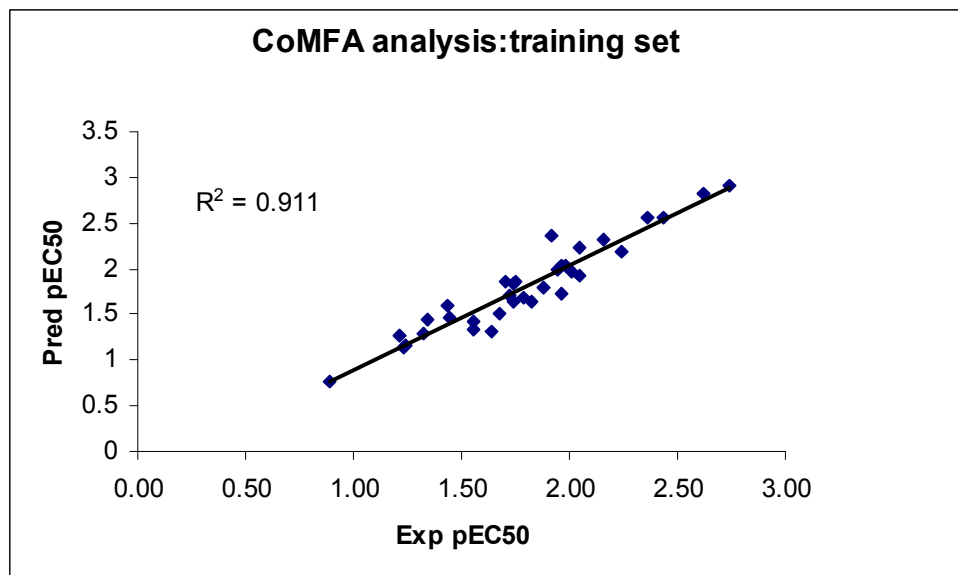


Fig. 5.2: Scatter plot depicting predicted pEC_{50} versus Experimental pEC_{50} data using CoMFA analysis for training set compounds

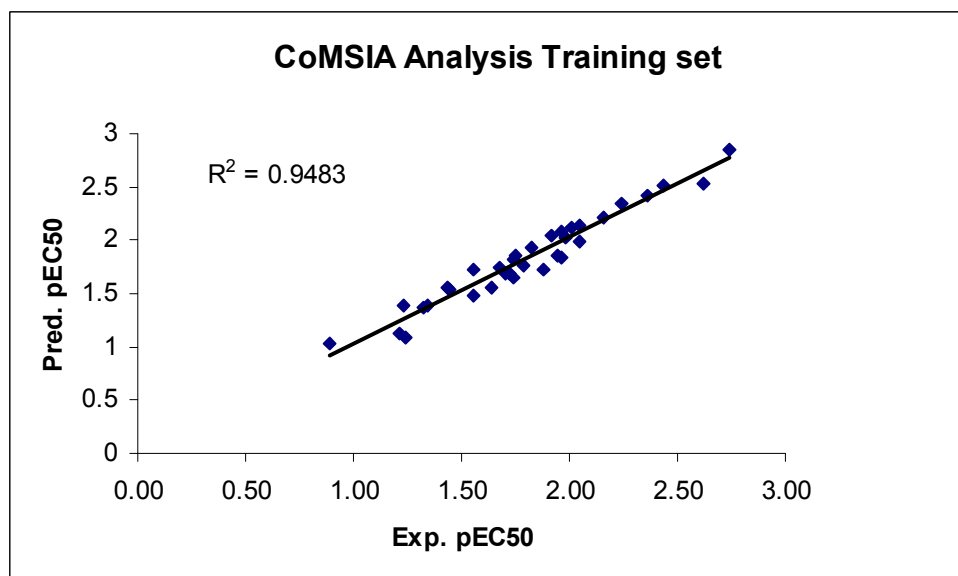


Fig 5.3: Scatter plot depicting predicted pEC_{50} versus Experimental pEC_{50} data using CoMSIA analysis for training set compounds.

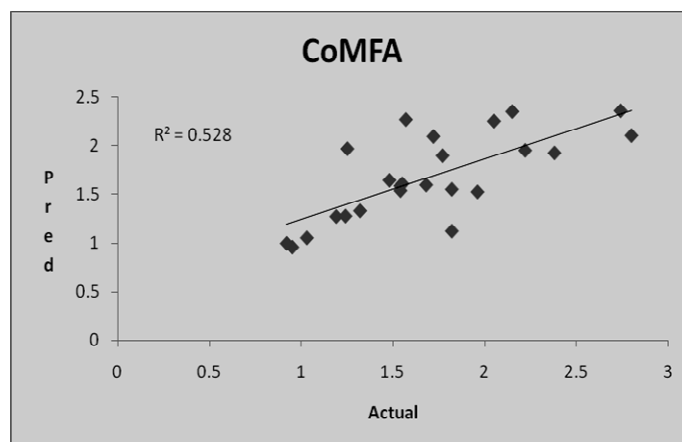


Fig. 5.4: Scatter plot depicting predicted pEC₅₀ versus Experimental pEC₅₀ data using CoMFA analysis for test set compounds

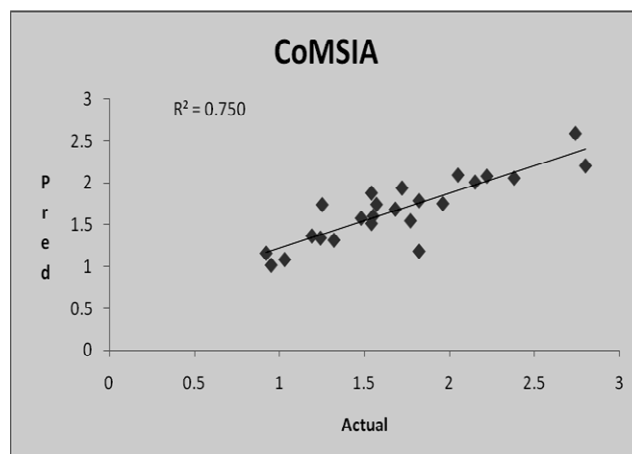


Fig. 5.5: Scatter plot depicting predicted pEC₅₀ versus Experimental pEC₅₀ data using CoMSIA analysis for test set compounds.

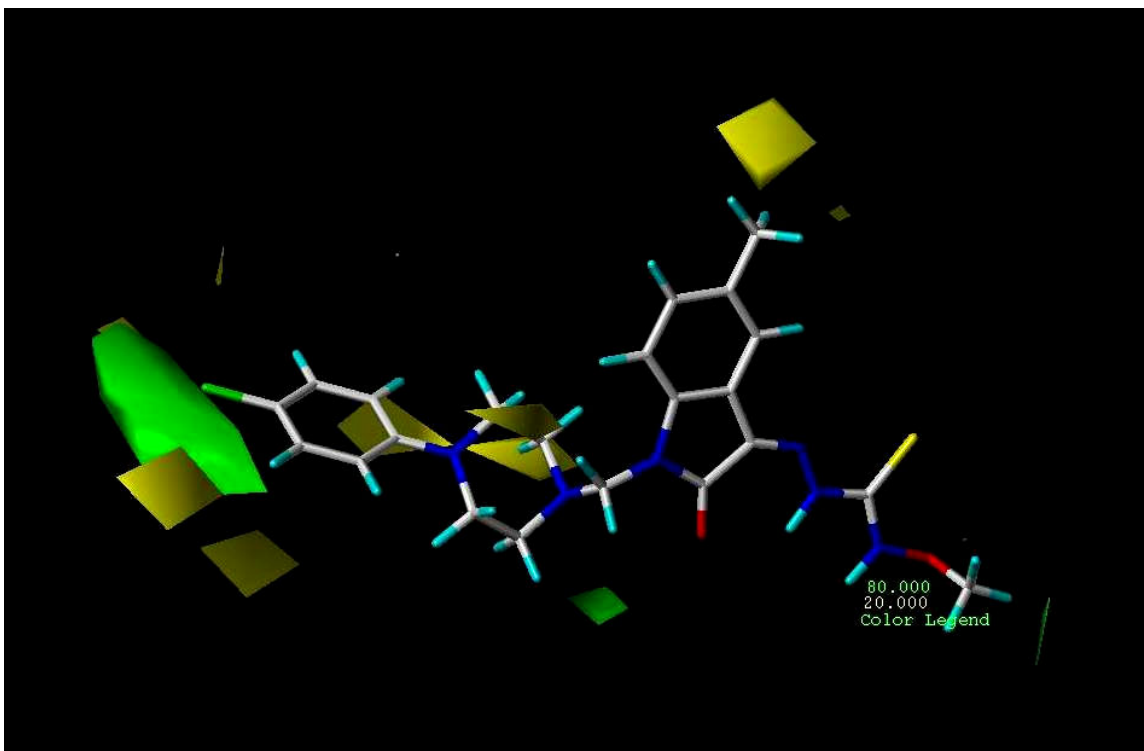


Fig. 5.6: CoMFA contour map of steric regions (green, favored; yellow; disfavored) around M21

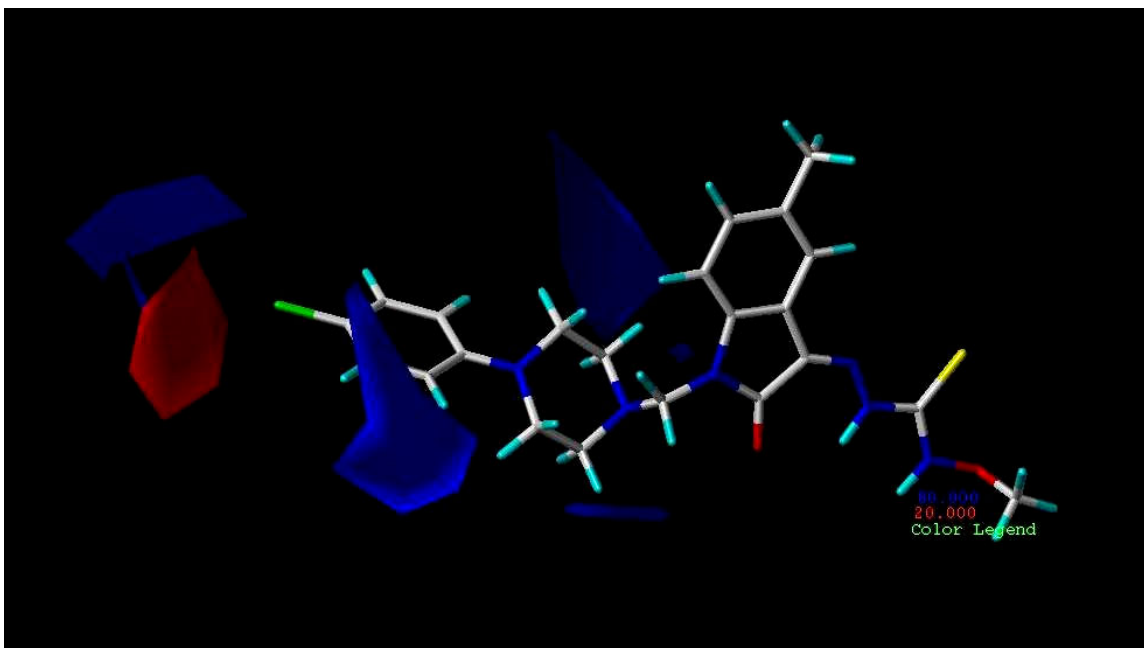


Fig. 5.7: CoMFA contour map of electrostatic regions around M21. Blue regions are favored by positively charged groups and red regions favored by negatively charged groups.

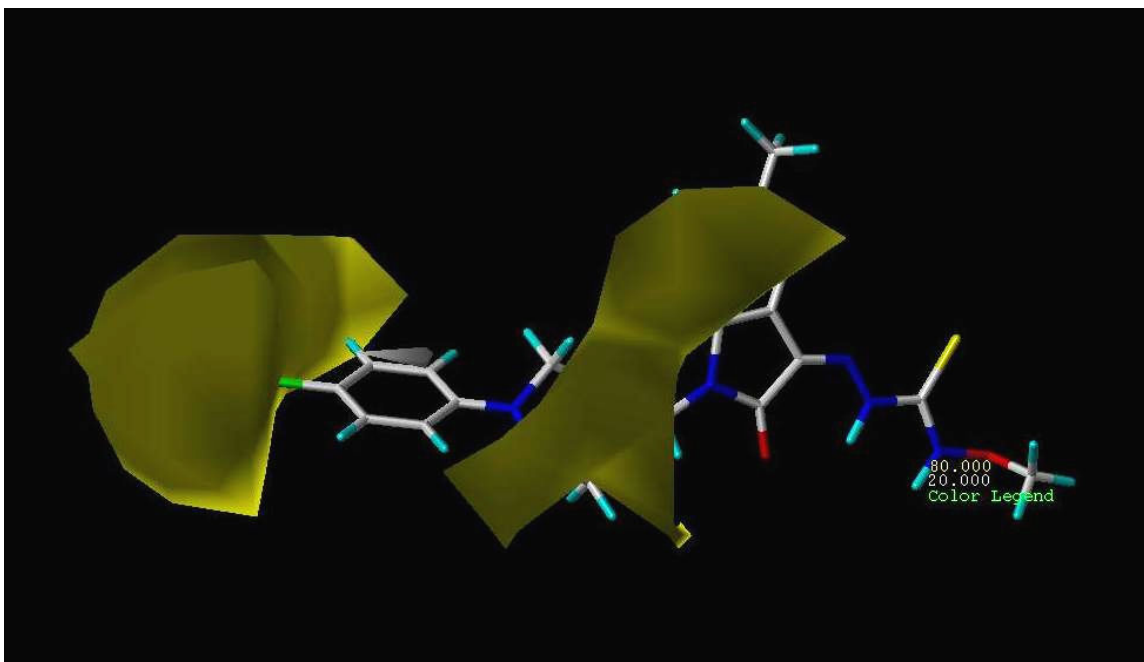


Fig. 5.8: CoMSIA contour map of hydrophobic regions (yellow favored; white disfavored) around M21

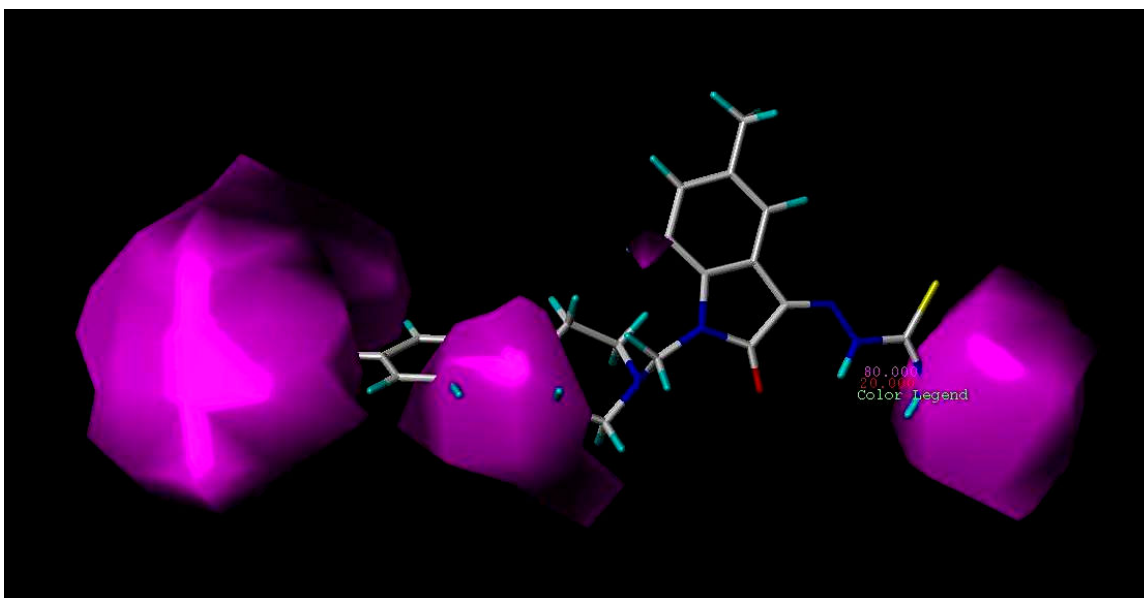


Fig. 5.9: CoMSIA hydrogen bonding acceptor contour map (magenta favored; green disfavored) around M21

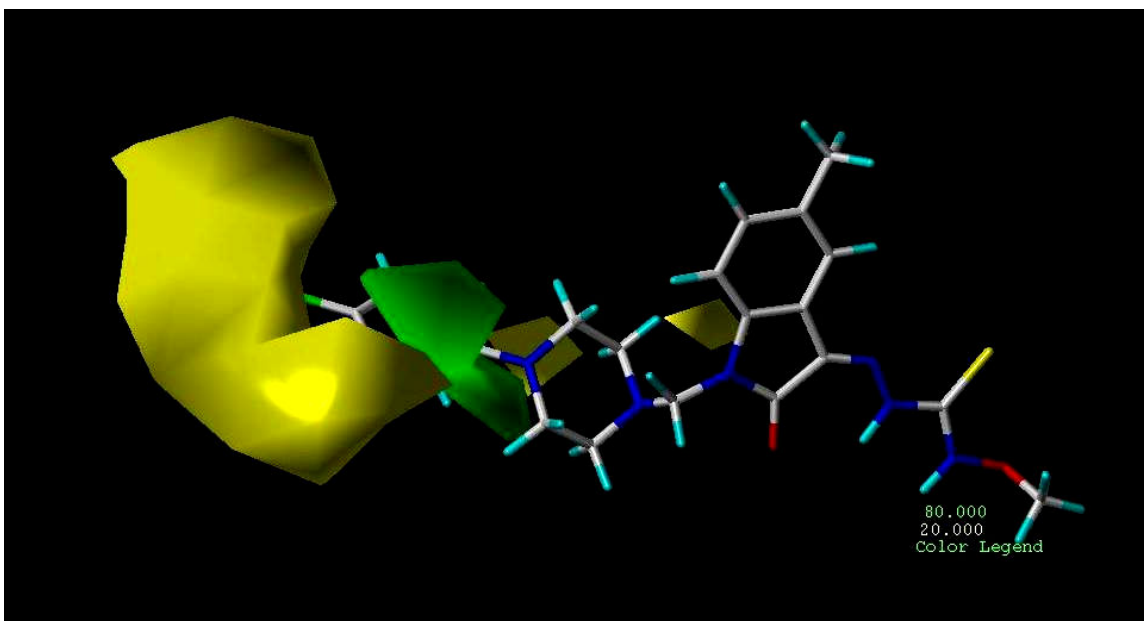


Fig. 5.10: CoMSIA steric contour map (green favored; yellow disfavored) around M21

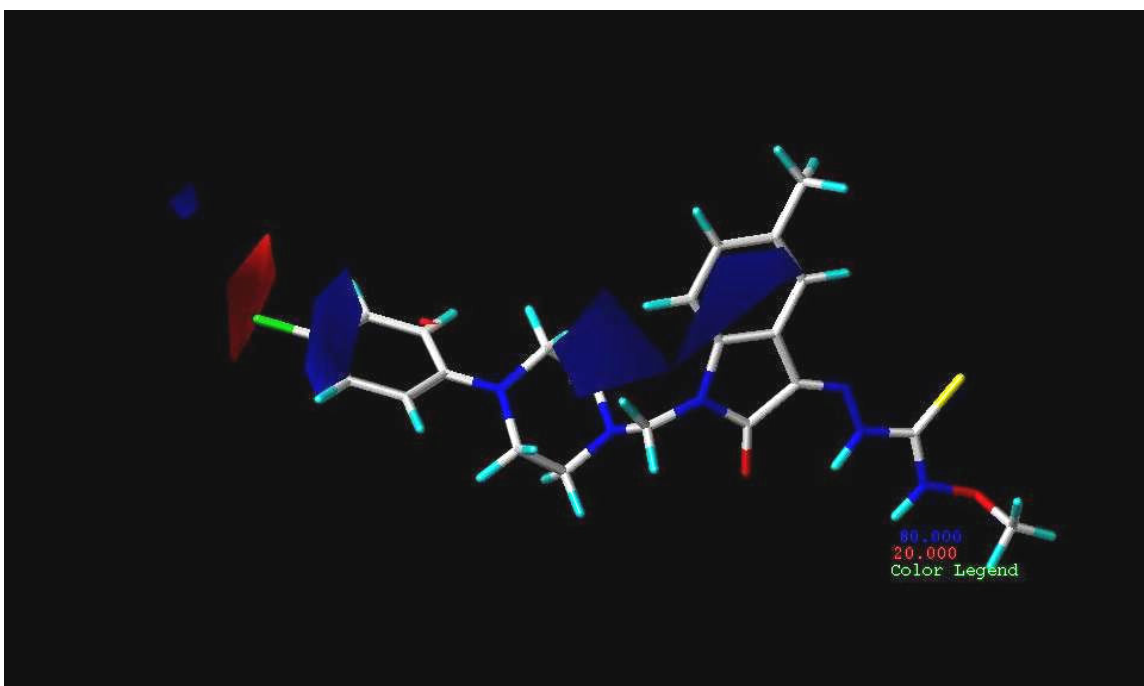


Fig. 5.11: CoMSIA electrostatic contour map around (red favored; blue disfavored) M21

Discussion:

CoMFA and CoMSIA Analyses based on HIV-1 screening. The CoMFA analysis was performed by dividing the array of compounds into training set of 34 compounds for model development and test set of 20 analogues, which were used for validation of this model. CoMFA study was developed using steric and electrostatic fields as independent variable and pEC₅₀ as dependent variable. CoMSIA study was developed based on steric, electrostatic, hydrophobic, hydrogen bond donor and hydrogen bond acceptor similarity fields as independent variables and pEC₅₀ as dependent variable [142].

The final CoMFA model was generated using cross-validated PLS analysis. PLS analysis showed a high q^2 value of 0.642 at 6 components with parabolic field (advanced CoMFA). The other fields like the indicator field and H-bonding field showed q^2 of 0.586 and 0.356 at 4 and 6 components respectively. When all these regions were focused, the q^2 improved and the parabolic field produced the highest q^2 of 0.666 at 6 components with high conventional r^2 . The obtained model was statistically significant as was evident from the q^2 , s_{press} , SE , F -value and r^2_{bs} values tabulated in the table for CoMFA and Advanced CoMFA fields. This final CoMFA model, had a cross-validated r^2 (q^2) of 0.666 with 6 principal components. The non cross-validated r^2 was determined to be 0.955 with standard error of estimate (SE) being 0.108 and covariance ratio (F) being 99.186 (significant at 99% level). This model was further validated using the test set compounds, which confirmed its reliable predictive ability. Bootstrapping results also supported the reliability of this model. The statistical parameters of this model are listed in Table 5.27.

In the CoMFA model, the steric and electrostatic field contributions were 0.669 and 0.331 respectively. The steric and electrostatic contour maps of this model are shown in Figs 5.6 and 5.7 respectively. The red regions in the contour maps refer to the electrostatically favored region and the blue region corresponds to electrostatically unfavored region. The green polyhedric regions correspond to sterically favored regions and yellow region refer to the sterically unfavored region. The red region near the *para* position of the phenyl ring of the phenyl piperazinyl methyl moiety suggests that introduction of more electronegative group at this position would enhance the anti-HIV activity of this class of compounds by virtue of some strong electrostatic interactions. The

blue regions near the 5th and 6th carbons of the phenyl ring indicate that presence of any electronegative moiety at these positions would be detrimental for anti-viral activity. The blue polyhedra around C₇ of isatin and C₂ of piperazine also indicated that introduction of any electronegative group at these positions would diminish the potential of these compounds to inhibit HIV. In the steric contour maps the green contour zone around *para* position of phenyl ring depicts that bulkier groups would enhance the anti-HIV activity. The diminutive green polyhedra near the methoxy group attached to the thiourea revealed that introduction of moderate bulky groups would be beneficial for anti-HIV activity. The yellow region near the methyl group at C₅ of isatin demonstrates that presence of bulky substituents would negatively influence the anti-HIV profile.

The best CoMSIA model, with q^2 of 0.823 is the one when all steric, electrostatic, hydrophobic, acceptor and donor fields were taken into account, and the contributions by these fields were 0.123, 0.241, 0.329, 0.242 and 0.064 respectively (Table 5.22). The donor field being comparatively insignificant was ignored for further calculations. The CoMSIA hydrogen bond acceptor contour illustrates (Fig 5.9) that presence of hydrogen bond acceptor groups (magenta colored) at the position adjacent to the thiourea moiety, around the piperazine moiety and the phenyl ring attached to the piperazine ring are conducive for the antiretroviral activity of this series. The CoMSIA hydrophobic contour map (Fig 5.8) depicted that presence of more hydrophobic moieties around the phenyl ring of isatin, piperazine and surrounding the phenyl appended to the piperazinyl methyl groups would prove to increase anti-HIV activity. The yellow polyhedron, in the CoMSIA steric contour, (Fig 5.10) near the chlorine attached to the *para* position of phenyl ring and C₅ of phenyl ring demonstrates that presence of bulky groups at these positions would hinder antiviral activity. The green region around C₁, C₂ and C₆ of phenyl ring emphasizes that bulky groups at these positions would further enhance the anti-HIV activity. The CoMSIA electrostatic contour map (Fig 5.11) demonstrated that presence of electronegative group at *para* position of the phenyl ring would further increase the antiretroviral activity as evident by the red region.

B. HIV-1 RT Docking

Results & Discussion:

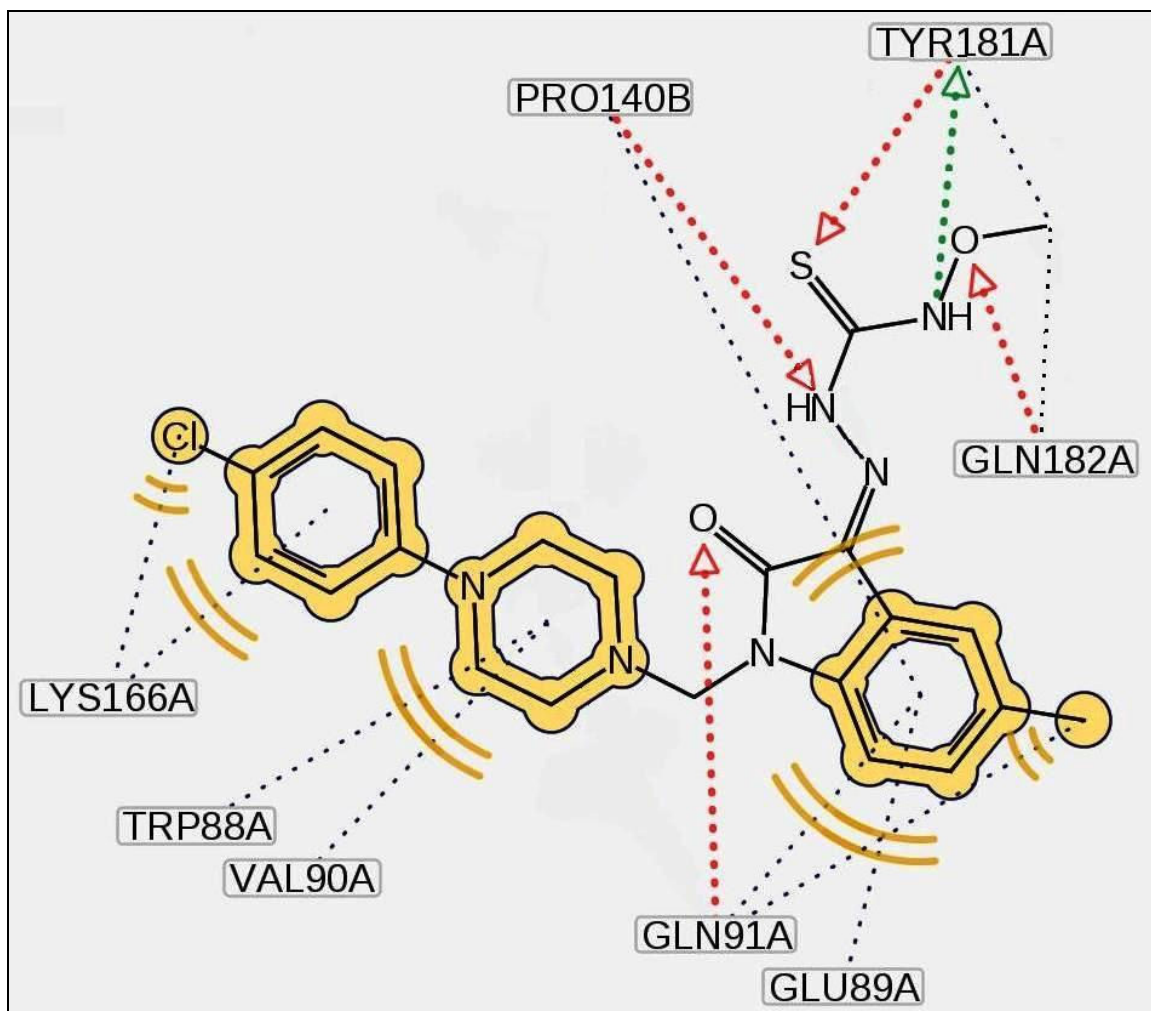


Fig. 5.12: Contact residues of M21 when docked onto HIV-1 RT

In order to probe the binding mode of our newly synthesized compounds in the HIV- RT active site, a modeling study was performed by means of GOLD [143, 144] for docking. Compound **M21** was docked onto the active site pocket of HIV-1 RT, the coordinates of which were taken from the crystal structure of RT/Nevirapine complex.

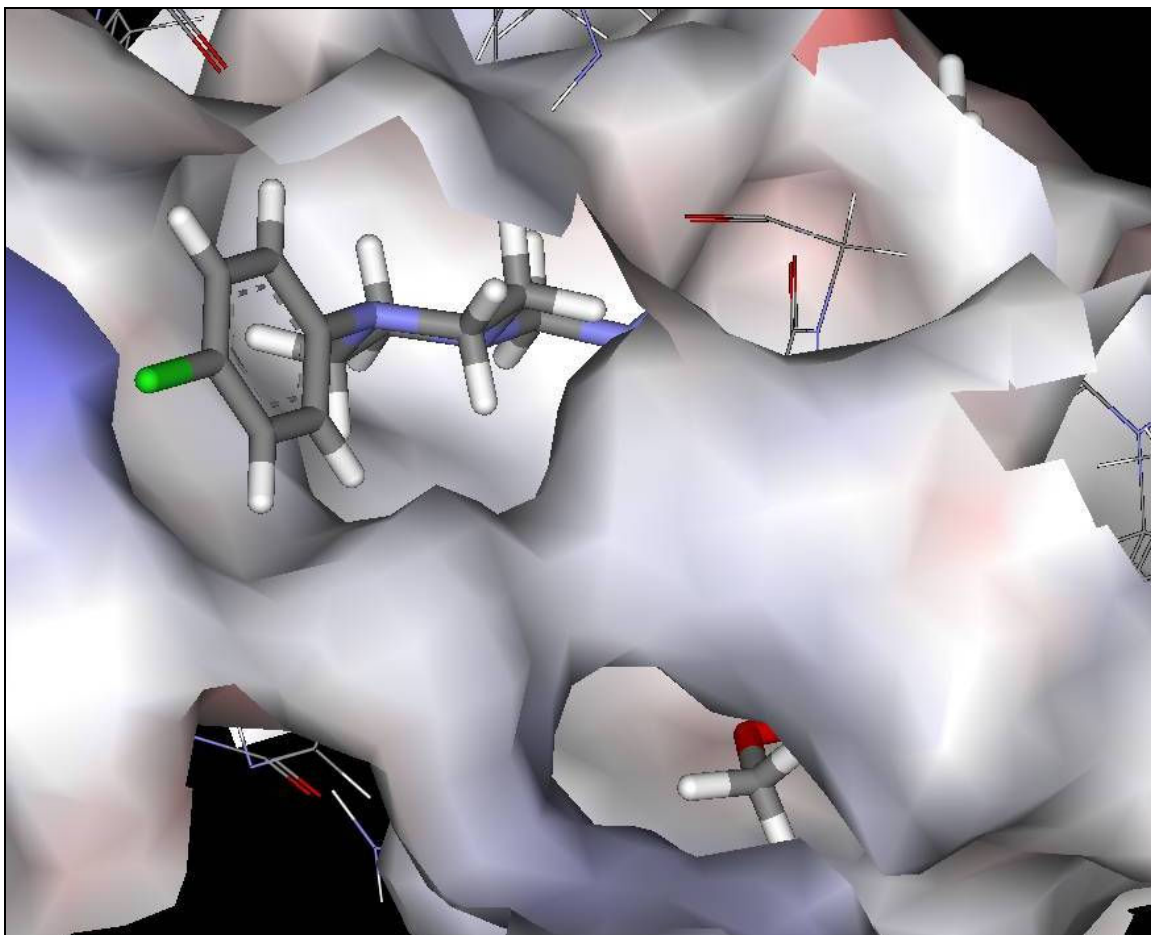


Fig. 5.13: Electrostatic surface view of active site pocket of HIV-1 RT bound to M21

The docking view of **M21** (Fig. 5.12 & 5.13), exhibited that the NH moiety of the methoxythioamido group was engaged in a hydrogen bonding interaction with the ring nitrogen of Pro140. The nitrogen of the terminal N-methoxy group was hydrogen bonded to the alcoholic oxygen of Tyr 181. The oxygen atom of the methoxy group was hydrogen bonded to the nitrogen of Gln 182's amide. The oxygen at C₂ of the indole ring was involved in hydrogen bond formation with the backbone nitrogen of Gln 91. The thioamido sulfur formed a hydrogen bond with Tyr 181. The chlorine functional group at the *para* position of the phenyl ring of the phenyl piperazinyl methyl group was involved in electrophilic interaction with Lys 166. Pro 140 was the major contributor of hydrophobic interaction for the aromatic indole nucleus. The aliphatic chains of Glu 89 and Gln 91 also interacted hydrophobically with the indole moiety. The aromatic ring of Tyr 181 and the aliphatic chain of Gln 182 were involved in steric interaction with the

terminal methoxy group. The chlorophenyl ring was well accommodated in the pocket bordered by the hydrophobic amino acid residues Trp 88, Val 90 and Lys 166. These residues also form the binding pocket for standard NNRTIs [145]. In summary, the results of the GOLD docking results supported our designed and synthesized compounds. Further structural optimization of **M21** for enhanced anti-HIV activity will be based on these facts highlighted by this docking simulation.

C. MTB ICL Docking

Results & Discussion:

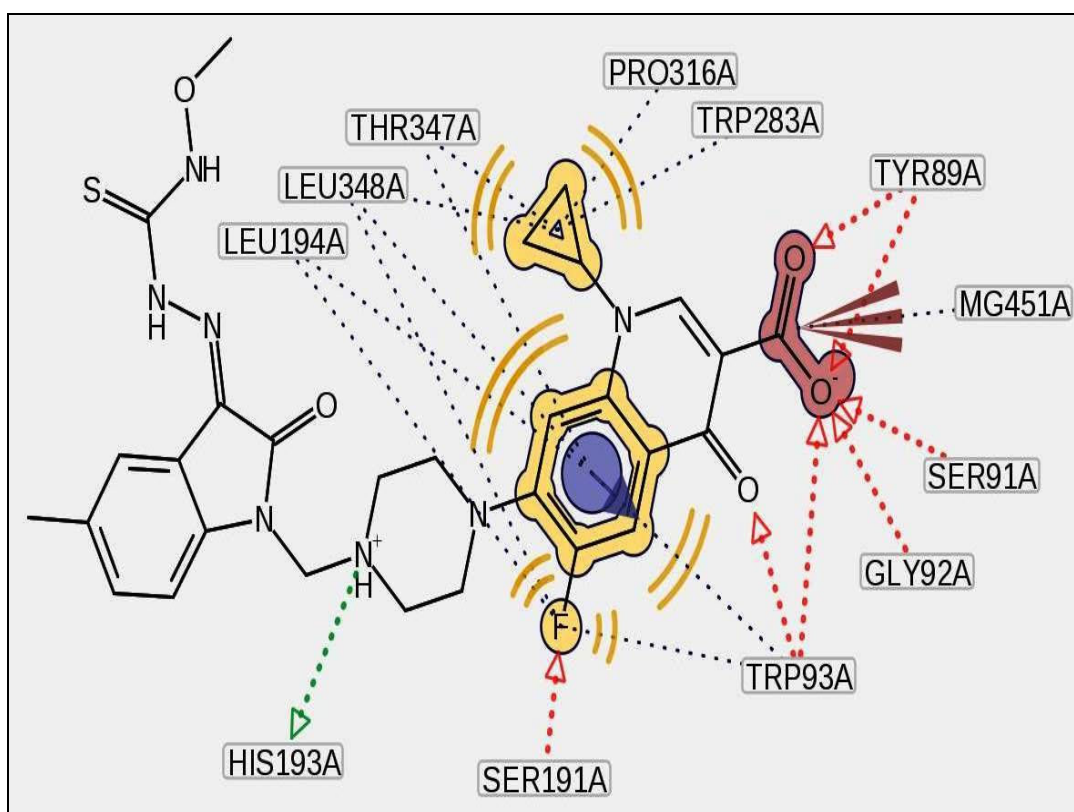


Fig. 5.14: Contact residues of M30 when docked onto MTB ICL

With the intention of investigating the binding manner of our designed analogues, a docking simulation was performed using Autodock 4.0. Compound **M30** was docked into the active site pocket of MTB ICL, the coordinates of which were taken from the crystal structure of ICL/Pyruvate complex.

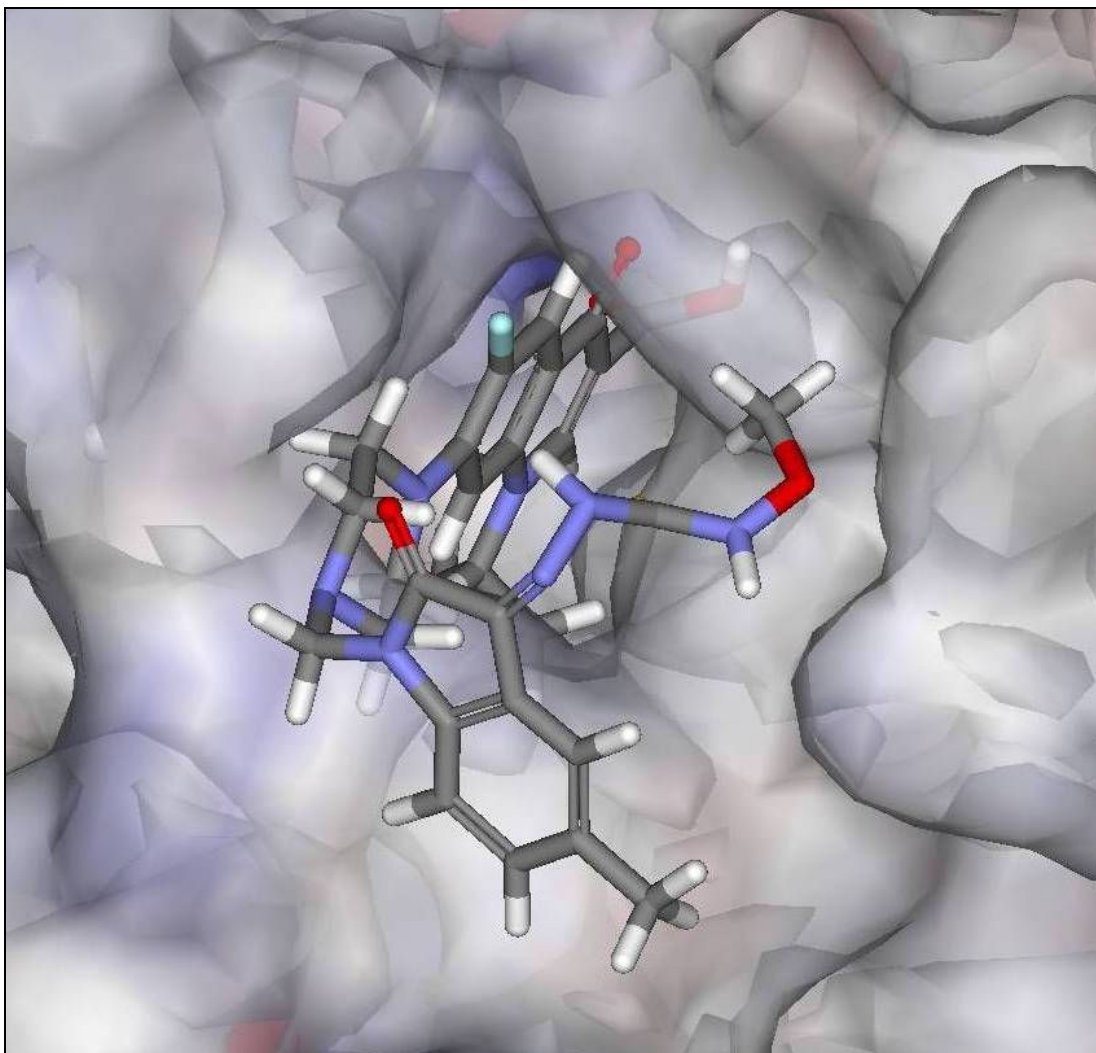


Fig. 5.15: Electrostatic surface view of active site pocket of MTB ICL bound to M30.

Eleven residues were present in the active site pocket, which was defined by a distance of 11.0 Å from the center of the active site. The docking analysis afforded a view (Fig. 5.14 & 5.15) of the hydrogen bonding interactions between the ligand and the active site residues of the protein. The hydroxyl of the quinolinyl carboxylate was engaged in hydrogen bonding interactions with Tyr 89, Ser 91, Gly 92 and Trp 93. The carbonyl oxygen of the quinolinyl carboxylate was hydrogen bonded to Tyr 89. The carbonyl oxygen at C₄ of quinoline moiety was involved in hydrogen bonding with the nitrogen of the peptide backbone of Trp 93. The N₄ of piperazine was found to be hydrogen bonded to imidazolyl nitrogen of His 193. The fluoroquinoline moiety was nestled in the hydrophobic pocket formed by the aromatic Trp 93, Leu 194, Thr 347 and Leu 348. Specifically, Trp 93 by virtue of its π -cloud provided favorable aromatic

interaction with the quinolinyl moiety. The cyclopropyl moiety attached to the N-1 of quinoline was located in the pocket formed by Trp 283, Pro 316, Thr 347 and Leu348. The fluorine atom at C₆ of quinoline was hydrogen bonded to Ser191 and it also possessed electrophilic interactions with Trp 93, Leu 194 and Leu 348. The carboxylate moiety at C₃ was also hydrogen bonded to the metal atom, Mg⁺⁺ ion of the protein. These residues also have significant implications in binding prototype ICL inhibitors viz. 3-NP and 3-bromo pyruvate [141].

5.4. Structure-activity-relationship (SAR) analysis:

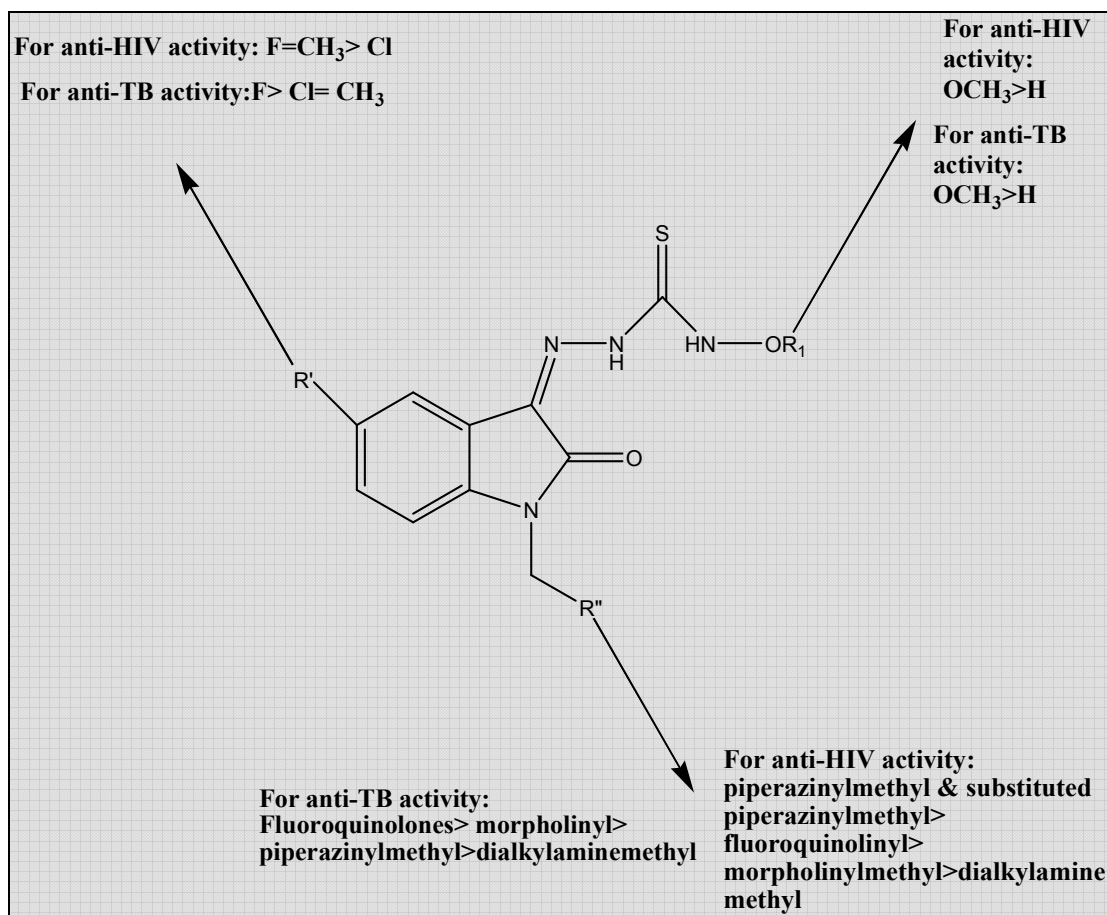


Fig 5.16: Schematic representation of SAR of *N*-Mannich bases of 5-substituted 1H-indole-2,3-dione 3-(*N*-hydroxy/methoxythiosemicarbazones)

CHAPTER 6

SYNTHESIS, BIOLOGICAL INTERVENTION AND COMPUTATIONAL STUDY OF *N*-MANNICH BASES OF 5-SUBSTITUTED-1*H*-INDOLE-2, 3-DIONE 3-(*N,N*-DIALLYL/DIPHENYL THIOSEMICARBAZONES)

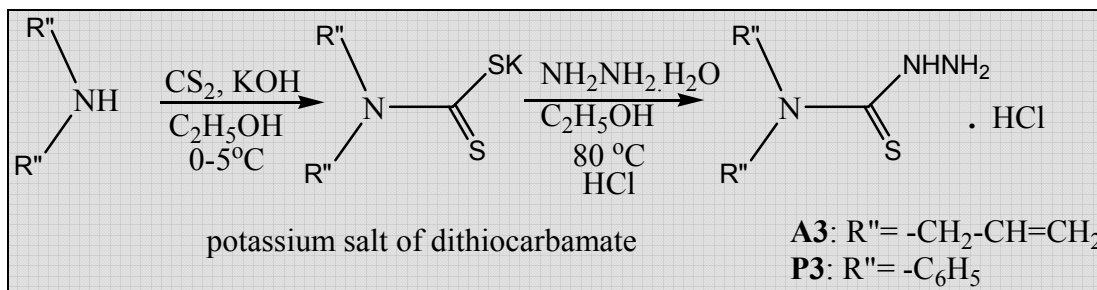
This chapter describes the synthesis, biological intervention and computational study of *N*-Mannich bases of 5-substituted-1*H*-indole-2, 3-dione 3-(*N,N*-diallyl/diphenyl thiosemicarbazones), since it was observed from earlier works that *N*-Mannich bases of 1*H*-indole-2,3-dione-3-(*N,N*-diethylthiosemicarbazone) have considerable potential against the replication of HIV-1 cells along with broad-spectrum chemotherapeutic properties [93]. The effect of increasing the lipophilicity of the molecules by appending bulky aryl or aliphatic moiety at the terminal end of the thiosemicarbazide was investigated by designing these molecules. Considering the isatinyl diethylthiosemicarbazone as the lead compound, these analogues were designed and synthesized and investigated for their ability to combat the HIV retrovirus as well as tackle the accompanying opportunistic infection viz. tuberculosis.

6.1 Synthesis

Step I: Synthesis of Isatin

The synthetic protocol is mentioned in Chapter 5.

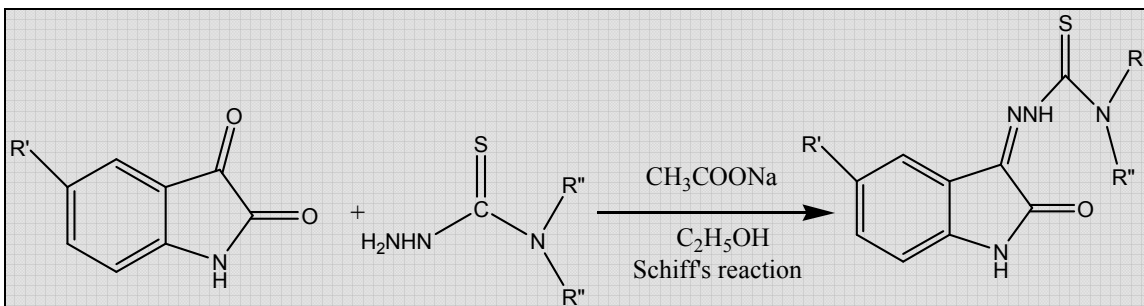
Step II: Synthesis of diallyl/diphenyl thiosemicarbazides (A3, P3)



To a solution of *N,N*-diallylamine(**A1**)/*N,N*-diphenylamine(**P1**) (0.01 mol) in absolute ethanol (20 ml) was added potassium hydroxide (0.01 mol) and carbon disulphide (0.75 ml), and the mixture was stirred at 0-5°C for 1 h to form the corresponding potassium salt

of dithiocarbamates (**A2,P2**). To the stirred mixture of dithiocarbamate salts was added hydrazine hydrate (0.01 mol) and the stirring was continued at 80°C for 1 h and on adding upon crushed ice the corresponding thiosemicarbazide was obtained which is converted to hydrochloride salts. **A3**: Yield : 32.8% ; M.P: >270 °C; **P3**: Yield: 17.28%; M.P: 231°C.

Step III: Synthesis of diallyl/diphenyl isatin-β-thiosemicarbazones (**A4-6, P4-6**)



To a hot dispersion of **A3/P3** (0.001M) in ethanol was added an equimolar aqueous solution of sodium acetate. To this solution further an equimolar ethanolic solution of various 5-substituted isatins was added and the mixture was stirred while being heated on a hot plate for 4-15 minutes, with immediate precipitation of a bulky solid. The resultant precipitate was filtered off and dried. The product was recrystallized from 95% ethanol.

Table 6.1: Physical data of synthesized Schiff base of isatins

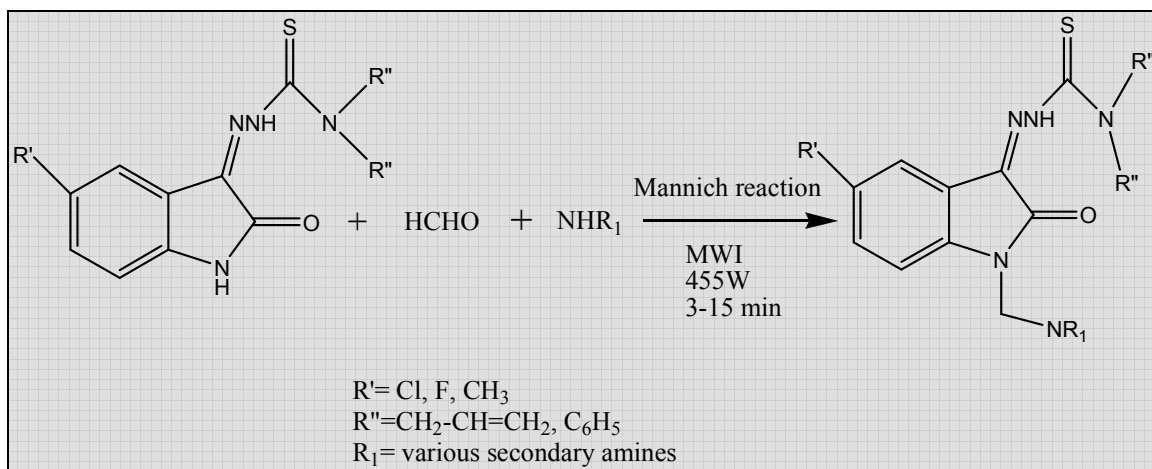
Compound code	R'	R''	% Yield	M.P (°C)	Molecular formula	Mol. Wt.
A4	Cl	CH ₂ -CH=CH ₂	65.9	216-218	C ₁₅ H ₁₅ ClN ₄ OS	270.7
A5	F	CH ₂ -CH=CH ₂	50.81	164-166 ^a	C ₁₅ H ₁₅ FN ₄ OS	254.24
A6	CH ₃	CH ₂ -CH=CH ₂	38.28	>260	C ₁₆ H ₁₈ N ₄ OS	250.28
P4	Cl	C ₆ H ₅	66.5	202-204	C ₂₁ H ₁₅ ClN ₄ OS	284.72
P5	F	C ₆ H ₅	48.7	198-200	C ₂₁ H ₁₅ FN ₄ OS	268.27
P6	CH ₃	C ₆ H ₅	41.93	210-211	C ₂₂ H ₁₈ N ₄ OS	264.3

^a Melting point of the compounds at their decomposition.

Table 6.2: Spectral data of the synthesized Schiff base

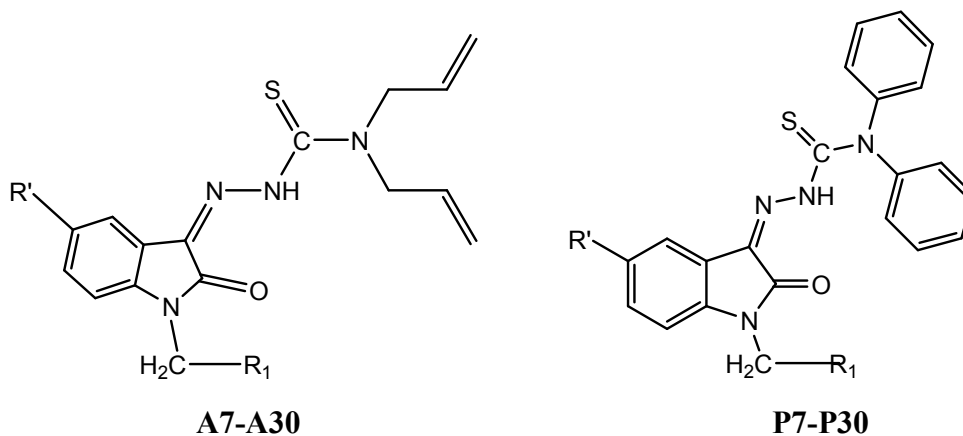
Compound code	IR spectroscopy (cm⁻¹; KBr pellet)	¹H-NMR (δ ppm, DMSO-d₆)
A4	1740 (amide stretch), 1625 (C=N stretch), 1645 (C=C stretch of alkene) 3010 (Aromatic C-H stretch), 3300 (amide NH stretch)	4.12 (m, 4H, -CH ₂ of diallyl), 5.18 (dd, 2H, C-3 H _{cis} of allyl), 5.21 (dd, 2H, C-3 H _{trans} of allyl), 5.84 (t, 2H, CH of CH=CH ₂), 7.03 (s, 1H, NH of hydrazino), 7.6 (m, 3H, isatiny), 8.1 (isatin NH).
P5	1740 (amide stretch), 1625 (C=N stretch), 3010 (Aromatic C-H stretch), 3300 (amide NH stretch)	6.46 (d, 4H, C ₂ , C ₆ of diphenyl), 7.11 (s, 1H, NH of hydrazino), 7.8 (m, 3H, isatiny), 8.1 (isatin NH).

Step IV: Synthesis of *N*-Mannich bases of isatin- β -thiosemicarbazones (A7-30, P7-30)



To an ethanolic solution of *N, N*-diallyl/diphenyl isatinyl thiosemicarbazones (0.00045M) was added an equimolar amount of various secondary amines, dissolved in ethanol or dimethyl sulfoxide. To this mixture, an equimolar amount of 30% formaldehyde solution was then added and this mixture was then irradiated with microwave of 455W in a scientific microwave reactor accompanied by continuous stirring, which was attained by means of a magnetic plate, placed underneath the floor of the magnetic cavity and a Teflon-coated magnetic bead in the reaction vessel, for approximately three to fifteen minutes. At the end of the reaction period, the product precipitated out, which was filtered off and dried. The resultant precipitate was recrystallized from ethanol. The physical data of the Mannich bases are given in Tables **6.3-6.5**. The spectral and elemental data of representative compounds are presented in Table **6.6-6.11**.

Table 6.3: Physical data of *N*-Mannich bases of isatin- β -thiosemicarbazones (A7-P14)



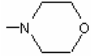
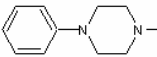
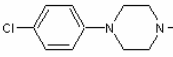
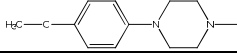
Compound code	Substituents		M.P (°C)	% Yield	Molecular Formula	Mol. Wt.	R _f ^b	logP ^c
	R'	R ₁						
A7	Cl	---N(CH ₃) ₂	112-114	92.13	C ₁₈ H ₂₂ ClN ₅ OS	391.92	0.47	3.61
P7	Cl	-do-	158-160	53.17	C ₂₄ H ₂₂ ClN ₅ OS	463.98	0.63	5.72
A8	F	-do-	106-110	65.01	C ₁₈ H ₂₂ FN ₅ OS	375.46	0.43	3.21
P8	F	-do-	151-153	38.93	C ₂₄ H ₂₂ FN ₅ OS	447.53	0.58	5.32
A9	CH ₃	-do-	104-108	90.27	C ₁₉ H ₂₅ N ₅ OS	371.5	0.48	3.54
P9	CH ₃	-do-	164-166	23.49	C ₂₅ H ₂₅ N ₅ OS	443.56	0.64	5.64
A10	Cl	---N(C ₂ H ₅) ₂	116-120	42.52	C ₂₀ H ₂₆ ClN ₅ OS	419.97	0.51	4.29
P10	Cl	-do-	97-98	31.76	C ₂₆ H ₂₆ ClN ₅ OS	492.04	0.66	6.39
A11	F	-do-	90-92	21.04	C ₂₀ H ₂₆ FN ₅ OS	403.52	0.47	3.89
P11	F	-do-	103-104	21.06	C ₂₆ H ₂₆ FN ₅ OS	475.58	0.58	5.99
A12	CH ₃	-do-	98-100	83	C ₂₁ H ₂₉ N ₅ OS	399.55	0.54	4.21
P12	CH ₃	-do-	95-96	74.52	C ₂₇ H ₂₉ N ₅ OS	471.62	0.65	6.32
A13	Cl		108-110	59	C ₂₀ H ₂₄ ClN ₅ O ₂ S	433.95	0.45	3.21
P13	Cl	-do-	64-66	45.85	C ₂₆ H ₂₄ ClN ₅ O ₂ S	506.02	0.53	5.32
A14	F	-do-	162-164	99.13	C ₂₀ H ₂₄ FN ₅ O ₂ S	417.5	0.42	2.81
P14	F	-do-	58-59	39.74	C ₂₆ H ₂₄ FN ₅ O ₂ S	489.56	0.57	4.92

^a Melting point of the compound at its decomposition.

^b Mobile phase CHCl₃ : CH₃OH (9 : 1).

^c LogP was calculated using ChemOffice 2004

Table 6.4: Physical data of *N*-Mannich bases of isatin- β -thiosemicarbazones (A15-P23)

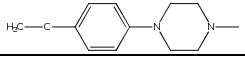
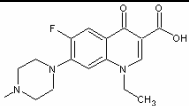
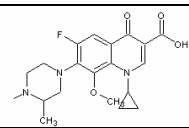
Compound code	Substituents		M.P (°C)	% Yield	Molecular Formula	Mol. Wt.	R _f ^b	logP ^c
	R'	R ₁						
A15	CH ₃		152-154	55.75	C ₂₁ H ₂₇ N ₅ O ₂ S	413.54	0.48	3.14
P15	CH ₃	-do-	48-50	54.12	C ₂₇ H ₂₇ N ₅ O ₂ S	485.6	0.53	5.24
A16	Cl		106-108	36.83	C ₂₆ H ₂₉ ClN ₆ OS	509.07	0.52	5.44
P16	Cl	-do-	102-104	62.38	C ₃₂ H ₂₉ ClN ₆ OS	581.13	0.64	7.55
A17	F	-do-	112-114	90.48	C ₂₆ H ₂₉ FN ₆ OS	492.61	0.49	5.04
P17	F	-do-	106-108	28.87	C ₃₂ H ₂₉ FN ₆ OS	564.08	0.61	7.15
A18	CH ₃	-do-	102-103	24.57	C ₂₇ H ₃₂ N ₆ OS	488.65	0.53	5.37
P18	CH ₃	-do-	114-116	68.93	C ₃₃ H ₃₂ N ₆ OS	560.71	0.67	7.48
A19	Cl		110-112	87	C ₂₆ H ₂₈ Cl ₂ N ₆ OS	543.51	0.49	6.0
P19	Cl	-do-	198-200	82.87	C ₃₂ H ₂₈ Cl ₂ N ₆ OS	615.58	0.61	8.1
A20	F	-do-	132-133	80	C ₂₆ H ₂₈ ClFN ₆ OS	527.06	0.48	5.6
P20	F	-do-	96-97	78.20	C ₃₂ H ₂₈ ClFN ₆ OS	599.12	0.59	7.7
A21	CH ₃	-do-	116-117	23.94	C ₂₇ H ₃₁ ClN ₆ OS	523.09	0.53	5.93
P21	CH ₃	-do-	108-110	67.53	C ₃₃ H ₃₁ ClN ₆ OS	595.16	0.65	8.03
A22	Cl		146-147	94	C ₂₇ H ₃₁ ClN ₆ O ₂ S	538.19	0.48	5.31
P22	Cl	-do-	192-194	64.22	C ₃₃ H ₃₁ ClN ₆ O ₂ S	611.16	0.54	7.42
A23	F	-do-	124-126	38.27	C ₂₇ H ₃₁ FN ₆ O ₂ S	522.64	0.46	4.91
P23	F	-do-	92-94	38.38	C ₃₃ H ₃₁ FN ₆ O ₂ S	594.7	0.52	7.02

^a Melting point of the compound at its decomposition.

^b Mobile phase CHCl₃ : CH₃OH (9 : 1).

^c LogP was calculated using ChemOffice 2004

Table 6.5: Physical data of *N*-Mannich bases of isatin- β -thiosemicarbazones (A24-P30)

Compound code	Substituents		M.P (°C)	% Yield	Molecular Formula	Mol. Wt.	R _f ^b	logP ^c
	R'	R ₁						
A24	CH ₃		153-154	31.26	C ₂₈ H ₃₄ N ₆ O ₂ S	518.67	0.51	5.24
P24	CH ₃	-do-	108-110	26.17	C ₃₄ H ₃₄ N ₆ O ₂ S	590.74	0.67	7.35
A25	Cl		133-134	46.91	C ₃₂ H ₃₃ ClFN ₇ O ₄ S	666.17	0.61	5.11
P25	Cl	-do-	174-176 ^a	46.82	C ₃₈ H ₃₃ ClFN ₇ O ₄ S	738.23	0.68	7.21
A26	F	-do-	172-174 ^a	96.04	C ₃₂ H ₃₃ F ₂ N ₇ O ₄ S	649.71	0.59	4.71
P26	F	-do-	166-168 ^a	26.54	C ₃₈ H ₃₃ F ₂ N ₇ O ₄ S	721.77	0.67	6.81
A27	CH ₃	-do-	146-147	94	C ₃₃ H ₃₆ FN ₇ O ₄ S	645.75	0.64	5.04
P27	CH ₃	-do-	170-172	23.69	C ₃₉ H ₃₆ FN ₇ O ₄ S	717.81	0.71	7.14
A28	Cl		160-164	46.36	C ₃₅ H ₃₇ ClFN ₇ O ₅ S	722.23	0.64	5.26
P28	Cl	-do-	198-200	56.71	C ₄₁ H ₃₇ ClFN ₇ O ₅ S	794.29	0.72	7.36
A29	F	-do-	146-148	92.02	C ₃₅ H ₃₇ F ₂ N ₇ O ₅ S	705.77	0.62	4.86
P29	F	-do-	203-205	26.73	C ₄₁ H ₃₇ F ₂ N ₇ O ₅ S	777.84	0.69	6.96
A30	CH ₃	-do-	108-110	35.84	C ₃₆ H ₄₀ FN ₇ O ₅ S	701.81	0.66	5.19
P30	CH ₃	-do-	207-208	29.99	C ₄₂ H ₄₀ FN ₇ O ₅ S	773.87	0.73	7.29

^a Melting point of the compound at its decomposition.

^b Mobile phase CHCl₃ : CH₃OH (9 : 1).

^c LogP was calculated using ChemOffice 2004

Table 6.6: Spectral and elemental data of *N*-Mannich bases of isatin- β -thiosemicarbazones

Compound	IR Spectroscopy (cm ⁻¹ ; KBr)	¹ H-NMR (δ ppm, DMSO-d ₆)	Elemental Analyses (Calculated/Found) ^a			Mass Spectrometry (m/z)
			C (%)	H (%)	N (%)	
A7	3035, 2846, 1732, 1645, 1618, 1215, 845.	2.23 (s, 6H, dimethylamine), 4.11 (s, 2H, -NCH ₂ N-), 4.26 (m, 4H, -CH ₂ of diallyl), 5.17 (dd, 2H, C-3 H _{cis} of allyl), 5.2 (dd, 2H, C-3 H _{trans} of allyl), 5.81 (t, 2H, CH of CH=CH ₂), 7.1 (s, 1H, NH of hydrazino), 7.4 (m, 3H, isatinyl)	55.16 55.14	5.66 5.67	17.87 17.85	391.12
A9	3030, 2850, 1730, 1643, 1620, 1210, 850.	2.26 (s, 6H, dimethylamine), 2.35 (s, 3H, CH ₃ at isatin C ₅), 4.03 (s, 2H, -NCH ₂ N-), 4.11 (m, 4H, -CH ₂ of diallyl), 5.17 (dd, 2H, C-3 H _{cis} of allyl), 5.2 (dd, 2H, C-3 H _{trans} of allyl), 5.81 (dd, 2H, CH of CH=CH ₂), 7.1 (s, 1H, NH of hydrazino), 7.4 (m, 3H, isatinyl)	61.43 61.41	6.78 6.81	18.85 18.87	371.18
A15	3033, 2847, 1725, 1650, 1625, 1195, 848.	2.35 (s, 3H, methyl at isatin C ₅), 2.37 (t, 4H, C ₂ , C ₆ of morpholinyl), 3.68 (t, 4H, C ₃ , C ₅ of morpholinyl), 4.04 (s, 2H, -NCH ₂ N-), 4.13 (m, 4H, -CH ₂ of diallyl), 5.17 (dd, 2H, C-3 H _{cis} of allyl), 5.2 (dd, 2H, C-3 H _{trans} of allyl), 5.83 (dd, 2H, CH of CH=CH ₂), 7.1 (s, 1H, NH of hydrazino), 7.5 (m, 3H, isatinyl)	60.99 60.96	6.58 6.55	16.94 16.92	413.19

^a Elemental analyses for C, H, N were within ± 0.4 % of the theoretical values.

Table 6.7: Spectral and elemental data of *N*-Mannich bases of isatin- β -thiosemicarbazones

Compound	IR Spectroscopy (cm ⁻¹ ; KBr)	¹ H-NMR (δ ppm, DMSO-d ₆)	Elemental Analyses (Calculated/Found) ^a			Mass Spectrometry (m/z)
			C (%)	H (%)	N (%)	
A17	3026, 2846, 1731, 1643, 1614, 1205, 855.	3.45 (t, 8H, piperazinyl), 4.02 (s, 2H, -NCH ₂ N-), 4.12 (m, 4H, -CH ₂ of diallyl), 5.17 (dd, 2H, C-3 <i>Hcis</i> of allyl), 5.2 (dd, 2H, C-3 <i>Htrans</i> of allyl), 5.84 (dd, 2H, CH of CH=CH ₂), 6.78 (m, 5H, phenylic), 7.1 (s, 1H, NH of hydrazino), 7.6 (m, 3H, isatinyl)	63.39 63.37	5.93 5.96	17.06 17.04	492.21
A19	3024, 2855, 1726, 1652, 1618, 1208, 846.	3.45 (t, 8H, piperazinyl), 4.04 (s, 2H, -NCH ₂ N-), 4.14 (m, 4H, -CH ₂ of diallyl), 5.17 (dd, 2H, C-3 <i>Hcis</i> of allyl), 5.2 (dd, 2H, C-3 <i>Htrans</i> of allyl), 5.81 (dd, 2H, CH of CH=CH ₂), 6.61 (d, 2H, C ₂ , C ₆ of phenyl), 7.11 (d, 2H, C ₃ , C ₅ of phenyl), 7.2 (s, 1H, NH of hydrazino), 7.8 (m, 3H, isatinyl)	57.46 57.44	5.19 5.18	15.46 15.43	542.14
A23	3032, 2848, 1731, 1647, 1623, 1202, 851.	2.89 (t, 8H, piperazinyl), 3.71 (s, 3H, methoxy), 4.02 (s, 2H, -NCH ₂ N-), 4.11 (m, 4H, -CH ₂ of diallyl), 5.17 (dd, 2H, C-3 <i>Hcis</i> of allyl), 5.2 (dd, 2H, C-3 <i>Htrans</i> of allyl), 5.84 (dd, 2H, CH of CH=CH ₂), 6.47 (d, 2H, C ₂ , C ₆ of methoxyphenyl), 6.73 (d, 2H, C ₃ , C ₅ of methoxyphenyl), 7.09 (s, 1H, NH of hydrazino), 7.47 (m, 3H, isatinyl)	62.05 62.03	5.98 5.96	16.08 16.09	522.22

^a Elemental analyses for C, H, N were within ± 0.4 % of the theoretical values.

Table 6.8: Spectral and elemental data of *N*-Mannich bases of isatin- β -thiosemicarbazones

Compound	IR Spectroscopy (cm ⁻¹ ; KBr)	¹ H-NMR (δ ppm, DMSO-d ₆)	Elemental Analyses (Calculated/Found) ^a			Mass Spectrometry (m/z)
			C (%)	H (%)	N (%)	
A25	3455, 3035, 2853, 1726, 1655, 1620, 1206, 850.	1.14 (t, 3H, CH ₃ of ethyl), 2.74 (t, 8H, piperazinyl), 3.13 (q, 2H, CH ₂ of ethyl), 4.01 (s, 2H, -NCH ₂ N-), 4.13 (m, 4H, -CH ₂ of diallyl), 5.17 (dd, 2H, C-3 H _{cis} of allyl), 5.2 (dd, 2H, C-3 H _{trans} of allyl), 5.82 (dd, 2H, CH of CH=CH ₂), 7.09 (s, 1H, NH of hydrazino), 7.3 (s, 1H, C ₅ of quinolone), 7.6 (m, 3H, isatiny), 11.4 (s, 1H, carboxylic acid)	57.69 57.71	4.99 4.96	14.72 14.71	665.20
A29	3452, 3025, 2852, 1725, 1653, 1625, 1205, 845.	0.51 (m, 4H, CH ₂ of cyclopropyl), 1.14 (d, 3H, CH ₃ at C ₃ of piperazinyl), 1.34 (t, 1H, CH of cyclopropyl), 3.07 (m, 1H, C ₃ of piperazinyl), 3.76 (s, 3H, methoxy at C ₈ of quinolone), 4.01 (s, 2H, -NCH ₂ N-), 4.13 (m, 4H, -CH ₂ of diallyl), 5.17 (dd, 2H, C-3 H _{cis} of allyl), 5.2 (dd, 2H, C-3 H _{trans} of allyl), 5.87 (dd, 2H, CH of CH=CH ₂), 7.03 (s, 1H, NH of hydrazino), 7.6 (m, 3H, isatiny), 11.05 (s, 1H, carboxylic acid)	59.56 59.53	5.28 5.31	13.89 13.86	705.25
P8	3032, 2847, 1728, 1622, 1195, 849.	2.21 (s, 6H, dimethylamine), 4.07 (s, 2H, -NCH ₂ N-), 6.82 (m, 10H, phenylic), 7.01 (d, 1H, isatin C ₆), 7.4 (s, 1H, isatin C ₄), 7.8 (d, 1H, isatin C ₇)	64.41 64.38	4.95 4.96	15.65 15.62	447.15

^a Elemental analyses for C, H, N were within ± 0.4 % of the theoretical values.

Table 6.9: Spectral and elemental data of *N*-Mannich bases of isatin- β -thiosemicarbazones

Compound	IR Spectroscopy (cm ⁻¹ ; KBr)	¹ H-NMR (δ ppm, DMSO-d ₆)	Elemental Analyses (Calculated/Found) ^a			Mass Spectrometry (m/z)
			C (%)	H (%)	N (%)	
P10	3028, 2851, 1732, 1617, 1209, 850.	1.03 (t, 6H, CH ₃ of diethylamine), 2.41 (q, 4H, CH ₂ of diethylamine), 4.04 (s, 2H, -NCH ₂ N-), 6.98 (m, 10H, phenylic), 7.4 (s, 1H, NH of hydrazino), 7.3 (m, 3H, isatiny)	63.47 63.46	5.33 5.34	14.23 14.21	491.15
P12	3035, 2850, 1727, 1621, 1207, 854.	1.02 (t, 6H, CH ₃ of diethylamine), 2.38 (s, 3H, CH ₃ at isatin C ₅), 2.45 (q, 4H, CH ₂ of diethylamine), 4.04 (s, 2H, -NCH ₂ N-), 6.85 (m, 10H, phenylic), 7.2 (m, 3H, isatiny), 7.6 (s, 1H, NH of hydrazino)	68.76 68.74	6.20 6.17	14.85 14.86	471.21
P16	3036, 2845, 1735, 1618, 1198, 852.	3.25 (t, 8H, piperazinyl), 4.01 (s, 2H, -NCH ₂ N-), 6.69 (m, 15H, phenylic), 7.2 (s, 1H, NH of hydrazino), 7.7 (m, 3H, isatiny)	66.14 66.13	5.03 5.05	14.46 14.49	580.18
P20	3026, 2853, 1730, 1622, 1209, 850.	3.28 (t, 8H, piperazinyl), 4.02 (s, 2H, -NCH ₂ N-), 6.56 (d, 2H, C ₂ , C ₆ of phenyl), 6.8 (m, 10H, phenylic), 7.1 (s, 1H, NH of hydrazino), 7.3 (d, 2H, C ₃ , C ₅ of phenyl), 7.6 (m, 3H, isatiny)	64.15 64.13	4.71 4.70	14.03 14.06	598.17

^a Elemental analyses for C, H, N were within ± 0.4 % of the theoretical values.

Table 6.10: Spectral and elemental data of *N*-Mannich bases of isatin- β -thiosemicarbazones

Compound	IR Spectroscopy (cm ⁻¹ ; KBr)	¹ H-NMR (δ ppm, DMSO-d ₆)	Elemental Analyses (Calculated/Found) ^a			Mass Spectrometry (m/z)
			C (%)	H (%)	N (%)	
P24	3029, 2853, 1726, 1619, 1210, 848.	2.33 (s, 3H, CH ₃ at isatin C ₅), 2.88 (t, 8H, piperazinyl), 3.72 (s, 3H, methoxy), 4.05 (s, 2H, -NCH ₂ N-), 6.45 (d, 2H, C ₂ , C ₆ of methoxyphenyl), 6.57 (d, 2H, C ₃ , C ₅ of methoxyphenyl), 6.92 (m, 10H, diphenyl), 7.2 (s, 1H, NH of hydrazino), 7.52 (m, 3H, isatinyl)	69.13 69.11	5.80 5.81	14.23 14.25	590.25
P26	3505, 3035, 2846, 1726, 1617, 1211, 848.	1.12 (t, 3H, CH ₃ of ethyl), 2.73 (t, 8H, piperazinyl), 3.15 (q, 2H, CH ₂ of ethyl), 4.05 (s, 2H, -NCH ₂ N-), 6.82 (m, 10H, diphenyl), 7.13 (s, 1H, NH of hydrazino), 7.3 (s, 1H, C ₅ of quinolone), 7.56 (m, 3H, isatinyl), 11.7 (s, 1H, carboxylic acid)	63.23 63.26	4.61 4.58	13.58 13.59	721.23
P28	3475, 3032, 2848, 1732, 1615, 1204, 845.	0.47 (m, 4H, CH ₂ of cyclopropyl), 1.13 (d, 3H, CH ₃ at C ₃ of piperazinyl), 1.37 (t, 1H, CH of cyclopropyl), 3.04 (m, 1H, C ₃ of piperazinyl), 3.74 (s, 3H, methoxy at C ₈ of quinolone), 4.05 (s, 2H, -NCH ₂ N-), 6.86 (m, 10H, diphenyl), 7.02 (s, 1H, NH of hydrazino), 11.09 (s, 1H, carboxylic acid)	62.00 61.97	4.70 4.73	12.34 12.37	793.22

^a Elemental analyses for C, H, N were within ± 0.4 % of the theoretical values.

Table 6.11: Spectral and elemental data of *N*-Mannich bases of isatin- β -thiosemicarbazones

Compound	IR Spectroscopy (cm ⁻¹ ; KBr)	¹ H-NMR (δ ppm, DMSO-d ₆)	Elemental Analyses (Calculated/Found) ^a			Mass Spectrometry (m/z)
			C (%)	H (%)	N (%)	
P30	3455, 3024, 2851, 1728, 1622, 1208, 851.	0.52 (m, 4H, CH ₂ of cyclopropyl), 1.13 (d, 3H, CH ₃ at C ₃ of piperaziny), 1.37 (t, 1H, CH of cyclopropyl), 2.34 (s, 3H, CH ₃ at isatin C ₅), 3.05 (m, 1H, C ₃ of piperaziny), 3.71 (s, 3H, methoxy at C ₈ of quinolone), 4.06 (s, 2H, -NCH ₂ N-), 6.84 (m, 10H, phenyl), 7.01 (s, 1H, NH of hydrazino), 11.05 (s, 1H, carboxylic acid)	65.18 65.15	5.21 5.18	12.67 12.66	773.28

^a Elemental analyses for C, H, N were within ± 0.4 % of the theoretical values.

Results and Discussion

Synthesis & Characterization:

The *N*-Mannich bases of the isatin- β -thiosemicarbazones (**A7-P30**) were synthesized by condensing the acidic imino group of isatin with formaldehyde and various secondary amines.

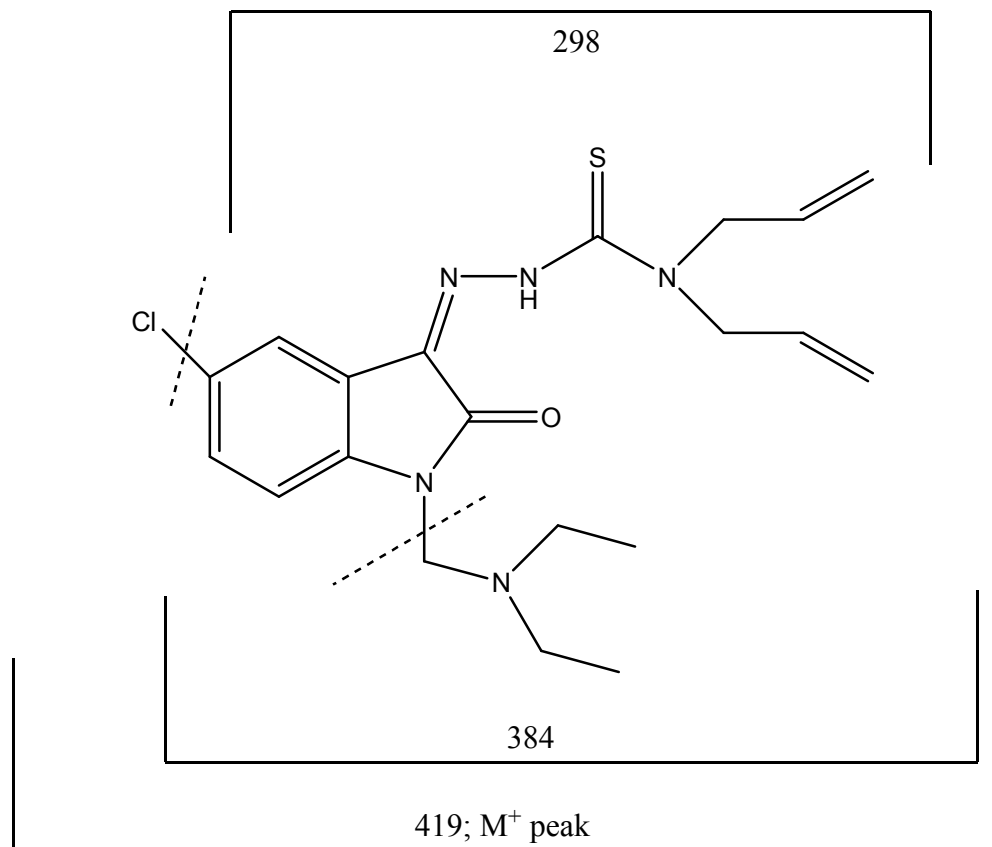
The % yield of these final products ranged from 21.04 to 99.13 % following recrystallization from ethanol. The purity of the compounds was assessed by ascending TLC using chloroform and methanol in the ratio of 9:1 as eluant. The elemental analysis of the compounds for C, H and N were within ± 0.04 % of the theoretical values.

The logP values ranged between 2.81 and 8.1 with **A14** having the lowest logP value and **P19** being the most lipophilic with a logP of 8.1. It was observed that the

compounds belonging to this series were in general more lipophilic due in part to their bulky aromatic or aliphatic side chain. Many of the analogues had logP greater than 5.0 and hence were not obeying Lipinski's rule of five [131].

The assignments of structures were based on elemental and spectroscopic methods and the chemical shifts obtained from $^1\text{H-NMR}$ spectra supported the proposed structures. The IR spectra displayed new absorption band in the region of 2850 cm^{-1} due to the methylene group ($-\text{CH}_2-$). Absence of peak at 3200 cm^{-1} , due to amide group (N-H group), indicated the replacement of active hydrogen atom of isatin with aminomethyl group. The aromatic CH stretching was observed at 3030 cm^{-1} , the C=O stretch of $-\text{amide}$ at 1620 cm^{-1} , the C=N peak at 1730 cm^{-1} , the C=S peak at 1210 cm^{-1} , and the aromatic CH bending vibrations at 850 cm^{-1} . A peak was also observed at around 1650 cm^{-1} in case of the diallyl analogues due to the alkene C=C stretching. In the case of molecules like **P28**, **P30** which has a fluoroquinolone moiety a broad OH stretch, due to the carboxylic acid, was observed around 3500cm^{-1} , along with a C=O stretch around 1710 cm^{-1} .

In the NMR spectra for the isatin- β -thiosemicarbazones (Schiff bases), sharp singlet was observed at δ 10.6 ppm due to $-\text{NH}$ group of isatin; whereas in the case of the N-Mannich bases this singlet disappeared and a new singlet appeared at δ 5.92 ppm due to the $-\text{NCH}_2\text{N}-$ protons of the methylene Mannich group.



The mass spectrum of **A10** showed a molecular ion peak at m/z 419 and an M+2 peak at m/z 421. The other remaining major fragmentation peaks were at m/z 384 and 298.

6.2 Biological activity

Results:

The titled compounds were screened for their anti-HIV activity and cytotoxicity against HIV-1 (HTLV-III_B) in MT-4 cell line.

Table 6.12: Anti-HIV activity and cytotoxicity of compounds (A7-P16) against HIV-1 (HTLV-III_B) in MT-4 cell line

Compound code	EC₅₀^a (μM)	CC₅₀^b (μM)	S.I.^c
A7	5.36	>510.20	95.19
P7	9.25	336.65	36.39
A8	2.62	>532.76	203.34
P8	6.57	295.17	44.93
A9	0.64	>538.36	841.19
P9	4.19	328.25	78.34
A10	3.88	>476.19	122.73
P10	14.83	125.68	8.47
A11	0.61	>495.66	812.56
P11	8.46	112.34	13.28
A12	0.30	>500.63	1668.77
P12	11.72	135.96	11.60
A13	5.99	>460.83	76.93
P13	22.42	156.74	6.99
A14	2.61	>479.04	183.54
P14	19.54	132.47	6.78
A15	2.02	>483.68	239.45
P15	13.51	218.49	16.17
A16	15.95	385.06	24.14
P16	17.38	141.28	8.13

^a Effective concentration of the drug that reduces HIV-1 induced cytopathic effect by 50% in MT-4 cells. ^b Cytotoxic concentration of the drug that decreases MT-4 cell's viability by 50.

^c Selectivity index or ratio of CC₅₀ to EC₅₀.

Table 6.13: Anti-HIV activity and cytotoxicity of compounds (A17-P26) against HIV-1 (HTLV-III_B) in MT-4 cell line

Compound code	EC₅₀^a (μM)	CC₅₀^b (μM)	S.I^c
A17	18.11	383.67	21.19
P17	41.48	110.62	2.67
A18	14.47	324.03	22.39
P18	9.98	81.68	8.18
A19	13.11	287.29	21.91
P19	10.12	105.95	10.47
A20	19.22	364.33	18.96
P20	19.90	72.94	3.67
A21	15.76	176.58	11.20
P21	3.53	87.88	24.90
A22	11.39	333.95	29.32
P22	13.74	128.12	9.32
A23	11.78	340.60	28.91
P23	35.01	66.92	1.91
A24	9.14	316.52	34.63
P24	5.43	64.157	11.82
A25	8.71	193.69	22.24
P25	12.95	97.83	7.55
A26	4.8	256.92	53.53
P26	7.93	125.49	15.82

^a Effective concentration of the drug that reduces HIV-1 induced cytopathic effect by 50% in MT-4 cells.

^b Cytotoxic concentration of the drug that decreases MT-4 cell's viability by 50.

^c Selectivity index or ratio of CC₅₀ to EC₅₀.

Table 6.14: Anti-HIV activity and cytotoxicity of compounds (A27-P30) against HIV-1 (HTLV-III_B) in MT-4 cell line

Compound code	EC₅₀^a (μM)	CC₅₀^b (μM)	S.I^c
A27	3.19	>309.59	97.05
P27	3.94	168.98	42.89
A28	5.97	>276.93	46.39
P28	10.27	113.45	11.05
A29	2.93	>283.28	96.68
P29	5.61	65.79	11.73
A30	1.33	>284.9	214.21
P30	4.91	169.56	34.53
Nevirapine	0.13	156	1200.00
Trovirdine	0.016	87	5437.50

^a Effective concentration of the drug that reduces HIV-1 induced cytopathic effect by 50% in MT-4 cells.

^b Cytotoxic concentration of the drug that decreases MT-4 cell's viability by 50.

^c Selectivity index or ratio of CC₅₀ to EC₅₀.

Selected compounds were analysed for their ability to repress HIV-1 RT enzyme.

Table 6.15: HIV-1 RT enzyme inhibition data for substituted isatin-β-thiosemicarbazones^a

Compound code	IC₅₀ (μM) against HIV-1 RT^b
A8	11.0±3.2
A9	9.2±1.3
A11	10.1±2.8
A12	8.4±1.8
A15	14.5±4.2
Nevirapine	0.25
Trovirdine	0.017 ± 0.007

^a Enzyme assays done with WT RT. ^b IC₅₀ is the quantity of drug that reduced WT RT enzyme activity by 50%.

All the analogues were screened for their ability to inhibit the growth of H37 Rv strain of MTB in logarithmic phase. MIC was the concentration at which the H37Rv MTB strain showed complete inhibition.

Table 6.16: Anti-tubercular activity of compounds (A7-P30) against H37Rv strain of MTB in logarithmic phase

Compound code	MIC in μM	Compound code	MIC in μM
A7	63.77	A19	23.02
P7	13.47	P19	2.53
A8	8.337	A20	2.96
P8	19.52	P20	1.30
A9	33.647	A21	10.58
P9	3.516	P21	1.31
A10	>59.52	A22	23.19
P10	22.45	P22	5.12
A11	7.757	A23	5.98
P11	20.83	P23	2.62
A12	62.57	A24	7.62
P12	5.71	P24	2.64
A13	28.8	A25	2.34
P13	12.08	P25	1.04
A14	7.497	A26	0.615
P14	6.38	P26	0.35

Table 6.16: Anti-tubercular activity of compounds (A7-P30) against H37Rv strain of MTB in logarithmic phase (Contd.)

Compound code	MIC in μM	Compound code	MIC in μM
A15	30.229	A27	1.207
P15	6.445	P27	0.27
A16	24.557	A28	0.276
P16	5.386	P28	0.26
A17	12.68	A29	0.283
P17	2.765	P29	0.136
A18	19.61	A30	0.569
P18	2.78	P30	0.258
Isoniazid	0.36	Rifampicin	0.12

Few of the analogues were screened for their ability to suppress dormant MTB.

Table 6.17: Anti-tubercular activity of selected compounds against dormant MTB

Compound code	Dormant MTB MIC (μM)^a
A7	>127.35
A10	>119.13
A12	31.34
A13	57.21
A26	19.239
A28	34.615
A30	17.811
P27	34.828
P30	32.305
Isoniazid	182.31
Rifampicin	15.19

^aMIC was the concentration at which the dormant H37Rv MTB strain showed complete inhibition.

Few of the analogues were analyzed for their ability to inhibit MTB ICL enzyme.

Table 6.18: MTB ICL suppression by selected compounds

Compound code	MTB ICL % Inhibition (conc. of stock solution used)
A7	8.32 (10mM)
A10	6.15 (10mM)
A12	40.45 (10mM)
A13	31.42 (10mM)
A26	20.74 (10mM)
A28	10.74 (10mM)
A30	23.41 (10mM)
P27	11.23 (10mM)
P30	10.63 (10mM)
3-NPA	65.99 (100mM)

Few of the analogues were tested for their ability to inhibit supercoiling of DNA gyrase of *Mycobacterium smegmatis* (MC₂).

Table 6.19: *Mycobacterium smegmatis* DNA gyrase supercoiling inhibition by selected compounds

Compound code	IC₅₀ (μM)
A25	60.04
A26	>76.96
A27	61.94-77.43
A28	27.69
A29	70.84
A30	42.75
P27	41.79-55.73
P30	51.69
Ciprofloxacin	15.09
Moxifloxacin	12.46

Selected analogues were analysed for their activity against influenza type A and B virus in MDCK cell line.

Table 6.20: Activity of selected compounds against Influenza Type A virus

Compound code	EC₅₀ (μM)	IC₅₀ (μM)	SI
A14	31.14	>81.44	>2.62
A25	22.52	51.04	2.27

Table 6.21: Activity of selected compounds against Influenza Type B virus

Compound code	EC₅₀ (μM)	IC₅₀ (μM)	SI
A14	74.25	79.04	1
A22	>7.43	7.43	0
A25	>46.53	46.53	0
A29	45.34	141.69	3

Selected compounds were tested for their antiviral activity against SARS virus in Vero 76 cell line.

Table 6.22: Activity of selected compounds against SARS virus

Compound code	EC₅₀ (μM)	IC₅₀ (μM)	SI
A14	62.28	76.65	1.23
A25	48.04	121.59	2.53
A29	45.34	>69.43	>1.53

Discussion:

A. *In vitro* anti-HIV assays:

The forty-eight titled compounds were evaluated for their ability to inhibit the replication of HIV-1 (III_B) cells in MT-4 cell line. EC₅₀ of the entire series were found to lie between the range of 0.3028 to 41.4835 μM (**Table 6.12-6.14**), with N,N-diallyl-2-(1-((diethylamino)methyl)-5-methyl-2-oxoindolin-3-ylidene)hydrazinecarbothioamide (**A12**), displaying the maximum inhibition of 0.3028 μM against HIV-1 replication. Comparison between the twenty-four diallyl thiosemicarbazone Mannich bases reveals that three of these, namely **A9**, **A11** and **A12** have EC₅₀ value less than 1 μM. At N₁ of isatin (R₁), the presence of dialkylamine substituents yielded compounds with better antiviral activity than the ones with piperazinyl/ substituted piperazinyl or flouroquinolone substituents. Diethylamine substituted derivatives (**A10-A12**) were found to have higher anti-viral activity than those of dimethylamine substituted ones (**A7-A9**). In contrast to analogues with piperazinyl substitution at R₁ (**A16-A24**), morpholinyl substitution yielded compounds (**A13-A15**) with higher anti-HIV activity. Substitution at R₁ with various piperazines lead to compounds possessing anti-HIV activity of the following order: 4-fluoro-phenyl piperazine < phenyl piperazine < 4-methoxy phenyl piperazine. Flouroquinolone substitution at R₁ gave compounds with greater anti-HIV activity than those with piperazinyl substitution but lesser than dialkylamine substitution. In contrast to norfloxacin analogues (**A25-A27**), gatifloxacin analogues (**A28-A30**) were found to be more promising in terms of anti-HIV activity. At the 5th position of the indolyl moiety (R'), the presence of methyl group resulted in compounds with superior anti-HIV activity followed by fluoro and then chloro group. **A12**, the compound with the highest anti-viral potency probably is involved in steric and hydrophobic interaction with bulky residues of the active site pocket by virtue of its methyl group at R' and also due to the diallylic moiety, attached to the thiourea group. The diallyl moiety might also be involved in some dipole-dipole interaction with some charged residues of the protein. While comparing between the diallyl and diphenyl thiosemicarbazone Mannich bases it was observed that diallyl derivatives had higher anti-viral activity. This can be ascribed to the allyl moiety present at the terminal of the hydrazino carbothiamido group, contributing to possible dipole-dipole interaction with certain charged groups of the

active site residues of the protein. The diminished activity of the diphenyl analogues may be due to the bulky phenyl groups which may be hindering the molecule from reaching inside the active pocket of the protein and interacting with the active residues. Amongst the diphenyl thiosemicarbazones, 2-(1-((4-(4-chlorophenyl)piperazin-1-yl)methyl)-5-methyl-2-oxoindolin-3-ylidene)-N,N diphenylhydrazinecarbothioamide (**P21**) was found to be most effective against HIV-1 replication with an EC_{50} of 3.53 μ M. At R_1 , presence of piperazinyl/substituted piperazinyl substitution (**P16-P24**) results in better anti-viral leads when compared to morpholinyl substitution (**P13-P15**). The morpholinylmethyl analogues in general had diminished anti-viral activity which can be attributed to the repulsion experienced by the oxygen of morpholine ring. Presence of dialkylamine at R_1 gave compounds with enhanced anti-HIV profile (**P7-P12**). Substitution at R_1 with flouroquinolones (**P25-P30**) resulted in compounds with improved anti-HIV activity in comparison to piperazinyl substitution. The antiviral potency of **P21** can be credited to the combined presence of the substituents at R' and R_1 . At R_1 , the 4-chlorophenyl piperazinyl methyl moiety might be engaged in some H-bonding interaction due to the piperazinyl group and also may be forming some polar bond due to the halogen at the *para* position of the phenyl ring.

The cytotoxic effect of these molecules was measured in MT-4 cells in parallel with the antiviral activity. **A9**, was found to be the least cytotoxic with a CC_{50} value of >538.36 μ M. The cytotoxicity of these forty-eight compounds was found to lie in the range of 64.17 to 538.36 μ M (**Table 6.12-6.14**). In general, these compounds portrayed lesser cytotoxicity profile than that of clinically used anti-HIV agents viz. nevirapine and trovirdine. Between diallyl thiosemicarbazones and diphenyl thiosemicarbazones, diallyl analogues were found to be less cytopathic to MT-4 cells. The greater cytotoxicity of the diphenyl derivatives may be because of the phenyl rings being involved in non-specific binding other than the active site due to its steric nature.

B. HIV-1 RT enzyme inhibition assay:

HIV-1 Reverse Transcriptase (RT) is the prime target for many anti-AIDS drugs that are being used clinically and are there in the developmental phases. RT is the only enzyme that catalyses the transformation of single-stranded viral RNA into double-stranded DNA which further gets incorporated into the host's chromosomes [25]. Drugs targeting RT can be broadly categorized into two classes: Nucleoside reverse transcriptase inhibitors (NRTIs) and Non-nucleoside reverse transcriptase inhibitors (NNRTIs). NNRTIs inhibit the polymerase activity of RT [146]. NNRTIs are specific to HIV-1 RT and hence are comparatively less toxic to the host. Though NNRTIs are structurally diverse, they act on RT by inducing conformational changes that form the NNRTI binding pocket (NNIBP). In the absence of any NNRTI, the NNIBP does not exist [24]. The NNIBP is primarily made up of hydrophobic amino acid residues and the cavity is created due to torsional rotation of Tyr181 and Tyr188 [117]. These Tyr residues skirt the catalytic aspartates, Asp-185 and Asp 186, whose movements distort the polymerase active site [26].

Five out of the entire battery of compounds were analyzed for their ability to inhibit HIV-1 RT. Two out of these five, namely **A9** and **A12**, displayed IC_{50} values below 10 μ M. N,N-diallyl-2-(1-(((diethylamino)methyl)-5-methyl-2-oxoindolin-3-ylidene)hydrazinecarbothioamide (**A12**) manifested the greatest inhibition of RT with IC_{50} value of 8.4 ± 1.8 μ M. The higher potency of **A9** and **A12** to repress RT can be accredited to the dialkylamine methyl moiety attached at N-1 of the indolyl group, which might possibly be having some favorable interaction with the hydrophobic residues of the NNIBP. The diallyl group appended to the thiourea moiety may also have a role in interacting with the active site residues by virtue of the π -electrons present in it.

C. *In vitro* anti-tubercular evaluation:

The titled compounds when evaluated for their inhibitory activity against the replication of MTB in logarithmic growth phase displayed activity ranging from 0.14 to 63.77 μM (**Table 6.16**). Nine of these derivatives had MIC below 1 μM . The compound which displayed the greatest inhibition of MTB culture in logarithmic phase was found to be 1-cyclopropyl-7-(4-((3-(2-(diphenylcarbamothioyl)hydrazono)-5-fluoro-2-oxoindolin-1-yl)methyl)-3-methylpiperazin-1-yl)-6-fluoro-8-methoxy-4-oxo-1,4-dihydroquinoline-3-carboxylic acid (**P29**), with an MIC value of 0.14 μM . In contrast to the diallyl analogues the diphenyl derivatives portrayed much higher inhibition of MTB multiplication in logarithmic phase. Amongst the compounds belonging to the diallyl series, the most significant anti-tubercular potency was shown by 7-(4-((5-chloro-3-(2-(diallylcarbamothioyl)hydrazono)-2-oxoindolin-1-yl)methyl)-3-methylpiperazin-1-yl)-1-cyclopropyl-6-fluoro-8-methoxy-4-oxo-1,4-dihydroquinoline-3-carboxylic acid (**A28**) with MIC of 0.28 μM . The prominent anti-tubercular activity of **A28** can be ascribed to many of the functional groups present on the fluoroquinolone moiety namely, the carboxylic acid group being involved in hydrogen bonding interaction; the cyclopropyl group being responsible for hydrophobic interaction; the fluoro group possibly being involved in some ion-dipole interaction with some charged residues of the active site pocket; and the methoxy group also contributing to some hydrogen bonding interaction with hydrogen-donor groups present in the active site. While considering the effect of the substituent attached to N_1 (R_1), presence of piperazinylmethyl/substituted piperazinylmethyl groups led to compounds (**A16-A24**) which had higher anti-TB activity than those with morpholinylmethyl groups (**A13-A15**). Sequence of anti-TB activity followed by the compounds when diverse piperazines were present at R_1 is: 4-chloro-phenyl piperazine > 4-methyl-phenyl piperazine > phenyl piperazine. When R_1 is occupied by fluoroquinolones, it gives rise to compounds with anti-tubercular activity higher than those with piperazinyl and dialkylamine substituents. Amongst the fluoroquinolone analogues the gatifloxacin substituted ones (**A28-A30**) exhibited improved inhibitory profile than those with norfloxacin (**A25-A27**). Amongst the twenty-four derivatives belonging to diallyl series, the dialkylamine substituents had the highest MIC values.

In the diphenyl thiosemicarbazone series, five of the analogues exhibited MIC below 1.0 μM (**Table 6.16**). The substituent at C₅ of isatin (R') being kept constant, when R₁ was varied amongst the diphenyl series, the order of activity conformed to the following sequence: diethylamine < dimethylamine < Morpholine < phenyl piperazine < 4-methyl phenyl piperazine < 4-chloro-phenyl piperazine < norfloxacin < gatifloxacin; except for 5-flouro derivatives were morpholinyl derivatives had the least activity and the remaining substituents following the same order. The greater activity profile of the flouroquinolone substituted analogues can be accredited to their increased lipophilicity permitting them to penetrate into the mycolic acid cell wall of the bacilli. While studying the presence of various functional groups at R', it was observed that flouro analogues have higher inhibitory action on MTB growth, which might possibly be owing to flourine's electronegativity contributing to some interaction with some positively charged residues in the active site.

D. Anti-tubercular activity of compounds against dormant MTB:

Mycobacterium tuberculosis is a pathogen that is wreaking havoc globally due to its ability to persist for long periods of time in the macrophages of the alveoli, by remaining disguised from the human immune system. The assemblage of genes that permits the organism to enter phases of dormancy and then re-emerge later during endogenous re-infection are now being revealed. Latent bacilli are generated by the launching of specific immunity which forces the bacilli to remain in a stationary phase inside the necrotic tissue. This tissue is crucial because it maintains a stable bacilli population and protracts the production of foamy macrophages which thereby helps the bacillus to escape to the alveolar spaces. In the alveolar spaces, the bacillus regrows and, when it is released into the alveolar space, it induces new granulomas which are less developed due to the effective immunity of the immunocompetent host. Hence newer chemotherapeutic agents are needed which would target the necrotic tissues which harbor these dormant mycobacteria [147].

These compounds were also screened for their activity against suppression of dormant MTB culture and nine of them demonstrated inhibition superior by many degrees to that of prototype drug INH (**Table 6.17**). 1-cyclopropyl-7-(4-((3-(2-

(diallylcarbamoithioyl)hydrazono)-5-methyl-2-oxoindolin-1-yl)methyl)-3-methylpiperazin-1-yl)-6-fluoro-8-methoxy-4-oxo-1,4-dihydroquinoline-3-carboxylic acid (**A30**), was found to be most effective in inhibiting dormant MTB with an MIC of 17.81 μM . It was observed that the compounds which inhibited starvation induced MTB culture were all fluoroquinolone analogues, which perhaps owing to their bulkiness were better able to penetrate the waxy cell wall of the quiescent mycobacterial spores. Hence these drugs could prove effective for treating reactivation tuberculosis. Amongst the non-fluoroquinolonated derivatives, **A12** displayed reasonably good activity in inhibiting the dormant MTB with an MIC of 31.34 μM . The aliphatic chain at the N-1 of the isatin moiety in case of **A12** may be permitting it to penetrate the waxy mycolic acid layer.

E. MTB ICL enzyme inhibition assay:

Persistence and reactivation are two typical hallmarks of TB, which makes this disease incurable even after prolonged chemotherapy with currently available anti-tubercular agents. The tubercle bacilli exist in dormant form in the macrophages of infected patients by entailing a metabolic shift to glyoxalate shunt, where it utilizes C_2 substrates. It was observed that there was a marked increase in concentration of isocitrate lyase, an essential enzyme in the glyoxalate pathway, in the lungs of mice, infected with chronic tuberculosis [137]. The glyoxalate pathway being absent in vertebrates, and since it has strong implications in maintaining chronicity of tubercular infection, ICL is considered a significant target for tackling reactivation TB [141]. As the compounds reported in this article, exhibited excellent inhibition of dormant mycobacterium, we decided to explore the possible mechanism by screening some compounds against ICL enzyme of MTB. Several small-molecule inhibitors have been described [140] as MTB ICL inhibitors; however, none has been developed as a drug for MTB. In this work, isocitrate lyase activity was determined at 37°C by measuring the formation of glyoxylate-phenylhydrazone in the presence of phenylhydrazine and isocitrate lyase at 324 nm based on the method described [119]. The compounds were screened with a single concentration of 10 μM and percentage inhibitions of the screened compounds along with the standard MTB ICL inhibitor 3-nitropropionic acid (3-NP) (at 100 μM) for comparison are reported.

Nine compounds were evaluated for their ability to inhibit MTB ICL and only two of these, namely **A12** and **A13**, showed significant suppression of ICL activity (**Table 6.18**). N,N-diallyl-2-(1-((diethylamino)methyl)-5-methyl-2-oxoindolin-3-ylidene)hydrazinecarbothioamide (**A12**), showed the highest inhibition at 40.45 % when tried at 10mM concentration level; whereas N,N-diallyl-2-(5-chloro-1-(morpholinomethyl)-2-oxoindolin-3-ylidene)hydrazinecarbothioamide (**A13**), inhibited ICL by 31.42% at 10mM level, in comparison to 65.99% inhibition by NP at 100mM concentration level. The superior inhibition of ICL by **A12** and **A13**, when compared to the other molecules, can be imputed to the π -electrons of the diallyl group attached to the thiourea moiety which perhaps might be interacting with some electron-deficient groups present in the active site pocket.

F. MTB DNA Gyrase enzyme assay:

Eight of the analogues belonging to this series were subjected to evaluation for their ability to inhibit supercoiling of *Mycobacterium smegmatis* DNA gyrase enzyme (**Table 6.19**). These compounds had IC₅₀ ranging between 20 and 50 $\mu\text{g/mL}$ with **A28** being the most active against DNA gyrase.

G. Antiviral and Cytotoxicity activity against Influenza Type A virus:

Two compounds belonging to this series, namely **A14** and **A25** were also analyzed for their ability to inhibit the replication of influenza type A virus, strain Vietnam/1203/2004H in MDCK cell line (**Table 6.20**). Both these analogues were found to be inactive against the replication of influenza A virus.

H. Antiviral and Cytotoxicity activity against Influenza Type B virus:

Selected compounds, namely **A14**, **A22**, **A25** and **A29** were analyzed for their ability to inhibit the replication of Influenza type B virus, strain Malaysia/2506/2004 in MDCK cell line (**Table 6.21**). All of them failed to inhibit influenza B virus.

I. Antiviral and Cytotoxicity activity against SARS virus:

Three of the analogues, viz. **A14**, **A25** and **A29** were analyzed for their ability to inhibit the replication of SARS virus, Urbani strain in Vero 76 cell line (**Table 6.22**). All of them were found to be inactive against SARS virus.

6.3 Computational studies

A. HIV-1 RT Docking

Results & Discussion:

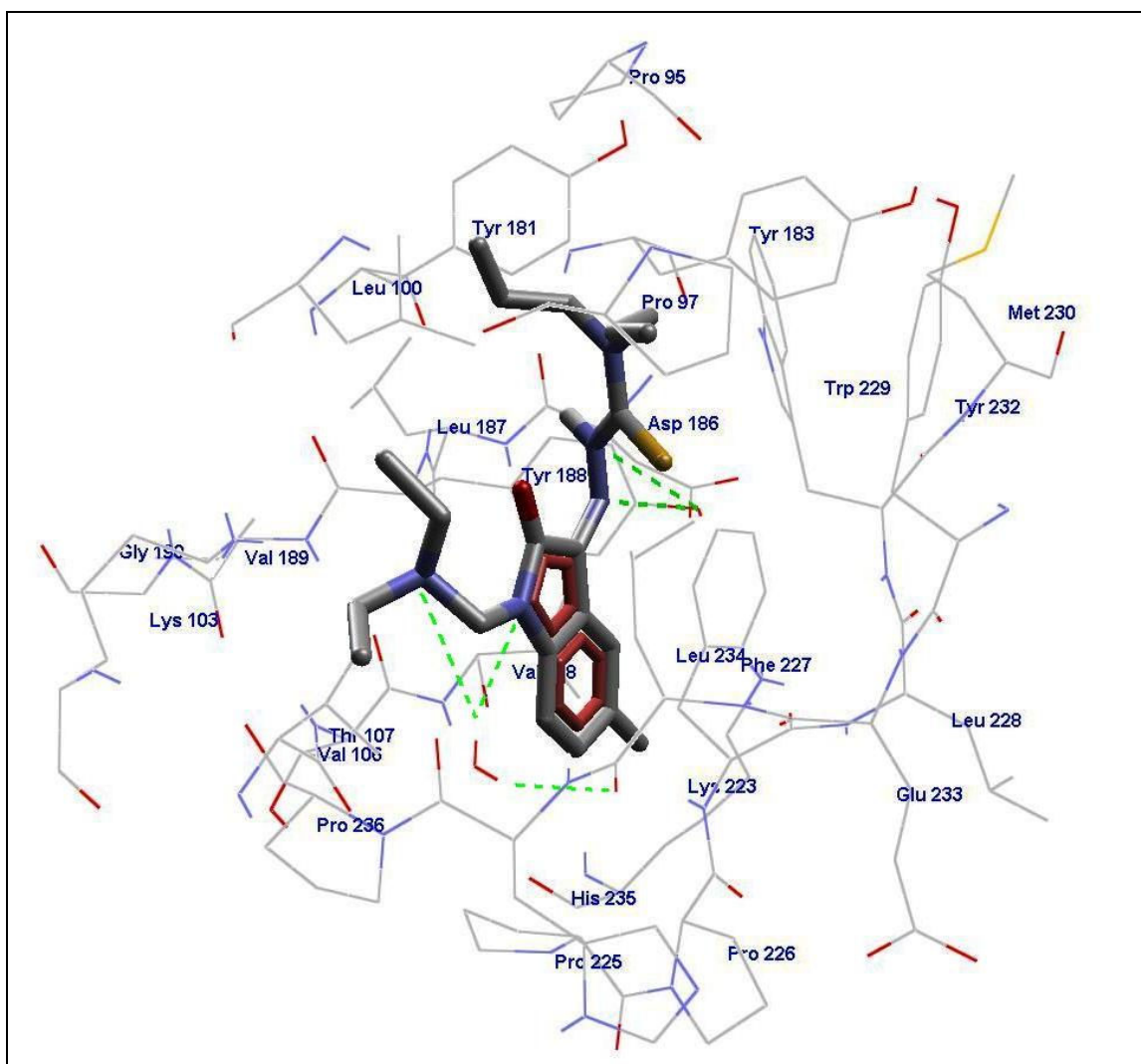


Fig. 6.1: Contact residues of A12 when docked onto HIV-1 RT

With the intention of exploring the binding mode of these synthesized molecules in the HIV-1 RT pocket, these molecules were subjected to molecular docking simulation using the docking software, AutoDock 4.0 [148, 149]. The coordinates of the NNIBP were taken from the PDB crystal structure of RT/Nevirapine complex (PDB ID: 1VRT).

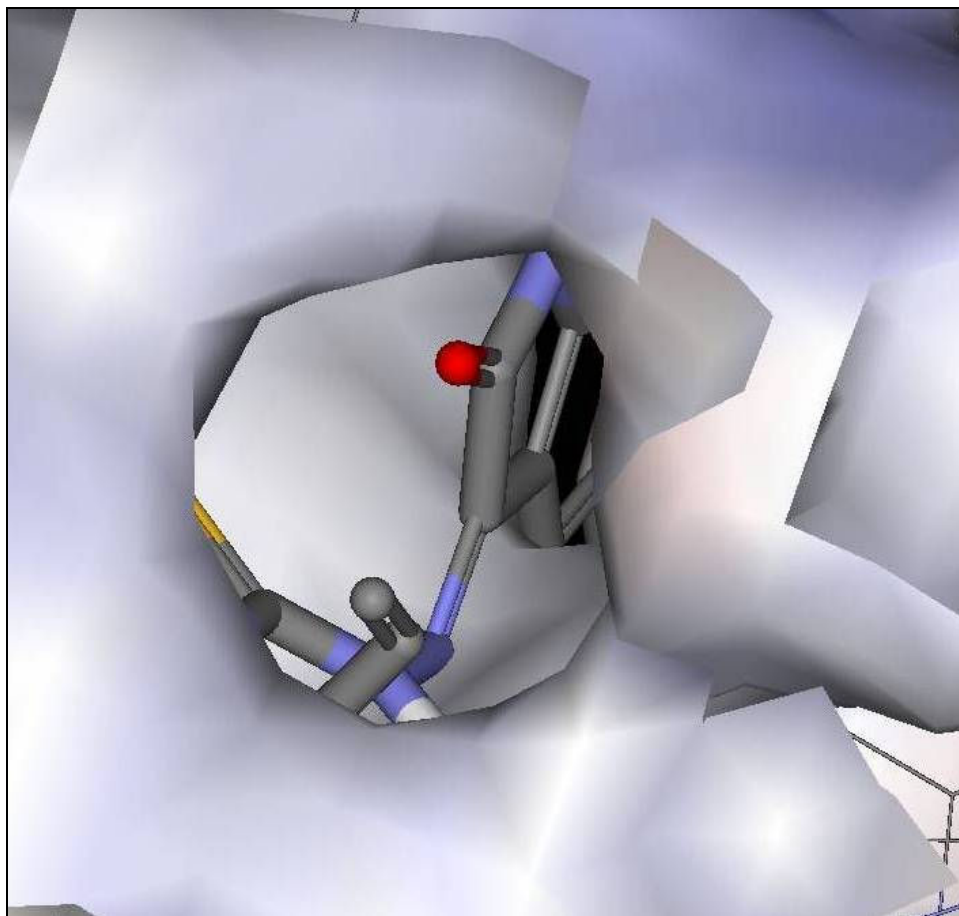


Fig. 6.2: Electrostatic surface view of active site pocket of HIV-1 RT bound to A12

A12 demonstrated the best binding affinity amongst the entire series of compounds. Visual inspection (**Fig. 6.1**) of the best docked pose of **A12** revealed that its hydrazine moiety established hydrogen bonds with the OH group of Tyr 188. The isatinyl ring nitrogen and the nitrogen of diallylamine also formed bridged hydrogen bonds with Leu 234 via water 67. The isatinyl ring was found to be well seated in a hydrophobic pocket bordered by Val 106, Val 108, Tyr 188, Lys 223, Pro 225 and Phe 227. The diethylaminomethyl moiety was seen to be having considerable hydrophobic interactions

with Leu 100, Lys 103, Leu 234 and Pro 236. The diallyl moiety at the terminal of the thiosemicarbazide group had hydrophobic interactions with Pro 95, Tyr 181 and Trp 229. These key residues and the interactions undergone by **A12** focus light on the structural criterion to be met by these compounds in order to inhibit HIV-1 RT and would help in further modifications of these compounds.

B. MTB ICL Docking

Results & Discussion:

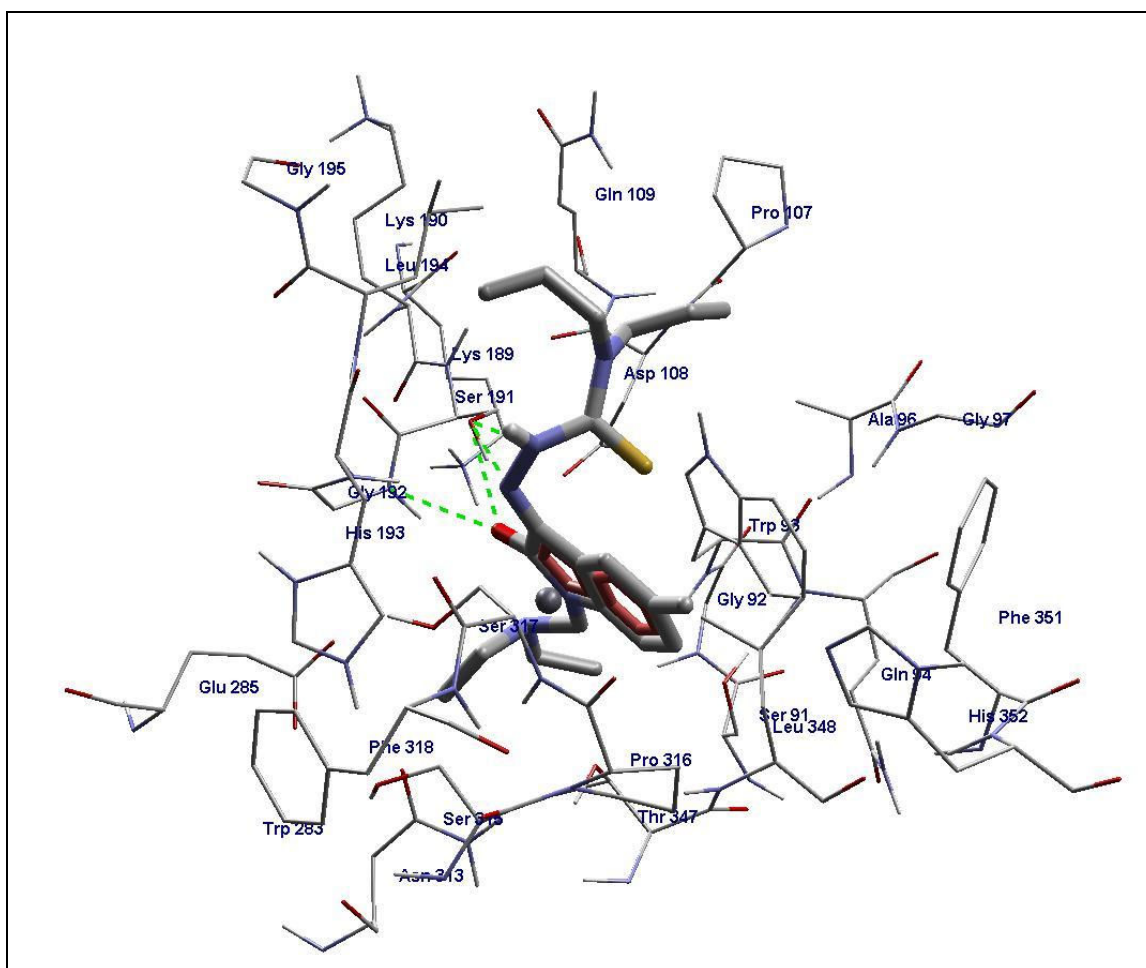


Fig. 6.3: Contact residues of A12 when docked onto MTB ICL

In order to probe the binding mode of our designed molecules, a docking simulation was performed using AutoDock 4.0 [149]. Compound **A12** was docked into

the active site pocket of MTB ICL, the coordinates of which were taken from the crystal structure of ICL/Pyruvate complex.

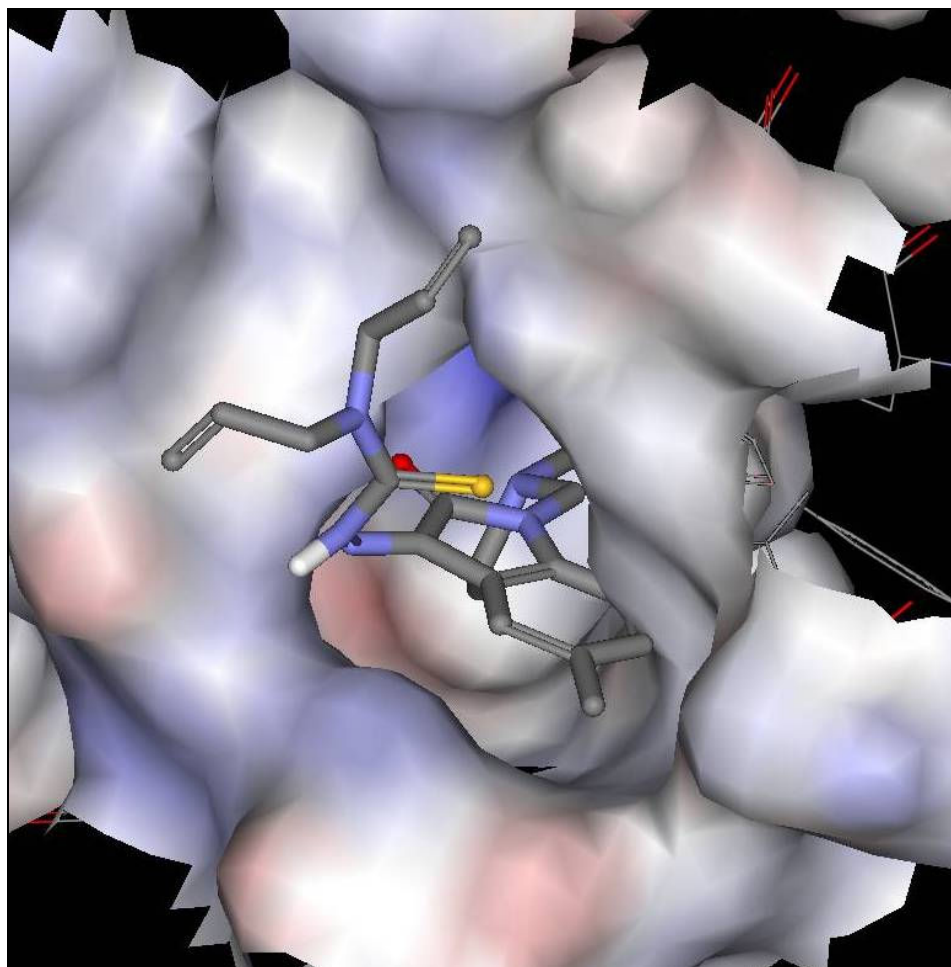


Fig. 6.4: Electrostatic surface view of active site pocket of MTB ICL bound to A12.

The docking results provided an aspect of the interactions between the ligand and the active site residues. The oxygen atom at C₂ of the indole nucleus was engaged in hydrogen bonding interactions with the peptide backbone's nitrogen atom of Gly 192 and the alcoholic oxygen of Ser191 as shown in **Fig. 6.3**. The Ser191 was also involved in hydrogen bonding interactions with the hydrazine group, which is appended to C₃ of isatin nucleus. The indole nucleus was well accommodated in the pocket formed by Trp 93, His 193, Pro316, Leu 348 and His 352. The isatinyl moiety is engaged in aromatic interaction with Trp93, His193 and His 352 forming a favorable π -stacking interaction.

The diethylamine group at N₁ of indole showed some polar interaction with the side chain of Asp 153.

So it can be concluded that these docking results were in accordance with the experimental data. Further structural optimization of **A12** will be based on these facts highlighted by this docking simulation.

6.4: Structure activity relationship (SAR) analysis

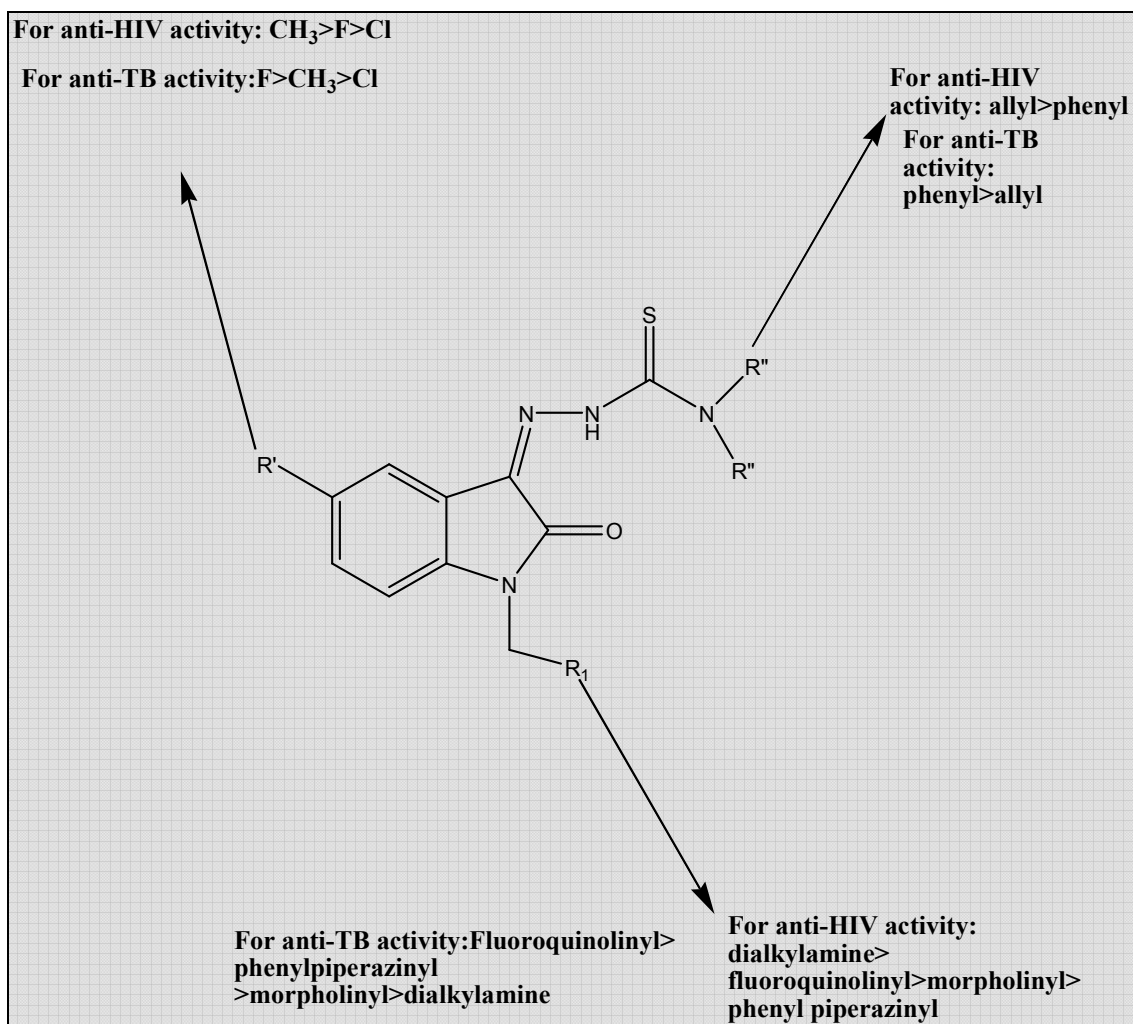


Fig. 6.5: Schematic representation of SAR of N-Mannich bases of 5-substituted- 1H-indole-2,3-dione 3- (N, N-diallyl/diphenyl thiosemicarbazones)

CHAPTER 7

SUMMARY & CONCLUSIONS

The present work was oriented towards the synthesis, biological evaluation and computational studies of various novel isatin- β -thiosemicarbazones in the treatment of AIDS and its most often accompanying opportunistic co-infection tuberculosis.

- An array of substituted aliphatic and aromatic thiosemicarbazides was synthesized, which on condensation with various 5-substituted isatins yielded a range of isatin- β -thiosemicarbazones.
- These on reaction with formaldehyde and various secondary amines in the presence of microwave irradiation resulted in *N*-Mannich bases of isatin- β -thiosemicarbazones, which were evaluated for their ability to treat HIV-TB co-infection.
- The structures of these final synthesized compounds were elucidated with the aid of their spectral and elemental data.
- These final analogues were subjected to anti-HIV screening against HIV-1 (HTLV-III_B) strain in MT-4 cell line, which employed an MTT assay based method.
- Few of the analogues were tested for their inhibitory effect on HIV-1 RT enzyme.
- All the compounds were evaluated for their ability to inhibit the growth of MTB in both logarithmic as well as dormant phase.
- Selected analogues were tested for their activity to inhibit MTB ICL, an enzyme with significant implication in dormant TB, and also against MC₂ DNA gyrase supercoiling.
- Few of the analogues were evaluated for their ability to act against the replication of various viruses viz. HCV, SARS virus, Influenza type A and B viruses.

- With the help of docking softwares namely, GOLD and AutoDock 4.0, the binding mode of these compounds were investigated when bound to HIV-1 RT and MTB ICL enzymes.
- In the first series, **M21** was found to be the most potent against HIV-1 replication in MT-4 cell line with an EC₅₀ of 1.69 μM.
- In the second series, **A12** displayed the most promising activity against HIV-1 replication with an EC₅₀ of 0.3028 μM.
- In general the compounds of the second series proved better in inhibiting HIV-1 replication, which may be due to their bulky moiety present at the terminal of the thiosemicarbazide in comparison to the hydrophilic hydroxy or methoxy group in the first series.
- Substitution at R₁ also ruled the pattern of activity followed by the compounds. Presence of piperazinylmethyl and substituted piperazinylmethyl group at N-1 enhanced the anti-HIV activity when compared to morpholinylmethyl group in case of the N-hydroxy/methoxy analogues; whereas for the *N,N*-diallyl/diphenyl analogues presence of dialkylamine substituents yielded compounds with better antiviral activity than the ones with piperazinyl/ substituted piperazinyl or fluoroquinolone substituents .
- At the 5th position of the indolyl moiety, the presence of methyl group results in compounds with superior anti-HIV activity followed by fluoro and then chloro group.
- Nine compounds were evaluated for their ability to repress the activity of HIV-1 RT enzyme. **M21** and **A12** emerged as the most promising ones against HIV-1 RT inhibition. **A12** was found to be better than **M21**, with a lower IC₅₀ value.
- Against logarithmic phase of MTB, **M35** and **P29** displayed exemplary inhibitory activity. It was observed that most of the fluoroquinolone analogues in both the series showed promising inhibition of MTB growth which might be due to their bulky nature permitting them to penetrate the waxy mycolic acid layer of the bacilli.

- When tested against starvation-induced MTB, seven of these analogues proved beneficial than standard drug, rifampicin and twenty-nine analogues were more effective than isoniazid.
- Eighteen compounds were tested for their ability to repress the activity of MTB ICL, out of which **M30** displayed the most promising ICL suppression of 63.44%, followed by **A12** at 40.45 %.
- Isatin analogues since having momentous activity against a wide panoply of microorganisms, these synthesized derivatives were put to test against the replication of HCV, SARS virus, Influenza Type A and B viruses; but were found to be ineffective. Hence it can be explicitly stated that these derivatives are selective towards HIV replication.

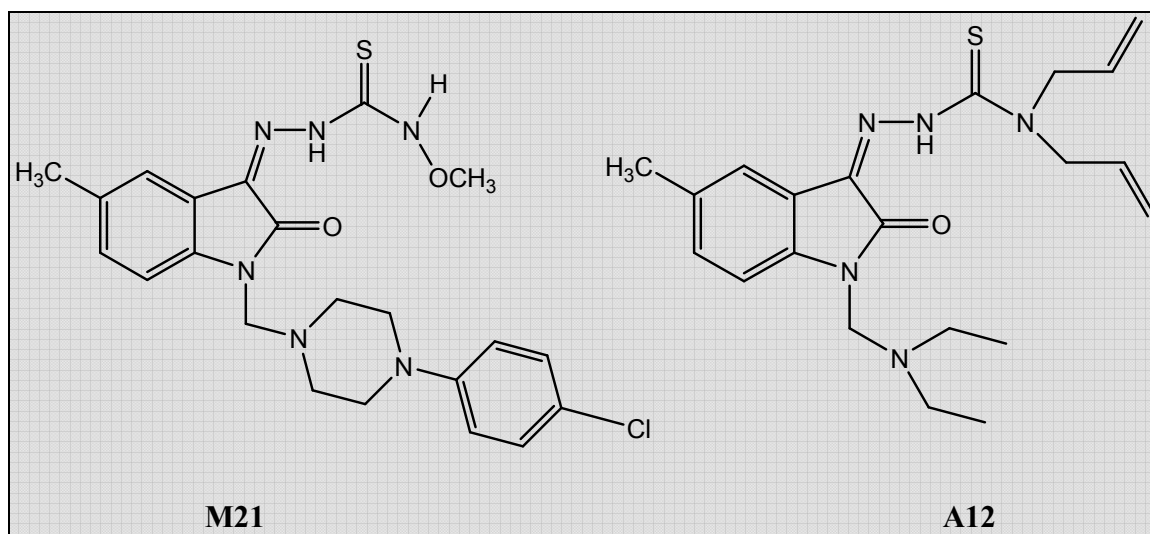


Fig. 7.1: Structure of most active compounds

FUTURE PERSPECTIVES

The present work generated compounds which were effective as NNRTIs in combating HIV as well as possessed considerable anti-tubercular activity. Further structural modifications of these leads would give rise to molecules which would be capable to treat HIV-TB co-infection; thereby decreasing the pill burden encountered by the patients and hence increasing treatment adherence.

Further studies are needed to be performed to assess the pharmacokinetic profile of these analogues to assess the bioavailability and effective plasma concentration of these analogues.

A perplexing drawback of treatment with NNRTIs is the development of resistance to these molecules by the HIV virion by undergoing genetic mutations. Hence these novel molecules need to be evaluated against the resistant HIV strains; in order to establish their efficacy against mutated and non-mutated strains of the retrovirus.

Where anti-tubercular assays are concerned, these derivatives need to be evaluated for their capacity to act against MDR-TB and XDR-TB. Also due to the significant difference existing between *in vitro* and *in vivo* studies, these analogues are required to undergo *in vivo* and *ex vivo* anti-tubercular assays in suitable animal models.

A plethora of gene products have been elucidated which have significant implication in maintaining the TB bacilli in dormant phase in the infected host. These compounds have a scope of being explored against all these gene products to reveal the exact mechanism by which they are acting against starvation-induced MTB.

References

1. Barre-Sinoussi, F.; Chermann, J. C.; Rey, F. ; Nugeyre, M. T.; Chamaret, S.; Gruest, J.; Dauguet, C.; Axler-Blin, C.; Vezinet-Brun, F.; Rouzioux, C.; Rozenbaum, W.; Montagnier, L. Isolation of a T-lymphotropic retrovirus from a patient at risk for acquired immune deficiency syndrome (AIDS). *Science*. **1983**, *220*, 868-871.
2. Gallo, R. C.; Salahuddin, S. Z.; Popovic, M.; Shearer, G. M.; Kaplan, M.; Haynes, B. F.; Palker, T. J.; Redfield, R.; Oleske, J.; Safai, B.; White, G.; Foster, P.; Markham P. D. Frequent detection and isolation of cytopathic retroviruses (HTLV-III) from patients with AIDS and at risk for AIDS. *Science*. **1984**, *224*, 500-503.
3. Sharp, P. M.; Bailes, E.; Chaudhuri, R. R.; Rodenburg, C. M.; Santiago, M. O.; Hahn B. H. The origins of acquired immune deficiency syndrome viruses: where and when? *Phil. Trans. R. Soc. Lond. B*. **2001**, *356*, 867-876.
4. Fauci, A. S. 25 years of HIV. *Nature*. **2008**, *453*, 289-290.
5. 2008 Report on the global AIDS epidemic. [Online]. 2008. Available from: URL: www.unaids.org.
6. UNGASS Country progress report 2008, India. Released by National AIDS Control Organization, Ministry of health and family welfare, Government of India, New Delhi.
7. Cann, A. J.; Karn, J. Molecular biology of HIV: new insights into the virus life-cycle. *AIDS*. **1989**, *3 Suppl 1*, S19-S34.
8. Briggs, J. A.; Wilk, T.; Welker, R.; Kräusslich, H. G.; Fuller, S. D. Structural organization of authentic, mature HIV-1 virions and cores. *EMBO J*. **2003**, *22*, 1707-1715.
9. Welker, R.; Hohenberg, H.; Tessmer, U.; Huckhagel, C.; Kräusslich, H. G. Biochemical and structural analysis of isolated mature cores of human immunodeficiency virus type 1. *J. Virol*. **2000**, *74*, 1168-1177.

10. Michael, N. L.; Moore, J. P. HIV-1 entry inhibitors: Evading the issue. *Nat. Med.* **1999**, *5*, 740-742.
11. Goto, T.; Nakai, M.; Ikuta, K. The life-cycle of human immunodeficiency virus type 1. *Micron.* **1998**, *29*, 123-138.
12. Haseltine, W. A. Replication and pathogenesis of the AIDS virus. *J. Acquir. Immune. Defic. Syndr.* **1988**, *1*, 217-240.
13. Ganser-Pornillos, B. K.; Yeager, M.; Sundquist, W.I. The structural biology of HIV assembly. *Curr. Opin. Struct. Biol.* **2008**, *18*, 203-217.
14. "HIV and its treatment: what you should know". Health information for the patients. Fact sheet released by US Department of health and human services. 2008. Available online from the URL: <http://aidsinfo.nih.gov>.
15. Richman, D.D. HIV chemotherapy. *Nature.* **2001**, *410*, 995-1001.
16. Flexner, C. HIV-protease inhibitors. *N. Engl. J. Med.* **1998**, *338*, 1281-1292.
17. Kilby, J. M.; Hopkins, S.; Venetta, T. M.; DiMassimo, B.; Cloud, G. A.; Lee, J. Y.; Alldredge, L.; Hunter, E.; Lambert, D.; Bolognesi, D.; Matthews, T.; Johnson, M. R.; Nowak, M. A.; Shaw, G. M.; Saag, M. S. Potent suppression of HIV-1 replication in humans by T-20, a peptide inhibitor of gp41-mediated virus entry. *Nat. Med.* **1998**, *4*, 1302-1307.
18. Root, M. J.; Kay, M. S.; Kim, P. S. Protein design of an HIV-1 entry inhibitor. *Science.* **2001**, *291*, 884-888.
19. Donzella, G. A.; Schols, D.; Lin, S.W.; Esté, J. A.; Nagashima, K. A.; Maddon, P. J.; Allaway, G. P.; Sakmar, T. P.; Henson, G.; De Clercq, E.; Moore, J. P. AMD3100, a small molecule inhibitor of HIV-1 entry via the CXCR4 co-receptor. *Nat. Med.* **1998**, *4*, 72-77.
20. Baba, M.; Nishimura, O.; Kanzaki, N.; Okamoto, M.; Sawada, H.; Iizawa, Y.; Shiraishi, M.; Aramaki, Y.; Okonogi, K.; Ogawa, Y.; Meguro, K.; Fujino, M. A small-molecule, nonpeptide CCR5 antagonist with highly potent and selective anti-HIV-1 activity. *Proc. Natl. Acad. Sci. U. S. A.* **1999**, *96*, 5698-5703.
21. Hazuda, D. J.; Felock, P.; Witmer, M.; Wolfe, A.; Stillmock, K.; Grobler, J. A.; Espeseth, A.; Gabryelski, L.; Schleif, W.; Blau, C.; Miller, M. D. Inhibitors of

- strand transfer that prevent integration and inhibit HIV-1 replication in cells. *Science*. **2000**, *287*, 646-650.
22. Arnold, E.; Sarafianos, S. G. Molecular biology: an HIV secret uncovered. *Nature*. **2008**, *453*, 169-170.
 23. Ren, J.; Esnouf, R.; Garman, E.; Somers, D.; Ross, C.; Kirby, I.; Keeling, J.; Darby, G.; Jones, Y.; Stuart, D.; Stammers, D. High resolution structures of HIV-1 RT from four RT-inhibitor complexes. *Nat. Struct. Biol.* **1995**, *2*, 293-302.
 24. Rodgers, D. W.; Gamblin, S. J.; Harris, B. A.; Ray, S.; Culp, J. S.; Hellmig, B.; Woolf, D. J.; Debouck, C.; Harrison, S. C. The structure of unliganded reverse transcriptase from the human immunodeficiency virus type 1. *Proc. Natl. Acad. Sci. U. S. A.* **1995**, *92*, 1222-1226.
 25. Jacobo-Molina, A.; Ding, J.; Nanni, R. G.; Clark, A. D. Jr.; Lu, X.; Tantillo, C.; Williams, R. L.; Kamer, G.; Ferris, A. L.; Clark, P.; Hizi, A.; Hughes, S. H.; Arnold, E. Crystal structure of human immunodeficiency virus type 1 reverse transcriptase complexed with double-stranded DNA at 3.0 Å resolution shows bent DNA. *Proc. Natl. Acad. Sci. U. S. A.* **1993**, *90*, 6320-6324.
 26. Rittinger, K.; Divita, G.; Goody, R. S. Human immunodeficiency virus reverse transcriptase substrate-induced conformational changes and the mechanism of inhibition by nonnucleoside inhibitors. *Proc. Natl. Acad. Sci. U. S. A.* **1995**, *92*, 8046-8049.
 27. Peletskaya, E. N.; Kogon, A. A.; Tuske, S.; Arnold, E.; Hughes, S. H. Nonnucleoside inhibitor binding affects the interactions of the fingers subdomain of human immunodeficiency virus type 1 reverse transcriptase with DNA. *J. Virol.* **2004**, *78*, 3387-3397.
 28. Esnouf, R.; Ren, J.; Ross, C.; Jones, Y.; Stammers, D.; Stuart, D. Mechanism of inhibition of HIV-1 reverse transcriptase by non-nucleoside inhibitors. *Nat. Struct. Biol.* **1995**, *2*, 303-308.
 29. De Clercq, E. Non-Nucleoside Reverse Transcriptase Inhibitors (NNRTIs): Past, Present, and Future. *Chem. Biodiver.* **2004**, *1*, 44-64.
 30. Ji, L.; Chen, F. E.; Feng, X. Q.; De Clercq, E.; Balzarini, J.; Pannecouque, C. Non-nucleoside HIV-1 reverse Transcriptase inhibitors, Part 7, Synthesis,

- antiviral activity, and 3D-QSAR investigations of novel 6-(1-naphthoyl) HEPT analogues. *Chem. Pharm. Bull. (Tokyo)*. **2006**, *54*, 1248-1253.
31. D'Cruz, O.J.; Uckun, F.M. Novel tight binding PETT, HEPT and DABO based non-nucleoside inhibitors of HIV-1 reverse Transcriptase. *J. Enz. Inhib. Med. Chem.* **2006**, *21*, 329-350.
 32. Genin, M. J.; Poel, T. J.; May, P. D.; Kopta, L. A.; Yagi, Y.; Olmsted, R. A.; Friis, J. M.; Voorman, R. L.; Adams, W. J.; Thomas, R. C.; Romero, D. L. Synthesis and Structure-activity relationships of the (alkylamino) piperidine-containing BHAP class of non-nucleoside reverse Transcriptase inhibitors: effect of 3-alkylpyridine ring substitution. *J. Med. Chem.* **1999**, *42*, 4140-4149.
 33. Rodriguez-Barrios, F.; Perez, C.; Lobaton, E.; Velazquez, S.; Chamorro, C.; San-Felix, A.; Perez-Perez, M. J.; Camarasa, M. J.; Pelemans, H.; Balzarini, J.; Gago, F. Identification of a putative binding site for [2',5'-bis-O-(tert-butyl)dimethylsilyl]-beta-D-ribofuranosyl]-3'-spiro-5''-(4''-amino-1'',2''-oxathiole-2'',2''-dioxide)thymine (TSAO) derivatives at the p51-p66 interface of HIV-1 reverse Transcriptase. *J. Med. Chem.* **2001**, *44*, 1853-1865.
 34. Pauwels, R.; Andries, K.; Debyser, Z. Potent and Highly Selective HIV-1 Inhibition by a Series of α -Anilinophenylacetamide Derivatives Targeted at HIV-1 Reverse Transcriptase. *Proc. Natl. Acad. Sci. USA*. **1993**, *90*, 1711-1715.
 35. Maggiolo, F.; Quinzan, G.; Gregis, G.; Ripamonti, D.; Ravasio, L.; Suter, F. HAART regimens with lower metabolic effect: a randomized, controlled trial. 15th International Conference on AIDS. Jul 11-16, 2004, Bangkok, Thailand). Abstract no. WePeB5865.
 36. Subsai, K.; Kanoksri, S.; Siwaporn, C.; Helen, L.; Kanokporn, O.; Wantana, P. Neurological complications in AIDS patients receiving HAART: a 2-year retrospective study. *Eur. J. Neurol.* **2006**, *13*, 233-239.
 37. Global Tuberculosis Control. WHO Report 2008. [Online]. 2008. Available from: URL: http://www.who.int/tb/publications/global_report/2008/en/index.html.
 38. Lee, J.; Hartman, M.; Kornfeld, H. Macrophage apoptosis in tuberculosis. *Yonsei Med. J.* **2009**, *50*, 1-11.

39. Vermund, S. H.; Yamamoto, N. Co-infection with human immunodeficiency virus and tuberculosis in Asia. *Tuberculosis (Edinb)*. **2007**, *87 Suppl 1*, S18-S25.
40. Vaidyanathan P. S.; Singh, S. TB-HIV Co-infection in India. *Natl. Tuberc. Inst. Bull.* **2003**, *39*, 11-18.
41. Garrait, V.; Cadranet, J.; Esvant, H.; Herry, I.; Morinet, P.; Mayaud, C.; Israël-Biet, D. Tuberculosis generates a microenvironment enhancing the productive infection of local lymphocytes by HIV. *J. Immunol.* **1997**, *159*, 2824-2830.
42. Goletti, D.; Weissman, D.; Jackson, R.W.; Graham, N. M.; Vlahov, D.; Klein, R. S.; Munsiff, S. S.; Ortona, L.; Cauda, R.; Fauci, A. S. Effect of Mycobacterium tuberculosis on HIV replication. Role of immune activation. *J. Immunol.* **1996**, *157*, 1271-1278.
43. Havlir, D. V.; Barnes, P. F. Tuberculosis in patients with human immunodeficiency virus infection. *N. Engl. J. Med.* **1999**, *340*, 367-373.
44. Aaron, L.; Saadoun, D.; Calatroni, I.; Launay, O.; Mémain, N.; Vincent, V.; Marchal, G.; Dupont, B.; Bouchaud, O.; Valeyre, D.; Lortholary, O. Tuberculosis in HIV-infected patients: a comprehensive review. *Clin. Microbiol. Infect.* **2004**, *10*, 388-398.
45. Hoshino, Y.; Tse, D. B.; Rochford, G.; Prabhakar, S.; Hoshino, S.; Chitkara, N.; Kuwabara, K.; Ching, E.; Raju, B.; Gold, J. A.; Borkowsky, W.; Rom, W. N.; Pine, R.; Weiden, M. *Mycobacterium tuberculosis*-Induced CXCR4 and Chemokine Expression Leads to Preferential X4 HIV-1 Replication in Human Macrophages. *J. Immunol.* **2004**, *172*, 6251-6258.
46. Idemyor, V. HIV and Tuberculosis Coinfection: Inextricably Linked Liaison. *J. Natl. Med. Assoc.* **2007**, *99*, 1414-1419.
47. Narita, M.; Ashkin, D.; Hollender, E. S.; Pitchenik, A. E. Paradoxical worsening of tuberculosis following antiretroviral therapy in patients with AIDS. *Am. J. Respir. Crit. Care. Med.* **1998**, *158*, 157-161.
48. Pepper, D. J.; Meintjes, G. A.; McIlleron, H.; Wilkinson, R. J. Combined therapy for tuberculosis and HIV-1: the challenge for drug discovery. *Drug. Discov. Today.* **2007**, *12*, 980-989.

49. Dean, G. L.; Edwards, S. G.; Ives, N. J.; Matthews, G.; Fox, E. F.; Navaratne, L.; Fisher, M.; Taylor, G. P.; Miller, R.; Taylor, C. B.; de Ruiter, A.; Pozniak, A. L. Treatment of tuberculosis in HIV-infected persons in the era of highly active antiretroviral therapy. *AIDS*. **2002**, *16*, 75-83.
50. Rae, J. M.; Johnson, M. D.; Lippman, M. E.; Flockhart, D. A. Rifampin is a selective, pleiotropic inducer of drug metabolism genes in human hepatocytes: studies with cDNA and oligonucleotide expression arrays. *J. Pharmacol. Exp. Ther.* **2001**, *299*, 849-857.
51. Burman, W. J.; Gallicano, K.; Peloquin, C. Therapeutic implications of drug interactions in the treatment of human immunodeficiency virus-related tuberculosis. *Clin. Infect. Dis.* **1999**, *28*, 419-429.
52. Chiyanzu, I.; Hansell, E.; Gut, J.; Rosenthal, P. J.; McKerrow, J. H.; Chibale, K. Synthesis and evaluation of isatins and thiosemicarbazone derivatives against cruzain, falcipain-2 and rhodesain. *Bioorg. Med. Chem. Lett.* **2003**, *13*, 3527-3530.
53. D'Ischia, M.; Palumbo, A.; Protà, G. Adrenalin oxidation revisited. New products beyond the adrenochrome stage. *Tetrahedron*. **1988**, *44*, 6441-6446.
54. Bauer, D. J. Clinical experience with the antiviral drug marboran (1-methylisatin 3-thiosemicarbazone). *Ann. N. Y. Acad. Sci.* **1965**, *130*, 110-117.
55. Varma, R. S.; Nobles, W. L. Synthesis and antiviral and antibacterial activity of certain N-dialkylaminomethylisatin beta-thiosemicarbazones. *J. Med. Chem.* **1967**, *10*, 972-974.
56. Woodson, B.; Joklik, W. K. The inhibition of vaccinia virus multiplication by isatin-beta-thiosemicarbazone. *Proc. Natl. Acad. Sci. U. S. A.* **1965**, *54*, 946-953.
57. Bauer, D. J.; Sadler, P. W. The structure-activity relationships of the antiviral chemotherapeutic activity of isatin beta-thiosemicarbazone. *Br. J. Pharmacol. Chemother.* **1960**, *15*, 101-110.
58. Bauer, D. J.; Dumbell, K. R.; Fox-Hulme, P.; Sadler, P. W. The chemotherapy of variola major infection. *Bull. World. Health. Organ.* **1962**, *26*, 727-732.

59. Bauer, D. J.; St. Vincent, L.; Kempe, C. H.; Downiw, A. W. Prophylactic treatment of small pox contacts with N-methylisatin beta-thiosemicarbazone (Compound 33T57, Marboran). *Lancet*. **1963**, *2*, 494-496.
60. Turner, W.; Bauer, D. J.; Nimmo-Smith, R. H. Eczema vaccinatum treated with n-methylisatin beta-thiosemicarbazone. *Br. Med. J.* **1962**, *1*, 1317-1319.
61. Bauer, D. J.; Apostolov, K. Adenovirus multiplication: inhibition by methisazone. *Science*. **1966**, *154*, 796-797.
62. Levinson, W.; Faras, A.; Woodson, B.; Jackson, J.; Bishop, J. M. Inhibition of RNA-dependent DNA polymerase of Rous sarcoma virus by thiosemicarbazones and several cations. *Proc. Natl. Acad. Sci. U. S. A.* **1973**, *70*, 164-168.
63. Logan, J. C.; Fox, M. P.; Morgan, J. H.; Makohon, A. M.; Pfau, C. J. Arenavirus inactivation on contact with N-substituted isatin beta-thiosemicarbazones and certain cations. *J. Gen. Virol.* **1975**, *28*, 271-283.
64. Tonew, M.; Tonew, E. Effects of some antiviral isatinisothiosemicarbazones on cellular and viral ribonucleic acid synthesis in Mengovirus-infected FL cells. *Antimicrob. Agents. Chemother.* **1974**, *5*, 393-397.
65. Francis, R. D.; Bradford, H. B. Jr. Some biological and physical properties of molluscum contagiosum virus propagated in cell culture. *J. Virol.* **1976**, *19*, 382-388.
66. Chen, T. C.; Weng, K. F.; Chang, S. C.; Lin, J. Y.; Huang, P. N.; Shih, S. R. Development of antiviral agents for enteroviruses. *J. Antimicrob. Chemother.* **2008**, *62*, 1169-1173.
67. Lieberman, M.; Pascale, A.; Schafer, T. W.; Came, P. E. Effect of antiviral agents in equine abortion virus-infected hamsters. *Antimicrob. Agents. Chemother.* **1972**, *1*, 143-147.
68. Levinson, W.; Coleman, V.; Woodson, B.; Rabson, A.; Lanier, J.; Whitcher, J.; Dawson, C. Inactivation of herpes simplex virus by thiosemicarbazones and certain cations. *Antimicrob. Agents. Chemother.* **1974**, *5*, 398-402.
69. Katz, E.; Margalith, E. Antiviral activity of SK&F 21681 against herpes simplex virus. *Antimicrob. Agents. Chemother.* **1984**, *25*, 195-200.

70. Katz, E.; Margalith, E.; Winer, B. An isatin beta-thiosemicarbazone (IBT)-dependent mutant of vaccinia virus: the nature of the IBT-dependent step. *J. Gen. Virol.* **1973**, *21*, 477-484.
71. Katz, E.; Margalith, E.; Winer, B. The effect of isatin beta thiosemicarbazone (IBT)-related compounds on IBT-resistant and on IBT-dependent mutants of vaccinia virus. *J. Gen. Virol.* **1974**, *25*, 239-244.
72. Sherman, L.; Edelstein, F.; Shtacher, G.; Avramoff, M.; Teitz, Y. Inhibition of Moloney leukaemia virus production by N-methylisatin-beta-4':4'-diethylthiosemicarbazone. *J. Gen. Virol.* **1980**, *46*, 195-203.
73. Ronen, D.; Teitz, Y. Inhibition of the synthesis of Moloney leukemia virus structural proteins by N-methylisatin-beta-4',4'-diethylthiosemicarbazone. *Antimicrob. Agents. Chemother.* **1984**, *26*, 913-916.
74. Ronen, D.; Sherman, L.; Bar-Nun, S.; Teitz, Y. N-methylisatin-beta-4',4'-diethylthiosemicarbazone, an inhibitor of Moloney leukemia virus protein production: characterization and in vitro translation of viral mRNA. *Antimicrob. Agents. Chemother.* **1987**, *31*, 1798-1802.
75. Teitz, Y.; Ladizensky, E.; Barko, N.; Burstein, E. Selective repression of v-abl-encoded protein by N-methylisatin-beta-4',4'-diethylthiosemicarbazone and N-allylisatin-beta-4',4'-diallylthiosemicarbazone. *Antimicrob. Agents. Chemother.* **1993**, *37*, 2483-2485.
76. Polatnick, J.; Bachrach, H. L. Effect of zinc and other chemical agents on foot-and-mouth-disease virus replication. *Antimicrob. Agents. Chemother.* **1978**, *13*, 731-734.
77. Sebastian, L.; Desai, A.; Shampur, M. N.; Perumal, Y.; Sriram, D.; Vasanthapuram, R. N-methylisatin-beta-thiosemicarbazone derivative (SCH 16) is an inhibitor of Japanese encephalitis virus infection in vitro and in vivo. *Virol. J.* **2008**, *5*, 64-75.
78. Krausslich, H.-G.; Wimmer, E. Viral Proteinases. *Annu. Rev. Biochem.* **1988**, *57*, 701-754.
79. Matthews, D. A.; Dragovich, P. S.; Webber, S. E.; Fuhrman, S. A.; Patick, A. K.; Zalman, L. S.; Hendrickson, T. F.; Love, R. A.; Prins, T. J.; Marakovits, J. T.;

- Zhou, R.; Tikhe, J.; Ford, C. E.; Meador, J. W.; Ferre, R. A.; Brown, E. L.; Binford, S. L.; Brothers, M. A.; DeLisle, D.M.; Worland, S. T. Structure-assisted design of mechanism-based irreversible inhibitors of human rhinovirus 3C protease with potent antiviral activity against multiple rhinovirus serotypes. *Proc. Natl. Acad. Sci. U. S. A.* **1999**, *96*, 11000-11007.
80. Webber, S. E.; Tikhe, J.; Worland, S. T.; Fuhrman, S. A.; Hendrickson, T. F.; Matthews, D. A.; Love, R. A.; Patick, A. K.; Meador, J. W.; Ferre, R. A.; Brown, E. L.; DeLisle, D. M.; Ford, C. E.; Binford, S. L. Design, synthesis, and evaluation of nonpeptidic inhibitors of human rhinovirus 3C protease. *J. Med. Chem.* **1996**, *39*, 5072-5082.
81. Drosten, C.; Günther, S.; Preiser, W.; Van der Werf, S.; Brodt, H. R.; Becker, S.; Rabenau, H.; Panning, M.; Kolesnikova, L.; Fouchier, R. A.; Berger, A.; Burguière, A. M.; Cinatl, J.; Eickmann, M.; Escriou, N.; Grywna, K.; Kramme, S.; Manuguerra, J. C.; Müller, S.; Rickerts, V.; Stürmer, M.; Vieth, S.; Klenk, H. D.; Osterhaus, A. D.; Schmitz, H.; Doerr, H.W. Identification of a novel coronavirus in patients with severe acute respiratory syndrome. *N. Engl. J. Med.* **2003**, *348*, 1967-1976.
82. Zhou, L.; Liu, Y.; Zhang, W.; Wei, P.; Huang, C.; Pei, J.; Yuan, Y.; Lai, L. Isatin compounds as noncovalent SARS coronavirus 3C-like protease inhibitors. *J. Med. Chem.* **2006**, *49*, 3440-3443.
83. Chen, L. R.; Wang, Y. C.; Lin, Y. W.; Chou, S. Y.; Chen, S. F.; Liu, L. T.; Wu, Y. T.; Kuo, C. J.; Chen, T. S.; Juang, S. H. Synthesis and evaluation of isatin derivatives as effective SARS coronavirus 3CL protease inhibitors. *Bioorg. Med. Chem. Lett.* **2005**, *15*, 3058-3062.
84. Pirrung, M. C.; Pansare, S. V.; Sarma, K. D.; Keith, K. A.; Kern, E. R. Combinatorial optimization of isatin-beta-thiosemicarbazones as anti-poxvirus agents. *J. Med. Chem.* **2005**, *48*, 3045-3050.
85. Teitz, Y.; Ronen, D.; Vansover, A.; Stematsky, T.; Riggs, J. L. Inhibition of human immunodeficiency virus by N-methylisatin-beta 4':4'-diethylthiosemicarbazone and N-allylisatin-beta-4':4'-diallythiosemicarbazone. *Antiviral. Res.* **1994**, *24*, 305-314.

86. Pandeya, S. N.; Sriram, D.; Nath, G.; De Clercq, E. Synthesis, antibacterial, antifungal and anti-HIV activities of Schiff and Mannich bases derived from isatin derivatives and N-[4-(4'-chlorophenyl)thiazol-2-yl] thiosemicarbazide. *Eur. J. Pharm. Sci.* **1999**, *9*, 25-31.
87. Pandeya, S. N.; Sriram, D.; Nath, G.; De Clercq, E. Synthesis, antibacterial, antifungal and anti-HIV evaluation of Schiff and Mannich bases of isatin derivatives with 3-amino-2-methylmercapto quinazolin-4(3H)-one. *Pharm. Acta. Helv.* **1999**, *74*, 11-17.
88. Pandeya, S. N.; Sriram, D.; Nath, G.; De Clercq, E. Synthesis and antimicrobial activity of Schiff and Mannich bases of isatin and its derivatives with pyrimidine. *Farmaco.* **1999**, *54*, 624-628.
89. Pandeya, S. N.; Sriram, D.; Nath, G.; De Clercq, E. Synthesis, antibacterial, antifungal and anti-HIV activities of norfloxacin mannich bases. *Eur. J. Med. Chem.* **2000**, *35*, 249-255.
90. Selvam, P.; Chandramohan, M.; De Clercq, E.; Witvrouw, M.; Pannecouque, C. Synthesis and anti-HIV activity of 4-[(1,2-dihydro-2-oxo-3H-indol-3-ylidene) amino]-N(4,6-dimethyl-2-pyrimidinyl)-benzene sulfonamide and its derivatives. *Eur. J. Pharm. Sci.* **2001**, *14*, 313-316.
91. Sriram, D.; Bal, T. R.; Yogeewari, P. Design, synthesis and biological evaluation of novel non-nucleoside HIV-1 reverse transcriptase inhibitors with broad-spectrum chemotherapeutic properties. *Bioorg. Med. Chem.* **2004**, *12*, 5865-5873.
92. Sriram, D.; Bal, T. R.; Yogeewari, P. Newer aminopyrimidinimino isatin analogues as non-nucleoside HIV-1 reverse transcriptase inhibitors for HIV and other opportunistic infections of AIDS: design, synthesis and biological evaluation. *Farmaco.* **2005**, *60*, 377-384.
93. Bal, T. R.; Anand, B.; Yogeewari, P.; Sriram, D. Synthesis and evaluation of anti-HIV activity of isatin beta-thiosemicarbazone derivatives. *Bioorg. Med. Chem. Lett.* **2005**, *15*, 4451-4455.
94. Sriram, D.; Yogeewari, P.; Meena, K. Synthesis, anti-HIV and antitubercular activities of isatin derivatives. *Pharmazie.* **2006**, *61*, 274-277.

95. De Oliveira, M. R.; Torres, J. C.; Garden, S. J.; dos Santos, C. V.; Alves, T. R.; Pinto, A. C.; Pereira, H. de S.; Ferreira, L. R.; Moussatché, N.; Frugulhetti, I. C.; Ferreira, V. F.; De Souza, M. C. Synthesis and antiviral evaluation of isatin ribonucleosides. *Nucleosides. Nucleotides. Nucleic. Acids.* **2002**, *21*, 825-835.
96. Pandeya, S. N.; Sriram, D.; Yogeewari, P.; Ananthan, S. Antituberculous activity of norfloxacin mannich bases with isatin derivatives. *Chemotherapy.* **2001**, *47*, 266-269.
97. Dandia, A.; Sati, M.; Arya, K.; Sharma, R.; Loupy, A. Facile one pot microwave induced solvent-free synthesis and antifungal, antitubercular screening of spiro [1,5]-benzothiazepin-2,3'[3H]indol-2[1H]-ones. *Chem. Pharm. Bull.* **2003**, *51*, 1137-1141.
98. Sriram, D.; Yogeewari, P.; Gopal, G. Synthesis, anti-HIV and antitubercular activities of lamivudine prodrugs. *Eur. J. Med. Chem.* **2005**, *40*, 1373-1376.
99. Sriram, D.; Yogeewari, P.; Basha, J. S.; Radha, D. R.; Nagaraja, V. Synthesis and antimycobacterial evaluation of various 7-substituted ciprofloxacin derivatives. *Bioorg. Med. Chem.* **2005**, *13*, 5774-5778.
100. Ramachandran, J. Antimycobacterial Isatin and Oxindole Derivatives for the Treatment of Mycobacterial Diseases, *Swed. Pat.* 9,944,608, **20 Apr 1998**.
101. Varma, R. S.; Pandeya, R. K. Synthesis of 3-(p-(p-alkoxy carbonyl)phenyl)-carbonyl)-phenyl)imino)-2-indolinones as potentially biologically active agents. *Indian. J. Pharm. Sci.* **1982**, *46*, 132-135.
102. Sriram, D.; Yogeewari, P.; Thirumurugan, R.; Pavana, R. K. Discovery of new antitubercular oxazolyl thiosemicarbazones. *J. Med. Chem.* **2006**, *49*, 3448-3450.
103. Sriram, D.; Aubry, A.; Yogeewari, P.; Fisher, L. M. Gatifloxacin derivatives: synthesis, antimycobacterial activities, and inhibition of Mycobacterium tuberculosis DNA gyrase. *Bioorg. Med. Chem. Lett.* **2006**, *16*, 2982-2985.
104. Sriram, D.; Yogeewari, P.; Dhakla, P.; Senthilkumar, P.; Banerjee, D. N-Hydroxythiosemicarbazones: synthesis and in vitro antitubercular activity. *Bioorg. Med. Chem. Lett.* **2007**, *17*, 1888-1891.

105. Güzel, O.; Karali, N.; Salman, A. Synthesis and antituberculosis activity of 5-methyl/trifluoromethoxy-1H-indole-2,3-dione 3-thiosemicarbazone derivatives. *Bioorg. Med. Chem.* **2008**, *16*, 8976-8987.
106. Kumar, R. R.; Perumal, S.; Senthilkumar, P.; Yogeewari, P.; Sriram, D. Discovery of antimycobacterial spiro-piperidin-4-ones: an atom economic, stereoselective synthesis, and biological intervention. *J. Med. Chem.* **2008**, *51*, 5731-5735.
107. Sumpter, W. C. The Chemistry of Isatin. *Chem. Rev.* **1944**, *34*, 393-434.
108. Sandmeyer, T. Über Isonitrosoacetanilide und deren Kondensation zu Isatinen. *Helv. Chim. Acta.* **1919**, *2*, 234-242.
109. Gassman, P. G.; Cue Jr., B. W.; Luh, T. Y. A general method for the synthesis of isatins. *J. Org. Chem.* **1977**, *42*, 1344-1348.
110. Lamberton, B. J. A.; Price, J. R. Alkaloids of the Australian Rutaceae: *Medicosma cunninghamii* Hook. *Aust. J. Chem.* **1953**, *6*, 173-179.
111. Giovannini, E.; Portmann P. Sur quelques dérivés de l'oxindole et de l'isatine. III. Les acides isatine-carboxyliques-5 et -6. *Helv. Chim. Acta.* **1948**, *31*, 1392-1396.
112. Pauwels, R.; Balzarini, J.; Baba, M.; Snoeck, R.; Schols, D.; Herdewijn, P.; Desmyter, J.; De Clercq, E. Rapid and automated tetrazolium-based colorimetric assay for the detection of anti-HIV compounds. *J. Virol. Methods.* **1988**, *20*, 309-321.
113. Balzarini, J.; Karlsson, A.; Pérez-Pérez, M. J.; Vrang, L.; Walbers, J.; Zhang, H.; Oberg, B.; Vandamme, A. M.; Camarasa, M. J.; De Clercq, E. HIV-1-specific reverse transcriptase inhibitors show differential activity against HIV-1 mutant strains containing different amino acid substitutions in the reverse transcriptase. *Virology.* **1993**, *192*, 246-253.
114. Popovic, M.; Sarngadharan, M. G.; Read, E.; Gallo, R. C. Detection, isolation, and continuous production of cytopathic retroviruses (HTLV-III) from patients with AIDS and pre-AIDS. *Science.* **1984**, *224*, 497-500.
115. Pauwels, R.; De Clercq, E.; Desmyter, J.; Balzarini, J.; Goubau, P.; Herdewijn, P.; Vanderhaeghe, H.; Vandeputte, M. Sensitive and rapid assay on MT-4 cells

- for detection of antiviral compounds against the AIDS virus. *J. Virol. Methods*. **1987**, *16*, 171-185.
116. Sriram, D.; Bal, T.R.; Yogeewari, P. Design, synthesis and biological evaluation of novel non-nucleoside HIV-1 reverse transcriptase inhibitors with broad-spectrum chemotherapeutic properties. *Bioorg. Med. Chem.* **2004**, *12*, 5865-5873.
117. National Committee for Clinical Laboratory Standards. Antimycobacterial susceptibility testing for Mycobacterium tuberculosis. Proposed standard M24-T. National Committee for Clinical Laboratory Standards, Villanova, PA, 1995.
118. Xie, Z.; Siddiqi, N.; Rubin, E. R. Differential antibiotic susceptibilities of starved Mycobacterium tuberculosis isolates. *Antimicrob. Agents. Chemother.* **2005**, *49*, 4778-4780.
119. Bentrup, K. H. Z.; Miczak, A.; Swenson, D. L.; Russell, D. G. Characterization of activity and expression of isocitrate lyase in *Mycobacterium avium* and *Mycobacterium tuberculosis*. *J. Bacteriol.* **1999**, *181*, 7161-7167.
120. Manjunatha, U. H.; Dalal, M.; Chatterji, M.; Radha, D. R.; Visweswariah, S. S.; Nagaraja, V. Functional characterisation of mycobacterial DNA gyrase: an efficient decatenase. *Nucleic. Acids. Res.* **2002**, *30*, 2144-2153.
121. Saito, Y.; Escuret, V.; Durantel, D.; Zoulim, F.; Schinazi, R. F.; Agrofoglio, L. A. Synthesis of 1,2,3-triazolo-carbanucleoside analogues of ribavirin targeting an HCV in replicon. *Bioorg. Med. Chem.* **2003**, *11*, 3633-3639.
122. Krieger, N.; Lohmann, V.; Bartenschlager, R. Enhancement of hepatitis C virus RNA replicon replication by cell culture-adaptive mutations. *J. Virol.* **2001**, *75*, 4614-4624.
123. Sidwell, R. W.; Smee, D. F. *In vitro* and *in vivo* assay systems for study of influenza virus inhibitors. *Antiviral Res.* **2000**, *48*, 1-16.
124. Smee, D.F.; Morrison, A.; Barnard, D.; Sidwell, R. Comparison of colorimetric, fluorometric, and visual methods for determining anti-influenza (H1N1 and H3N2) virus activities and toxicities of compounds. *J. Virol. Methods.* **2002**, *106*, 71-79.

125. Klebe, G.; Abraham, U. On the prediction of binding properties of drug molecules by comparative molecular field analysis. *J. Med. Chem.* **1993**, *36*, 70-80.
126. Klebe, G.; Abraham, U.; Mietzner, T. Molecular similarity indices in a comparative analysis (CoMSIA) of drug molecules to correlate and predict their biological activity. *J. Med. Chem.* **1994**, *37*, 4130-4146.
127. RCSB Protein Data Bank ID. 1VRT. Available from: URL: www.rcsb.pdb.org.
128. Carlsson, J.; Boukharta, L.; Aqvist, J. Combining docking, molecular dynamics and the linear interaction energy method to predict binding modes and affinities for non-nucleoside inhibitors to HIV-1 reverse transcriptase. *J. Med. Chem.* **2008**, *51*, 2648-2656.
129. De Martino, G.; La Regina, G.; Di Pasquali, A.; Ragno, R.; Bergamini, A.; Ciaprini, C.; Sinistro, A.; Maga, G.; Crespan, E.; Artico, M.; Silvestri, R. Novel 1-[2-(diarylmethoxy)ethyl]-2-methyl-5-nitroimidazoles as HIV-1 non-nucleoside reverse transcriptase inhibitors. A structure-activity relationship investigation. *J. Med. Chem.* **2005**, *48*, 4378-88.
130. RCSB Protein Data Bank ID. 1F8M. Available from: URL: www.rcsb.pdb.org.
131. Lipinski, C. A.; Lombardo, F.; Dominy, B. W.; Feeney, P. J. Experimental and computational approaches to estimate solubility and permeability in drug discovery and development settings. *Adv. Drug Deliv. Rev.* **1997**, *23*, 3-25.
132. Ren, J.; Stammers, D. K.; HIV reverse transcriptase structures: designing new inhibitors and understanding mechanisms of drug resistance. *Trends Pharmacol. Sci.* **2005**, *26*, 4-7.
133. Kohlstaedt, L. A.; Wang, J.; Fiedman, J. M.; Rice, P. A.; Steitz, T. A.; Crystal structure at 3.5 Å resolution of HIV-1 reverse transcriptase complexed with an inhibitor. *Science.* **1992**, *256*, 1783-1790.
134. Bentrup, K. H. Z.; Russell, D. G. Mycobacterial persistence: adaptation to a changing environment. *Trends Microbiol.* **2001**, *9*, 597-605.
135. Manabe, Y. C.; Bishai, W. R. Latent Mycobacterium tuberculosis-persistence, patience, and winning by waiting. *Nat. Med.* **2000**, *6*, 1327-1329.

136. Zhang, Y. The magic bullets and tuberculosis drug targets. *Annu. Rev. Pharmacol. Toxicol.* **2005**, *45*, 529–564.
137. Mc Kinney, J.D.; Höner zu Bentrup, K.; Muñoz-Elias, E. J.; Miczak, A.; Chen, B.; Chan, W. T.; Swenson, D.; Sacchettini, J. C.; Jacobs, W. R. Jr.; Russell, D. G. Persistence of *Mycobacterium tuberculosis* in macrophages and mice requires the glyoxylate shunt enzyme isocitrate lyase. *Nature.* **2000**, *406*, 735–738.
138. Glickman, M.S. A novel mycolic acid cyclopropane synthetase is required for cording, persistence, and virulence of *Mycobacterium tuberculosis*. *Mol. Cell* **2000**, *5*, 717–727.
139. Dahl, J. L. The role of RelMtb-mediated adaptation to stationary phase in long-term persistence of *Mycobacterium tuberculosis* in mice. *Proc. Natl. Acad. Sci. U. S. A.* **2003**, *100*, 10026–10031.
140. Park, H.D. Rv3133c/dosR is a transcription factor that mediates the hypoxic response of *Mycobacterium tuberculosis*. *Mol. Microbiol.* **2003**, *48*, 833–843.
141. Sharma, V.; Sharma, S.; Hoener zu Bentrup, K.; McKinney, J. D.; Russell, D. G.; Jacobs, W. R. Jr.; Sacchettini, J. C.; Structure of isocitrate lyase, a persistence factor of *Mycobacterium tuberculosis*. *Nat. Struct. Biol.* **2000**, *7*, 663-668.
142. Ravichandran, V.; Agrawal, R. K. Predicting anti-HIV activity of PETT derivatives: CoMFA approach. *Bioorg. Med. Chem. Lett.* **2007**, *17*, 2197-2202.
143. Willett, P. Genetic algorithms in molecular recognition and design. *Trends. Biotechnol.* **1995**, *13*, 516-521.
144. Jones, G.; Willett, P.; Glen, R. C.; Leach, A. R.; Taylor, R. Development and validation of a genetic algorithm for flexible docking. *J. Mol. Biol.* **1997**, *267*, 727-748.
145. Das, K.; Lewi, P.J.; Hughes, S.H.; Arnold, E. Crystallography and the design of anti-AIDS drugs: conformational flexibility and positional adaptability are important in the design of non-nucleoside HIV-1 reverse transcriptase inhibitors. *Prog. Biophys. Mol. Biol.* **2005**, *88*, 209-231.
146. Sarafianos, S. G.; Das, K.; Hughes, S. H.; Arnold, E. Taking aim at a moving target: designing drugs to inhibit drug-resistant HIV-1 reverse transcriptases. *Curr. Opin. Struct. Biol.* **2004**, *14*, 716-730.

147. Cardona, P. J. New insights on the nature of latent tuberculosis infection and its treatment. *Inflamm. Allergy. Drug. Targets.* **2007**, *6*, 27-39.
148. Hunter, R.; Younis, Y.; Muhanji, C. I.; Curtin, T. L.; Naidoo, K. J.; Petersen, M.; Bailey, C. M.; Basavapathruni, A.; Anderson, K. S. C-2-aryl O-substituted HI-236 derivatives as non-nucleoside HIV-1 reverse-transcriptase inhibitors. *Bioorg. Med. Chem.* **2008**, *16*, 10270-10280.
149. Morris, G. M.; Huey, R.; Olson, A. J. Using AutoDock for ligand-receptor docking. *Curr Protoc Bioinformatics.* 2008 Dec; Chapter 8: Unit 8.14.

APPENDIX

List of Publications

1. Dharmarajan Sriram, **Debjani Banerjee**, Perumal Yogeewari, Pritesh Bhat, Anisha Thomas, “Novel isatinyl derivatives as potential molecule in the crusade against HIV-TB co-infection”, *J. Med. Chem.*, Communicated, **2009**.
2. **Debjani Banerjee**, Perumal Yogeewari, Pritesh Bhat, Anisha Thomas, Dharmarajan Sriram, “Synthesis, in-vitro evaluation and computational studies of novel isatinyl derivatives for their activity against HIV-TB co-infection”, *Int. J. Antimicrob. Agents.*, Communicated, **2009**.
3. Sriram, D.; Yogeewari, P.; Dhakla, P.; Senthilkumar, P.; **Banerjee, D.**; Manjashetty, T. H. “5-Nitrofuranyl derivatives: synthesis and inhibitory activities against growing and dormant mycobacterium species.”, *Bioorg. Med. Chem Lett.* **2009**, *19*, 1152-1154.
4. Sriram, D.; **Banerjee, D.**; Yogeewari, P. “Efavirenz Mannich bases: synthesis, anti-HIV and antitubercular activities.”, *J. Enzyme. Inhib. Med. Chem.* **2009**, *24*, 1-5.
5. Senthilkumar, P.; Dinakaran, M.; **Banerjee, D.**; Devakaram, R. V.; Yogeewari, P.; China, A.; Nagaraja, V.; Sriram, D. “Synthesis and antimycobacterial evaluation of newer 1-cyclopropyl-1,4-dihydro-6-fluoro-7-(substituted secondary amino)-8-methoxy-5-(sub)-4-oxoquinoline-3-carboxylic acids.”, *Bioorg. Med. Chem.* **2008**, *16*, 2558-2569.
6. Sriram, D.; Yogeewari, P.; Senchani, G.; **Banerjee, D.** “Newer tetracycline derivatives: synthesis, anti-HIV, antimycobacterial activities and inhibition of HIV-1 integrase.”, *Bioorg. Med. Chem. Lett.* **2007**, *17*, 2372-2375.

7. Sriram, D.; Yogeewari, P.; Dhakla, P.; Senthilkumar, P.; **Banerjee, D.** “N-Hydroxythiosemicarbazones: synthesis and in vitro antitubercular activity.”, *Bioorg. Med. Chem. Lett.* **2007**, *17*, 1888-1891.
8. Sriram, D.; Yogeewari, P.; Senthilkumar, P.; Sangaraju, D.; Nelli, R.; **Banerjee, D.**; Bhat, P.; Veugopal, B.; Pavan, V. V. S.; Manjashetty, T. H. “Novel pthalazinyl derivatives: Synthesis, antimycobacterial activities, and inhibition of Mycobacterium tuberculosis isocitrate lyase enzyme”, *Med. Chem. Communicated*, **2009**.
9. Sriram, D.; **Banerjee, D.**; Varuna, T. S. T. V. N. V.; Sankar, M.; Yogeewari, P. “Antitubercular activities of novel diallyl/dibenzyl thiosemicarbazones endowed with high activity toward multi-drug resistant tuberculosis”, *Med. Chem. Res. Communicated*, **2009**.

Papers Presented At National/International Conferences

1. **Debjani Banerjee**, Perumal Yogeeswari, Dharmarajan Sriram, “Synthesis and Biological Evaluation of Isatin- β -thiosemicarbazone derivatives as Novel NNRTIs with Broad-spectrum Chemotherapeutic Properties”, Poster, “MEDCHEM 2009 Conference Cum Workshop on Current Trends in Medicinal Chemistry” held from April 2-4, Chennai, India, 2009.
2. Anisha Thomas, **Debjani Banerjee**, Perumal Yogeeswari, Dharmarajan Sriram, “Synthesis of N-Hydroxy thiosemicarbazone derivatives and their anti-retroviral evaluation”, Poster, “59th Indian Pharmaceutical Congress”, held from December 20-23, Varanasi, India, 2007.
3. **Debjani Banerjee**, Tanushree R. Bal, P. Yogeeswari, D.Sriram, Liba Sebastian, Anita Desai, S.N. Madhusudhana, V. Ravi, “Isatin derivatives inhibit japanese encephalitis virus entry and replication *in vitro*”, Poster, “3rd International Symposium on Current Trends in Drug Discovery Research (CTDDR)” held from February 17-21, Lucknow, India, 2007.
4. **Debjani Banerjee**, M. Dinakaran, P. Senthil Kumar, Ruth Vandana Devakaram, P. Yogeeswari, D. Sriram, “Synthesis and Antibacterial Evaluation of Phenothiazine Derivatives”, Poster, National Symposium on “Challenges in Drug Discovery Research: Networking Opportunities between Academia & Industries”, held from April 7-8, Pilani, India, 2006.

BIOGRAPHY OF DEBJANI BANERJEE

Debjani Banerjee completed her Bachelor's degree in Pharmacy from KLE College of Pharmacy, Bangalore (Rajiv Gandhi University of Health Sciences, Karnataka), in the year 2003. She then did her Master's in Pharmacy (M.Pharm) from Birla Institute of Technology & Science, Pilani, Rajasthan and graduated in the year 2006. She has been working as a research scholar since 2006-2009, in the same institute under the supervision of Dr. D. Sriram. During her post graduation studies she availed GATE scholarship and during her doctoral studies she was awarded Senior Research Fellowship (SRF) by the Indian Council of Medical Research, New Delhi, India. She has few publications and presentations to her credit.

BIOGRAPHY OF Dr. D. SRIRAM

Dr. D. Sriram is presently working in the capacity of Assistant Professor at the Pharmacy Group, Birla Institute of Technology & Science (BITS), Pilani, Hyderabad Campus. He received his Ph.D. degree in the year 2000 from Banaras Hindu University (BHU), Varanasi, having finished his doctoral studies in a record period of 2 years. He has been involved in research for the past thirteen years and in teaching for twelve years. He is the recipient of "*YOUNG PHARMACY TEACHER OF THE YEAR 2006*" awarded by the Association of Pharmacy Teachers of India. He is involved in collaborative research with TAACF, Southern Research Institute, Alabama, USA, National Institute of Health, Bethesda, USA, Indian Institute of Science, Bangalore, India, National Institute of Mental Health and Neurosciences, Bangalore, India, National Institute of AIDS, USA, Central Drug Research Institute, Lucknow, India. He has to his credit more than 109 research publications and also is the expert reviewer of many international journals like Bioorganic Medicinal Chemistry (Elsevier), Bioorganic Medicinal Chemistry Letters (Elsevier), Letters in Drug Design & Discovery (Bentham), Combinatorial Chemistry & High Throughput Screening (Bentham), Current Enzyme Inhibition (Bentham), Archives der Pharm. Pharm. Med. Chem, Indian Journal of Chemistry, Section B (CSIR), Recent Patents on Anti-infective drug discovery (Bentham), Current Bioactive Agents

(Bentham), European Journal of Medicinal chemistry (Elsevier), Journal of Medicinal Chemistry (ACS). Due to his remarkable accomplishments his biographical profile has been included in the prestigious registry of the 6th edition of “*Marquis Who’s Who in Science and Engineering*”. He has also co-authored a textbook on organic medicinal chemistry with Dr. P. Yogeewari titled “Medicinal Chemistry”, published by Pearson Education. He is currently handling two major research projects, one of Department of Biotechnology and the other funded by Indian Council of Medical Research, India. He has guided four PhD students and is presently guiding two PhD students.